Quantum Measurement and Feedback Control of highly nonclassical Photonic States

Jared Lolli

Université Sorbonne Paris Cité

Université Paris Diderot

Laboratoire Matériaux et Phénomènes Quantiques

École doctorale: Physique en Ile-de-France

Jared Lolli

Quantum Measurement and Feedback Control of highly nonclassical Photonic States

---

Thèse dirigée par Cristiano Ciuti

Soutenue le 10 novembre 2017 devant le jury composé de:

M.	Mauro Paternostro	Rapporteur
M.	Johannes Fink	Rapporteur
M.	Nicolas Roch	Examinateur
Mme	Pérola Milman	Présidente du jury
M.	Cristiano Ciuti	Directeur de thèse

A Sofia, Gea, Pietro, Blu, Inés, Nina e al futuro.

Acknowledgments, Remerciements e Ringraziamenti

I have always found the acknowledgment pages in PhD manuscripts curious. From a formal point of view, they should be strictly aimed at acknowledging the people that contributed to the scientific production reported in the thesis. On the other hand it is often transformed in a true declaration of friendship, affection or even love, to the many people that we encounter during these intense years.

I will not be an exception to this habit. I think that these pages are a unique opportunity, to acknowledge the amazing people that helped me to understand who I am, as a scientist and as a man.

First of all I would like to thank my supervisor Cristiano Ciuti. I am sincerely thankful for the huge experience that you shared with me, and for supporting me in many of my ideas and projects. Nel bene e nel male, non dimenticherò mai le ultime settimane di redazione, la tua completa disponibilità e le correzioni persino durante il fine settimana, grazie.

While my supervisor and colleagues "had" to read and correct my manuscript, the jury members freely accepted this tedious task! For this reason I am sincerely thankful to Mauro Paternostro, Johannes Fink, Nicolas Roch and Pérola Milman. Thank you for going through the pages of this manuscript, for the corrections, and for the very interesting questions and the discussion held during the defense of my thesis.

A very special thanks goes to Fabrizio Minganti, it has been a true privilege to work with you, Fabrizio. Your passion and ideas enlighten our work, I will never forget the profoundness and the rigouresness of our discussions, I think that we have learnt a lot together. You helped me a lot during these years, I am sincerely thankful to your unique generosity. I have no doubt that you are going to be a great researcher and teacher, sta solo a te decidere se preferisci il pianoforte a coda dei tuoi sogni! Grazie mille Fabrissione.

Then I would like to spend few words for my most direct collaborators: Alexandre Baksic, Nicola Bartolo and Gernot Schaller. Quel chance d'avoir rencontré quelqu'un comme toi au début de ma thèse, Alexandre, merci pour ton humour et pour tes capacités pédagogiques. Grazie Nicola, è stato un piacere capire insieme che i gatti saltano invece che trotterellare. Vielen Dank Gernot for hosting me in Berlin and for the attention that you devoted to our project. I also thank our collaboration with Wim Casteels, David Nagy, Vladimir E. Manucharian, and particularly Tobias Brandes, of which I keep a very nice memory of his kindness and ability to listen. I finally would like to thank Ruediger Schack for helping me to clarify some of the

concepts that we used in this theses, the discussion that we had in March 2017 was probably the most exciting exchange of my scientific career.

In 4 years at the MPQ laboratory I have sat in 6 different offices, I would like to thank the many people of this community that enriched my experience. On a commencé cette aventure ensemble, cela aurait été cool de compter le nombre de "galettes" qu'on a achetées à la machine du 3ème étage: merci pour tout ce qu'on a partagé Florent, on se retrouvera en manif ou en randonnée! Toujours en marche, mais jamais à la façon de Macron! Quel belle surprise de te retrouver Alexandre (Le Boité), merci pour ton aide en fin de rédaction et pour les belles discussions. Gracias à Juan, la terrasse du 7ème n'a plus été la même sans toi. Grazie Riccardo, Alberto, Simone, per le belle chiacchiere e per avermi sopportato quando vi assillavo con i fondamenti della quantistica. Merci aux derniers arrivés et aux "partis trop tôt" du groupe: Cassia, les 2 Filippos, Matthieux, Michael, Arthur, Stefano. Merci aussi aux membres du laboratoire, pour les beaux échanges qu'on a eus: Adrian (que j'aurais du écouter plus), Nabeel, Ouafi, Andreas, Tom, Hélene, Zahra, Dimitri, Ian et tous les autres thésards, j'aurais du venir dans le "thésarium" plus tôt! Merci aussi à Carlo et Anne pour votre humanité, merci à Jaysen, à Walid et à toutes les autres personnes qui ont enrichi mes journées. Merci à Jocelyne, à Sandrine et à toutes les autres personnes qui font marcher cette grande machine, y compris les gardiens et le personnel du nettoyage.

I think that teaching has been one of the most interesting experiences of my PhD. For this reasons I would like to thank the staff and teachers of the *Rue Pajol IUT*. I would also like to thank the *EnAct* teachers, whose trainings have helped me a lot in the teaching activity. I had the chance to devote a lot of energy in this activity, sadly it is not the case for all PhD students. A selection system based only on publications obviously discourages to invest time on teaching, and this also leads to the deterioration of the teaching quality.

Out of the lab many amazing people made these years in Paris a unique experience. Grazie a Nico: nelle nostre tante discese di Rue de Ménilmontant cercavamo noi stessi e finivamo sempre per trovare la solita crêpe...ma quanto era bona?! Un merci à toutes les personnes spéciales rencontrées pendant cette inoubliable première année parisienne: Olivia, Enri, Onder, Giulia, Eli, Fede, Chiara... Grazie a Dudo: le feste, l'acrobazia, la musica, chissá quante altre passioni condivideremo, l'intensità con cui le vivi rimane per me un esempio! Merci Fred, la rigueur avec laquelle tu vis tes principes est un exemple pour moi, ça me permettra d'être un peu moins bobo un jour. A dirla tutta a Parigi ho trovato una vera famiglia, e di questo ne sarò sempre grato. Ci sono la zia Camilla, e gli zii Giulio e Joseba, la vostra cucina è l'espressione della vostra estrema generosità. Ci sono i nonni Marco e Marzia, su cui si può contare sempre. Il y a la tante LUize, du français au Hip-hop elle n'arrêtera jamais de nous apprendre des choses. C'è il cugino Vito che è profondo e che è anche un gran melomane! C'è

il cugino Valerio, chi se non tu poteva darci la prima nipotina?! Ahi! La famiglia di Ritals è grande, non finisce più! Ci sono Rita, Martino, Giulia, Fede, Mattia, Rembaduzzo... quanti cugini, ognuno con il suo superpotere!

Molte altre persone devo ringraziare per aver arricchito la mia vita parigina. La mia coinquilina Silvia, esempio di generosità, et toute la clique des architectes, vous savez comment on fait la fête! Marco (trombonista) e Filippo, cercare di inserirmi nella vostra pienissima agenda varrà sempre la pena.

Merci à toute la Fanfare Invisible, qui, comme un super-héros, est toujours là même quand on ne la voit pas. Merci au ZFO pour sa richesse et surtout pour m'emmener si loin. Merci à Lin et à tous ses élèves avec lesquels tous les jours on essaye de voler, et on y est presque!

À Paris on se trouve et on se perd tout le temps, mais ce n'est pas pour ça qu'on s'oublie... Merci Oriane, Arthur, Jasko et Yann, pour les beaux moments qu'on a vécus ensemble. "Drôle l'idée de faire une thèse pour quelqu'un comme toi", merci Oriane, cette discussion m'a permis de comprendre beaucoup de choses. Grazie anche a Ricky e alle sue bolle, che mi hanno accompagnato in un anno duro e pieno di emozioni.

Bon bref, merci à Paris et à toutes tes richesses qui m'ont permis de vivre une période de découverte sans égale.

Grazie anche a tutte le mie famiglie lontane, ma sempre vicine! Grazie a tutta la mia famiglia, e soprattutto a mia madre e i miei fratelli che mi hanno sempre indicato il camino, comunque lasciandomi la libertà di disegnare il mio. Grazie a mio padre per l'energia che ci ha dato. Grazie alla famiglia di iMAGiNARiA e a quella elfica: fare scienza è prima di tutto ispirazione, con voi ho vissuto alcuni dei più forti momenti d'ispirazione della mia vita. Grazie in particolare ad Aca per avermi invitato e convinto a parlare a un TEDx talk, è stata un'esperienza unica e indimenticabile. Grazie ai "fisici de merda", grazie a Jacosbracci e al suo salame, a Nik e le sue minchiate, a Giangi e la sua gioia de vive', a GM che resterà sempre il leader, a Federico, Biko, Ilaria, Gianpaolo, Giovanni, Marzie, ancora Camilla. Che squadretta che formavamo, che bello scoprire la fisica insieme a voi!

Fa piacere accorgersi che anche le esperienze più lontane nel tempo hanno influenzato queste pagine di tesi. Grazie al Prof. Litterio, che ora chiamo Marco, lui mi ha fatto amare la fisica, lui mi ha guidato per tanti anni. E grazie anche alle altre bellissime persone che ho incontrato al liceo. Celeste, e la tua profonda sensibilità. Federica la ragazza più zizza del mondo! Alessio e Giova, compagni di banco e di avventure, siamo cresciuti insieme, che fortuna trovarvi. E Digio, l'altro dei Cantina-Boys, ho-detto-tutto! Grazie anche al Biondo, a mamma Letizia, e tutti i compagni di quella bella avventura, eravamo forti!

E poi in fondo ci sei tu, Giulia, che non sei in cima solo per una questione di forma. C'è molto di te in questa pagine. Mi ha sempre colpito la tua capacità di ascoltare

come lo sai fare tu, ed è proprio raccontandoti quel poco che so di scienza che ho chiarito molte delle mie idee. Il poster a nido d'ape, la preparazione del TEDx, gli ultimi mesi di scrittura insieme, grazie per avermi sostenuto nei momenti più intensi di questa avventura. Ovviamente c'è molto di più, ogni giorno mi regali il sorriso, ogni giorno mi aiuti a capire chi sono, ogni giorno mi aiuti ad immaginare la mia e la nostra "Itaca".

Abstract

In recent years, the field of quantum optics has thrived thanks to the possibility of controlling light-matter interaction at the quantum level. This is relevant for the study of fundamental quantum phenomena, the generation of artificial quantum systems, and for quantum information applications. In particular, it has been possible to considerably increase the intensity of light-matter interaction and to shape the coupling of quantum systems to the environment, so to realise unconventional and highly nonclassical states. However, in order to exploit these quantum states for technological applications, the question of how to measure and control these systems is crucial.

Our work is focused on proposing and exploring new protocols for the measurement and the control of quantum systems, in which strong interactions and peculiar symmetries lead to the generation of highly nonclassical states. The first situation that we consider is the ultrastrong coupling regime in cavity (circuit) quantum electrodynamics. In this regime, it becomes energetically favourable to have photons and atomic excitations in the ground state, that is no more represented by the standard vacuum. In particular, in case of parity symmetry, the ground state is given by a light-matter Schrödinger cat state. However, according to energy conservation, the photons contained in these exotic vacua are bound to the cavity, and cannot be emitted into the environment. This means that we can not explore and control them by simple photodetection. In our work we propose a protocol that is especially designed to overcome this issue. We show that we can infer the photonic properties of the ground state from the Lamb shift of an ancillary two-level system.

Another class of systems in which the fundamental parity symmetry leads to very unconventional quantum states is given by two-photon driven-dissipative resonators. Thanks to the reservoir engineering, it is today possible to shape the interaction with the environment to stabilize the system in particularly interesting quantum states. When a resonator (an optical cavity) exchanges with the environment by pairs of photons, it has been possible to observe the presence of optical Schrödinger cat states in the transient dynamics of the system. However, the quantum correlations of these states quickly decays due to the unavoidable presence of one-photon dissipation. Protecting the system against this perturbation is the goal of the parity triggered feedback protocol that we present in this thesis.

Key words: quantum physics; quantum optics; quantum measurement; quantum trajectory; quantum feedback; ultrastrong coupling; Schrödinger's cat; reservoir engineering; light-matter interaction; atoms and photons.

Résumé

Ces dernières années, les progrès réalisés dans le contrôle de l'interaction lumière-matière au niveau quantique ont conduit à de nombreuses avancées en optique quantique, en particulier dans l'étude de phénomènes quantiques fondamentaux, dans la conception de systèmes quantiques artificiels et dans les applications en information quantique. Il a notamment été possible d'augmenter considérablement l'intensité de l'interaction lumière-matière et de contrôler le couplage de systèmes quantiques à leur environnement, afin d'obtenir des états non conventionnels et fortement non classiques. Cependant, pour exploiter ces états quantiques en vue d'applications technologiques, il est crucial de pouvoir mesurer et contrôler ces systèmes avec précision.

Dans ce contexte, ce travail de thèse est consacré à l'étude de nouveaux protocoles pour la mesure et le contrôle de systèmes quantiques dans lesquels des fortes interactions et des symétries particuliers conduisent à la génération d'états fortement non classiques. Nous nous intéressons dans un premier temps au régime de couplage ultra-fort de l'électrodynamique quantique en cavité (et de circuit). Plus précisément, l'état de fondamental n'est plus le vide standard, car il devient énergiquement favorable qu'il contienne des photons. Dans ce régime on peut même obtenir des chat de Schrödinger comme état fondamental. En revanche, pour assurer la conservation de l'énergie, les photons contenus dans ce vide exotique sont liés à la cavité et ne peuvent pas s'échapper dans l'environnement. Cela signifie qu'ils ne peuvent être mesurés par simple photodétection. Nous proposons dans ce travail un protocole spécialement conçu pour surmonter cette difficulté. Nous montrons qu'il est possible de déduire les propriétés photoniques de l'état fondamental à partir du déplacement de Lamb d'un système à deux niveaux auxiliaire.

Les résonateurs optiques à paires de photons constituent une autre classe de systèmes dans lesquels la symétrie de parité conduit à des états quantiques non conventionnels. Grâce à "l'ingénierie de réservoir", il est aujourd'hui possible de contrôler l'interaction d'un système avec son environnement, de façon à le stabiliser dans des états quantiques particulièrement intéressants. En particulier, quand un résonateur (une cavité optique) est couplé à l'environnement par échange de paires de photons, il est possible de créer de chats de Schrödinger optiques dans la dynamique transitoire du système. Les corrélations quantiques de ces états sont par contre rapidement perdues en raison de la présence inévitable de dissipation à un photon. Protéger le système contre cette perturbation est le but du protocole de feedback basé sur la parité que nous présentons dans cette thèse.

Mot clefs: physique quantique; optique quantique; mesure quantique; trajectoires quantiques; feedback quantique; couplage ultrafort; chat de Schrödinger; ingénierie de réservoirs; interaction lumière-matière; atomes et photons.

Contents

Chapter 1
Introduction

When Neil Amstrong set his left foot on the lunar surface, he pronounced the following famous words: "That's one small step for [a] man, one giant leap for mankind". Today I look at my PhD thesis and I think the exact contrary: "This is a small step for science, one giant leap for a young man (me)". Indeed, these years working on quantum physics represented a radical change in my vision of reality and science: from a very realist vision of the world, I gradually developed a more subjective point of view. As a young student in high school and later in my university studies, I grew up with the idea that, with science, we are more and more approaching the understanding of an absolute and unique reality. In this vision, reality is something objective and independent from any cognitive being, and science is the description of what we receive, as passive spectators, from this external world. This kind of questions belong to a very long-standing philosophical debate that, in our occidental culture, finds its roots in the ancient Greek thinking [1], and follows into the formalised doctrines of modern epistemology. Probably conditioned by traditional philosophies, science today is still largely dominated by the point of view of scientific realism [2]. However, the revolutionary developments of science in the 20th century, and quantum physics in particular, are strongly challenging this vision of reality.

Quantum physics is probably the most influential theory for our contemporary life. It allows to understand the world at the atomic scale and, by capturing the physics of light and of the solid state, it determined the technological revolution that we are living today. Mobile phones, computers, the internet: a very large part of human wealth today is due to the knowledge of quantum physics.

Nevertheless and despite its enormous success, the ontological meaning of quantum physics is still the matter of an intense debate [3–7]. It is enough to visit the *Wikipedia* page for *"Interpretations of quantum mechanics"* to understand the level of disagreement around this theory [8]. The table in Fig. 1.1 is extracted from this page. It summarises the manifold of existing interpretations and their position on various questions: in few words, "a map of madness" (quote from [9]).

The seventh column of this table is about "collapsing wave function". In most formulations of quantum physics, wave function collapse is a founding postulate of quantum physics and is related to what happens when we perform a measurement on a system. However, according to the table in Fig. 1.1, only half of the interpretations consider it as fundamental, and among them every interpretation gives a different meaning to the postulate. The way in which a measurement happens is one of the

Interpretation	Author(s)	Deter-ministic?	Wave function real?	Unique history?	Hidden variables?	Collapsing wave functions?	Observer role?	Local?	Counter-factual definite-ness?	Universal wave function exists?
Ensemble interpretation	Max Born, 1926	Agnostic	No	Yes	Agnostic	No	No	No	No	No
Copenhagen interpretation	N. Bohr, W. Heisenberg, 1927	No	No	Yes	No	Yes	Causal	No	No	No
de Broglie–Bohm theory	L. de Broglie, 1927, D. Bohm, 1952	Yes	Yes	Yes	Yes	No	No	No	Yes	Yes
Quantum logic	G. Birkhoff, 1936	Agnostic	Agnostic	Yes	No	No	Interpreta-tional	Agnostic	No	No
Time-symmetric theories	S. Watanabe, 1955	Yes	Yes	Yes	Yes	No	No	Yes	No	Yes
Many-worlds interpretation	H. Everett, 1957	Yes	Yes	No	No	No	No	Yes	Ill-posed	Yes
Consciousness causes collapse	E. Wigner, 1961	No	Yes	Yes	No	Yes	Causal	No	No	Yes
Stochastic interpretation	E. Nelson, 1966	No	No	Yes	Yes	No	No	No	Yes	No
Many-minds interpretation	H. D. Zeh, 1970	Yes	Yes	No	No	No	Interpreta-tional	Yes	Ill-posed	Yes
Consistent histories	R. B. Griffiths, 1984	No	No	No	No	No	No	Yes	No	Yes
Transactional interpretation	J. G. Cramer, 1986	No	Yes	Yes	No	Yes	No	No	Yes	No
Objective collapse theories	Ghirardi–Rimini–Weber, Penrose, 1986-89	No	Yes	Yes	No	Yes	No	No	No	No
Relational interpretation	C. Rovelli, 1994	Agnostic	No	Agnostic	No	Yes	Intrinsic	Yes	No	No
QBism	C. Fuchs, R. Schack, 2010	No	No	Agnostic	No	Yes	Intrinsic	Yes	No	No

Figure 1.1 Table resuming the different positions of the known interpretations of quantum physics. From the *Wikipedia* page for "Interpretations of quantum mechanics" [8]. A more detailed description of physicist attitudes toward quantum mechanics is given in Ref. [3].

most non-trivial aspects in interpriting quantum physics, indeed the "only mystery" (quote of R. Feynman et al. [10])

What are the changes that quantum physics has brought about? And what does quantum physics tell about the measurement? One of the biggest changes introduce by quantum physics is the fact that any observable quantity must satisfy the Heisenberg's uncertainty principle [11]. In our classical conception of reality, one can determine all the properties of a system, and once that this condition of total knowledge is reached, it is in principle possible to predict the outcome of any future observation on the system. This is the idea of *Isaac Newton's clockwork universe* [12], where everything follows precise laws and any prediction is easy if one knows the starting conditions. Quantum physics, and precisely the Heisenberg's uncertainty principle, tells that this idea is an illusory misconception of our classical vision. Our predictions around the observables quantities of any system have intrinsic limits that are not due to the imperfection of our measurement, but are rather the expression of a fundamental behaviour of nature.

In this thesis we will consider the measurement and control of quantum optics systems in which the limits of Heisenberg's principle are attained. At the risk of boring some experts, and in an attempt to include the broadest audience to this discussion, in Figure 1.2 we will try to illustrate this principle in a very simplified

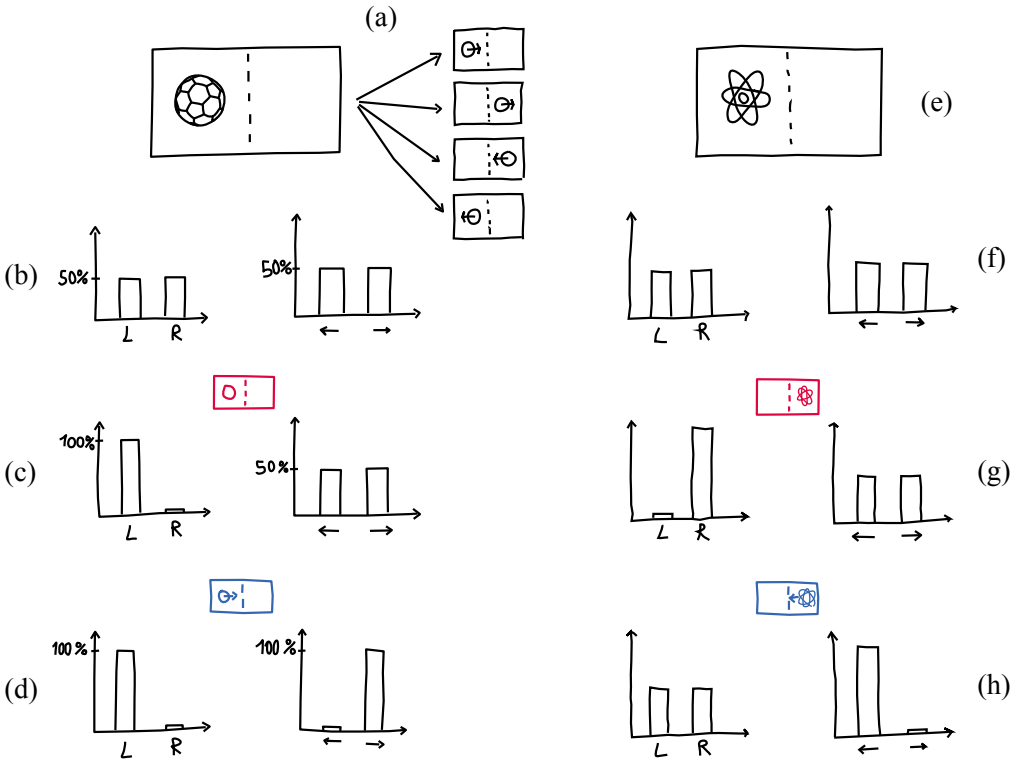

Figure 1.2 A very simplified illustration of the Heisenberg principle. The update of probability distributions (the histograms) after the measurement of position (magenta little boxes) and the direction (blue little boxes) for a large object (a ball) and a microscopic object (an atom).

form and language. Let us consider a ball that can move left and right inside a box that is ideally divided into two sectors. In this simplified model the ball can be in four possible configurations (see Fig. 1.2 (a)): 1, left side moving to the right; 2, right side moving to the right; 3, right side moving to the left; 4, left side moving to the left. Imagine that the box is closed and that we do not know anything about the ball. The only thing that we can say is that the ball has the same probability, 50%, of being in the left or in the right side of the box. And the same probability is valid for the two possible directions, label (b) in Figure 1.2.

By opening the box and sequentially measuring the position (c) and the direction of the ball (d), we can update our knowledge about the ball, up to a condition of total knowledge. We have indeed been able to determine the "real" configuration of the ball (the first one listed in (a)), that in principle allows us to predict with absolute certainty, the ball position and direction at every subsequent observation.

This reasoning, that works in our classical conception of reality, is not valid anymore in the quantum world. Let us consider now an atom inside the box (Fig. 1.2(e)),

and let us follow the same argumentation as for the ball. Starting from total ignorance (f), and by measuring the atom position (g) and direction (h), we may think to know everything about the atom. In particular, by measuring the position quickly again, we are sure to find the atom in the same position as suddenly before. Here comes the big surprise: in the quantum world we can not be sure about this anymore. Indeed when we measured the direction we lost all certainty about the position (h) and if we measure the position we lose all information about the direction (g). Either we perfectly know the position or the direction, we can not know both.

This behaviour is at odds with our intuition, but we have no explanation for it: this is a fact, something that we see and that we have to account for. Why do not we have the same picture for the ball? Actually, something similar is happening for the ball as well, but on large objects the effect is too small to be noticed. That we can reach a condition of total knowledge, in which all the propriety of a system are perfectly predictable, it is an illusion. And this illusion is due to the large size of the objects composing our daily life experiences.

Since the condition of total knowledge is unaccessible, thinking in term of configurations for the atom is misleading. The only thing that we can do is to handle the atom's probability distributions, that are describing our knowledge about the atom and defining the likelihood to observe a certain position or direction. In this regard, quantum physics is a tool (a very sophisticated one) to handle our *a priori* knowledge and our information of reality. And this idea can be indeed extended to science in general. Atoms, particles, fields, equations of motion: all the concepts and elements of the theories in science, are not a representation of something "out there", they are rather the abstract tools that we use to elaborate our knowledge about what we observed in the past and what we are going to observe in the future. Indeed many modern formulations of science are based on the concept of information (some examples in mathematics [13, 14], in thermodynamics and physics [15–17], and in neuroscience [18, 19]).

Translated into the language of quantum physicists, the idea is to interpret the wave function as a description of the *a priori* information that an observer has on the considered system. In other words, the wave function is more similar to a probability distribution than to a configuration of the system. This represents a possible solution to the long-standing debate around the measurement problem in quantum physics [7, 20–23]. The wave function collapse is nothing else then the (Bayesian) update of this probability distribution. A pure state is a state of maximal knowledge, quantum entanglement is a particular class of correlations, and decoherence describes a peculiar form of information losses.

As we have mentioned above: in the physical conditions of our "normal life", the consequences of the Heisenberg uncertainty principle are not apparent. Indeed, even if quantum physics is needed to explain the nature of the most basic elements of our reality (the colour of the sun, the structure of matter, etc.), the specific consequences

of this principle are invisible to our "normal eyes". Nevertheless, the advances in experimental quantum optics allow today to approach the limits of the Heisenberg principle. In this kind of experiments the role of the measurement becomes crucial.

Quantum optics has always been very central in the development of quantum physics. It is indeed by studying the light that the use of a quantum description has been necessary the first time. In order to explain the spectral shape of solar radiation (or more general, of the black body radiation), Max Planck in 1899 suggested that light energy was formed by discrete quantities called *quanta* [24]: the theory of quanta, later renamed as quantum mechanics, was just born. Few years later, this new theory had its first important successes by explaining the photoelectric effect (Einstein, 1905 [25]) and the structure of the hydrogen atom (Born, 1913 [26]).

Since its first stages, quantum physics has revolutionised our understanding of light, matter, and of their interaction. One hundred years later, light-matter interaction is still among the most important fields in which quantum physics is tested and exploited. Indeed, by improving the control of light-matter interaction, it is possible to reach regimes in which quantum physics is crucially at play, and in which we can observe and exploit properties that are otherwise unaccessible. This is precisely the aim of cavity Quantum Electrodynamics (cavity QED) [27]. In simple words, cavity QED studies the physics of one or more atoms interacting with an electromagnetic field that is confined inside an optical cavity. Even if the way to model this physics in terms of two-level systems (for the atoms) and of bosonic modes (for the electromagnetic field) is known since more then fifty years [28–32], it is only in the last decades that the technological advances have permitted to access these systems in a controlled way. The big challenge has been to reduce the effects of dissipation, and then, to reach regimes of increasingly large light-matter coupling [33, 34]. When the interaction strength becomes larger than the dissipation, the system enters the so called *strong coupling regime*. In this regime, the system energy spectrum is resolvable [35], and the relatively long lifetime of atom-cavity correlations allows to perform accurate estimations of the system state [36].

In this audacious exploration of the quantum world, cavity QED has more recently be joined by two relatively new disciplines of solid-state physics: semiconductor cavity QED [37, 38], and superconducting circuit QED [39, 40]. Exploiting the quantized degrees of freedom of a superconductive circuit, it is indeed possible to realise the same physics of cavity QED [41–48]. On a superconducting chip, optical cavities are replaced by transmission line resonators and the artificial two-level atoms are realised by exploiting the nonlinearity of Josephson junctions [49, 50]. The high degree of control in these systems makes these systems very promising candidates as quantum information devices. In semiconductor microcavities [51, 52], the electromagnetic field is confined between two semiconductor mirrors and the role of atoms is played by the electronic transitions in semiconductor nanostructures [53, 54]. It is in that kind of structures, that the so called field of quantum fluids of light was born [55]. In the strong

light-matter coupling regime, intra-cavity photons are mixed to electronic excitations, defining a new kind of quasiparticles, the *polaritons* [29]. It has been proved that the effective interactions between polaritons are strong enough to generate collective many-body phenomena, such as the Bose-Einstein condensation [56], or superfluidity [57].

Another reason why superconducting circuit QED and semiconductor cavity QED are particularly interesting is their suitability to reach the so called *ultrastrong coupling regime*, in which the vacuum Rabi frequency (quantifying light-matter interaction strength) is comparable to the bare transition frequencies of the atom and of the cavity. This regime of intense interaction is attained in circuit QED experiments thanks to the strong confinement of light in transmission lines [58–63], while in semiconductor realisations the interaction with the many electronic transitions can be recast into a very large effective interaction with a single collective transition momentum [64–67].

One of the reason why ultrastrong coupling regime has recently attracted a growing interest, is that in this regime the ground state can contain non-trivial population and correlation of light and matter. Indeed in this regime, it becomes energetically favourable to have photons and light-matter correlations in the ground state. When the number of artificial atoms becomes large, some ultrastrong coupling models even predict the emergence of the so called *superradiant phase transition* [68–72]. According to the particular symmetry of the model, the ground state can be for example a *Schrödinger cat state* of correlated light and matter [73], or it can be a squeezed vacuum [63].

The interest of Schrödinger cat states both for fundamental and for technological developments, is witnessed by the literature [27, 74–77]. Another way to yield this kind of states is through *reservoir engineering*. Indeed, recently it has been possible to engineer the environment with precise tailored symmetries, and to let a system relax to a target, non-trivial steady state [78–85].

Given the possibility to generate these highly nonclassical states, a question arises rather naturally: how can we measure and control them? This important question, finds today a renewed meaning. Indeed, in the past it was only possible to test the ensemble properties of quantum systems. The advances in the protection of quantum systems from decoherence, and in the precision of the measurements, allow today to track the quantum state trajectory even on single shot experiments [86–89]. For this reason quantum measurement and trajectories represent today a key topic for new disciplines such as quantum control and quantum thermodynamics [90–93].

The work reported here is part of this field. This thesis presents original results about: i) measurement protocols to detect exotic quantum optical ground states with photons in the ultrastrong coupling regime; ii) a theory of quantum feedback for the stabilisation of photonic Schrödinger cat states in driven-dissipative resonators.

The manuscript is structured as follows. In Chapter 2 we introduce the paradigmatic models of quantum optics, that we will use along this manuscript. After a

derivation of the electromagnetic field quantization, we introduce the paradigmatic models of light-matter interaction. Chapter 3 presents the theoretical framework that is necessary to include the out-of-equilibrium nature of the considered open quantum system. In particular we derive and present in detail the master equation approach, and discuss its validity in the ultrastrong coupling regime. In Chapter 4, we introduce the basic elements of quantum measurement and trajectories. Starting with a presentation of interpretative framework of quantum mechanics, we derive the stochastic equations of quantum trajectories, and discuss their relation with the master equation approach. In Chapter 5 we present our proposal for a non-destructive measurement of light-matter populations and correlations in the exotic vacua achieved in the ultrastrong coupling regime [94]. Finally, Chapter 6 presents our analysis of quantum trajectories for a resonator with two-photon drive and dissipation [95]. Moreover we present a parity-triggered feedback control protecting photonic Schrödinger cat states against one-photon decoherence [96].

Chapter 2

Paradigmatic models in quantum optics

This chapter is aimed at introducing the reader to the theoretical description of the physical systems investigated in this thesis.

At the heart of our work is *light* and its quantum description. In all the systems that we considered, the electromagnetic field plays the central role. For this reason the chapter begins with a detailed derivation of the quantum description of light (Sec. 2.1).

The second important ingredient of our investigation is *light-matter interaction*. Recent advances in controlling light and matter degrees of freedom have allowed physicists to reach new regimes in which a quantum model of light-matter interaction is required. While in free space photons are mostly independent particles, in some particular realisations it has been possible to enhance significant matter-mediated effective interaction between photons [55]. In Section 2.2.1 we describe the quantization of the electromagnetic field in a dielectric medium, in which the nonlinearities can mediate an effective interaction between hybrid light-matter particles, called polaritons.

The high level of control recently reached in the fields of cavity and circuit Quantum Electrodynamics (QED), allows physicist to realise a variety of quantum models of interacting atoms and photons. Section 2.2.2 provides an introduction to the paradigmatic cavity QED models, and Sec. 2.2.3 discusses their peculiar behaviour when the regime of ultrastrong coupling is attained.

2.1 Quantum description of light

In this section we present the quantization of electromagnetic field, i.e. the formal path from the classical to the quantum description of electrodynamics. The classical frame of electrodynamics is basically defined by the real valued electric and magnetic vector fields governed by Maxwell's equations. It turns out that the electromagnetic field can be decomposed as a sum of independent harmonic oscillators. Furthermore, the harmonic oscillator is a very convenient model to introduce the formal steps of the quantization process. For these reasons, we start this section by reviewing the canonical quantization of an harmonic oscillator (sec 2.1.1). In Sec. 2.1.2 and in Sec. 2.1.3 we introduce the canonical description and the mode decomposition of the

electromagnetic field, and in Sec. 2.1.4 we derive the final quantum description of the electromagnetic field modes.

We point that this section is based on the very comprehensive textbooks in Refs. [97–99] and on the lecture notes in Refs. [100, 101].

2.1.1 The harmonic oscillator

The aim of this section is to introduce, in the simplified framework of an harmonic oscillator, the formal steps of canonical quantization that we will follow in the more complicated situation of the electromagnetic field.

The harmonic oscillator is probably the most used dynamic model in physics. Many physical system, such as the electromagnetic field, can be recast or approximated in terms of harmonic oscillators and, most importantly, it is a solvable model. The dynamics of a classical harmonic oscillator in one dimension is described by the following differential equation for the coordinate x:

$$m\ddot{x} = -kx \tag{2.1}$$

where m is the mass of the system that is experiencing the elastic force $F = -kx$.

This dynamics is alternatively described by the system Lagrangian

$$L(x, \dot{x}) = \frac{m\dot{x}^2}{2} - \frac{kx^2}{2}\,, \tag{2.2}$$

in its generalised coordinate x. The differential Equation (2.1) is easily regained through the Euler-Lagrange equation

$$\frac{\mathrm{d}}{\mathrm{d}t}\left(\frac{\partial L}{\partial \dot{x}}\right) - \frac{\partial L}{\partial x} = 0\,. \tag{2.3}$$

The conjugate momentum p and the Hamiltonian H are determined from this Lagrangian:

$$p = \frac{\partial L}{\partial \dot{x}} = m\dot{x}\,, \tag{2.4}$$

$$H(x, p) = p\dot{x} - L = \frac{p^2}{2m} + \frac{kx^2}{2} = \frac{p^2}{2m} + \frac{m}{2}\omega^2 x^2\,, \tag{2.5}$$

where $\omega = \sqrt{k/m}$ is the angular frequency of the oscillator.

To quantize the classical Hamiltonian, the first step is to formally substitute x and p in Eq. (2.5) with some operators $\hat{x}$ and $\hat{p}$ on the system Hilbert space, playing the role of their quantum counterparts. The expression Hamiltonian is therefore:

$$\hat{H} = \frac{\hat{p}^2}{2m} + \frac{m}{2}\omega^2\hat{x}^2\,. \tag{2.6}$$

The key point is now to determine $\hat{x}$ and $\hat{p}$. The operator $\hat{x}$ and $\hat{p}$ are now Hermitian operators acting on the same Hilbert space. One can, in particular, express one in terms of the other. Indeed, from the Heisenberg uncertainty principle, one can show that $[\hat{x}, \hat{p}] = i\hbar$ [102–104].

In a more rigorous and general way this was postulated by Born [105] and later generalised by Dirac [98, 106, 107]: the commutator of two quantum observables $\hat{o}_1$ and $\hat{o}_2$ is related to the Poisson bracket of their classical counterparts via:

$$[\hat{o}_1, \hat{o}_2] = i\hbar \{o_1, o_2\}\,, \tag{2.7}$$

where $\{o_1, o_2\}$ is the Poisson bracket between two classical observables.[1] In the particular case in which o_1 and o_2 are the conjugate generalised coordinate and momentum (like x and p) the relation (2.7) reduces to

$$[\hat{o}_1, \hat{o}_2] = i\hbar\,. \tag{2.8}$$

Once that the quantum description of the harmonic oscillator is settled, we are interested in diagonalising its Hamiltonian, since its eigenvalues and eigenvector allows to solve the system dynamics. The common way to do so is by recasting the Hamiltonian through the annihilation and creation operators, respectively

$$\hat{a} \overset{\text{def}}{=} \sqrt{\frac{m\omega}{2\hbar}}\left(\hat{x} + \frac{i}{m\omega}\hat{p}\right), \quad \hat{a}^\dagger \overset{\text{def}}{=} \sqrt{\frac{m\omega}{2\hbar}}\left(\hat{x} - \frac{i}{m\omega}\hat{p}\right). \tag{2.9}$$

Employing the commutation relation of $\hat{x}$ and $\hat{p}$ it is straightforward to prove that

$$[\hat{a}, \hat{a}^\dagger] = 1\,. \tag{2.10}$$

Inverting the definitions in Eqs. (2.9), one attains:

$$\hat{x} = \sqrt{\frac{\hbar}{2m\omega}}(\hat{a}^\dagger + \hat{a})\,, \quad \hat{p} = i\sqrt{\frac{\hbar m\omega}{2}}(\hat{a}^\dagger - \hat{a})\,. \tag{2.11}$$

These expressions can be inserted in the Hamiltonian Equation (2.6), obtaining the following expression:

$$\hat{H} = \hbar\omega\left(\hat{a}^\dagger\hat{a} + \frac{1}{2}\right) = \hbar\omega\left(\hat{N} + \frac{1}{2}\right), \tag{2.12}$$

[1] In the canonical coordinates q_i and p_i, the Poisson bracket between two observables $o_1(q_i, p_i, t)$ and $o_2(q_i, p_i, t)$ is defined as

$$\{o_1, o_2\} = \sum_{i=1}^{N}\left(\frac{\partial o_1}{\partial q_i}\frac{\partial o_2}{\partial p_i} - \frac{\partial o_1}{\partial p_i}\frac{\partial o_2}{\partial q_i}\right).$$

It follows that $\{q_i, p_j\} = \delta_{ij}$.

where $\hat{N} \overset{\text{def}}{=} \hat{a}^\dagger \hat{a}$ is called the number operator. From the commutator of $\hat{a}$ and $\hat{a}^\dagger$ one can show that

$$[\hat{N}, \hat{a}^\dagger] = \hat{a}^\dagger \quad \text{and} \quad [\hat{N}, \hat{a}] = -\hat{a}\,. \tag{2.13}$$

Using this commutation relation it can be proved that the spectrum of $\hat{N}$ is given by the positive natural numbers n, and that $\hat{a}$ and $\hat{a}^\dagger$ allow to climb down and up the corresponding eigenstates $|n\rangle$:

$$\hat{N}\,|n\rangle \overset{\text{def}}{=} n\,|n\rangle \;; \quad \hat{a}^\dagger\,|n\rangle = \sqrt{n+1}\,|n+1\rangle \;; \quad \hat{a}\,|n\rangle = \sqrt{n}\,|n-1\rangle \;. \tag{2.14}$$

The observable $\hat{N}$ represents the number of energy quanta contained in the system. In this regard $\hat{a}$ and $\hat{a}^\dagger$ are called the annihilation and creation operators, coherently with the relations (2.14).

2.1.2 Canonical quantization of the electromagnetic field

In the previous section we saw that the main ingredients to define a quantum system are the Hamiltonian and the commutation relations between the operators intervening in its expression. We also saw that the commutator between two canonical conjugate variables is postulated equal to $i\hbar$. In the case of the harmonic oscillator, it was easy to recognise the two canonical conjugate variables are x and p. However for the electromagnetic field this is not so direct. That is the reason why in this section we will take the time to review the Lagrangian description of the electromagnetic field, and to retrace the steps of its canonical quantization.

The dynamics of the electromagnetic field in vacuum and absence of charges is encoded by the four Maxwell's equations:

$$\begin{aligned} \nabla \cdot \boldsymbol{E} &= 0\,, \\ \nabla \cdot \boldsymbol{B} &= 0\,, \\ \nabla \times \boldsymbol{E} &= -\frac{\partial \boldsymbol{B}}{\partial t}\,, \\ \nabla \times \boldsymbol{B} &= \frac{1}{c^2}\frac{\partial \boldsymbol{E}}{\partial t}\,. \end{aligned} \tag{2.15}$$

The electric and magnetic fields $\boldsymbol{E}$ and $\boldsymbol{B}$ are typically described through the electric scalar potential ϕ and the magnetic vector potential $\boldsymbol{A}$ as

$$\boldsymbol{E} = -\nabla\phi - \frac{\partial \boldsymbol{A}}{\partial t} \quad \text{and} \quad \boldsymbol{B} = \nabla \times \boldsymbol{A}\,. \tag{2.16}$$

These two potentials define the so called four-potential $A_\mu \overset{\text{def}}{=} (\phi/c, -\boldsymbol{A})$, whose components are typically chosen as generalised coordinates in the Lagrangian description of electrodynamics. They completely define the electromagnetic field and, contrary to the 6 components of the electric and magnetic fields ($\boldsymbol{E}$ and $\boldsymbol{B}$) that are constrained

by the Maxwell's equations, the components of the four-potential only have to respect a minimal set of constraints that depend on the chosen gauge.

In the covariant formulation of electrodynamics, the Lagrangian density in vacuum and absence of external charges reads (we use the Einstein notation for indices):

$$\mathcal{L}(A_\mu, \partial_t A_\mu) = -\frac{1}{4\mu_0} F^{\mu\nu} F_{\mu\nu} \,, \tag{2.17}$$

where the electromagnetic tensor $F_{\mu\nu}$ is a covariant antisymmetric tensor defined as:

$$F_{\mu\nu} \stackrel{\text{def}}{=} \partial_\mu A_\nu - \partial_\nu A_\mu \quad \text{and} \quad F^{\mu\nu} = \eta^{\mu\alpha} F_{\alpha\beta} \eta^{\beta\nu} \,. \tag{2.18}$$

Here $\eta^{\mu\nu}$ is the Minkowsky metric tensor and the time-space derivatives ∂_μ are defined as:

$$x^\mu = (ct, \boldsymbol{x}) = (ct, x, y, z) \quad \text{and} \quad \partial_\mu = \frac{\partial}{\partial x^\mu} = \left(\frac{1}{c}\frac{\partial}{\partial t}, \nabla \right) \,.$$

Note that the potentials ϕ and $\boldsymbol{A}$ are unique only after a gauge choice. The most comfortable choice for the quantization of the electromagnetic field is the Coulomb gauge, defined by the condition

$$\nabla \cdot \boldsymbol{A} = 0 \,. \tag{2.19}$$

In this gauge and in absence of charges, ϕ can be fixed to an arbitrary constant and Eq. (2.16) simplifies to

$$\boldsymbol{E} = -\frac{\partial \boldsymbol{A}}{\partial t} \quad \text{and} \quad \boldsymbol{B} = \nabla \times \boldsymbol{A} \,. \tag{2.20}$$

Through these relations we can now express the tensor $F_{\mu\nu}$ as a function of $\boldsymbol{E}$ and $\boldsymbol{B}$:

$$F_{\mu\nu} = \begin{pmatrix} 0 & E_x/c & E_y/c & E_z/c \\ -E_x/c & 0 & -B_z & B_y \\ -E_y/c & B_z & 0 & -B_x \\ -E_z/c & -B_y & B_x & 0 \end{pmatrix} \tag{2.21}$$

and

$$F^{\mu\nu} = \begin{pmatrix} 0 & -E_x/c & -E_y/c & -E_z/c \\ E_x/c & 0 & -B_z & B_y \\ E_y/c & B_z & 0 & -B_x \\ E_z/c & -B_y & B_x & 0 \end{pmatrix} \,. \tag{2.22}$$

The validity of the Lagrangian density (2.17) is proved by its invariance with respect to Lorentz transformations and by the fact that it reproduces the Maxwell's equations through the use of the Euler-Lagrange equations:

$$\partial_\nu \left[\frac{\partial \mathcal{L}}{\partial(\partial_\nu A_\mu)} \right] - \frac{\partial \mathcal{L}}{\partial A_\mu} = 0 \,. \tag{2.23}$$

With the target of defining the Hamiltonian and the commutators, the first thing to do is to identify the canonical coordinates, i.e. to determine the conjugate momenta Π^μ of the coordinate A_μ. They can be computed from the Lagrangian density in Eq. (2.17):

$$\Pi^\mu \stackrel{\text{def}}{=} \frac{\partial \mathcal{L}}{\partial(\partial_t A_\mu)} = \frac{1}{c}\frac{\partial \mathcal{L}}{\partial(\partial_0 A_\mu)} \,. \tag{2.24}$$

Note that

$$\begin{aligned} \frac{\partial(F^{\alpha\beta}F_{\alpha\beta})}{\partial(\partial_\nu A_\mu)} &= 2F^{\alpha\beta}\frac{\partial F_{\alpha\beta}}{\partial(\partial_\nu A_\mu)} \\ &= 2F^{\alpha\beta}\left(\frac{\partial(\partial_\alpha A_\beta)}{\partial(\partial_\nu A_\mu)} - \frac{\partial(\partial_\beta A_\alpha)}{\partial(\partial_\nu A_\mu)}\right) \\ &= 2F^{\alpha\beta}(\delta^\nu_\alpha\delta^\mu_\beta - \delta^\nu_\beta\delta^\mu_\alpha) \\ &= 2F^{\nu\mu} - 2F^{\mu\nu} \\ &= 4F^{\nu\mu} \end{aligned} \tag{2.25}$$

Using equations (2.25), (2.21) and (2.22) it is thus possible to show that:

$$\Pi^\mu = -\frac{1}{c\mu_0}F^{0\mu} = \epsilon_0(0, \boldsymbol{E}) \,. \tag{2.26}$$

The fact the $\Pi_0 = 0$ is not unimportant: it means that $A_0 \stackrel{\text{def}}{=} \phi/c$ is not an independent field. Indeed as we already reminded above, in the Coulomb gauge, the absence of charges implies that the electric scalar potential ϕ is an arbitrary constant, and it can be fixed to zero.

Using Eq. (2.8) and reminding that A_μ, Π^μ and E_i are space-dependent fields, one might be tempted to introduce the following canonical commutation relations for the quantum observables of the problem:

$$\begin{aligned} &\left[\hat{A}_\mu(\boldsymbol{r}), \hat{\Pi}^\nu(\boldsymbol{r}')\right] \stackrel{?}{=} i\hbar\,\delta_{\mu\nu}\delta^3(\boldsymbol{r}-\boldsymbol{r}') \,, \\ \text{i.e.} \quad &\left[\hat{A}_i(\boldsymbol{r}), \hat{E}_j(\boldsymbol{r}')\right] \stackrel{?}{=} -\frac{i\hbar}{\epsilon_0}\,\delta_{ij}\delta^3(\boldsymbol{r}-\boldsymbol{r}') \,. \end{aligned} \tag{2.27}$$

Unfortunately these relations are wrong! The Coulomb gauge imposes an additional constraint to the electromagnetic field. Equation (2.19) implies that not all the components of $\boldsymbol{A}$ and $\boldsymbol{E}$ are independent and for this reason the correct commutation relations for the corresponding quantum operator are:

$$\begin{aligned} &\left[\hat{A}_\mu(\boldsymbol{r}), \hat{\Pi}^\nu(\boldsymbol{r}')\right] = i\hbar\,\delta^{(tr)}_{\mu\nu}(\boldsymbol{r}-\boldsymbol{r}') \,, \\ \text{i.e.} \quad &\left[\hat{A}_i(\boldsymbol{r}), \hat{E}_j(\boldsymbol{r}')\right] = -\frac{i\hbar}{\epsilon_0}\,\delta^{(tr)}_{ij}(\boldsymbol{r}-\boldsymbol{r}') \,, \end{aligned} \tag{2.28}$$

where we have introduced the so-called "transverse delta function", which has the same effect as the usual delta function on transverse fields and which is defined as

$$\delta_{ij}^{(tr)}(\boldsymbol{r}) = \int \frac{\mathrm{d}^3k}{2\pi} e^{i\boldsymbol{k}\cdot\boldsymbol{r}} \left(\delta_{ij} - \frac{k_i k_j}{\boldsymbol{k}^2}\right) . \tag{2.29}$$

Note that here and above Latin letter indexes refer to the components of 3-dimensional space fields such as the vector potential $\boldsymbol{A}$ and the electric field $\boldsymbol{E}$, while the Greek letter indexes refer to covariant four-vectors or matrices such as A_μ or $F^{\nu\mu}$. The function $\delta_{\mu\nu}^{(tr)}(\boldsymbol{r}-\boldsymbol{r}')$ that we use in the first of Eqs. (2.28) is only defined for $\mu,\nu \neq 0$. The complete justification for the use of the traverse delta function and the complete derivation of these commutation relations go beyond the aim of this section. The target here is to provide an idea of the formal steps to follow for a rigorous quantization of the electromagnetic field, according to the postulates of quantum mechanics. For more details on the traverse delta function and on the derivation of this commutation relations we address the reader to the paragraph 7.7 of Ref. [97] in which one can find a very complete description of this derivation.

The next step toward the quantization of the electromagnetic field is to determine its Hamiltonian. The Hamiltonian density is defined through the Legendre transformation

$$\mathcal{H} \overset{\text{def}}{=} \Pi^\mu(\partial_t A_\mu) - \mathcal{L} . \tag{2.30}$$

Using equations (2.26), (2.21) and (2.22) one can show that

$$\begin{aligned}
\mathcal{H}(A_\mu, \Pi^\mu) &= -\frac{1}{\mu_0} F^{0\mu}\partial_0 A_\mu + \frac{1}{4\mu_0} F^{\mu\nu}F_{\mu\nu} \\
&= -\frac{1}{\mu_0} F^{0\mu}(F_{0\mu} + \partial_\mu A_0) + \frac{1}{4\mu_0}\left(2\boldsymbol{B}^2 - 2\frac{\boldsymbol{E}^2}{c^2}\right) \\
&= -\frac{1}{\mu_0} F^{0\mu}F_{0\mu} + \frac{1}{2\mu_0}\left(\boldsymbol{B}^2 - \frac{\boldsymbol{E}^2}{c^2}\right) \\
&= \frac{1}{\mu_0}\frac{\boldsymbol{E}^2}{c^2} + \frac{1}{2\mu_0}\left(\boldsymbol{B}^2 - \frac{\boldsymbol{E}^2}{c^2}\right) \\
&= \frac{1}{2}\left(\frac{\boldsymbol{B}^2}{\mu_0} + \epsilon_0\boldsymbol{E}^2\right)
\end{aligned} \tag{2.31}$$

where we used the fact that, since A_0 is fixed to zero then also $\partial_\mu A_0 = 0$. This expression coherently corresponds to the usual formula of the energy density for the electric and magnetic field. Using Eq. (2.20), we can now expres the Hamiltonian as a function of the only field $\boldsymbol{A}$, or as a function of its canonical conjugate fields $\boldsymbol{A}$ and $\boldsymbol{\Pi}$:

$$\begin{aligned}
H(A_\mu, \Pi^\mu) \overset{\text{def}}{=} \int \mathrm{d}^3r\, \mathcal{H} &= \frac{\epsilon_0}{2}\int \mathrm{d}^3r \left[\left(\frac{\partial \boldsymbol{A}}{\partial t}\right)^2 + c^2(\nabla\times\boldsymbol{A})^2\right] \\
&= \frac{1}{2\epsilon_0}\int \mathrm{d}^3r \left[\boldsymbol{\Pi}^2 + \frac{1}{\mu_0}(\nabla\times\boldsymbol{A})^2\right]
\end{aligned} \tag{2.32}$$

Here the parallelism with the harmonic oscillator is nearly settled. In Eq. (2.5) we have a quadratic form of the Lagrangian generalised coordinates $\boldsymbol{A}$ and of its conjugate momentum $\boldsymbol{\Pi} \stackrel{\text{def}}{=} \epsilon_0 \boldsymbol{E}$, that commute according to the commutation relation in Eq. (2.28). It can be shown that this Hamiltonian can be diagonalised in a structure very similar to that of the harmonic oscillator. In order to achieve this diagonalisation we first need to introduce the mode decomposition of the electromagnetic field. This is the topic of the next section.

2.1.3 Mode decomposition

In this section we will show that the electromagnetic field can be expressed as a linear superposition of wave modes. This will suggest the right variable change leading to the diagonalisation of the electromagnetic field Hamiltonian. First of all we recall the 3rd and 4th Maxwell's equation in absence of charges:

$$\nabla \times \boldsymbol{E} = -\frac{\partial \boldsymbol{B}}{\partial t} \quad \text{and} \quad \nabla \times \boldsymbol{B} = \frac{1}{c^2}\frac{\partial \boldsymbol{E}}{\partial t}\,. \tag{2.33}$$

From this last equation and replacing the fields $\boldsymbol{E}$ and $\boldsymbol{B}$ with the expressions given by equations (2.20) one finds

$$\nabla \times (\nabla \times \boldsymbol{A}) = -\frac{1}{c^2}\frac{\partial^2 \boldsymbol{A}}{\partial t^2} \tag{2.34}$$

Given that $\nabla \times (\nabla \times \boldsymbol{A}) = \nabla(\nabla \cdot \boldsymbol{A}) - \nabla^2 \boldsymbol{A}$ and that $\nabla \cdot \boldsymbol{A} = 0$ (see Eq. (2.19)), it is straightforward to show that the vector potential $\boldsymbol{A}$ evolves according to the following wave equation:

$$\frac{1}{c^2}\frac{\partial^2 \boldsymbol{A}}{\partial t^2} - \nabla^2 \boldsymbol{A} = 0\,. \tag{2.35}$$

The solution of this differential equation depends on the initial condition and on the boundary conditions. Without loss of generality, we will consider here the simplest situation in which the field is confined in a cubic box of size L and satisfies periodic boundary conditions. Under these conditions the electromagnetic field can be expressed as a sum of plane-wave modes:

$$\boldsymbol{A}(\boldsymbol{r}, t) \stackrel{\text{def}}{=} \sum_{\boldsymbol{k},\boldsymbol{\epsilon}} \sqrt{\frac{\hbar}{2\epsilon_0 L^3 \omega_k}} \left[\, \alpha_{\boldsymbol{k},\boldsymbol{\epsilon}}\, \boldsymbol{\epsilon}\, e^{i\boldsymbol{k}\cdot\boldsymbol{r} - \omega_k t} + \alpha^*_{\boldsymbol{k},\boldsymbol{\epsilon}}\, \boldsymbol{\epsilon}^* e^{-i\boldsymbol{k}\cdot\boldsymbol{r} + \omega_k t} \,\right]\,, \tag{2.36}$$

where the sum runs over the possible wave vectors $\boldsymbol{k}$ and polarisation complex unit vectors $\boldsymbol{\epsilon}$. In order to fulfill the wave Equation (2.34), the wave frequency ω_k is a function of the wave vector: $\omega_k = c|\boldsymbol{k}|$. According to the box confinement and boundary condition the allowed wave vectors are $\boldsymbol{k} = 2\pi\boldsymbol{n}/L$, where $\boldsymbol{n}$ is a set of three integers $\boldsymbol{n} = (n_x, n_y, n_z)$. For every wave vector we have two possible orthogonal

unit vectors $\boldsymbol{\epsilon}$, they are orthogonal and they lay on the plane orthogonal to the wave vectors, such $\boldsymbol{\epsilon} \cdot \boldsymbol{k} = 0$.

Every couple of $\boldsymbol{k}$ and $\boldsymbol{\epsilon}$ defines a wave mode that evolves independently to the others at the frequency ω_k. The complex coefficients $\alpha_{(\boldsymbol{k},\boldsymbol{\epsilon})}$ define the amplitude of the mode and depend on the initial and boundary conditions, the field $\boldsymbol{A}(\boldsymbol{r}, t)$ is completely defined by these coefficients.

2.1.4 Quantum description of the electromagnetic field

The mode decomposition given by Eq. (2.36) suggests the change of variables that can diagonalise the electromagnetic Hamiltonian. Let us recast the quantum field operator $\hat{\boldsymbol{A}}(\boldsymbol{r})$ of the vector potential field as:

$$\hat{\boldsymbol{A}}(\boldsymbol{r}) \stackrel{\text{def}}{=} \sum_{\boldsymbol{k},\boldsymbol{\epsilon}} \sqrt{\frac{\hbar}{2\epsilon_0 L^3 \omega_k}} \left[\hat{a}_{\boldsymbol{k},\boldsymbol{\epsilon}}\, \boldsymbol{\epsilon}\, e^{i\boldsymbol{k}\cdot\boldsymbol{r}} + \hat{a}^\dagger_{\boldsymbol{k},\boldsymbol{\epsilon}}\, \boldsymbol{\epsilon}^* e^{-i\boldsymbol{k}\cdot\boldsymbol{r}} \right] . \tag{2.37}$$

Using Eq. (2.36) and Eqs. (2.20) the mode decomposition of quantum field operators $\hat{\boldsymbol{\Pi}}(\boldsymbol{r})$, $\hat{\boldsymbol{E}}(\boldsymbol{r})$ and $\hat{\boldsymbol{B}}(\boldsymbol{r})$ reads

$$\hat{\boldsymbol{\Pi}}(\boldsymbol{r}) = -\epsilon_0 \hat{\boldsymbol{E}}(\boldsymbol{r}) = -i \sum_{\boldsymbol{k},\boldsymbol{\epsilon}} \sqrt{\frac{\hbar\, \omega_k \epsilon_0}{2L^3}} \left[\hat{a}_{\boldsymbol{k},\boldsymbol{\epsilon}}\, \boldsymbol{\epsilon}\, e^{i\boldsymbol{k}\cdot\boldsymbol{r}} - \hat{a}^\dagger_{\boldsymbol{k},\boldsymbol{\epsilon}}\, \boldsymbol{\epsilon}^* e^{-i\boldsymbol{k}\cdot\boldsymbol{r}} \right] \tag{2.38a}$$

$$\hat{\boldsymbol{B}}(\boldsymbol{r}) = i \sum_{\boldsymbol{k},\boldsymbol{\epsilon}} \sqrt{\frac{\hbar}{2\epsilon_0 L^3 \omega_k}} \left[\hat{a}_{\boldsymbol{k},\boldsymbol{\epsilon}}\, (\boldsymbol{k} \times \boldsymbol{\epsilon})\, e^{i\boldsymbol{k}\cdot\boldsymbol{r}} - \hat{a}^\dagger_{\boldsymbol{k},\boldsymbol{\epsilon}}\, (\boldsymbol{k} \times \boldsymbol{\epsilon}^*) e^{-i\boldsymbol{k}\cdot\boldsymbol{r}} \right] . \tag{2.38b}$$

By using these expressions for the operators of the electromagnetic field we can rewrite the Hamiltonian (Eqs. (2.31) and (2.32)) in the following diagonalised form:

$$\hat{H} = \sum_{\boldsymbol{k},\boldsymbol{\epsilon}} \hbar\, \omega_k \left(\hat{a}^\dagger_{\boldsymbol{k},\boldsymbol{\epsilon}} \hat{a}_{\boldsymbol{k},\boldsymbol{\epsilon}} + \frac{\hat{\mathbb{1}}}{2} \right) = \sum_{\boldsymbol{k},\boldsymbol{\epsilon}} \hbar\, \omega_k \left(\hat{N}_{\boldsymbol{k},\boldsymbol{\epsilon}} + \frac{\hat{\mathbb{1}}}{2} \right) , \tag{2.39}$$

where we have defined the mode number operator $N_{\boldsymbol{k},\boldsymbol{\epsilon}} \stackrel{\text{def}}{=} \hat{a}^\dagger_{\boldsymbol{k},\boldsymbol{\epsilon}} \hat{a}_{\boldsymbol{k},\boldsymbol{\epsilon}}$, in perfect analogy with what we did for the harmonic oscillator.

The last ingredient to define our quantum system are the commutation relations. One can prove that the canonical commutation relations postulated for the conjugate variables of the electromagnetic field, equations (2.28), imply that the mode operators $\hat{a}_{\boldsymbol{k},\boldsymbol{\epsilon}}$ and $\hat{a}^\dagger_{\boldsymbol{k},\boldsymbol{\epsilon}}$ respect the following commutation relations:

$$[\hat{a}_{\boldsymbol{k},\boldsymbol{\epsilon}}, \hat{a}^\dagger_{\boldsymbol{k}',\boldsymbol{\epsilon}'}] = \delta_{kk'} \delta_{\epsilon\epsilon'} . \tag{2.40}$$

The proof of this equivalence is a simple calculation: see Section 7.7 of Ref. [97] or Chapter 3 of Ref. [99] for more details.

As a consequence of the commutator Eq. (2.40)

$$[\hat{N}_{\boldsymbol{k},\boldsymbol{\epsilon}}, \hat{a}^\dagger_{\boldsymbol{k},\boldsymbol{\epsilon}}] = \hat{a}^\dagger_{\boldsymbol{k},\boldsymbol{\epsilon}}\,, \quad [\hat{N}_{\boldsymbol{k},\boldsymbol{\epsilon}}, \hat{a}_{\boldsymbol{k},\boldsymbol{\epsilon}}] = -\hat{a}_{\boldsymbol{k},\boldsymbol{\epsilon}}\,, \tag{2.41}$$

and the action of $\hat{a}_{\boldsymbol{k},\boldsymbol{\epsilon}}$ and $\hat{a}^\dagger_{\boldsymbol{k},\boldsymbol{\epsilon}}$ on the eigenstates of $\hat{N}_{\boldsymbol{k},\boldsymbol{\epsilon}}$ are given by the following equations:

$$\begin{aligned} &\hat{N}_{\boldsymbol{k},\boldsymbol{\epsilon}} |n_{\boldsymbol{k},\boldsymbol{\epsilon}}\rangle \stackrel{\text{def}}{=} n_{\boldsymbol{k},\boldsymbol{\epsilon}} |n_{\boldsymbol{k},\boldsymbol{\epsilon}}\rangle\,, \\ &\hat{a}^\dagger_{\boldsymbol{k},\boldsymbol{\epsilon}} |n_{\boldsymbol{k},\boldsymbol{\epsilon}}\rangle = \sqrt{n_{\boldsymbol{k},\boldsymbol{\epsilon}}+1}\, |n_{\boldsymbol{k},\boldsymbol{\epsilon}}+1\rangle\,, \quad \hat{a}_{\boldsymbol{k},\boldsymbol{\epsilon}} |n_{\boldsymbol{k},\boldsymbol{\epsilon}}\rangle = \sqrt{n_{\boldsymbol{k},\boldsymbol{\epsilon}}}\, |n_{\boldsymbol{k},\boldsymbol{\epsilon}}-1\rangle\,. \end{aligned} \tag{2.42}$$

The eigenvalues of $\hat{N}_{\boldsymbol{k},\boldsymbol{\epsilon}}$ are the positive integers and its eigenstates are the so called Fock states $|n_{\boldsymbol{k},\boldsymbol{\epsilon}}\rangle$. This observable quantifies the number of quanta in the considered mode of the electromagnetic field. These quanta are called photons, and $\hat{a}_{\boldsymbol{k},\boldsymbol{\epsilon}}$, $\hat{a}^\dagger_{\boldsymbol{k},\boldsymbol{\epsilon}}$ are the photon annihilation and creation operators,

$$\hat{a}_{\boldsymbol{k},\boldsymbol{\epsilon}} = \sqrt{\frac{\epsilon_0}{2\hbar L^3}} \int \mathrm{d}^3 r\, e^{-i\boldsymbol{k}\cdot\boldsymbol{r}} \boldsymbol{\epsilon} \left[\sqrt{\omega_k}\, \hat{\boldsymbol{A}}(\boldsymbol{r}) - \frac{i}{\sqrt{\omega_k}} \hat{\boldsymbol{E}}(\boldsymbol{r}) \right] \tag{2.43}$$

Troughout this thesis we will study the electromagnetic field confined inside optical cavities. The fact of confining the light in a small space (combined with the very good quality of the confining mirrors) results in a large frequency spacing. This allows to discern the different modes and most of the times it is possible to work in a condition in which only one cavity mode enters in the field dynamics. Using this assumption the quantum description take the very simplified form

$$\hat{H}_c = \hbar\, \omega_c\, \hat{a}^\dagger \hat{a} \qquad \text{and} \qquad [\hat{a}, \hat{a}^\dagger] = \hat{\mathbb{1}}\,, \tag{2.44}$$

where we introduced the frequency ω_c of the relevant cavity mode and where we fixed to zero the energy of the vacuum state. This Hamiltonian is the first brick of all the systems that we will consider along this manuscript.

2.2 Light-matter interaction

In this section we will introduce some important models of light-matter interaction. In Section 2.2.1 we derive the Hamiltonian of the effective photon-photon interaction that is mediated by a generic dielectric medium. Section 2.2.2 provides an introduction to the most important Hamiltonians modelling the interaction of atoms with the cavity electromagnetic field. Finally, Sec. 2.2.3 introduces to the fundamental peculiarities of cavity (circuit) QED in the regime of the ultrastrong coupling.

2.2.1 Interacting photons

Even if photon-photon interactions have been predicted to occur even in vacuum via virtual excitation of electron-positron pairs [108], the cross section of this process is too

small to play any significant role in realistic optical systems. For this reason photons in vacuum are typically considered independent. However, an effective interaction between photons can arise as mediated by interaction of light with matter. The most simple situation in which light-matter interaction happens is in the presence of a dielectric medium.

The effect of the electric field on a dielectric medium is quantified by polarisation $\boldsymbol{P}$, that is the dipole momentum created in the medium per unit volume. When the field is weak the response of the medium can be assumed to be linear, i.e.

$$P_i = \epsilon_0 \chi^{(1)}_{ij} E_j \,, \tag{2.45}$$

where $\chi^{(1)}_{ij}$ is the linear susceptibility tensor of the medium (repeated indexes are summed). If the electric field is strong enough, then the linear response is not sufficient anymore to describe the response of the dialectic medium, and nonlinear susceptibility must be considered:

$$P_i = \epsilon_0 \left[\chi^{(1)}_{ij} E_j + \chi^{(2)}_{ijk} E_j E_k + \chi^{(3)}_{ijkl} E_j E_k E_l + \dots \right] . \tag{2.46}$$

Here the susceptibility tensors $\boldsymbol{\chi}^{(n)}$ define the expansion of the response function.

In absence of external charges or currents, the electromagnetic field is governed by the following Maxwell's equations:

$$\begin{aligned} \nabla \cdot \boldsymbol{D} &= 0 \,, \\ \nabla \cdot \boldsymbol{B} &= 0 \,, \\ \nabla \times \boldsymbol{E} &= -\frac{\partial \boldsymbol{B}}{\partial t} \,, \\ \nabla \times \boldsymbol{B} &= \mu_0 \frac{\partial \boldsymbol{D}}{\partial t} \,, \end{aligned} \tag{2.47}$$

where $\boldsymbol{D} = \epsilon_0 \boldsymbol{E} + \boldsymbol{P}$ is the displacement vector. Very similarly to what we did in the previous section, these fields and dynamics can be translated to the quantum description through the canonical quantization. We will only consider here the most simple case in which the medium response is homogeneous and non-dispersive, i.e. the tensors $\boldsymbol{\chi}^{(n)}$ do not depend on the space position and on the field frequency.

Under these assumptions an appropriate Lagrangian density is

$$\begin{aligned} \mathcal{L}(A_\mu, \partial_t A_\mu) = \frac{\epsilon_0}{2} \left(\boldsymbol{E}^2 - c^2 \boldsymbol{B} \right) \\ + \epsilon_0 \left[\frac{1}{2} \chi^{(1)}_{ij} E_i E_j + \frac{1}{3} \chi^{(2)}_{ijk} E_i E_j E_k + \frac{1}{4} \chi^{(3)}_{ijkl} E_i E_j E_k E_l + \dots \right] , \end{aligned} \tag{2.48}$$

that can then be recast in the generalised coordinates $A_\mu \stackrel{\text{def}}{=} (\phi/c, -\boldsymbol{A})$, by substituting $\boldsymbol{E}$ and $\boldsymbol{B}$ with their expression as a function of the potentials $\boldsymbol{A}$ and $A_0 = \phi/c$:

$$\boldsymbol{E} = -\frac{\partial \boldsymbol{A}}{\partial t} - c \nabla A_0 \quad \text{and} \quad \boldsymbol{B} = \nabla \times \boldsymbol{A} \,. \tag{2.49}$$

This Lagrangian density reproduces Maxwell's Equation (2.47) through the Euler-Lagrange equations and it allows to define the conjugate momenta of A_μ:

$$\Pi^\mu \overset{\text{def}}{=} \frac{\partial \mathcal{L}}{\partial(\partial_t A_\mu)} = (0, \boldsymbol{D}) \,. \tag{2.50}$$

Once again the momentum Π_0 is zero, meaning that A_0 is not an independent field. On the other hand, contrary to the case of vacuum, we can not fix A_0 to zero, see Ref. [109] for more details.

The Hamiltonian can then be defined using the Legendre transformation in Eq. (2.30):

$$\begin{aligned} H(A_\mu, \Pi^\mu) = &\int \mathrm{d}^3 r \, \frac{\epsilon_0}{2} \left(\boldsymbol{E}^2 + c^2 \boldsymbol{B}^2 \right) \\ &+ \int \mathrm{d}^3 r \epsilon_0 \left[\frac{1}{2} \chi^{(1)}_{ij} E_i E_j + \frac{2}{3} \chi^{(2)}_{ijk} E_i E_j E_k + \frac{3}{4} \chi^{(3)}_{ijkl} E_i E_j E_k E_l + \dots \right] \\ &+ \int \mathrm{d}^3 r \, \boldsymbol{D} \cdot \nabla A_0 \,. \end{aligned} \tag{2.51}$$

Integrating by parts and using the fact that $\nabla \cdot \boldsymbol{D} = 0$ allows to eliminate the last term. Since $\boldsymbol{E}$ is no longer the canonical momentum, it is useful to express the Hamiltonian as a function of $\boldsymbol{D}$:

$$\begin{aligned} H(A_\mu, \Pi^\mu) = &\int \mathrm{d}^3 r \frac{1}{2\mu_0} \left(\nabla \times \boldsymbol{A} \right)^2 \\ &+ \int \mathrm{d}^3 r \left[\frac{1}{2} \beta^{(1)}_{ij} D_i D_j + \frac{1}{3} \beta^{(2)}_{ijk} D_i D_j D_k + \frac{1}{4} \beta^{(3)}_{ijkl} D_i D_j D_k D_l + \dots \right] , \end{aligned} \tag{2.52}$$

where we introduced the tensors $\boldsymbol{\beta}^{(n)}$ allowing to express $\boldsymbol{E}$ as a function of $\boldsymbol{D}$,

$$\begin{aligned} \boldsymbol{\beta}^{(1)} &= \left[\epsilon_0 \left(\mathbf{1} + \boldsymbol{\chi}^{(1)} \right) \right]^{-1} \\ \beta^{(2)}_{ijk} &= -\epsilon_0 \, \beta^{(1)}_{il} \beta^{(1)}_{jm} \beta^{(1)}_{kn} \chi^{(2)}_{lmn} \\ \beta^{(3)}_{ijkl} &= -\epsilon_0 \, \beta^{(1)}_{im} \beta^{(1)}_{jn} \beta^{(1)}_{kp} \beta^{(1)}_{lq} \chi^{(3)}_{mnpq} \,. \end{aligned} \tag{2.53}$$

We suggest again the Ref. [109] for more details on these last expression.

Now we are ready to quantize these fields, first of all we introduce the canonical commutation relation:

$$\begin{aligned} \left[\hat{A}_\mu(\boldsymbol{r}), \hat{\Pi}^\nu(\boldsymbol{r}') \right] &= i\hbar \, \delta^{(tr)}_{\mu\nu}(\boldsymbol{r} - \boldsymbol{r}') \,, \\ \text{i.e.} \quad \left[\hat{A}_i(\boldsymbol{r}), \hat{D}_j(\boldsymbol{r}') \right] &= -i\hbar \, \delta^{(tr)}_{ij}(\boldsymbol{r} - \boldsymbol{r}') \,, \end{aligned} \tag{2.54}$$

where $\delta^{(tr)}_{ij}(\boldsymbol{r})$ is defined in Eq. (2.29). Similarly to what we did in the case of the free field, it is useful to introduce the annihilation and creation operators, $\hat{a}_{\boldsymbol{k},\boldsymbol{\epsilon}}$ and $\hat{a}^\dagger_{\boldsymbol{k},\boldsymbol{\epsilon}}$:

$$\hat{a}_{\boldsymbol{k},\boldsymbol{\epsilon}} = \frac{1}{\sqrt{2\hbar L^3}} \int \mathrm{d}^3 r \, e^{-i\boldsymbol{k}\cdot\boldsymbol{r}} \boldsymbol{\epsilon} \left[\sqrt{\epsilon_0 \omega_k} \, \hat{\boldsymbol{A}}(\boldsymbol{r}) - \frac{i}{\sqrt{\epsilon_0 \omega_k}} \hat{\boldsymbol{D}}(\boldsymbol{r}) \right] , \tag{2.55}$$

where the usual commutation relations Eq. (2.40) also hold for these operators. Note that, contrary to the free-field case (see Eq. (2.43)), these operators contain both light and matter degree of freedom. They define an hybrid light-matter excitation that is a sort of "dressed" photon.

Only a few more assumptions allow to show a very simplified expression of the matter-madiated interaction between these "dressed" photons. Let us assume that the medium is not only non-dispersive and homogeneous, but also symmetric under spatial inversion ($r \to -r$). Spatial inversion symmetry implies that $\boldsymbol{\chi}^{(2)}$ is negligible.[2] The second assumption is to reduce the problem to a single mode. This is valid provided that the frequency spacing of the modes is large compared to the nonlinear frequency shift, that is typically true when the field is confined in an optical cavity. At this point it is just a formal calculation to prove that the 3rd order susceptibility can be accounted through the so called *Kerr Hamiltonian* interaction term

$$\hat{H}_{Kerr}/\hbar = \frac{U}{2}\hat{a}^\dagger\hat{a}^\dagger\hat{a}\hat{a}\,, \tag{2.56}$$

where U is a scalar proportional to $|\boldsymbol{\chi}^{(3)}|$, quantifying the strength of the interactions between the "dressed" photons.

2.2.2 Interacting photons and atoms

As we have mentioned in the introduction, cavity QED studies the physics of atoms interacting with an electromagnetic field that is confined inside an optical cavity. We also have mentioned that this physics is efficiently modeled in terms of two-level systems (for the atoms) and of bosonic modes (for the electromagnetic field) [28–32], Here we introduce the microscopic origin of these paradigmatic models of interacting atoms and photons.

Let us consider the most simple case of a single atom interacting with the electromagnetic field. Neglecting relativistic corrections, such a system is described by the following Hamiltonian [27, 110–112]:

$$\hat{H} = \sum_{j=1}^{N_{el}} \frac{\left[\hat{\boldsymbol{p}}_j - q\hat{\boldsymbol{A}}(\hat{\boldsymbol{r}}_j)\right]^2}{2m} + \phi(\hat{\boldsymbol{r}}_1, ..., \hat{\boldsymbol{r}}_{N_{el}}) + \sum_i \hbar\,\omega_i\left(\hat{a}_i^\dagger\hat{a}_i + \frac{\hat{\mathbb{1}}}{2}\right)\,, \tag{2.57}$$

where q and m are the charge and the mass of the N_{el} electrons of the atom, whose momenta and positions are depicted by the operator $\hat{\boldsymbol{p}}_j$ and $\hat{\boldsymbol{r}}_j$. The first two terms of the Hamiltonian describe respectively the kinetic and the electric potential energy

[2] For a medium presenting such a symmetry the susceptibility tensors $\boldsymbol{\chi}^{(n)}$ are invariant under spatial inversion ($\boldsymbol{r} \to -\boldsymbol{r}$). This means that under spatial inversion $\boldsymbol{\chi}^{(2)} \to \boldsymbol{\chi}^{(2)}$, $\boldsymbol{P}(\boldsymbol{r},t) \to -\boldsymbol{P}(\boldsymbol{r},t)$ and $\boldsymbol{E}(\boldsymbol{r},t) \to -\boldsymbol{E}(\boldsymbol{r},t)$. But $\boldsymbol{P} \to -\boldsymbol{P}$ implies $\boldsymbol{\chi}^{(2)}\boldsymbol{E}\boldsymbol{E} \to -\boldsymbol{\chi}^{(2)}\boldsymbol{E}\boldsymbol{E}$, which can be satisfied if and only if $\boldsymbol{\chi}^{(2)} = 0$.

of the electrons. The operator $\hat{a}_i^\dagger$ ($\hat{a}_i$) describes the creation (annihilation) of the cavity field mode with frequency ω_i, and $\hat{\boldsymbol{A}}(\hat{\boldsymbol{r}}_j)$ is the vector potential at the electron position, that we assume to be of the form

$$\hat{\boldsymbol{A}}(\hat{\boldsymbol{r}}_j) = \sum_i \sqrt{\frac{\hbar}{2\epsilon_0 V \omega_i}}\, f_i(\hat{\boldsymbol{r}}_j)\, \boldsymbol{\epsilon}_i \left(\hat{a}_i + \hat{a}_i^\dagger \right) . \tag{2.58}$$

This expression is an analog of Eq. (2.37), where plane waves have been replaced by real cavity-mode functions $f_i(\boldsymbol{r})$ depending on the specific geometry of the cavity. We choose the normalisation of this function to be equal to the cavity total volume, i.e. $\int \mathrm{d}^3 r\, |f_i(\boldsymbol{r})|^2 = V$, moreover, from the wave equation (Eq. (2.35)) we have that

$$\nabla^2 f_i(\boldsymbol{r}) + \frac{\omega_i}{c^2} f_i(\boldsymbol{r}) = 0 . \tag{2.59}$$

Note from the expression of $\hat{\boldsymbol{A}}(\hat{\boldsymbol{r}}_j)$ in Eq. (2.58), that this operator acts on both the spaces of the atomic electrons and of the cavity field.

Let us spend a few words on the atom kinetic energy, to explain why the usual expression $\hat{\boldsymbol{p}}_j^2/2m$ has been replaced by $[\hat{\boldsymbol{p}}_j - q\hat{\boldsymbol{A}}(\boldsymbol{r}_j)]^2/2m$. The dynamics of a charged particle in an electromagnetic field is described by the differential equation

$$m\,\ddot{\boldsymbol{r}} = \boldsymbol{F} = q(\boldsymbol{E} + \dot{\boldsymbol{r}} \times \boldsymbol{B}) \tag{2.60}$$

that is equivalently generated by the Lagrangian

$$L = m\,\dot{\boldsymbol{r}}^2/2 + q(\boldsymbol{A} \cdot \dot{\boldsymbol{r}} - \phi) . \tag{2.61}$$

The resulting conjugate momentum of the generalised coordinate $\boldsymbol{r}$ is

$$\boldsymbol{p} = \frac{\partial L}{\partial \dot{\boldsymbol{r}}} = m\,\dot{\boldsymbol{r}} + q\boldsymbol{A} . \tag{2.62}$$

Thus the kinetic energy is

$$E_k = m\dot{\boldsymbol{r}}^2 = (\boldsymbol{p} - q\boldsymbol{A})^2/2m . \tag{2.63}$$

Once the square in the kinetic energy of the electrons is expanded, it is possible to distinguish three terms composing the Hamiltonian, $\hat{H} = \hat{H}_{at} + \hat{H}_{ph} + \hat{H}_{int} + \hat{H}_{A^2}$:

$$\begin{aligned}
\hat{H}_{at} &= \sum_{j=1}^{N_{el}} \frac{\hat{\boldsymbol{p}}_j^{\,2}}{2m} + \phi(\hat{\boldsymbol{r}}_1, ..., \hat{\boldsymbol{r}}_{N_{el}}) , \\
\hat{H}_{ph} &= \sum_i \hbar\,\omega_i \left(\hat{a}_i^\dagger \hat{a}_i + \frac{\hat{\mathbb{1}}}{2} \right) , \\
\hat{H}_{int} &= -\frac{q}{m} \sum_{j=1}^{N_{el}} \hat{\boldsymbol{p}}_j \cdot \hat{\boldsymbol{A}}(\hat{\boldsymbol{r}}_j) , \\
\hat{H}_{A^2} &= \frac{q^2}{2m} \sum_{j=1}^{N_{el}} \hat{\boldsymbol{A}}^2(\hat{\boldsymbol{r}}_j) .
\end{aligned} \tag{2.64}$$

The first two terms are respectively referred to the atom and the cavity field degrees of freedom. The third and the fourth terms represent the light-matter interaction.

The first term $\hat{H}_{at}$ is the usual Hamiltonian of an atom, with its characteristic spectrum $\{E_k\}$ and eigenstates $|k\rangle$, the atomic orbitals. In these terms the Hamiltonian can be recast into

$$\hat{H}_{at} = \sum_k E_k \, |k\rangle\langle k| \; . \tag{2.65}$$

The third term describing the interaction between the atom and the cavity field has been obtained by considering that $\hat{\boldsymbol{p}}_j$ commutes with $\hat{\boldsymbol{A}}(\hat{\boldsymbol{r}}_j)$, which follows from the Coulomb gauge condition $\nabla \cdot \boldsymbol{A} = 0$. Let us make use of the so called electric-dipole approximation, assuming that the wave lengths of the significant cavity modes are much larger than the atom size, $\lambda \gg a_0$. In this approximation, the space dependence of the electromagnetic field can be neglected, and $\hat{\boldsymbol{A}}(\hat{\boldsymbol{r}}_j) \simeq \hat{\boldsymbol{A}}(\boldsymbol{r}_0)$, where $\boldsymbol{r}_0$ is the position of the atom inside the cavity. The matrix elements of the interaction Hamiltonian on the atomic eigenstates read:

$$\begin{aligned}
\langle k|\hat{H}_{int}|k'\rangle &= -\frac{q}{m}\,\hat{\boldsymbol{A}}(\boldsymbol{r}_0)\cdot\sum_{j=1}^{N_{el}}\langle k|\hat{\boldsymbol{p}}_j|k'\rangle \\
&= \frac{iq}{\hbar}\,\hat{\boldsymbol{A}}(\boldsymbol{r}_0)\cdot\sum_{j=1}^{N_{el}}\langle k|\Big[\hat{\boldsymbol{r}}_j,\hat{H}_{at}\Big]|k'\rangle \\
&= \frac{iq}{\hbar}\,\hat{\boldsymbol{A}}(\boldsymbol{r}_0)\cdot\sum_{j=1}^{N_{el}}(E_{k'}-E_k)\langle k|\hat{\boldsymbol{r}}_j|k'\rangle \; ,
\end{aligned} \tag{2.66}$$

where we have used the relation $[\hat{\boldsymbol{r}}_j, \hat{H}_{at}] = i\hbar\,\hat{\boldsymbol{p}}_j/m$, which follows from the canonical commutation relations $[\hat{\boldsymbol{r}}_i, \hat{\boldsymbol{p}}_j] = i\hbar\delta_{i,j}$. Note from the last line that on the basis of the atomic eigenstates the diagonal elements of $\hat{H}_{int}$ vanish.

Another very important simplification is to reduce the problem to only two states of the atom, and to only one cavity field mode, as illustrated in Fig. 2.1. Let us call $|g\rangle$ the ground state and $|e\rangle$ the excited state. The interaction matrix element reads

$$\begin{aligned}
\langle g|\hat{H}_{int}|e\rangle &= \frac{iq}{\hbar}\,\hat{\boldsymbol{A}}(\boldsymbol{r}_0)\cdot\sum_{j=1}^{N_{el}}(E_e-E_g)\langle g|\hat{\boldsymbol{r}}_j|e\rangle \\
&= i\,\omega_a\,\boldsymbol{A}(\boldsymbol{r}_0)\cdot\langle g|\,q\sum_{j=1}^{N_{el}}\hat{\boldsymbol{r}}_j|e\rangle\,\big(\hat{a}+\hat{a}^\dagger\big) \\
&= \hbar\,g\,\big(\hat{a}+\hat{a}^\dagger\big) \; ,
\end{aligned} \tag{2.67}$$

where $\hbar\,\omega_a = E_e - E_g > 0$ quantifies the atomic transition frequency, and where

$$\boldsymbol{A}(\boldsymbol{r}_0) \stackrel{\text{def}}{=} \sqrt{\frac{\hbar}{2\epsilon_0 V\omega_c}}\,f_c(\boldsymbol{r}_0)\,\boldsymbol{\epsilon}_c \, , \tag{2.68}$$

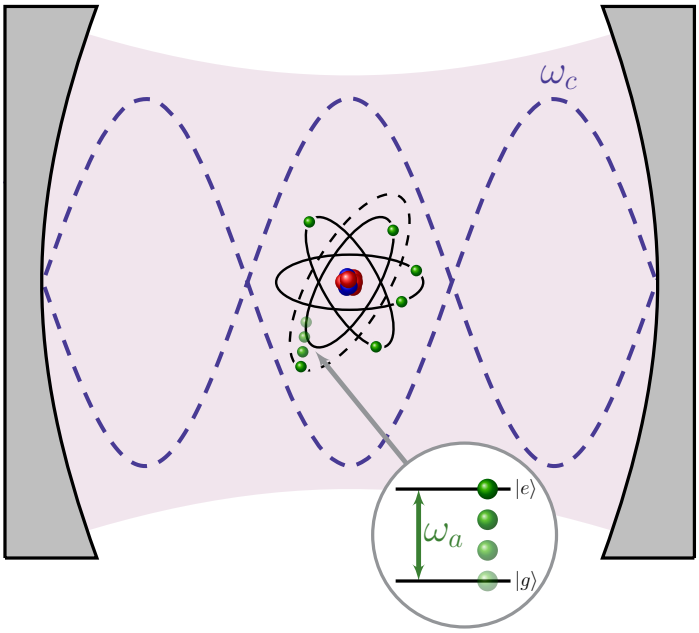

Figure 2.1 The simplified model of an electromagnetic field mode interacting with a resonant two-level system, corresponding to an electronic atomic transition.

follows from the expression in Eq. (2.58) of the vector potential for the selected cavity mode of frequency ω_c and the ladder operators $\hat{a}$ and $\hat{a}^\dagger$. In the last line we have introduce the real parameter

$$g \stackrel{\text{def}}{=} \frac{i\omega_a}{\hbar} \boldsymbol{A}(\boldsymbol{r}_0) \cdot \boldsymbol{d}_{ge} \,, \tag{2.69}$$

where $\boldsymbol{d}_{ge} = \langle g | \, q \sum_{j=1}^{N_{el}} \hat{\boldsymbol{r}}_j | e \rangle$ is the electric dipole of the considered transition. Note that g is in general a complex number, however we can always choose the relative phase between $|e\rangle$ and $\langle g|$, in such a way that g becomes real and positive.

By neglecting the term $\hat{H}_{A^2}$, we obtain a very simplified model, the Rabi Hamiltonian:

$$\hat{H}_{Rabi}/\hbar = \omega_c \, \hat{a}^\dagger \hat{a} + \frac{\omega_a}{2} \hat{\sigma}_z + g(\hat{a} + \hat{a}^\dagger)(\hat{\sigma}_+ + \hat{\sigma}_-), \tag{2.70}$$

where we have introduced the atomic operators, defined as

$$\begin{aligned} \hat{\sigma}_z &= |e\rangle\langle e| - |g\rangle\langle g| \,, \\ \hat{\sigma}_- &= \hat{\sigma}_+^\dagger = |g\rangle\langle e| \,. \end{aligned} \tag{2.71}$$

Note that the interaction strength g is proportional to $f_c(\boldsymbol{r}_0)/\sqrt{V}$. This means that in order to reach a stronger interaction, in experimental realisation it is important to position the atom at the maximum of the cavity-mode function $f_c(\boldsymbol{r})$, and to reduce the volume V in which the electromagnetic field is confined.

When the interaction strength is weak, this Hamiltonian can be approximated to a further simplified form. Let us perform the product in the interaction term

$$g(\hat{a}+\hat{a}^\dagger)(\hat{\sigma}_+ + \hat{\sigma}_-) = g(\hat{a}\,\hat{\sigma}_+ + \hat{a}^\dagger\hat{\sigma}_- + \hat{a}\,\hat{\sigma}_- + \hat{a}^\dagger\hat{\sigma}_+)\,. \tag{2.72}$$

The first two terms of the right side conserve the excitation number

$$\hat{N}_{exc} = \hat{a}^\dagger\hat{a} + (\hat{\sigma}_z + \hat{\mathbb{1}})/2\,. \tag{2.73}$$

Instead, the last two terms, also called anti-resonant terms, do not conserve $\hat{N}_{exc}$ since they respectively annihilate and create pairs of atomic and photon excitations. The first two processes are energetically more favourable than the two others. Indeed, by considering the Rabi Hamiltonian in the interaction picture we get

$$\hat{H}'_{Rabi}(t) = \hbar\, g\left(\hat{a}\,\hat{\sigma}_+ e^{i(-\omega_c+\omega_a)t} + \hat{a}^\dagger\hat{\sigma}_- e^{i(\omega_c-\omega_a)t} + \hat{a}\,\hat{\sigma}_- e^{-i(\omega_c+\omega_a)t} + \hat{a}^\dagger\hat{\sigma}_+ e^{i(\omega_c+\omega_a)t}\right), \tag{2.74}$$

we see that it contains both slowly $(\omega_c - \omega_a)$ and quickly $(\omega_c + \omega_a)$ oscillating terms. In a regime of weak coupling in which $g, |\omega_c - \omega_a| \ll (\omega_c + \omega_a)$, when integrating the system time evolution, the contribution of the quickly oscillating terms averages to zero.

In this approximation, that is typically referred to as the rotating wave approximation (RWA), the anti-rotating terms of the Rabi model can be neglected, and we obtain the so called the Jaynes-Cummings Hamiltonian:

$$\hat{H}_{JC}/\hbar = \omega_c\,\hat{a}^\dagger\hat{a} + \frac{\omega_a}{2}\hat{\sigma}_z + g(\hat{a}\,\hat{\sigma}_+ + \hat{a}^\dagger\hat{\sigma}_-). \tag{2.75}$$

Despite its simplicity, this Hamiltonian provides an accurate description of a large range of cavity QED experiments, explaining its broad exploitation in this field [33, 34].

Symmetries and conserved quantities

Note that these Hamiltonians have some conserved quantities. From what was discussed above, it is clear that the Jaynes-Cummings Hamiltonian $\hat{H}_{JC}$ conserves the total number of excitations $\hat{N}_{exc}$, that is in contrary not conserved in the Rabi Hamiltonian $\hat{H}_{Rabi}$, due to the presence of the anti-resonant terms in the interaction. On the other hand, the anti-resonant terms act by creating or annihilating pairs of excitation, so that $\hat{H}_{Rabi}$ conserves the excitation parity

$$\hat{P}_{exc} = e^{i\pi\hat{N}_{exc}}\,. \tag{2.76}$$

Dispersive regime

Let us consider the Jaynes-Cummings Hamiltonian $\hat{H}_{JC}$ in the dispersive regime in which the atom and cavity are largely detuned compared to the coupling strength, i.e.

$g \ll |\omega_c - \omega_a|$. In this regime, the exchanges of excitations between the atom and the cavity are energetically unfavourable. The bare spectra of the atom and the cavity are only perturbatively shifted by the interaction.

Under these conditions, one can approximate the Hamiltonian in a form that commutes with both $\hat{a}^\dagger\hat{a}$ and $\hat{\sigma}_z$. This is concretely done by applying the unitary transformation

$$\hat{U}(\xi) = e^{\xi \hat{X}_-}\,, \tag{2.77}$$

where we introduced the operator $\hat{X}_- = (\hat{a}^\dagger\hat{\sigma}_- - \hat{a}\,\hat{\sigma}_+)$ and the small parameter

$$\xi = \frac{g}{\omega_a - \omega_c}\,. \tag{2.78}$$

Note that an unitary transformation leaves the spectrum of the Hamiltonian unchanged: $\hat{H}_{JC}$ and its transformed $\hat{U}^\dagger(\xi)\hat{H}_{JC}\hat{U}(\xi)$, have the same spectrum. By expanding $\hat{U}^\dagger(\xi)\hat{H}_{JC}\hat{U}(\xi)$ to the second order in ξ, we obtain an effective Hamiltonian that has approximatively the same spectrum of $\hat{H}_{JC}$:

$$\hat{H}_{JC}^{(disp)} = \hat{U}^\dagger(\xi)\hat{H}_{JC}\hat{U}(\xi) \simeq \hat{H}_{JC} + \xi\left[\hat{H}_{JC}, \hat{X}_-\right] + \frac{\xi^2}{2}\left[\left[\hat{H}_{JC}, \hat{X}_-\right], \hat{X}_-\right]\,. \tag{2.79}$$

By performing the commutators in this expansion, one obtains the effective Hamiltonian of the Jaynes-Cummings model in the dispersive regime

$$\hat{H}_{JC}^{(disp)}/\hbar \simeq \omega_c\,\hat{a}^\dagger\hat{a} + \frac{\omega_a}{2}\hat{\sigma}_z + \frac{g^2}{2(\omega_a - \omega_c)}\,(\hat{a}^\dagger\hat{a} + \hat{\mathbb{1}})\,\hat{\sigma}_z\,. \tag{2.80}$$

The unitary transformation that we used is the so called Schrieffer-Wolff transformation, and it is explicitly chosen to eliminate the interaction term to first order in g [3].

Let us spend a few words on the validity boundaries of this effective Hamiltonian. First of all, we recall that the Jaynes-Cummings Hamiltonian has been obtained using the RWA, that is valid for $|\omega_c - \omega_a| \ll \omega_c + \omega_a$. Combined with the definition of the dispersive regime, this implies that $\hat{H}_{JC}^{(disp)}$ is only valid for $g \ll |\omega_c - \omega_a| \ll \omega_c + \omega_a$. If the detuning $|\omega_c - \omega_a|$ is comparable to the excitation frequencies ω_c and ω_a for instance, the RWA breaks down and the approach outlined above is not valid anymore. However the dispersive effective Hamiltonian beyond the RWA has been derived in detail in Section 5.2.1 and in Ref. [115]. In Figure 2.2 we compare the spectra of $\hat{H}_{Rabi}$, $\hat{H}_{JC}$ and of $\hat{H}_{JC}^{(disp)}$, in the case of out-of-resonance tuning, $\omega_a/\omega_c = 1.5$. The three models have exactly the same spectra for $g \ll \omega_c$, but as g increases, the error of the approximations in the dispersive approach becomes quickly significant. For large values of g, also the Rabi and the Jaynes-Cumming models disagree significantly.

[3] Given the unitary transformation $\hat{U}(g)$ that diagonalises the Jaynes-Cummings Hamiltonian $\hat{H}_{JC}$, the Schrieffer-Wolff unitary transformation $\hat{U}(\xi)$ corresponds to the first order expansion of $\hat{U}(g)$[113, 114].

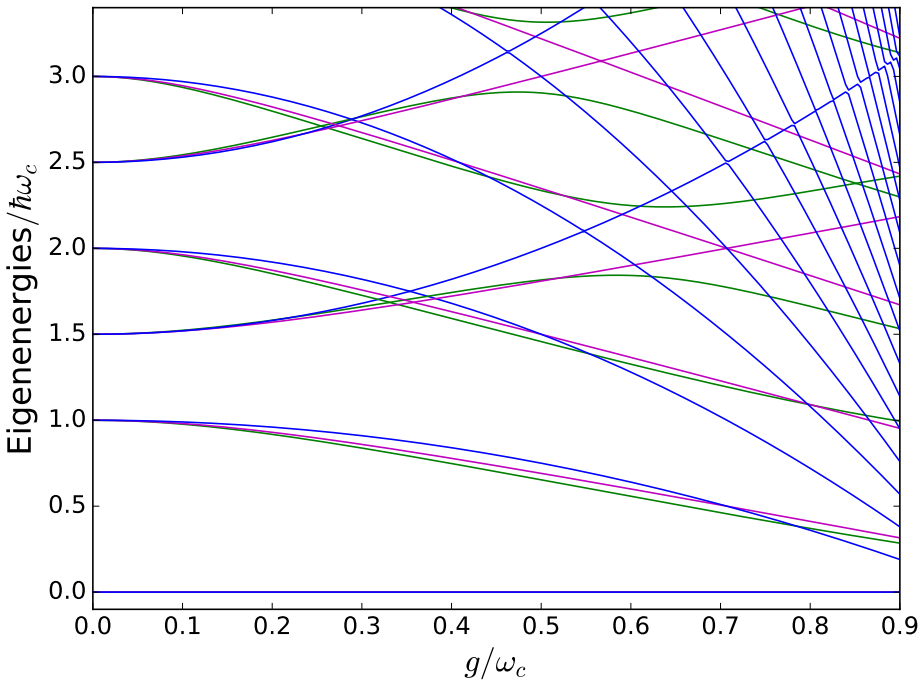

Figure 2.2 The spectra of $\hat{H}_{Rabi}$ (green), $\hat{H}_{JC}$ (magenta) and of $\hat{H}_{JC}^{(disp)}$ (blue), for $\omega_a/\omega_c = 1.5$.

The dispersive coupling described by $\hat{H}_{JC}^{(disp)}$, has a very important role in experimental circuit QED [41–43, 88]. In the dispersive limit it is indeed possible to extract information about the cavity field state from the measured value of the resonance frequency of the two-level system and *vice versa*. This is more apparent by rewriting $\hat{H}_{JC}^{(disp)}$ in the following forms:

$$\hat{H}_{JC}^{(disp)} \simeq \left[\omega_c + \frac{g^2}{2(\omega_a - \omega_c)}\hat{\sigma}_z\right]\hat{a}^\dagger\hat{a} + \left[\frac{\omega_a}{2} + \frac{g^2}{2(\omega_a - \omega_c)}\right]\hat{\sigma}_z \tag{2.81a}$$

$$\simeq \omega_c\,\hat{a}^\dagger\hat{a} + \left[\frac{\omega_a}{2} + \frac{g^2}{2(\omega_a - \omega_c)}\,\hat{a}^\dagger\hat{a} + \frac{g^2}{2(\omega_a - \omega_c)}\right]\hat{\sigma}_z\,. \tag{2.81b}$$

From the first line we see that the two-level atom induces a state-dependent shift of the cavity resonance frequency. In the same way, the resonance frequency of the atom linearly depends on the number of photons inside the cavity, and precisely its frequency shift is

$$\delta\omega_n = \frac{g^2}{2(\omega_a - \omega_c)}\,(n+1) \tag{2.82}$$

where n labels the considered number state of the cavity, as illustrated in the left panel of Fig.2.3. This means that a spectroscopic analysis on the atom would give information on the cavity state. For instance, in Ref. [88] Sun et al. used this kind of

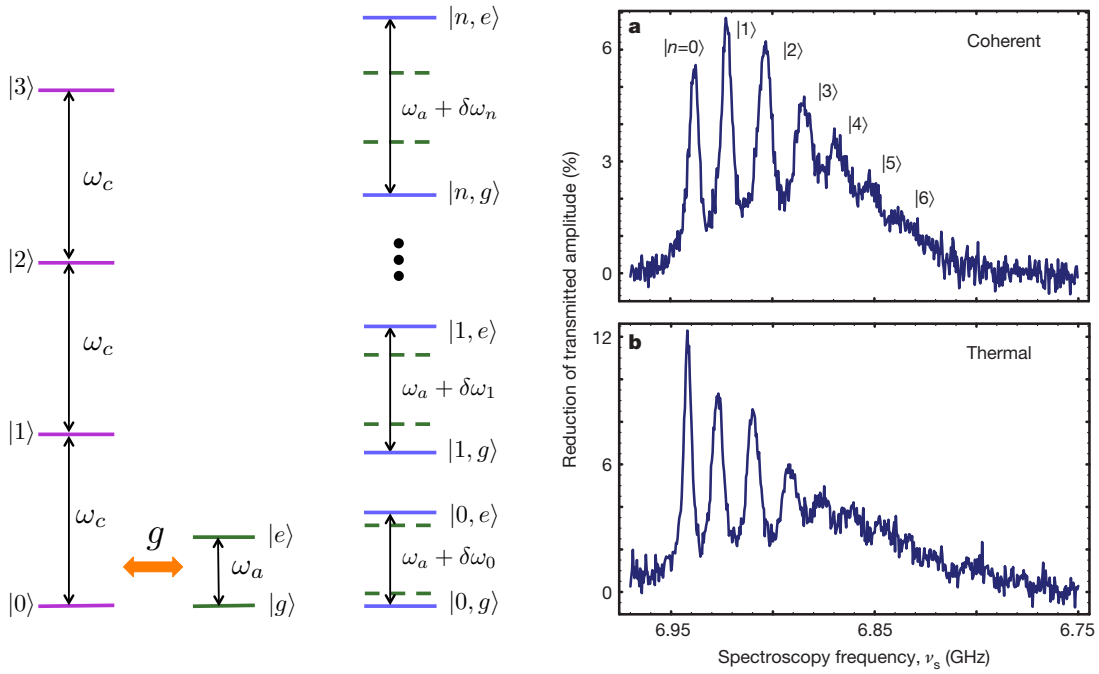

Figure 2.3 The dispersive coupling. Left panel: the modification of the atom frequency as a function of the cavity number state in the dispersive limit. Right panel: the spectral response of the qubit for two differently populated cavity fields. The relative area under the peaks quantifies the population of each cavity number state. It allows to clearly distinguish the two different photon distributions of the cavity, a coherent and a thermal state respectively. Figure extracted from Ref. [42].

coupling to repeatedly track the photon parity in a microwave cavity and in Ref. [42] Schuster et al. resolved the photon number occupation of both a coherent and a thermal state of the cavity, as shown in the right panel of Fig. 2.3.

Equation (2.81b) also suggests another important behaviour of atom-photon coupling: the so called Lamb shift [116, 117]. Even in absence of photon, i.e. $\langle \hat{a}^\dagger \hat{a} \rangle = 0$, the atom resonance frequency is shifted to $\omega_a + g^2/(\omega_a - \omega_c)$. This shift is due to vacuum fluctuations.

2.2.3 Ultrastrong coupling regime

The paradigmatic Hamiltonians presented above have proven to be very efficient to describe most cavity QED realisations [33–36]. However, typical experiments in cavity QED, are characterised by a relatively small interaction strength, more precisely $g \ll \sqrt{\omega_c \, \omega_a}$. Whether these models also work for higher values of light-matter interaction is a legitimate question. This explains the recent interest in exploring the ultrastrong coupling regime, in which the vacuum Rabi frequency (quantifying the intensity of light-matter interaction) is comparable to the bare transition frequencies of the atom

and of the cavity [58–67].

Indeed, the Rabi and the Jaynes-Cumming Hamiltonians, predict some very peculiar phenomena in the ultrastrong coupling regime. In this section, we will focus on the highly nonclassical nature of their ground states, which are characterised by a finite population of photons in the ultrastrong coupling regime. Importantly, the precise form of these exotic ground states depends on the model that is considered. Indeed, in the ultrastrong coupling regime, the precise properties of the system, drastically depend on the model that is considered [118–120]. This is the reason why the ultrastrong coupling regime is considered an important ground to test for validity of light-matter interaction models.

In the previous section we have seen that in a regime of weak coupling, in which the conditions $g, |\omega_c - \omega_a| \ll (\omega_c + \omega_a)$ for the rotating wave approximation are satisfied, the Rabi and the Jaynes-Cumming Hamiltonians produce comparable results. This is no more the case in the ultrastrong coupling regime. Let us consider first the Jaynes-Cumming Hamiltonian

$$\hat{H}_{JC}/\hbar = \omega_c \, \hat{a}^\dagger \hat{a} + \frac{\omega_a}{2}\hat{\sigma}_z + g(\hat{a}\,\hat{\sigma}_+ + \hat{a}^\dagger \hat{\sigma}_-), \tag{2.83}$$

in which the anti-resonant terms $(\hat{a}\,\hat{\sigma}_- + \hat{a}^\dagger\hat{\sigma}_+)$ of the Rabi model have been neglected. Since this Hamiltonian conserves the total number of excitations $\hat{N}_{exc}$, it can be diagonalised by blocks. Each block space is spanned by the basis $\{|n, g\rangle, |n-1, e\rangle\}$, where the first value labels the Fock states of the cavity. In this reduced space the Jaynes-Cumming Hamiltonian reads

$$\hat{h}^{(n)}_{J-C} = \begin{pmatrix} \omega n - \omega_0/2 & g\sqrt{n} \\ g\sqrt{n} & \omega(n-1) + \omega_0/2 \end{pmatrix} . \tag{2.84}$$

Each block of the Hamiltonian can be diagonalised analytically, giving the following eigenenergies

$$\begin{aligned} E^{(n)}_{\pm} &= \omega(n - 1/2) \pm \sqrt{(\omega - \omega_0)^2/4 + g^2 n} \\ E^{(0)} &= -\omega_a/2 \end{aligned} \tag{2.85}$$

and the associated eigenstates

$$\begin{aligned} |n, +\rangle &= \cos\theta_n \, |n, g\rangle + \sin\theta_n \, |n-1, e\rangle \ , \\ |n, -\rangle &= -\sin\theta_n \, |n, g\rangle + \cos\theta_n \, |n-1, e\rangle \ , \\ |0, g\rangle \ . \end{aligned} \tag{2.86}$$

where

$$\tan\theta_n = 2g\sqrt{n} / \left[\omega - \omega_0 + \sqrt{(\omega - \omega_0)^2 + 4g^2 n}\right] . \tag{2.87}$$

This spectrum is represented in Figure 2.4 for the case of perfect resonance $\omega_c = \omega_a$. Interestingly, we see that in the Jaynes-Cumming model, for $g/\omega_a > 1$, the energy

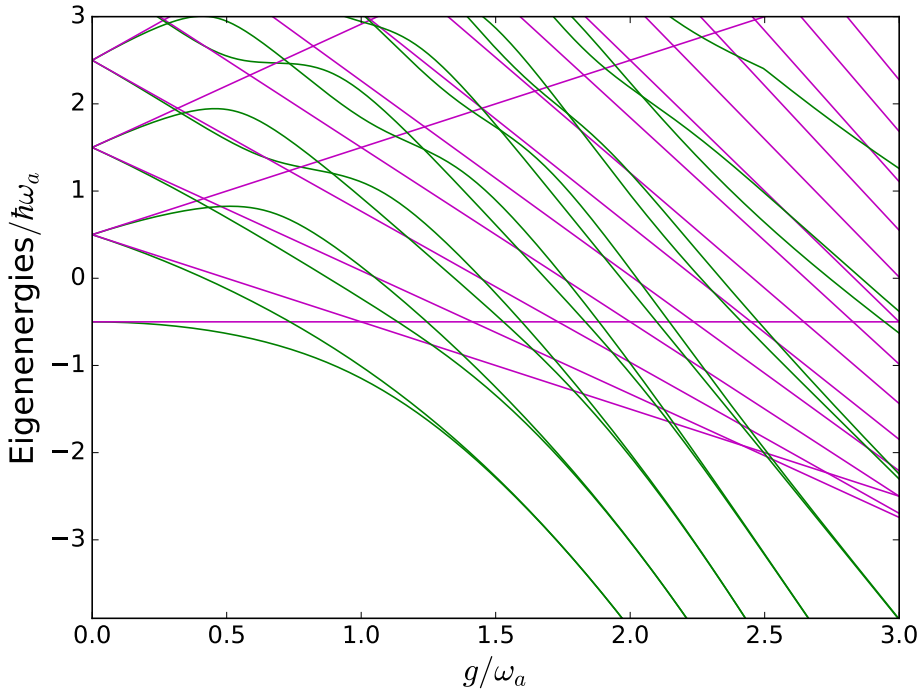

Figure 2.4 The spectrum of Jaynes-Cumming and of Rabi Hamiltonians (respectively in magenta and green) for $\omega_c = \omega_a$.

of $|1,-\rangle$ is smaller then the energy of $|0,g\rangle$. This means that in this regime the ground state is not represented by the standard vacuum $|0,g\rangle$, but it is a state $|n,-\rangle$ containing a finite number of photons that depends on the strength g of the interaction.

In Fig. 2.4 we also show the spectrum of the Rabi Hamiltonian

$$\hat{H}_{Rabi}/\hbar = \omega_c\,\hat{a}^\dagger\hat{a} + \frac{\omega_a}{2}\hat{\sigma}_z + g(\hat{a}+\hat{a}^\dagger)(\hat{\sigma}_+ + \hat{\sigma}_-). \tag{2.88}$$

By comparing the two spectra we see that, despite their agreement for small values of g, the eigenenergies of the two models considerably diverge in the ultrastrong coupling regime. Indeed, the role of the anti-resonant terms is crucial in this regime. These terms couple the excitation-number blocks of the Jaynes-Cumming model, eventually leading to the phenomenon of level anti-crossing.

Note that in the ultrastrong coupling regime, the two models considered here, not only differ for their spectrum, but they also have drastically different eigenstates. In Fig. 2.5 we compare the photon occupation of the ground states. The ground state of the Rabi model contains photons for any finite value of light-matter coupling. Furthermore, photon population of the Rabi ground state increases continuously, while in the Jaynes-Cumming model it increases by steps as expected by the presence of level crossing.

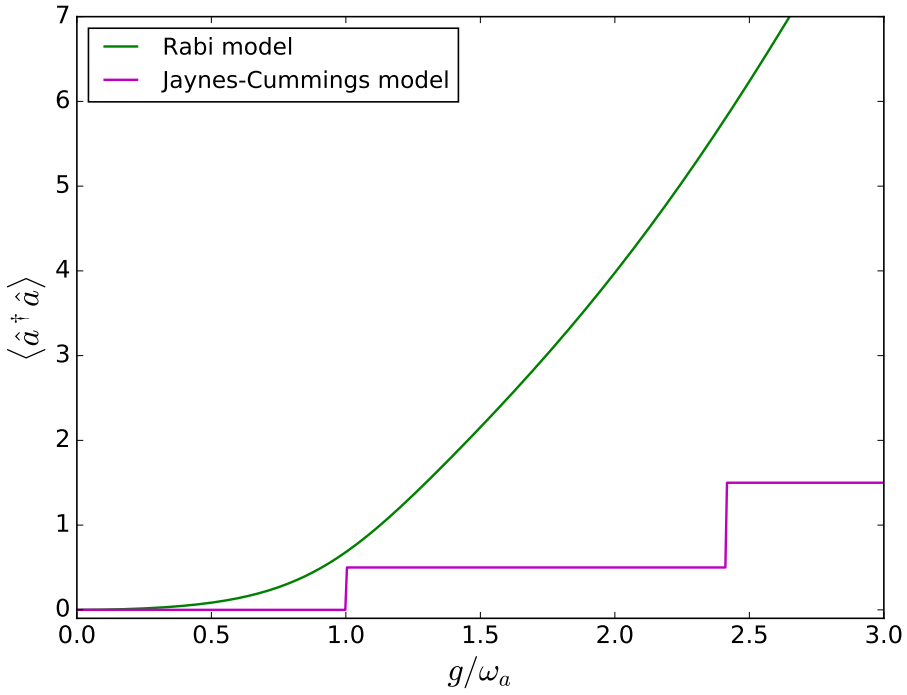

Figure 2.5 The average number of photons in the ground state of the Jaynes-Cumming and Rabi Hamiltonians (in magenta and green respectively) for $\omega_c = \omega_a$.

In order to better know the nature of the Rabi ground state, we explore the limit in which $g \gg \omega_a$. Indeed, in this limit, an analytic expression for the ground state of the Rabi model can be obtained by neglecting the only bound term of the Hamiltonian, i.e. $\omega_a \hat{\sigma}_z/2$:

$$\hat{H}_{Rabi}/\hbar \simeq \omega_c \, \hat{a}^\dagger \hat{a} + g(\hat{a} + \hat{a}^\dagger)(\hat{\sigma}_+ + \hat{\sigma}_-). \tag{2.89}$$

Since the only atomic operator in this approximated Hamiltonian is $\sigma_x = \hat{\sigma}_+ + \hat{\sigma}_-$, we search for a ground state of the form $|\alpha\rangle |\eta\rangle$, where α is a state of the cavity mode and $|\eta\rangle$ is an eigenstate of σ_x, more precisely $\sigma_x |\eta\rangle = \eta |\eta\rangle$ with $\eta = \pm 1$. We can thus rewrite the Hamiltonian as

$$\begin{aligned} \hat{H}_{Rabi}/\hbar &\simeq \omega \left(\hat{a}^\dagger + \frac{g}{\omega_c}\eta \right) \left(\hat{a} + \frac{g}{\omega_c}\eta \right) - \frac{g^2}{\omega_c}\eta^2 \\ &= \omega_c \, \hat{b}^\dagger \hat{b} - E_G \, , \end{aligned} \tag{2.90}$$

where we have introduced the operator $\hat{b} = \hat{a} + g\eta/\omega_c$ and defined the ground state energy $E_G = -g^2\eta^2/\omega_c$. From the last expression of the Hamiltonian, we see that finding the ground state is equivalent to determining the state $|\alpha\rangle$ such that $\hat{b} |\alpha\rangle = 0$. This expression is equivalent to $\hat{a} |\alpha\rangle = -g\eta/\omega_c |\alpha\rangle$, that is precisely the definition of a coherent state. This means that the ground state of this approximated Hamiltonian

is of the form $|\eta\rangle\,|-g\eta/\omega_c\rangle$, in which we note that the two values of $\eta = \pm 1$ lead to two state with the same energy $E_G = -g^2/\omega_c$, meaning that the ground state is double degenerate. However, this degeneracy can be lifted by reintroducing the term $\omega_a\hat{\sigma}_z/2$ as a perturbation. We consider the action of the complete Rabi Hamiltonian in Eq.(2.89) in the subspace spanned by $\{|+\rangle\,|-g/\omega_c\rangle\,, |-\rangle\,|g/\omega_c\rangle\}$:

$$\hat{h}^{(G)}_{Rabi} = \begin{pmatrix} -g^2/\omega_c & \frac{\omega_a}{2}e^{-2g^2/\omega_c^2} \\ \frac{\omega_a}{2}e^{-2g^2/\omega_c^2} & -g^2/\omega_c \end{pmatrix}. \tag{2.91}$$

By diagonalising this reduced Hamiltonian we obtain the ground state and for the first excited state (respectively $|G_-\rangle$ and $|G_+\rangle$)

$$|G_\pm\rangle = \frac{1}{\sqrt{2}}(|+\rangle\,|-g/\omega_c\rangle \pm |-\rangle\,|g/\omega_c\rangle), \tag{2.92}$$

and the associated energies

$$E_\pm/\hbar = -\frac{g^2}{\omega_c} \pm \frac{\omega_a}{2}e^{-2g^2/\omega_c^2}. \tag{2.93}$$

From these energies we obtain the energy gap between the ground state and the first exited state

$$\Delta E/\hbar = \omega_a e^{-2g^2/\omega_c^2}, \tag{2.94}$$

which decays to zero for $g \gg \omega_c$. We conclude that the ground state of the Rabi model is a, so called, *Schrödinger cat state* [27], in which light and matter are correlated in a highly nonclassical state. In the ultrastrong coupling regime, both the Rabi and the Jaynes-Cumming Hamiltonian have non-trivial light-matter populations and correlations in the ground states. Unfortunately, because of energy conservation, the photons and the atomic excitations contained in these *exotic vacua* are bound to the cavity, meaning that it is not possible to explore their property by simple photodetection. Hence, alternative protocols of measurement are required (Chapter 5)[121–123]. In Sec. 3.1.3, we will discuss in more detail the stability of ground state photons.

Superradiant phase transition

So far, we have considered the models of only one atom coupled to the cavity. However one could be interested in considering an arbitrary number of atoms interacting with the same cavity mode. This is for example the case in the microcavity semiconductors, in which the cavity field interact with the many intra-cavity electronic transitions that play the role of the atoms [53, 54, 64–67]. In this case an often studied model is represented by the Dicke Hamiltonian:

$$\hat{H}_{Dicke}/\hbar = \omega_c\hat{a}^\dagger\hat{a} + \frac{\omega_a}{2}\sum_i \hat{\sigma}_z^{(i)} + \frac{\lambda}{\sqrt{N_{at}}}\sum_i(\hat{\sigma}_+^{(i)} + \hat{\sigma}_-^{(i)})(\hat{a} + \hat{a}^\dagger)\,, \tag{2.95}$$

where the Pauli matrices here refer to each two-level atom. This model simply generalises the Rabi Hamiltonian to an arbitrary number of atoms N, in which we have recast the coupling strength of a single atom as $g = \lambda/N$. The Dicke Hamiltonian is most conveniently rewritten by considering the collective spin associated to the N two-level systems, namely

$$\hat{J}_z = \frac{1}{2}\sum_{i=1}^{N} \hat{\sigma}_z^{(i)}\,, \qquad \hat{J}_\pm = \sum_{i=1}^{N} \hat{\sigma}_\pm^{(i)}\,. \tag{2.96}$$

We can thus write

$$\hat{H}_{Dicke}/\hbar = \omega_c \hat{a}^\dagger \hat{a} + \omega_a \hat{J}_z + \frac{\lambda}{\sqrt{N}}\left(\hat{a}^\dagger + \hat{a}\right)\left(\hat{J}_+ + \hat{J}_-\right)\,. \tag{2.97}$$

From the rules of combining angular momenta, we know that the total spin quantum number here, can range over all the half-integers from 0 to $N/2$. However, since the Hamiltonian commutes with the operator of total spin magnitude $\hat{\boldsymbol{J}}^2$, we can reduce the problem to only one eigenspace of $\hat{\boldsymbol{J}}^2$. In particular we choose the space with maximal total spin, since it is the one in which the ground state is contained (this is straightforward for $\lambda = 0$ and for $\lambda \to \infty$). This means that the operators defined in Eq.(2.96) represent collective spin of size $N/2$. Note that by doing so we considerably reduce the dimension of the atomic Hilbert space from 2^N to N.

Similarly to the Rabi model, this Hamiltonian is characterised by parity symmetry, defined by the operator $\hat{\Pi} = \exp\{i\pi(\hat{a}^\dagger\hat{a} + \hat{J}_z + N/2)\}$. In the thermodynamical limit $N \to \infty$ the system is characterised by a phase transition that is associated to the breaking of this discrete symmetry. A detailed description of this quantum phase transition is provided by C. Emary and T. Brandes in Ref. [73], here we only briefly use their results to describe this transition and the relation with the finite size properties. It is indeed possible to show that at zero temperature and thermodynamic limit the Dicke model undergo a quantum phase transition at $\lambda = 0.5$. In the broken symmetry phase, also called superradiant phase, the system has two degenerate eigenstates $|\Psi_\pm\rangle = |\pm\alpha\rangle\,|\pm\beta\rangle$, where $|\pm\alpha\rangle$ is a coherent state of the cavity mode and $|\pm\beta\rangle$ is a polarised state of the atoms. The latter is defined as a coherent state on the bosonic operator introduced with the Holstein-Primakoff transformation [124] that is used in Ref. [73] to describe the superradiant phase transition. We have that

$$\begin{aligned} \alpha &= \mp\frac{\lambda\sqrt{N}}{\omega_c}\sqrt{1-\left(\frac{\omega_c\,\omega_a}{4g^2}\right)^2}\,, \\ \beta &= \pm\sqrt{\frac{N}{2}}\sqrt{1-\frac{\omega_c\,\omega_a}{4g^2}}\,. \end{aligned} \tag{2.98}$$

However, the degeneracy of the ground state mathematically only holds in the limit of an infinite number of atoms. For any finite N the two states are coupled, leading

to a lift of the degeneracy [62]. Similarly to what we did to determine the ground state of the Rabi model, we can consider the action of the Hamiltonian in Eq. (2.97) on the two states $|\Psi_\pm\rangle$. Diagonalising this reduced Hamiltonian, one obtains a good approximation of the ground and of the first excited state (respectively $|G_-\rangle$ and $|G_+\rangle$) for a finite number of atoms. Without going into the details of the calculations, we have

$$|G_\pm\rangle \simeq \frac{|\alpha\rangle\,|\beta\rangle \pm |-\alpha\rangle\,|-\beta\rangle}{\mathcal{N}_\pm}\,, \tag{2.99}$$

where $\mathcal{N}_\pm$ ensures the right normalisation of the state. Again the ground and first excited states are Schrödinger cat states with a nonclassical correlation between light and matter.

No-go theorem for superradiant quantum phase transitions in cavity QED

It is important to mention that a no-go theorem for superradiant quantum phase transitions has been predicted for cavity QED realisations [63]. Indeed the $\hat{\boldsymbol{A}}^2$ term in Eq. (2.64), that we have neglected to derive the Rabi Hamiltonian, can become crucial in the ultrastrong coupling regime. Adding the contribution of this term to the Dicke model, one obtains the Hamiltonian

$$\hat{H}/\hbar = \omega_c \hat{a}^\dagger \hat{a} + \omega_a \hat{J}_z + \frac{\lambda}{\sqrt{N}}\left(\hat{a}^\dagger + \hat{a}\right)\left(\hat{J}_+ + \hat{J}_-\right) + D\left(\hat{a}^\dagger + \hat{a}\right)^2, \tag{2.100}$$

and when $D = \lambda^2/\omega_a$ one obtains the Hopfield model, well known in semiconductor optics [29, 64]. It can be proven [63] that in cavity QED the sum rule implies $D \geq \lambda^2/\omega_a$. For these values of D, the quadratic renormalisation introduced by the $\hat{\boldsymbol{A}}^2$ term inhibits the superradiant phase transition at zero temperature. This shows that the way in which we model light-matter interaction is importantly tested in the ultrastrong coupling regime. Indeed, while the contribution of the $\hat{\boldsymbol{A}}^2$ term is unimportant in typical regimes of cavity QED realisations, in the ultrastrong coupling regime it can drastically modify the physics of the system.

Note that this no-go theorem only applies in the precise conditions of cavity QED system. In circuit QED, however, the systems can be tailored to make the $\hat{\boldsymbol{A}}^2$ term negligible [63], or to realise the physics of most atom-cavity models [48, 72].

Chapter 3

Open quantum systems and Lindblad master equation

An aspect that intrinsically distinguishes the physics of photons from other branches of physics is its out-of-equilibrium nature. Despite the efforts to isolate the electromagnetic field in more and more efficient cavities, the coupling to the environment is typically non-negligible. The photons generally escape through the optical mirrors of the cavities and dissipate in the infinite modes of the external electromagnetic field.

More general, in open quantum systems, the environment is represented by a second system with infinite degrees of freedom. Due to its large size, it is in principle impossible to have total control of the environment. Thus, except in specific cases, in which the environment is in a precisly known and controlled state, the coupling to an environment represents a loss of information on the system. In Section 3.1 we introduce a microscopical model of the coupling to the environment that allows to describe the system evolution in the form of a Lindblad master equation.

Since the photons tend to escape the cavity, in order to have a non-negligible population we need to constantly replace them. This is the role of the driving, which can for example be a laser field, that injects photons inside the cavity. In Section 3.2 we provide a simple microscopic description of this process.

3.1 Coupling to the environment and Lindblad master equation

The coupling to the environment is associated with some very important processes in quantum physics. It is responsible for the loss of quantum information, commonly called decoherence, impeding the control and exploitation of quantum systems, and it also explains the loss of energy, generally called dissipation.

In order to consider these processes, the Lindblad master equation often is a very convenient description [125, 126]. In its general form, a Lindblad master equation describes the time evolution of the density operator as

$$\partial_t \hat{\rho} = -\frac{i}{\hbar}\left[\hat{H}\,,\hat{\rho}\right] + \sum_i^{N^2-1}\left(2\hat{A}_i\hat{\rho}\hat{A}_i^\dagger - \hat{A}_i^\dagger\hat{A}_i\hat{\rho} - \hat{\rho}\hat{A}_i^\dagger\hat{A}_i\right) \tag{3.1}$$

where $\hat{H}$ is an Hermitian operator, and $\hat{A}_i$ are operators acting on the system Hilbert space of dimension N. The first term of Eq. (3.1) describes a unitary evolution, where $\hat{H}$ is typically the Hamiltonian of the system. The second term is associated to the coupling of the system to the environment, it produces a non-unitary dynamics, and is determined by the so called jump operators $\hat{A}_i$.

In Section 3.1.1, we provide a detailed derivation of the Lindblad master equation. This will allow us to describe the dissipation and decoherence of atoms and cavities (Sec. 3.1.2), and, importantly, to derive a master equation consistent with the ultrastrong coupling regime (Sec. 3.1.3). In Sec. 2.2.3 we have indeed seen, that when cavity QED systems reach the ultrastrong coupling regime, their ground state contains a finite population of photons and of atom excitations. In order to properly describe the stability of these ground state photons, a careful description of the environment coupling is needed.

3.1.1 Microscopic derivation of Lindblad master equation

In this subsection we provide a microscopic derivation of the Lindblad master equation based on Refs.[125–127]. From a mathematical point of view, the coupling to the environment can be described by considering the total Hamiltonian of the quantum system and the environment, that determines the dynamics of the total density operator. Here we follow a standard procedure, that permits to obtain an effective dynamics for only the system density operator, by tracing out the degrees of freedom of the environment degrees. The total Hamiltonian of the system S and the coupled environment B is

$$\hat{H} = \hat{H}_S + \hat{H}_B + \hat{H}_I \,, \tag{3.2}$$

where $\hat{H}_S$ and $\hat{H}_B$ are respectively the free Hamiltonian of the system and the environment and $\hat{H}_I$ describes the interaction between them. We assume all the Hamiltonian terms to be time independent.

A simple model of the environment is given by a bath of harmonic oscillators

$$\hat{H}_B = \sum_k \hbar\,\omega_k\,\hat{b}_k^\dagger \hat{b}_k \,, \qquad \left[\hat{b}_k, \hat{b}_{k'}^\dagger\right] = \delta_{k,k'} \,, \tag{3.3}$$

where ω_k is the frequency of the kth mode of the bath. The bath of harmonic oscillator can represent, for instance, the extra-cavity modes of the electromagnetic field, or it can describe the phonon modes of a solid environment. Here we consider the bath at thermal equilibrium

$$\hat{\rho}_{_B} = \frac{e^{-\beta \hat{H}_B}}{Z_B} = \prod_k \left(1 - e^{\beta\hbar\,\omega_k}\right) e^{\beta\hbar\,\omega_k \hat{b}_k^\dagger \hat{b}_k} \,, \tag{3.4}$$

where $\hat{\rho}_{_B}$ is the density operator of the bath and Z_B is its partition function. The

thermal equilibrium implies the following relations:

$$\begin{aligned} &\langle \hat{b}_k \rangle_{_T} = \langle \hat{b}_k^\dagger \rangle_{_T} = 0\,, \quad \langle \hat{b}_k \hat{b}_k \rangle_{_T} = \langle \hat{b}_k^\dagger \hat{b}_k^\dagger \rangle_{_T} = 0\,, \\ &\langle \hat{b}_k^\dagger \hat{b}_k \rangle_{_T} = \delta_{k,k'} N_{_T}(\omega_k) \quad \text{with} \quad N_{_T}(\omega_k) = \frac{1}{e^{\beta\hbar\,\omega_k - 1}}\,, \end{aligned} \tag{3.5}$$

where $\langle\,\cdot\,\rangle_{_T} = \mathrm{Tr}_B\{\,\cdot\,\hat{\rho}_{_B}\}$ represent the thermal equilibrium average at temperature T and where we have introduced the bosonic average occupation number $N_{_T}(\omega_k)$ of the kth mode.

A quite general assumption is to consider the following form for the interaction term

$$\hat{H}_I/\hbar = \hat{S} \otimes \hat{B}\,, \tag{3.6}$$

where $\hat{S}$ is a generic Hermitian operator acting on the system degrees of freedom, while $\hat{B}$ is an Hermitian operator acting on the bath, and that we choose to be of the form

$$\hat{B} = \sum_k \left(g_k \hat{b}_k + g_k^* \hat{b}_k^\dagger \right)\,. \tag{3.7}$$

In the Schrödinger picture, the time evolution of the total density operator for the system and environment is

$$\partial_t \hat{\rho} = -\frac{i}{\hbar}\left[\hat{H}_S + \hat{H}_B + \hat{H}_I, \hat{\rho}\right]\,. \tag{3.8}$$

The derivation of the Lindblad equation is most easily performed in the interaction picture, in which $\hat{\rho}$ is mapped into

$$\hat{\rho}'(t) \stackrel{\text{def}}{=} e^{\frac{i}{\hbar}(\hat{H}_S+\hat{H}_B)t}\,\hat{\rho}(t)\,e^{-\frac{i}{\hbar}(\hat{H}_S+\hat{H}_B)t}\,. \tag{3.9}$$

In the interaction frame, the equation of motion for $\hat{\rho}'$ reads:

$$\partial_t \hat{\rho}' = -\frac{i}{\hbar}\left[\hat{H}_I'(t), \hat{\rho}'(t)\right]\,, \tag{3.10}$$

where

$$\hat{H}_I'(t) \stackrel{\text{def}}{=} e^{\frac{i}{\hbar}(\hat{H}_S+\hat{H}_B)t}\,\hat{H}_I\,e^{-\frac{i}{\hbar}(\hat{H}_S+\hat{H}_B)t}\,. \tag{3.11}$$

This equation can be formally integrated as

$$\hat{\rho}'(t) = \hat{\rho}'(0) - \frac{i}{\hbar}\int_0^t \mathrm{d}t' \left[\hat{H}_I'(t'), \hat{\rho}'(t')\right]\,, \tag{3.12}$$

and injected again in Eq. (3.10) allowing to write the following time evolution:

$$\partial_t \hat{\rho}\,' = -\frac{i}{\hbar}\left[\hat{H}_I'(t), \hat{\rho}\,'(0)\right] - \frac{1}{\hbar^2}\int_0^t \mathrm{d}t' \left[\hat{H}_I'(t), \left[\hat{H}_I'(t'), \hat{\rho}\,'(t')\right]\right]\,. \tag{3.13}$$

At this point we have to do the first important assumption of the approach, the so called *Born approximation*. We assume that the interaction term $\hat{H}_I$ is too weak

to create a significant correlation between the system and the bath. Furthermore, one should keep in mind the large size of the bath. The effects of the interaction are dispersed on the many degrees of freedom of the bath, and we can assume that its state remains mostly unperturbed. This allows us to consider the following approximate factorised expression:

$$\hat{\rho}(t) \simeq \hat{\rho}_S(t) \otimes \hat{\rho}_B \,. \tag{3.14}$$

Injecting this expression in Eq. (3.13) and tracing out the bath degrees of freedom we find the time evolution of the reduced system density operator $\hat{\rho}'_S$ (in the interaction picture):

$$\partial_t \hat{\rho}'_S = -\frac{1}{\hbar^2} \int_0^t \mathrm{d}\tau \, \mathrm{Tr}_B \Big\{ \Big[\hat{H}'_I(t), \Big[\hat{H}'_I(t-\tau) \,, \hat{\rho}'_S(t-\tau) \otimes \hat{\rho}_B \Big] \Big] \Big\} \,, \tag{3.15}$$

where we have introduced the variable $\tau = t - t'$ and where we have used the fact that $\hat{\rho}'_B(t) = \hat{\rho}_B$, since $\hat{\rho}_B$ commute with $\hat{H}_B$ and $\hat{H}_S$. The fact that the first term in Eq. (3.13) vanishes is proven by noting that $\hat{H}_I/\hbar = \hat{S} \otimes \sum_k (g_k \hat{b}_k + g_k^* \hat{b}_k^\dagger)$ and that at thermal equilibrium $\langle \hat{b}_k \rangle_T = 0$.

In order to expand the Eq. (3.15) we first need to decompose the operator $\hat{S}$. Supposing a discrete spectrum, let us denote the eigenvalues and eigenstate of $\hat{H}_S$ by ϵ and $|\epsilon\rangle$ respectively. Then we can define the operators

$$\hat{S}(\omega) \overset{\text{def}}{=} \sum_{\epsilon' - \epsilon = \hbar\omega} \langle \epsilon \, | \hat{S} | \epsilon' \rangle \, | \epsilon \rangle\langle \epsilon' | \,, \tag{3.16}$$

where the sum in this expression is extended over all the eigenvalues ϵ' and ϵ of $\hat{H}_S$ with a fixed energy difference $\hbar\omega$. This means that the operators $\hat{S}(\omega)$ only couples energy levels with a difference in energy equal to $\hbar\omega$. They are not Hermitian, but they satisfy the relation $\hat{S}^\dagger(\omega) = \hat{S}(-\omega)$, and in the interaction picture frame they read

$$\begin{aligned} e^{\frac{i}{\hbar}\hat{H}_S t} \, \hat{S}(\omega) \, e^{-\frac{i}{\hbar}\hat{H}_S t} &= e^{-i\omega t} \, \hat{S}(\omega) \\ e^{\frac{i}{\hbar}\hat{H}_S t} \, \hat{S}^\dagger(\omega) \, e^{-\frac{i}{\hbar}\hat{H}_S t} &= e^{+i\omega t} \, \hat{S}^\dagger(\omega) \,. \end{aligned} \tag{3.17}$$

Summing over all the energy differences ω (positive and negative) and employing the completeness relation we get

$$\sum_\omega \hat{S}(\omega) = \sum_\omega \hat{S}^\dagger(\omega) = \hat{S} \,. \tag{3.18}$$

This allows us to recast the interaction Hamiltonian term into the form

$$\hat{H}_I/\hbar = \sum_\omega \hat{S}(\omega) \otimes \hat{B} = \sum_\omega \hat{S}^\dagger(\omega) \otimes \hat{B} \,. \tag{3.19}$$

This is translated in the interaction picture as

$$\hat{H}'_I(t)/\hbar = \sum_\omega e^{-i\omega t}\hat{S}(\omega)\otimes\hat{B}'(t) = \sum_\omega e^{+i\omega t}\hat{S}^\dagger(\omega)\otimes\hat{B}'(t) \tag{3.20}$$

where

$$\hat{B}'(t) = e^{\frac{i}{\hbar}\hat{H}_B t}\,\hat{B}\,e^{-\frac{i}{\hbar}\hat{H}_B t} = \sum_k \left(g_k\, e^{-i\omega t}\,\hat{b}_k + g_k^*\, e^{+i\omega t}\,\hat{b}_k^\dagger\right). \tag{3.21}$$

Injecting the expression of $\hat{H}'_I(t)$ into the Equation (3.15) we obtain the following expression for the time evolution of $\hat{\rho}'_S$:

$$\begin{aligned}
\partial_t\hat{\rho}'_S =& \frac{1}{\hbar^2}\int_0^t \mathrm{d}\tau\,\mathrm{Tr}_B\Big\{\hat{H}'_I(t-\tau)\,\left[\hat{\rho}'_S(t-\tau)\otimes\hat{\rho}_B\right]\,\hat{H}'_I(t)\Big\} \\
&- \frac{1}{\hbar^2}\int_0^t \mathrm{d}\tau\,\mathrm{Tr}_B\Big\{\hat{H}'_I(t)\,\hat{H}'_I(t-\tau)\,\left[\hat{\rho}'_S(t-\tau)\otimes\hat{\rho}_B\right]\Big\} + h.c. \\
=& \sum_{\omega,\omega'} e^{i(\omega'-\omega)t}\,\hat{S}(\omega)\left[\int_0^t \mathrm{d}\tau e^{i\omega\tau}\hat{\rho}'_S(t-\tau)\langle\hat{B}'(t)\hat{B}'(t-\tau)\rangle_T\right]\hat{S}^\dagger(\omega') \\
&- \sum_{\omega,\omega'} e^{i(\omega'-\omega)t}\,\hat{S}^\dagger(\omega')\,\hat{S}(\omega)\left[\int_0^t \mathrm{d}\tau e^{i\omega\tau}\hat{\rho}'_S(t-\tau)\langle\hat{B}'(t)\hat{B}'(t-\tau)\rangle_T\right] + h.c..
\end{aligned} \tag{3.22}$$

To simplify the integral in the square brackets we need to spend some words on the bath correlation $\langle\hat{B}'(t)\hat{B}'(t-\tau)\rangle_T$. First of all, we notice that the bath correlations are homogeneous in time, which implies that $\langle\hat{B}'(t)\hat{B}'(t-\tau)\rangle_T = \langle\hat{B}'(\tau)\hat{B}'(0)\rangle_T$.
We can express this bath correlation by injecting the expression for $\hat{B}'(t)$ in Eq (3.21):

$$\begin{aligned}
\langle\hat{B}'(\tau)\hat{B}'(0)\rangle_T &= \mathrm{Tr}_B\left\{\hat{\rho}_B\sum_k\left(g_k\,e^{-i\omega_k\tau}\,\hat{b}_k + g_k^*\,e^{+i\omega_k\tau}\,\hat{b}_k^\dagger\right)\sum_{k'}\left(g_{k'}\,\hat{b}_{k'} + g_{k'}^*\,\hat{b}_{k'}^\dagger\right)\right\} \\
&= \sum_k\left(|g_k|^2\,e^{-i\omega_k\tau}\langle\hat{b}_k\hat{b}_k^\dagger\rangle_T + |g_k|^2\,e^{+i\omega_k\tau}\langle\hat{b}_k^\dagger\hat{b}_k\rangle_T\right) \\
&= \sum_k |g_k|^2\left\{[1+N_T(\omega_k)]\,e^{-i\omega_k\tau} + N_T(\omega_k)\,e^{+i\omega_k\tau}\right\}
\end{aligned} \tag{3.23}$$

where we exploited the thermal equilibrium averages in Eqs. (3.5). It can be shown [125, 126], that for the typical models of thermal bath, this correlation decays to zero for large τ. This is heuristically explained by considering that, for τ larger then a characteristic decay time that we call τ_B, the oscillation of the different exponentials $e^{\pm i\omega_k\tau}$ from the different modes are dephased and interfere destructively. This destructive interference is more and more effective as the number of populated modes is large, requiring the bath to be "large" enough and implying that τ_B decreases as the temperature of the bath increases.

This analysis on the bath correlation function now allows us to simplify the integral in the square brackets in Eq. (3.22). To do so, we need to introduce the so called *Markov approximation*. We assume that the time scale $\tau_{_B}$ is much shorter than the time scale $\tau_{_S}$ in which the interaction picture density operator of the system changes significantly. It means that in the time in which $\langle \hat{B}'(t)\hat{B}'(t-\tau)\rangle_{_T}$ has a significant value, the density operator nearly is constant and we can approximate it as $\hat{\rho}'_{_S}(t-\tau) \simeq \hat{\rho}'_{_S}(t)$. The validity of this approximation is based on the large size of the thermal bath, which implies a small $\tau_{_B}$, and on the weakness of the interaction $\hat{H}_I$, that determines the time scale of the density operator $\hat{\rho}'_{_S}(t)$ relaxation. This is called the Markov approximation because the fast decay of bath correlation, implies that the time evolution is local in time. It means that the system time evolution at a certain time does not depend on the past states of the system and of the bath: this defines a Markovian memoryless evolution.

Applying the approximations introduced above, we can now simplify the integral inside the square brackets in Eq. (3.22):

$$\int_0^t \mathrm{d}\tau\, e^{i\omega\tau}\hat{\rho}'_{_S}(t-\tau)\langle \hat{B}'(t)\hat{B}'(t-\tau)\rangle_{_T} = \hat{\rho}'_{_S}(t)\int_0^t \mathrm{d}\tau\, e^{i\omega\tau}\langle \hat{B}'(\tau)\hat{B}'(0)\rangle_{_T}\,. \tag{3.24}$$

Considering that for $t \gg \tau_{_B}$ the bath correlation function is negligible, we can send the upper limit of the integral to infinity

$$\hat{\rho}'_{_S}(t)\,\Gamma(\omega) = \hat{\rho}'_{_S}(t)\int_0^\infty \mathrm{d}\tau\, e^{i\omega\tau}\langle \hat{B}'(\tau)\hat{B}'(0)\rangle_{_T}\,, \tag{3.25}$$

where we have introduced the Fourier transform of the bath correlation function

$$\Gamma(\omega) = \int_0^\infty \mathrm{d}\tau\, e^{i\omega\tau}\langle \hat{B}'(\tau)\hat{B}'(0)\rangle_{_T}\,. \tag{3.26}$$

Using this expression to simplify the time evolution in Eq. (3.22) we obtain

$$\partial_t\hat{\rho}'_{_S} = \sum_{\omega,\,\omega'} e^{i(\omega'-\omega)t}\,\Gamma(\omega)\left[\,\hat{S}(\omega)\hat{\rho}'_{_S}(t)\,\hat{S}^\dagger(\omega') - \,\hat{S}^\dagger(\omega')\,\hat{S}(\omega)\hat{\rho}'_{_S}(t)\,\right] + h.c.\,. \tag{3.27}$$

At this point we introduce the last important approximation toward the derivation of the Lindblad master equation: the *secular approximation*. The exponential factor is assumed to rotate rapidly compared to the time scale $\tau_{_S}$ of the system relaxation. Once again, this is justified by assuming that the interaction $\hat{H}_I$ is much weaker then the system typical energy differences $\epsilon' - \epsilon$, where the $\{\epsilon\}$ are the eigenvalues of $\hat{H}_S$. Under this assumption the terms of the summation in Eq. (3.27) with $\omega \neq \omega'$ are negligible in the time integration of the equation, and they can be neglected in the equation for the time evolution:

$$\partial_t\hat{\rho}'_{_S} = \sum_{\omega}\Gamma(\omega)\left[\,\hat{S}(\omega)\hat{\rho}'_{_S}(t)\,\hat{S}^\dagger(\omega) - \,\hat{S}^\dagger(\omega)\,\hat{S}(\omega)\hat{\rho}'_{_S}(t)\,\right] + h.c.\,. \tag{3.28}$$

In order to obtain the Lindblad master equation in its final form we need to compute the complex function $\Gamma(\omega)$. First of all, it is convenient to decompose $\Gamma(\omega)$ in its real and imaginary part

$$\Gamma(\omega) = \frac{1}{2}\gamma(\omega) + i\Lambda(\omega)\,, \tag{3.29}$$

where

$$\Lambda(\omega) = \frac{1}{2i}\left[\Gamma(\omega) - \Gamma^*(\omega)\right] \tag{3.30}$$

and

$$\gamma(\omega) = \frac{1}{2}[\Gamma(\omega) + \Gamma^*(\omega)] = \int_{-\infty}^{\infty} \mathrm{d}\tau\, e^{i\omega\tau}\langle \hat{B}'(\tau)\hat{B}'(0)\rangle_{_T}\,. \tag{3.31}$$

The imaginary part $\Lambda(\omega)$ induces a shift in the energy levels, it is also referred as the Lamb shift induced by the system-bath coupling. In most circumstances this term can be neglected [125, 126]. While the real part

$$\begin{aligned}
\gamma(\omega) &= \int_{-\infty}^{\infty} \mathrm{d}\tau\, e^{i\omega\tau}\langle \hat{B}'(\tau)\hat{B}'(0)\rangle_{_T} \\
&= \int_{-\infty}^{\infty} \mathrm{d}\tau\, e^{i\omega\tau} \sum_k |g_k|^2 \left\{[1 + N_{_T}(\omega_k)]\, e^{-i\omega_k\tau} + N_{_T}(\omega_k)\, e^{+i\omega_k\tau}\right\} \\
&= \sum_k |g_k|^2 \left\{[1 + N_{_T}(\omega_k)] \int_{-\infty}^{\infty} \mathrm{d}\tau\, e^{i(\omega-\omega_k)\tau} + N_{_T}(\omega_k) \int_{-\infty}^{\infty} \mathrm{d}\tau\, e^{i(\omega+\omega_k)\tau}\right\} \\
&= \sum_k 2\pi|g_k|^2 \left\{[1 + N_{_T}(\omega_k)]\, \delta(\omega - \omega_k) + N_{_T}(\omega_k)\, \delta(\omega + \omega_k)\right\}\,,
\end{aligned} \tag{3.32}$$

Where we used $\int_{-\infty}^{\infty} \mathrm{d}\tau\, e^{i\omega\tau} = 2\pi\delta(\omega)$, the integral definition of the Dirac delta function. Injecting this expression of $\Gamma(\omega)$ into the time evolution Eq. (3.28), we get

$$\begin{aligned}
\partial_t\hat{\rho}'_{_S} =& \sum_{\omega>0}\sum_k \pi|g_k|^2[1 + N_{_T}(\omega_k)]\, \delta(\omega - \omega_k)\left[2\hat{S}(\omega)\hat{\rho}'_{_S}(t)\hat{S}^\dagger(\omega) - \left\{\hat{S}^\dagger(\omega)\hat{S}(\omega), \hat{\rho}'_{_S}(t)\right\}\right] \\
&+ \sum_{\omega>0}\sum_k \pi|g_k|^2 N_{_T}(\omega_k)\, \delta(\omega - \omega_k)\left[2\hat{S}^\dagger(\omega)\hat{\rho}'_{_S}(t)\hat{S}(\omega) - \left\{\hat{S}(\omega)\,\hat{S}^\dagger(\omega), \hat{\rho}'_{_S}(t)\right\}\right]\,,
\end{aligned} \tag{3.33}$$

where the negative frequencies have been excluded by the summation considering that $\omega_k > 0$, while in the second term we used the property $\hat{S}(-\omega) = \hat{S}^\dagger(\omega)$. Now we can define the function

$$G(\omega) = \sum_k \pi|g_k|^2\, \delta(\omega - \omega_k)\,, \tag{3.34}$$

and we obtain

$$\begin{aligned}\partial_t\hat{\rho}'_{_S} =&\sum_{\omega>0} G(\omega)[1+N_{_T}(\omega)]\left[2\,\hat{S}(\omega)\hat{\rho}'_{_S}(t)\,\hat{S}^\dagger(\omega) - \left\{\hat{S}^\dagger(\omega)\,\hat{S}(\omega)\,,\,\hat{\rho}'_{_S}(t)\right\}\right]\\ &+\sum_{\omega>0} G(\omega)N_{_T}(\omega)\left[2\,\hat{S}^\dagger(\omega)\hat{\rho}'_{_S}(t)\,\hat{S}(\omega) - \left\{\hat{S}(\omega)\,\hat{S}^\dagger(\omega)\,,\,\hat{\rho}'_{_S}(t)\right\}\right].\end{aligned} \tag{3.35}$$

The function $G(\omega)$ depends on the spectral density of the harmonic oscillator bath and on the system-bath interaction strength g_k. Note that in most circumstances the spectrum of the harmonic oscillator bath is a continuum, thus the summation is replaced by an integral over ω_k and g_k is a continuous function $g(\omega_k)$. The function $G(\omega)$ is non-zero-valued only in correspondence of a bath mode frequency. Looking Eq. (3.35), the physical meaning of $G(\omega)$ is clear: it only allows an exchange of energy with the system if it is resonant with some frequency of the bath. The expression of $G(\omega)$ in Eq. (3.34) is reminiscent of the Fermi's golden rule, it quantifies the system rate of emission in the environment. The two terms of Eq. (3.35) describe the two directions of the system-bath energy exchange: the first term describes the system loss of energy while the second one depicts the transfer of bath excitations toward the system. Note that at zero temperature there are no excitations in the bath, indeed $N_{_T}(\omega)=0$ and the second term vanishes. On the other hand the first term remains finite, and the energy is only drained away from the system.

It can be convenient to recast the Eq. (3.35) as

$$\begin{aligned}\partial_t\hat{\rho}'_{_S} =&\frac{\gamma_{_S}}{2}\sum_{\omega>0} \widetilde{G}(\omega)[1+N_{_T}(\omega)]\left[2\,\hat{S}(\omega)\hat{\rho}'_{_S}(t)\,\hat{S}^\dagger(\omega) - \left\{\hat{S}^\dagger(\omega)\,\hat{S}(\omega)\,,\,\hat{\rho}'_{_S}(t)\right\}\right]\\ &+\frac{\gamma_{_S}}{2}\sum_{\omega>0} \widetilde{G}(\omega)N_{_T}(\omega)\left[2\,\hat{S}^\dagger(\omega)\hat{\rho}'_{_S}(t)\,\hat{S}(\omega) - \left\{\hat{S}(\omega)\,\hat{S}^\dagger(\omega)\,,\,\hat{\rho}'_{_S}(t)\right\}\right].\end{aligned} \tag{3.36}$$

where we have introduced the dissipation rate $\gamma_{_S} = 2G(\omega_{_S})$ and the dimensionless spectral function $\widetilde{G}(\omega) = G(\omega)/G(\omega_{_S})$, with $\omega_{_S}$ the characteristic frequency of the system: for instance the cavity mode frequency or atom transition frequency. It is the time to go back to the Schrödinger picture in which

$$\hat{\rho}_{_S} \overset{\text{def}}{=} e^{\frac{i}{\hbar}\hat{H}_S t}\hat{\rho}'_{_S}e^{-\frac{i}{\hbar}\hat{H}_S t}. \tag{3.37}$$

The two terms of Eq. (3.36) are invariant under this transformation and we obtain the following expression for the time evolution of $\hat{\rho}_{_S}$:

$$\partial_t\hat{\rho}_{_S} = \frac{i}{\hbar}\left[\hat{H}_{_S}\,,\,\hat{\rho}_{_S}\right] + \frac{\gamma_{_S}}{2}\mathcal{D}_{_T}(\hat{S})\hat{\rho}_{_S} \tag{3.38}$$

where $\mathcal{D}_{_T}(\hat{S})$ defines the dissipation superoperator at finite temperature T

$$\begin{aligned}\mathcal{D}_{_T}(\hat{S})\hat{\rho}_{_S} =&\sum_{\omega>0} \widetilde{G}(\omega)[1+N_{_T}(\omega)]\left[2\,\hat{S}(\omega)\hat{\rho}_{_S}\,\hat{S}^\dagger(\omega) - \left\{\hat{S}^\dagger(\omega)\,\hat{S}(\omega)\,,\,\hat{\rho}_{_S}\right\}\right]\\ &+\sum_{\omega>0} \widetilde{G}(\omega)N_{_T}(\omega)\left[2\,\hat{S}^\dagger(\omega)\hat{\rho}_{_S}\,\hat{S}(\omega) - \left\{\hat{S}(\omega)\,\hat{S}^\dagger(\omega)\,,\,\hat{\rho}_{_S}\right\}\right].\end{aligned} \tag{3.39}$$

Note that the dimensionless spectral function $\widetilde{G}(\omega)$ depends on the kind of bath that we are considering. For a 3D electromagnetic field, for instance, $\widetilde{G}(\omega) \propto \omega^3$ and it vanishes for $\omega \to 0$.

Let us go a few steps backward. Before applying the rotating wave approximation, the time evolution of $\hat{\rho}'_S$ was expressed by Eq. (3.27). If we follow the same steps detailed above we find that $\hat{\rho}'_S$ is evolving as

$$\begin{aligned}\partial_t \hat{\rho}'_S =& \frac{\gamma}{2} \sum_{\omega>0} \sum_{\omega'} e^{i(\omega'-\omega)t}\, \widetilde{G}(\omega)[1+N_T(\omega)] \Big[\hat{S}(\omega)\hat{\rho}'_S(t)\hat{S}^\dagger(\omega') - \hat{S}^\dagger(\omega')\hat{S}(\omega)\hat{\rho}'_S(t) \Big] + h.c. \\ &+ \frac{\gamma}{2} \sum_{\omega>0} \sum_{\omega'} e^{-i(\omega'-\omega)t}\, \widetilde{G}(\omega) N_T(\omega) \Big[\hat{S}^\dagger(\omega)\hat{\rho}'_S(t)\hat{S}(\omega') - \hat{S}(\omega')\hat{S}^\dagger(\omega)\hat{\rho}'_S(t) \Big] + h.c.\,. \end{aligned} \tag{3.40}$$

Now we apply a kind of rotating wave approximation by neglecting only the negative frequencies in the summation over ω'. This is justified by considering that, ω being positive, the factor $e^{-i(\omega'-\omega)t}$ rotates faster for those terms. At zero temperature, with the assumption that $\widetilde{G}(\omega) = 1$ is a constant, and going back to the Schrödinger picture we obtain that

$$\partial_t \hat{\rho}_S = \frac{i}{\hbar} \Big[\hat{H}_S \,,\, \hat{\rho}_S \Big] + \frac{\gamma}{2} \Big[2\, \hat{S}_- \hat{\rho}_S \hat{S}_-^\dagger - \Big\{ \hat{S}_-^\dagger \hat{S}_- \,,\, \hat{\rho}_S \Big\} \Big] \tag{3.41}$$

where we have introduced the jump operator

$$\hat{S}_- \overset{\text{def}}{=} \sum_{\omega>0} \hat{S}(\omega) = \sum_{\omega>0} \sum_{\epsilon' - \epsilon = \hbar\omega} \langle \epsilon \,|\hat{S}|\epsilon' \rangle \, |\epsilon \,\rangle\langle \epsilon'| = \sum_{\epsilon'>\epsilon} \langle \epsilon \,|\hat{S}|\epsilon' \rangle \, |\epsilon \,\rangle\langle \epsilon'| \;, \tag{3.42}$$

in which we recall that $\{\epsilon\}$ and $\{|\epsilon\rangle\}$ are the eigenvalues and eigenstates of $\hat{H}_S$ respectively. At $T = 0$, the bath can only absorb energy from the system, so only jumps going downward in the system eigenstates are permitted ($\epsilon' > \epsilon$).

3.1.2 Master equations for atoms and cavities

Let us apply the general Lindblad master equations that we have microscopically derived above to the two elementary bricks of cavity QED models: linear cavities, and two-level atoms. We will consider here the simplified case of zero temperature and constant spectral function $G(\omega)$. In this conditions a very convenient description is given by Equation (3.41).

Damped cavity master equation

Let us consider a single mode linear cavity, whose Hamiltonian is

$$\hat{H}_c/\hbar = \omega_c \hat{a}^\dagger \hat{a}, \tag{3.43}$$

where $\hat{a}^\dagger$ and $\hat{a}$ are the creation and annihilation operator of a cavity field mode of frequency ω_c. We assume that the cavity is coupled to the environment through the interaction Hamiltonian:

$$\hat{H}_I/\hbar = \hat{S} \otimes \hat{B} = (\hat{a} + \hat{a}^\dagger) \sum_k \left(g_k \hat{b}_k + g_k^* \hat{b}_k^\dagger \right) . \tag{3.44}$$

Let us compute the jump operator $\hat{S}_-$, using the eigenstates of H_c that are the Fock states $|n\rangle$, i.e. $\hat{H}_c |n\rangle = n \hbar \omega_c |n\rangle$:

$$\hat{S}_- = \sum_{n'>n} \langle n|\hat{a} + \hat{a}^\dagger|n'\rangle \ |n\rangle\langle n'| = \sum_{n'>n} \langle n|\hat{a}|n'\rangle \ |n\rangle\langle n'| = \hat{a} \, , \tag{3.45}$$

where we have used that $\langle n|\hat{a} + \hat{a}^\dagger|n'\rangle = 0$ for any $n' > n$. The resulting Lindblad master equation for a damped cavity at zero temperature is

$$\partial_t \hat{\rho} = -i \left[\omega_c \, \hat{a}^\dagger \hat{a} \, , \hat{\rho} \right] + \frac{\gamma_c}{2} \left(2\hat{a}\hat{\rho}\hat{a}^\dagger - \hat{a}^\dagger \hat{a} \hat{\rho} - \hat{\rho} \hat{a}^\dagger \hat{a} \right) , \tag{3.46}$$

where γ_c quantifies the intensity of the coupling to the environment, that depends on the values of the g_k and on the bath density of states (Eq. (3.34)). This equation efficiently describes the *dissipation* of photons (and energy) into the bath. Indeed, by considering the dynamics of the average number of photons $\hat{N}$, we get

$$\partial_t \langle \hat{N} \rangle = \mathrm{Tr}\left\{ \hat{a}^\dagger \hat{a} \, (\partial_t \hat{\rho}) \right\} = -\gamma_c \langle \hat{N} \rangle \quad \Rightarrow \quad \langle \hat{N} \rangle(t) = \langle \hat{N} \rangle(0) e^{-\gamma_c t} \, . \tag{3.47}$$

Here, we see that the mean number of photons and the energy inside the cavity decays exponentially to zero.

Dissipation and decoherence in a two-level atom

Let us now follow the same procedure for a two-level atom, whose Hamiltonian reads

$$\hat{H}_a/\hbar = \frac{\omega_a}{2} \, \hat{\sigma}_z \, , \tag{3.48}$$

and in which the interaction Hamiltonian between the system and the bath is chosen to be

$$\hat{H}_I/\hbar = \hat{S} \otimes \hat{B} = (\hat{\sigma}_- + \hat{\sigma}_+) \sum_k \left(g_k \hat{b}_k + g_k^* \hat{b}_k^\dagger \right) . \tag{3.49}$$

Here the $\hat{\sigma}$ operators are the usual Pauli matrices operating on the space of a two-level system with transition frequency ω_a. We compute the jump operator $\hat{S}_-$ for the two-level atom by using its eigenstate $|g\rangle$ and $|e\rangle$:

$$\hat{S}_- = \langle g|\hat{\sigma}_- + \hat{\sigma}_+|e\rangle \ |g\rangle\langle e| = \langle g|\hat{\sigma}_-|e\rangle \ |g\rangle\langle e| = \hat{\sigma}_- \, , \tag{3.50}$$

where we used the equality $\hat{\sigma}_+ |e\rangle = 0$. Using this result, we can now express the zero temperature Lindblad master equation of a damped two-level atom as

$$\partial_t \hat{\rho} = -i \left[\frac{\omega_a}{2} \hat{\sigma}_z \, , \hat{\rho} \right] + \frac{\gamma_a}{2} \left(2\hat{\sigma}_- \hat{\rho} \hat{\sigma}_+ - \hat{\sigma}_+ \hat{\sigma}_- \hat{\rho} - \hat{\rho} \hat{\sigma}_+ \hat{\sigma}_- \right) , \tag{3.51}$$

where, as for the damped linear cavity, γ_a quantifies the intensity of the coupling to the environment.

Two-level systems (also called qubits, as shortcut for quantum bits) are the elementary bricks of quantum computation. The idea is to store information in these systems and to exploit their quantumness to improve the performances of certain algorithms. However, the coupling to the environment is an obstacle to this exploitation, since the uncontrolled bath degrees of freedom represent a loss of information. Imagine to store the information in a superposition of $|g\rangle$ and $|e\rangle$, namely:

$$|\Psi(0)\rangle = (|g\rangle + |e\rangle)/\sqrt{2} \, . \tag{3.52}$$

This quantum information is gradually deteriorated by the presence of the environment. Indeed the superposition coherence $\langle e|\hat{\rho}|g\rangle$ exponentially vanishes as

$$\begin{aligned} \partial_t \langle e|\hat{\rho}|g\rangle \; &= \langle e|\partial_t \hat{\rho}|g\rangle \; = -(i\omega_a + \gamma_a/2) \langle e|\hat{\rho}|g\rangle \\ \Rightarrow \quad \langle e|\hat{\rho}(t)|g\rangle \; &= \langle e|\hat{\rho}(0)|g\rangle \, e^{-i\omega_a t - \gamma_a t/2} \, . \end{aligned} \tag{3.53}$$

This process of information loss in quantum systems is generally called *decoherence*.

3.1.3 Consistent master equation in the ultrastrong coupling regime

In the previous section we have obtained the description of dissipation for a cavity mode (Eq. (3.46)) and for a two-level system (Eq. (3.46)). At this point one could be interested in determining the master equation of a generic cavity QED system $\hat{H}_S$ in which cavity and atom are coupled. A first guess could be to simply combine the two dissipation terms of the cavity and the atom, into the following master equation:

$$\partial_t \hat{\rho} = -\frac{i}{\hbar} \left[\hat{H}_S, \hat{\rho} \right] + \frac{\gamma_c}{2} \left(2\hat{a} \hat{\rho} \hat{a}^\dagger - \hat{a}^\dagger \hat{a} \hat{\rho} - \hat{\rho} \hat{a}^\dagger \hat{a} \right) + \frac{\gamma_a}{2} \left(2\hat{\sigma}_- \hat{\rho} \hat{\sigma}_+ - \hat{\sigma}_+ \hat{\sigma}_- \hat{\rho} - \hat{\rho} \hat{\sigma}_+ \hat{\sigma}_- \right) . \tag{3.54}$$

While this master equation, that is broadly used in quantum optics, is a good approximation in the case of a weak coupling $g \ll \sqrt{\omega_c \omega_a}$ between the cavity and the atom, however, it can lead to very pathological results in the ultrastrong coupling regime.

Indeed, as we have seen in Section 2.2.3, the ground state of cavity QED models in the ultrastrong coupling regime contains a finite population of photons and atomic excitations. What happens to these excitations when the dissipation is considered? Are they going to be emitted in the environment? A naïve answer would be that,

since the ground state contains photons and that the mirrors of the cavity are not perfect, these photons should be able to escape the cavity. However this reasoning leads to a wrong conclusion. Indeed, since these photons are part of the system ground state, extracting a photon means to increase the state energy. At the same time, a dissipated photon contributes to increase the environment energy. So, we finish with the contradictory conclusion that the total energy of the system and the environment is clearly not conserved.

In order to better illustrate this idea, let us consider the concrete case of the resonant ($\omega_c = \omega_a = \omega$) Jaynes-Cumming model

$$\hat{H}_{JC}/\hbar = \omega\, \hat{a}^\dagger \hat{a} + \frac{\omega}{2}\hat{\sigma}_z + g(\hat{a}\,\hat{\sigma}_+ + \hat{a}^\dagger \hat{\sigma}_-)\,. \tag{3.55}$$

Considering the same cavity-to-environment coupling chosen in the previous section, we have

$$\hat{H}_I/\hbar = (\hat{a} + \hat{a}^\dagger) \sum_k \left(g_k \hat{b}_k + g_k^* \hat{b}_k^\dagger \right)\,. \tag{3.56}$$

Let us compute the jump operator $\hat{S}_-$ on the eigenstates of the Jaynes-Cumming Hamiltonian that are presented in Section 2.2.3. For $g \ll \omega$ we get

$$\begin{aligned} \hat{S}_- &\simeq \sum_{n'>n} \sum_{\eta,\eta'=\pm} \langle n,\eta|\hat{a} + \hat{a}^\dagger|n',\eta'\rangle \;|n,\eta\rangle\langle n',\eta'| \\ &= \sum_{n'>n} \sum_{\eta\eta'=\pm} \langle n,\eta|\hat{a}|n',\eta'\rangle \;|n,\eta\rangle\langle n',\eta'| = \hat{a}\,, \end{aligned} \tag{3.57}$$

where we used the fact that $\langle n,\eta|\hat{a}^\dagger|n',\eta'\rangle = 0$ for any $n' > n$. In a similar way, for an atomic coupling to the bath of the form in Eq. (3.49), and in the limit of weak coupling $g \ll \omega$, one can find that the jump operator is $\hat{\sigma}_-$. This means that in this limit the master equation in Eq. (3.54) is a valid description of dissipation for the Jaynes-Cumming model.

However, this is no more the case in the ultrastrong coupling regime. Indeed, for $g > \omega$ the state $|0,g\rangle$ is no more the ground state of the system, and, since we have that $\hat{a}\,|0,g\rangle = \hat{\sigma}_-\,|0,g\rangle = 0$, Eq. (3.54) predicts that this state is stable. That an excited state is stable in absence of driving and for a bath at zero temperature is not physical. Furthermore, since $\hat{a}\,|n,-\rangle\,, \hat{\sigma}_-\,|n,-\rangle \neq 0$, the ground state $|n,-\rangle$ of the system for $g > \omega$ is never stable under the action of the bare cavity and atom jump operators $\hat{a}$ and $\hat{\sigma}_-$.

Nevertheless, the general master equations that we have microscopically derived in Section 3.1.1 (Eqs. (3.41) and (3.38)), are consistent with the ultrastrong coupling regime and immune from the unphysical artefacts illustrated above.

3.2 External driving

Most of the experiments in quantum optics, particularly those in cavity and circuit QED, require the presence of an external driving, both to excite and to probe the considered system. The driving can be of different forms, electric or optical, coherent or incoherent.

Here we start by consider the microscopic description of cavity mode coherently driven by a laser beam. Let us consider the full quantum description of the laser field and cavity mode through the total Hamiltonian

$$\hat{H}_{tot}/\hbar = \omega_c\,\hat{a}^\dagger\hat{a} + \omega_p\,\hat{b}^\dagger\hat{b} + g\left(\hat{a}^\dagger + \hat{a}\right)\left(\hat{b}^\dagger + \hat{b}\right)\,, \tag{3.58}$$

where $\hat{b}$ is the annihilation operator of the the laser field, ω_p is its frequency, the $\hat{\sigma}$ operators describe the two-level system degrees of freedom, and g quantifies the strength of the coupling, as detailed in Sec. 2.2.2.

The common assumption here, and in general whenever a system-environment coupling is studied, is to consider the environment as unaffected by the system. Thus the laser field stays in a coherent state and the total density matrix will be of the form:

$$\hat{\rho}_{tot}(t) = \hat{\rho}(t) \otimes |\beta(t)\rangle\langle\beta(t)|\,. \tag{3.59}$$

Here $\hat{\rho}(t)$ is the density operator of the cavity and $|\beta(t)\rangle$ is the coherent state of the laser field that, neglecting the effect of the interaction with the cavity, evolves as:

$$|\beta(t)\rangle = e^{-i\omega_p\,\hat{b}^\dagger\hat{b}\,t}\,|\beta_0\rangle = |\beta_0 e^{-i\omega_p t}\rangle\,. \tag{3.60}$$

Injecting the density operator defined by Eqs. (3.59) and (3.60) into the Liouville-von Neumann equation

$$\partial_t\hat{\rho}_{tot}(t) = -\frac{i}{\hbar}\left[\hat{H}_{tot}, \hat{\rho}_{tot}(t)\right]\,, \tag{3.61}$$

and tracing out the laser mode degrees of freedom we see that the density operator of only the cavity evolves in time as

$$\partial_t\hat{\rho}(t) = -\frac{i}{\hbar}\left[\hat{H}(t), \hat{\rho}(t)\right]\,, \tag{3.62}$$

with

$$\hat{H}(t)/\hbar = \omega_c\,\hat{a}^\dagger\hat{a} + \Omega_p\cos(\omega_p t)(\hat{a} + \hat{a}^\dagger)\,, \tag{3.63}$$

and where we introduced the pumping strength $\Omega_p = g\beta_0/2$ (here we have chosen β_0 to be real).

Note that one can obtain a different expression for the driving by using the rotating wave approximation (see Sec. 2.2.2) on the complete Hamiltonian in Eq. (3.58). Neglecting the anti-resonant terms, and by following the same reasoning as above, leads to obtain the following Hamiltonian for the driven cavity

$$\hat{H}_{pump}(t)/\hbar = \omega_c\,\hat{a}^\dagger\hat{a} + Fe^{-i\omega_p t}\hat{a}^\dagger + F^* e^{i\omega_p t}\hat{a}\,, \tag{3.64}$$

where we have introduced the complex pumping strength $F = g\beta_0$ (for an arbitrary complex β_0). Very similar expressions can be obtained to describe the driving of a two-level atom, by simply replacing the creation and annihilation operators of the cavity mode with the ladder operators $\sigma_\pm$.

Note that here the coupling to an external environmental bosonic mode does not represent a loss of knowledge. Indeed, since the environment is in a precisely known state, it does not reduce our knowledge on the observables of the cavity mode. This explains why it has been possible to describe the coupling to this environment through an Hamiltonian term for the cavity. This will not be the case for other kind of environments in which a non-unitary time evolution is necessary, see subsection 3.1.

Rotating frame

It is in general not desirable to have a time dependence in the Hamiltonian. In the case of the Hamiltonian driving term in Eq. (3.64), it is possible to move to a rotating frame in which the time dependence is removed. This is done through the unitary transformation

$$\hat{U}(t) = e^{i\,\omega_p\,\hat{a}^\dagger\hat{a}\,t}\,. \tag{3.65}$$

The cavity density operator in the rotating frame reads

$$\hat{\rho}' = \hat{U}\,\hat{\rho}\,\hat{U}^\dagger\,, \tag{3.66}$$

and its time evolution is

$$\begin{aligned}\partial_t\hat{\rho}' &= (\partial_t\hat{U})\hat{\rho}\hat{U}^\dagger + \hat{U}\hat{\rho}(\partial_t\hat{U}^\dagger) + \hat{U}(\partial_t\hat{\rho})\hat{U}^\dagger \\ &= i\omega_p\left[\hat{a}^\dagger\hat{a},\hat{\rho}'\right] - \frac{i}{\hbar}\left[\hat{H}',\hat{\rho}'\right] = -\frac{i}{\hbar}\left[\hat{H}' - \hbar\,\omega_p\hat{a}^\dagger\hat{a}\,,\hat{\rho}'\right]\,.\end{aligned} \tag{3.67}$$

Thus the time evolution of the cavity density operator in the rotating frame is governed by the relative Hamiltonian

$$\begin{aligned}\hat{H}^{(rf)} &= \hat{H}' - \hbar\,\omega_p\hat{a}^\dagger\hat{a} = \hat{U}\hat{H}\hat{U}^\dagger - \hbar\,\omega_p\hat{a}^\dagger\hat{a} \\ &= -\Delta\,\hat{a}^\dagger\hat{a} + F\hat{a}^\dagger + F^*\hat{a}\,.\end{aligned} \tag{3.68}$$

where we introduced the frequency detuning $\Delta = \omega_p - \omega_c$ and where

$$\hat{U}(t)\,\hat{a}\,\hat{U}^\dagger(t) = e^{-i\,\omega_p\,t}\,\hat{a}\,. \tag{3.69}$$

Note that the populations are unchanged by this transformation, this means that computing the average of Hermitian operators, such as the number of photons $\hat{a}^\dagger\hat{a}$ does not requires to go back in the non-rotating frame.

Chapter 4

Theory of quantum measurement and trajectories

The degrees of control that experimental quantum optics has reached nowadays gives a renewed value to the question of quantum measurement. Indeed, while in the past it was only possible to test the ensemble properties of quantum systems, the improvements in reducing the decoherence, and the advances in the precision of the measurements, today allow physicists to track the quantum state trajectory even on single shot experiments [87–89]. This is paving the way to new physics, encompassing feedback control [86, 128] and quantum thermodynamics [90–93].

In this chapter we introduce the most basic elements of the theory of quantum measurement. Traditionally, quantum physics describes the measurement through the *projection postulate*. However, since the very early stages of the quantum theory this postulate has stimulated intense debates, whose relation with the foundations of quantum physics is reported in Section (4.1). In particular, we will show that in the framework of an informational interpretation of quantum mechanics, the projection measurement can be seen as an information update. While the projection postulate represents the most basic description of a quantum measurement, in Sec. 4.2 we will present a more general theory of measurement, in which other kinds of information updates can be considered. In particular we will consider the case of the continuous measurement, in which the continuous extraction of information allows to reconstruct the quantum state trajectory of the system. In Section 4.3 we will present the physics of stochastic quantum trajectories, and in particular their relation with the Lindblad master equation approach.

4.1 The measurement problem in the foundations of quantum physics

The measurement problem in quantum mechanics, and the associated *quantum state collapse*[1], is one of the most intriguing – and often misunderstood – concept in physics.

[1]Note that for traditional reasons "quantum state collapse" is less used than "wave function collapse". In order to stay more general, here we preferred to use the first expression, however there are no substantial differences between them. Furthermore this term is also an equivalent denomination of the projection postulate.

Since the origin of quantum mechanics, this problem has stimulated vivid debates, formulation of gedanken experiments and paradoxes [21, 129].

In quantum physics, a system is described by its quantum state that evolves deterministically, according to the Schrödinger equation. When a certain observable is measured, the quantum state collapses by projection into the eigenstate of the observable operator that corresponds to the observed output value (this process is further explained in section 4.2.1). This process, that is typically introduced as a postulate of quantum physics, is characterised by some counterintuitive features.

- Randomness: even if the measurement apparatus and the system evolve deterministically, the result of a measurement is in principle unpredictable. It is the first time that a physical theory has an *intrinsic randomness*, which is generally perceived as philosophically inconvenient. This unease is well expressed by the famous sentence by Einstein: "God doesn't play dice with the world" (p.58 of Ref. [20]).

- Nonlocality: the quantum state collapse is instantaneous and it changes the system description at a distance arbitrary large with respect to the place in which the measurement occurred. This seems to be at odds with the speed-of-light limit and is the subject of the largely debated EPR paradox [21].

- Two different evolution principles: there is no way to explain the random process of quantum state collapse from the deterministic Schrödinger equation; the origins of the quantum state collapse as a physical process are unclear.

Classically, through an ideal measurement, it is in principle possible to determine with certainty the values of all the system variables. In this condition of complete knowledge, the results of all subsequent measurements are perfectly predictable. Although measurement and probability are crucial for practical applications, they are completely irrelevant in the foundation of classical mechanics.

The picture is completely different in quantum physics. In this case, no matter the perfection of the measurement or the *degree of knowledge* on the system, there is always a measurement whose result is uncertain. The best one can do is to determine the probability distribution of the physical system observables. One could interpret this uncertainty as due to an incomplete knowledge of the considered quantum system. This is the idea of *"hidden" variable* interpretations of quantum physics. They attribute the randomness of quantum measurement to the existence of some "hidden" variables whose knowledge is incomplete.

Although many of these interpretations are consistent (the most famous is probably the Bohm or pilot-wave theory [130, 131]) they are generally rejected by most physicists. An important contribution in determining this rejection is probably due to the result of Bell in 1964, who showed that any deterministic "hidden" variable theory must be nonlocal [22]. The idea that a theory is based on nonlocal variables is indeed

undesired. Less famous than the Bell's result, another black mark for deterministic "hidden" variable theories is represented by the quantum contextuality. In any theory that explains quantum mechanics in deterministic terms, the result of an observable measurement depends on the specific setup of the measurement [7, 23].

Another viable option to reconcile these controversial aspects, is to interpret quantum mechanics in terms of the knowledge and the information that an observer has of a physical system. Rather then an element of reality, the quantum state can be seen as the description of observer's knowledge about the system. In these terms, for instance, the quantum state collapse is simply the update of the observer's knowledge due to the new information obtained by the measurement. Just like in the classical theory of probability and information, a knowledge update can be random, it can be nonlocal and instantaneous[2], and it happens in a very different fashion compared to the probability distribution time evolution.

Probably the first interpretation of quantum mechanics adopting this idea is due to the Copenhagen school, and particularly to the original thinking of Bohr: "It is wrong to think that the task of physics is to find out how nature is. Physics concerns what we can say about nature" [132]. In the same vein, QBism, a very recent interpretation of quantum physics, tries to extend the Bayesian conception of probability to the quantum frame [5, 6]. In this view the quantum state is a representation of the subjective *degrees of belief* of the observer, as defined by decision theory and the de Finetti's theorem [133, 134].

In the next sections, we will adopt this point of view. The quantum state is a representation of the observer's knowledge about the realisation of the measurement outcomes. The quantum state collapse is the update of the information that the observer has about the system. Only one more conceptual assumption is needed to justify certain properties of quantum measurements: any kind of measurement is always accompanied by an interaction between the measured and the measuring system. The measurement is an act of interaction. At the end of Sec. 4.2.1, we will show the importance of this last assumption in a concrete situation.

4.2 General theory of quantum measurement

In the previous section we have interpreted the quantum state collapse as an update of the information that an observer has on a system. In Sec. 4.2.1 we describe this information update, within the mathematical formalism of quantum mechanics, and in the form of a projective measurement. The projective measurement is not the only way to acquire information from a system. For this reason in Sec. 4.2.2 we present

[2]When one acquires new information about a system that is correlated to a second distant system, the knowledge update is instantaneous, and concerns both systems even if they are separated by large distances. It may seem to be a nonlocal process, however it is not the case, because no faster-than-light transmission of information occurs.

a more general description of quantum measurement. We point that this section is inspired by Ref. [135].

4.2.1 Projective measurement

In its traditional description, quantum measurement is defined in terms of projective measurements. Let us consider the measurement of the observable $\hat{\Lambda}$. This operator is Hermitian and can be written in a diagonal form, in terms of its eigenspace projectors $\hat{\Pi}_\lambda$ and the associated real eigenvalues λ:

$$\hat{\Lambda} = \sum_\lambda \lambda \hat{\Pi}_\lambda \,. \tag{4.1}$$

For simplicity, we will assume the ensemble $\{\lambda\}$ to be discrete.

When a measurement of the observable $\hat{\Lambda}$ is performed, one obtains as result one of the eigenvalues $\{\lambda\}$. The probability $p_\lambda(t)$ to observe a particular eigenvalue λ at time t, is provided by the Born rule [136]:

$$p_\lambda(t) = \mathrm{Tr}\Big\{\hat{\Pi}_\lambda \hat{\rho}(t)\Big\} \tag{4.2}$$

where $\hat{\rho}(t)$ represents the *a priori* knowledge of the system at time t.

We are interested in determining the *a posteriori* conditional state after the measurement, i.e. the state $\hat{\rho}_\lambda(t^+)$ that we deduce at a time t^+ just after obtaining from the measurement the result λ. This is determined by a projective update on the *a priori* state $\hat{\rho}(t)$:

$$\hat{\rho}_\lambda(t^+) = \frac{\hat{\Pi}_\lambda \hat{\rho}(t) \hat{\Pi}_\lambda}{p_\lambda(t)} \,. \tag{4.3}$$

If the system is in a pure state (a state of maximal knowledge) before the measurement, i.e. $\hat{\rho}(t) = |\psi(t)\rangle\langle\psi(t)|$, the Eqs. (4.2) and (4.3) can be simplified as

$$p_\lambda(t) = \langle\psi(t)|\, \hat{\Pi}_\lambda \,|\psi(t)\rangle \;, \tag{4.4}$$

$$|\psi_\lambda(t^+)\rangle = \frac{\hat{\Pi}_\lambda \,|\psi(t)\rangle}{\sqrt{p_\lambda(t)}} \,. \tag{4.5}$$

This is the mathematical formulation of the *projection postulate* or the quantum state collapse, as we referred to in Section (4.1). If, in addition, the spectrum of $\hat{\Lambda}$ is non-degenerate, then the eigenspace projectors can be expressed as $\hat{\Pi}_\lambda = |\lambda\rangle\langle\lambda|$ (where $|\lambda\rangle$ are the eigenstates of $\hat{\Lambda}$), and Equation (4.3) defines a *von Neumann measurement*.

Given Eqs. (4.2) and (4.3), it is possible to determine the unconditional state $\hat{\rho}(t^+)$, i.e. the state obtained when the measurement results are not retained:

$$\hat{\rho}(t^+) = \sum_\lambda p_\lambda(t) \hat{\rho}_\lambda(t^+) = \sum_\lambda \hat{\Pi}_\lambda \hat{\rho}(t) \hat{\Pi}_\lambda \,. \tag{4.6}$$

This implies that, if we do not keep track of the measurement results, an *a priori* pure state will be in general updated to a mixed state, increasing the entropy of the system.

From an information theory point of view, this is very strange: if one does not receive any information on the outcomes of the measurement, then the state of knowledge $\hat{\rho}$ should remain unchanged. To get out of this impasse, we recall an assumption on the nature of quantum measurement that we introduced at the end of Section (4.1): any kind of measurement is always accompanied by an interaction between the measured and measuring system. This interaction must be accounted for in the time evolution of the system, and this introduces a finite effect on the state of the measured system.

The picture is totally different in the classical conception, in which measurement is seen as a passive reception of information. From this point of view, rejecting the outcomes is equivalent to not performing any measurement, and in both cases it would leave the system state of knowledge unchanged.

4.2.2 General description of measurement

In undergraduate courses, the projective measurement is typically the only kind of quantum measurement to be introduced. However, this is not the most general kind of measurement. It describes an ideal measurement, and it is inadequate when the measurement extracts only partial information about the observable or when one needs to include the effect of errors.

Indeed, there are many situations in which the *a posteriori* conditional state $\hat{\rho}_\lambda(t^+)$ is clearly not obtained through a projective update of the *a priori* state $\hat{\rho}(t)$. This is for instance the case in photon counting. As we will see in detail later, when a photon is detected the state of the system is update by annihilating a photon:

$$\hat{\rho}_{_{det}}(t^+) \propto \hat{a}\,\hat{\rho}(t)\,\hat{a}^\dagger \tag{4.7}$$

where $\hat{a}$ is the photon annihilation operator and $\hat{\rho}_{_{det}}$ describes the system state conditional to the detection of a photon. The non-Hermitian operator $\hat{a}$ is clearly not a projector.

A more generalised description of quantum measurement is provided by the formalism of positive-operator valued measures (POVM). In this formalism every measurement outcome r is associated to an operator $\hat{M}_r$. When a measurement returns the value r the system state is updated as

$$\hat{\rho}_r(t + t_m) = \frac{\hat{M}_r \hat{\rho}(t) \hat{M}_r^\dagger}{p_r(t)}\,, \tag{4.8}$$

where t_m is the measurement duration time that, contrary to the projective measurement, is finite. The operators $\{\hat{M}_r\}$ are called *measurement operators*, and they are not required to be Hermitian.

The probability to measure the value r given the *a priori* state of knowledge $\hat{\rho}(t)$ is:

$$p_r(t) = \mathrm{Tr}\Big\{\hat{M}_r^\dagger \hat{M}_r \hat{\rho}(t)\Big\} \,. \tag{4.9}$$

Positive probabilities imply that the operators $\{\hat{M}_r^\dagger \hat{M}_r\}$ are positive semidefinite operators. The fact that the probability must sum to 1 for any *a priori* state, the set of operators $\{\hat{M}_r\}$ must satisfy the *completeness relation*:

$$\sum_r \hat{M}_r^\dagger \hat{M}_r = \hat{\mathbb{1}}_S \,, \tag{4.10}$$

where $\hat{\mathbb{1}}_S$ is the unit system operator. The set of operators $\{\hat{M}_r^\dagger \hat{M}_r\}$ is POVM, defines a set of semidefinite positive Hermitian operators respecting the completeness relation, explaining the name of the formalism.

Note that this formalism includes the projective measurement, however, it is not based on the concept of "observable". The outcomes $\{r\}$ are not necessarily eigenstates of an observable Hermitian operator. They represent the possible results of the measurement, but the kind of information that they bring (represented by $\hat{M}_r$) depends on the circumstances. This idea will be more clear when considering concrete situations. In section 4.3 we will use the formalism to derive the description of photon counting and homodyne detection.

The POVM formalism in terms of projective measurements

It is important to know, that any POVM can be obtained as an interaction with an ancillary quantum system followed by a projective measurement on the ancillary system.

Let us consider a system in the initial state $|\psi(t)\rangle$. The system interacts with an ancillary system whose initial state is $|\theta(t)\rangle$. The initial uncorrelated state of the total system is

$$|\Psi(t)\rangle = |\theta(t)\rangle\,|\psi(t)\rangle \,. \tag{4.11}$$

After a time t_m^- the total system evolves into the state ($\hbar = 1$)

$$|\Psi(t + t_m^-)\rangle = e^{-iH_I t_m^-}\,|\theta(t)\rangle\,|\psi(t)\rangle \,, \tag{4.12}$$

where H_I is the interaction between the two subsystems, which are now correlated. Measuring one of them gives information on the other. The idea is now to recover the measurement operator $\hat{M}_r$ for the original system by performing a projective measurement on the ancillary system.

Let us measure on the ancillary system the observable $\hat{R}$, whose spectrum $\{r\}$ is assumed to be discrete and non-degenerate. The *a posteriori* state of the system,

conditional to the observation of the outcome r is obtained by using the associated projector $\Pi_r = |r\rangle\langle r| \otimes \hat{\mathbb{1}}_S$:

$$|\Psi(t+t_m)\rangle = \frac{|r\rangle\langle r|\, e^{-iH_I t_m^-} |\theta(t)\rangle\, |\psi(t)\rangle}{\sqrt{p_r(t)}}\,, \tag{4.13}$$

where the probability of observing the value r is

$$p_r(t) = \langle\psi(t)|\, \langle\theta(t)|\, e^{+iH_I t_m^-} \left[\, |r\rangle\langle r| \otimes \hat{\mathbb{1}}_S \,\right] e^{-iH_I t_m^-} |\theta(t)\rangle\, |\psi(t)\rangle\ . \tag{4.14}$$

After the projective measurement the ancillary system is in the state $|r\rangle$, the total state is factorisable and the total system state can be written as:

$$|\Psi(t+t_m)\rangle = |r\rangle\, \frac{\hat{M}_r\, |\psi(t)\rangle}{\sqrt{p_r(t)}}\,. \tag{4.15}$$

Here we defined the measurement operator $\hat{M}_r$ acting on the original system Hilbert space, defined as

$$\hat{M}_r = \langle r|\, e^{-iH_I t_m^-} |\theta(t)\rangle\ . \tag{4.16}$$

It can be proven that any set of measurement operators $\{\hat{M}_r\}$ can be recast by the suitable unitary evolution and a projective measurement [137]. This explains why only the projective measurement is presented in undergraduate courses. Even if POVM measurements are more general and useful for concrete applications, the projective measurement is the fundamental description of measurement in quantum physics.

Imperfect measurement

It is important to note that the measurement formalism introduced above describe the situation of an ideal measurement. On the other hand, one could be interested in describing real measurements in which the role of experimental errors can not be neglected. Referring to the previous subsection this can be explained for instance by a mixed initial state of the ancilla or by imperfections in recording the projection measurement results.

In this more general case the measurement description requires to introduce *operation superoperators*. To every measurement outcome r is associated an operation superoperator

$$\mathcal{O}_r\, \hat{\rho} = \sum_j \hat{O}_{r,j}\, \hat{\rho}\, \hat{O}_{r,j}^\dagger \tag{4.17}$$

acting on the space of the system density operators $\hat{\rho}$.

After observing the outcome r the system state of knowledge is updated to the conditional state

$$\hat{\rho}_r(t+t_m) = \frac{\mathcal{O}_r \hat{\rho}_r(t)}{p_r(t)}\,, \tag{4.18}$$

where t_m is the measurement duration and

$$p_r(t) = \mathrm{Tr}\{\mathcal{O}_r \hat{\rho}_r(t)\} = \mathrm{Tr}\left\{ \sum_j \hat{O}_{r,j}^\dagger \hat{O}_{r,j}\, \hat{\rho} \right\} . \tag{4.19}$$

Continuous weak measurement

Among the many kind of possible measurement, continuous monitoring plays a crucial role, especially from an experimental point of view. Photon counting and homodyne detection, are among the most used techniques in experimental quantum optics and cavity QED [89, 126, 138–140]. In order to give a formal description of these measurement (Sec. 4.3), we need to define a continuous weak measurement. In simple words it consists of a measurement that continuously monitors the system, without introducing important perturbations on the system. Within the POVM formalism it is possible to give a precise definition of this kind of measurements.

In the POVM formalism the unconditional state of the system $\hat{\rho}(t + t_m)$ is given as

$$\hat{\rho}(t + t_m) = \sum_r p_r(t) \hat{\rho}_r(t + t_m) = \sum_r \hat{M}_r(t_m) \hat{\rho}(t) \hat{M}_r^\dagger(t_m) \,, \tag{4.20}$$

where we consider $\hat{M}_r(t_m)$ to depend on the measurement duration t_m, that is indeed justified by Equation (4.16).

Contrary to the case of projective measurement (Eq. (4.6)), it is now possible to have a set of measurement operators $\{\hat{M}_r(t_m)\}$ such that Eq. (4.20) describes a continuous evolution for any *a priori* state $\hat{\rho}(t)$. More precisely, it is possible to choose the measurement operators $\{\hat{M}_r(t_m)\}$ such that

$$\lim_{t_m \to 0} \frac{\hat{\rho}(t + t_m) - \hat{\rho}(t)}{t_m} = \frac{\mathrm{d}\hat{\rho}(t)}{\mathrm{d}t} \tag{4.21}$$

defines a finite differential when t_m goes to zero. This condition defines a special subclass of POVM measurements: the continuous weak measurements.

In some situation one can be interested in monitoring the system continuously. At all times one would have a result and a conditional state, defining a *quantum state trajectory*. In other words a continuous measurement is a measurement in which information is continually extracted from a system. The requirement in Eq. (4.21) means that the amount of information extracted goes to zero as the duration of the measurement goes to zero: the measurement is weak.

In section 4.3 we will study the quantum state trajectories arising from two continuous weak measurements that are crucially important in experimental quantum optics: photon counting and homodyne detection.

4.3 Quantum trajectories and stochastic Schrödinger equations

In Chapter 3 we have seen that the information stored in a quantum system is generally deteriorated by the coupling to the environment. Indeed, information is indeed lost into the unmonitored degrees of freedom of the environment. Our knowledge of the system is incomplete in this case, and the system is in general described through a mixed-state density operator. However by performing a continuous measurement on the environment it is possible to retrieve the lost information, and to track the *quantum trajectory* of the maximal-knowledge pure state of the system. In this section we consider two commonly used kinds of monitoring in quantum optics: *photon counting* and *homodyne detection*. In particular we will derive a microscopical description of photon counting in Sec. 4.3.1, and present the relation between stochastic evolutions and the Lindblad master equation (Sec. (4.3.2)). Finally in Sec. 4.3.3 we briefly report, the formal step that allows to define a diffusive stochastic evolution in the case of homodyne detection.

We pointout that this section takes inspiration from Refs. [126, 135].

4.3.1 Photon counting: microscopic description

Let us consider a cavity QED system continuously monitored through photon counting. The system is coupled to a bath represented by the modes of the extracavity electromagnetic field. Assuming to be able to monitor all theses modes one could detect all the photons that are released by the cavity QED system. This would allow to track the state of the system at all times, i.e. to follow the quantum trajectory of the system. The idea here is to model the system-bath energy exchanges and the detection of these exchanges by continuously monitoring the environment.

Very similarly to what we did to derive the Lindblad master equation in Sec. 3.1.1, we define the total Hamiltonian of the system S and the coupled environment B as

$$\hat{H} = \hat{H}_S + \hat{H}_B + \hat{H}_I \,, \tag{4.22}$$

where $\hat{H}_S$ and $\hat{H}_B$ are respectively the free Hamiltonian of the system and the environment, while $\hat{H}_I$ describes the interaction between them. For this derivation we find it convenient to use a bath of harmonic oscillators with a continuous spectrum:

$$\hat{H}_B = \int_0^\infty \mathrm{d}\omega\, \hbar\,\omega\, \hat{b}^\dagger(\omega)\hat{b}(\omega)\,, \qquad \left[\hat{b}(\omega), \hat{b}^\dagger(\omega')\right] = \delta(\omega - \omega')\,, \tag{4.23}$$

where $\hat{b}(\omega)$ is the annihilation operator of the bath mode with only positive energies ω.

The interaction is modeled as

$$\hat{H}_I = i\hbar \int_0^\infty \mathrm{d}\omega\; g(\omega)(\hat{a} - \hat{a}^\dagger)\left[\hat{b}(\omega) + \hat{b}^\dagger(\omega)\right]\,, \tag{4.24}$$

where $g(\omega)$ quantifies the interaction strength and $\hat{a}$ is an operator acting on the Hilbert space of the cavity QED system. More precisely, for this derivation we need $\hat{a}$ to be of the form

$$\hat{a} = \sum_{\epsilon' - \epsilon = \hbar\omega_0} c_{\epsilon\epsilon'} \left|\epsilon\right\rangle\!\left\langle\epsilon'\right| , \tag{4.25}$$

where $c_{\epsilon\epsilon'}$ are arbitrary complex coefficients and where the sum runs over all the eigenvalues ϵ' and ϵ of $\hat{H}_S$ with an arbitrary energy difference $\hbar\omega_0 > 0$. Thus the operator $\hat{a}$ encodes the loss of a precise amount of energy $\hbar\omega_0$ in the system (very similarly to an annihilation operator for a linear cavity). Note that this choice for $\hat{a}$ is quite general, indeed any interaction term can be decomposed in a sum of operators like those assumed here.

In the interaction picture the evolution is determined by only the interaction Hamiltonian term

$$\hat{H}'_I(t) = i\hbar \int_0^\infty \mathrm{d}\omega\, g(\omega)(\hat{a}\, e^{-i\omega_0 t} - \hat{a}^\dagger e^{i\omega_0 t}) \left[\hat{b}(\omega)e^{-i\omega t} + \hat{b}^\dagger(\omega)e^{i\omega t}\right] . \tag{4.26}$$

Adopting the rotating wave approximation, we neglect the anti-resonant terms, giving

$$\hat{H}'_I(t) = i\hbar \int_0^\infty \mathrm{d}\omega\, g(\omega) \left[\hat{a}\,\hat{b}^\dagger(\omega)e^{i(\omega-\omega_0)t} - \hat{a}^\dagger\hat{b}(\omega)e^{-i(\omega-\omega_0)t}\right] . \tag{4.27}$$

At this point we need to use the Markov approximation. Since the coupling is weak we can assume that in the time scale of the system-bath interaction, the exponential terms in Eq. (4.27) oscillate very rapidly. This means that only the modes that are very close to ω_0 give a significant contribution in the integral above. If $g(\omega)$ is smooth enough, we can replace it by the constant value $g(\omega) = g(\omega_0) \stackrel{\text{def}}{=} \sqrt{\gamma/2\pi}$. For the same reason we can also send the bottom limit of the integral to negative infinity. After this approximation the interaction Hamiltonian reads

$$\hat{H}'_I(t) = i\hbar\sqrt{\gamma} \left[\hat{a}\,\hat{b}^\dagger(t) - \hat{a}^\dagger\hat{b}(t)\right] , \tag{4.28}$$

where the time-dependent bath operators

$$\hat{b}(t) = \frac{1}{\sqrt{2\pi}} \int_{-\infty}^{\infty} \mathrm{d}\omega\, \hat{b}(\omega)e^{-i(\omega-\omega_0)t} , \tag{4.29}$$

can be shown to be related by the following commutation relation

$$\left[\hat{b}(t), \hat{b}^\dagger(t')\right] = \delta(t - t') . \tag{4.30}$$

In section Sec. 4.2.2 we have shown that is possible to justify a general measurement operator $\hat{M}_r$ on the system, as a projective measurement on a coupled ancillary system. Here the situation is pretty similar, the bath represents the ancillary system,

and we will derive the photon-counting measurement operators of only the system from a projective measurement on the bath mode.

Let us assume the bath at zero temperature, and in its vacuum state $|0\rangle$. The bath and the system are initially in a uncorrelated state

$$|\Psi'(t)\rangle = |\psi'(t)\rangle\,|0\rangle\ , \tag{4.31}$$

where $|\psi'(t)\rangle$ and $|\Psi'(t)\rangle$ are respectively the *a priori* state of the system and of the total system in the interaction picture ($|0\rangle$ is unchanged in this picture).

The evolution of this state after a small interval of time Δt is obtained through the following operator

$$\hat{U}(t+\Delta t,t) = e^{-\frac{i}{\hbar}\int_t^{t+\Delta t}\hat{H}'_I(t_1)\,\mathrm{d}t_1} = \exp\left\{\sqrt{\gamma}\int_t^{t+\Delta t}\left[\hat{a}\,\hat{b}^\dagger(t)-\hat{a}^\dagger\hat{b}(t)\right]\mathrm{d}t\right\}\ . \tag{4.32}$$

For small values of Δt the evolution can be developed using a Dyson expansion. As we will see below, due to delta function in the commutator in Eq. (4.30), we will need to keep the second-order expansion of the time evolution operator:

$$\hat{U}(t+\Delta t,t) \simeq \hat{\mathbb{1}} - \frac{i}{\hbar}\int_t^{t+\Delta t}\mathrm{d}t_1\,\hat{H}'_I(t_1) - \frac{1}{\hbar^2}\int_t^{t+\Delta t}\mathrm{d}t_1\int_t^{t_1}\mathrm{d}t_2\,\hat{H}'_I(t_1)\hat{H}'_I(t_2)\,. \tag{4.33}$$

Using this approximation and considering that $\hat{b}(t)\,|0\rangle = 0$ for all t we can compute the state change $|\Psi'(t+\Delta t)\rangle - |\Psi'(t)\rangle$:

$$|\Psi'(t+\mathrm{d}t)\rangle - |\Psi'(t)\rangle \simeq \sqrt{\gamma}\int_t^{t+\Delta t}\mathrm{d}t_1\,\hat{a}\,\hat{b}^\dagger(t_1)\,|\psi'(t)\rangle\,|0\rangle \tag{4.34a}$$

$$-\gamma\int_t^{t+\Delta t}\mathrm{d}t_1\int_t^{t_1}\mathrm{d}t_2\,\hat{a}^\dagger\hat{a}\,\hat{b}(t_1)\hat{b}^\dagger(t_2)\,|\psi'(t)\rangle\,|0\rangle \tag{4.34b}$$

$$+\gamma\int_t^{t+\Delta t}\mathrm{d}t_1\int_t^{t_1}\mathrm{d}t_2\,\hat{a}\,\hat{a}\,\hat{b}^\dagger(t_1)\hat{b}^\dagger(t_2)\,|\psi'(t)\rangle\,|0\rangle\ . \tag{4.34c}$$

Even if the second term of this equation seems to be of second order in $\mathrm{d}t$, it is not the case. Indeed, since

$$\hat{b}(t_1)\hat{b}^\dagger(t_2)\,|0\rangle = \left[\hat{b}(t_1),\hat{b}^\dagger(t_2)\right]|0\rangle = \delta(t_1-t_2)\,|0\rangle\,, \tag{4.35}$$

the first integral in the term can be solved obtaining

$$-\gamma\int_t^{t+\Delta t}\mathrm{d}t_1\int_t^{t_1}\mathrm{d}t_2\,\hat{a}^\dagger\hat{a}\,\hat{b}(t_1)\hat{b}^\dagger(t_2)\,|\psi'(t)\rangle\,|0\rangle = -\frac{\gamma}{2}\int_t^{t+\Delta t}\mathrm{d}t_1\,\hat{a}^\dagger\hat{a}\,|\psi'(t)\rangle\,|0\rangle\,. \tag{4.36}$$

Going to the limit $\Delta t \to \mathrm{d}t$ we find that $\int_t^{t+\Delta t}\mathrm{d}t_1 \to \mathrm{d}t$ and so we can finally express the first-order time evolution of the state

$$|\Psi'(t+\mathrm{d}t)\rangle = \left(\hat{\mathbb{1}} - \mathrm{d}t\,\gamma\,\frac{\hat{a}^\dagger\hat{a}}{2}\right)|\psi'(t)\rangle\,|0\rangle + \sqrt{\mathrm{d}t}\,\sqrt{\gamma}\,\hat{a}\,|\psi'(t)\rangle\,|1_{(t)}\rangle \tag{4.37}$$

where we introduced $|1_{(t)}\rangle \stackrel{\text{def}}{=} \sqrt{\mathrm{d}t}\,\hat{b}^\dagger(t)\,|0\rangle$ that represents the one-photon state in the bath mode labelled by t, and with the property

$$\langle 1_{(t)}|1_{(t')}\rangle = \mathrm{d}t\,\langle 0|\,\hat{b}(t)\hat{b}^\dagger(t')\,|0\rangle = \mathrm{d}t\,\delta(t-t') \tag{4.38}$$

Note that we dropped the third term in Eq. (4.34c), it is of order $\mathrm{d}t^2$ and thus negligible (as we will see, it corresponds to the detection of two photons).

Let us now perform a projective measurement with a photon-detector that is able to count the number of photons in the bath at time t. In other words a projective measurement of the observable $\hat{b}^\dagger(t)\hat{b}(t)$. By obtaining the result 0, the state of the system is updated by projection on the bath vacuum $|0\rangle$

$$|\Psi_0'(t+\mathrm{d}t)\rangle = \frac{1}{\sqrt{p_0(t,\mathrm{d}t)}}\left(\hat{\mathbb{1}} - \mathrm{d}t\,\gamma\,\frac{\hat{a}^\dagger\hat{a}}{2}\right)|\psi'(t)\rangle\,|0\rangle \tag{4.39}$$

where

$$p_0(t,\mathrm{d}t) = \langle\psi'(t)|\left(\hat{\mathbb{1}}_S - \mathrm{d}t\,\gamma\,\frac{\hat{a}^\dagger\hat{a}}{2}\right)\left(\hat{\mathbb{1}}_S - \mathrm{d}t\,\gamma\,\frac{\hat{a}^\dagger\hat{a}}{2}\right)|\psi'(t)\rangle\,\langle 0|0\rangle\ , \tag{4.40}$$

with $\hat{\mathbb{1}}_S$ is the unitary operator of only the system. The same state update is described by the measurement operator

$$\hat{M}_0' = \hat{\mathbb{1}}_S - \mathrm{d}t\,\gamma\,\frac{\hat{a}^\dagger\hat{a}}{2} \tag{4.41}$$

acting on the Hilbert space of only the system.

On the other hand, if the measurement returns the value 1 it means that a photon has been detected in the bath and the *a posteriori* conditional state is updated as:

$$|\Psi_1'(t+\mathrm{d}t)\rangle = \frac{\sqrt{\mathrm{d}t}\,\sqrt{\gamma}}{\sqrt{p_1(t,\mathrm{d}t)}}\hat{a}\,|\psi'(t)\rangle\,|1_{(t)}\rangle\,, \tag{4.42}$$

where p_1 the probability to detect a photon

$$p_1(t,\mathrm{d}t) = \mathrm{d}t\,\gamma\,\langle\psi'(t)|\,\hat{a}^\dagger\hat{a}\,|\psi'(t)\rangle\ \langle 1_{(t)}|1_{(t)}\rangle\ . \tag{4.43}$$

In the reduced space of only the system, the same update of the state is produce by the measurement operator

$$\hat{M}_1' = \sqrt{\mathrm{d}t}\,\sqrt{\gamma}\,\hat{a}\,. \tag{4.44}$$

Note that, after the detection, the projective measurement is supposed to leave the bath in the state $|1_{(t)}\rangle$, while the approach is based on a initial vacuum state. In reality, photon detection, at least at optical frequencies, is done by absorption, so the bath is always left in the vacuum state. However, this consideration is not essential to the validity of the approach presented. Indeed since the interaction with the bath in assumed Markovian, at time $t+\mathrm{d}t$ the system is not affected anymore by the bath mode $\hat{b}(t)$. The fact that this mode contains a photon is unimportant because the system is already interacting with other modes that are still in the vacuum state.

In conclusion this derivation allowed to determine the expression of the photon-counting measurement operators from a microscopic description.

Photon-counting description from a minimal measurement model

An alternative procedure to derive the equations that describe the system evolution under photon-counting monitoring is by defining the minimal model fulfilling the requirement in Eq. (4.21), namely

$$\frac{\hat{\rho}(t+\mathrm{d}t)-\hat{\rho}(t)}{\mathrm{d}t}=\frac{\sum_r \hat{M}_r(\mathrm{d}t)\hat{\rho}(t)\hat{M}_r^\dagger(\mathrm{d}t)-\hat{\rho}(t)}{\mathrm{d}t} \tag{4.45}$$

must define a finite differential for every *a priori* state $\hat{\rho}(t)$.

A minimal model for a continuous monitoring is a measurement that at all times t returns at least two possible outcomes, i.e. $r=0,1$. A general guess for $\hat{M}_0(\mathrm{d}t)$ is a linear expansion in $\mathrm{d}t$, namely

$$\hat{M}_0(\mathrm{d}t)=\hat{\mathbb{1}}_S-\left(\frac{\hat{R}}{2}+i\hat{H}\right)\mathrm{d}t \tag{4.46}$$

where $\hat{R}$ and $\hat{H}$ are Hermitian operators. Given this choice for $\hat{M}_0(\mathrm{d}t)$ the second measurement operator $\hat{M}_1(\mathrm{d}t)$ is determined from the completeness relation in Eq. (4.10):

$$\hat{M}_0(\mathrm{d}t)^\dagger\hat{M}_0(\mathrm{d}t)+\hat{M}_1(\mathrm{d}t)^\dagger\hat{M}_1(\mathrm{d}t)=\hat{\mathbb{1}}_S\,. \tag{4.47}$$

In order to satisfy this relation we have

$$\hat{M}_1(\mathrm{d}t)^\dagger\hat{M}_1(\mathrm{d}t)=\hat{\mathbb{1}}_S-\hat{M}_0(\mathrm{d}t)^\dagger\hat{M}_0(\mathrm{d}t)=\hat{R}\,\mathrm{d}t\,. \tag{4.48}$$

Then we conclude that a minimal model, fulfilling the requirements above (continuous unconditional evolution and the completeness relation), is given by the following measurement operators:

$$\hat{M}_0(\mathrm{d}t)=\hat{\mathbb{1}}_S-\left(\frac{\hat{c}^\dagger\hat{c}}{2}+i\hat{H}\right)\mathrm{d}t\,, \tag{4.49a}$$

$$\hat{M}_1(\mathrm{d}t)=\sqrt{\mathrm{d}t}\,\hat{c}\,, \tag{4.49b}$$

where we introduce the arbitrary operator $\hat{c}$ (replacing $\hat{R}=\hat{c}^\dagger\hat{c}$) and where $\hat{H}$ is an Hermitian operator that allows to include the Hamiltonian evolution in our description.

The two measurement operators that we derived here from a minimal model of continuous measurement are clearly equivalent to those we obtain by a microscopic approach, under the replacement $\hat{c}\to\sqrt{\gamma}\,\hat{a}$. Except for absence of the Hamiltonian that $\hat{H}$ (that is recovered by going back in the Schrödinger picture) the operator $\hat{M}_0'$ in Eq. (4.41) is indeed equivalent to the measurement operator $\hat{M}_0$ that we derived here.

According to Eq. (4.20), the unconditional evolution of the state under the action of this measurement is

$$\hat{\rho}(t+\mathrm{d}t) = \left[1 - \left(\frac{\hat{c}^\dagger\hat{c}}{2} + i\hat{H}\right)\mathrm{d}t\right]\hat{\rho}(t)\left[1 - \left(\frac{\hat{c}^\dagger\hat{c}}{2} - i\hat{H}\right)\mathrm{d}t\right] + \mathrm{d}t\,\hat{c}\,\hat{\rho}(t)\,\hat{c}^\dagger\,, \tag{4.50}$$

which is importantly equivalent to the following Lindblad master equation

$$\frac{\mathrm{d}\hat{\rho}(t)}{\mathrm{d}t} = -i\left[\hat{H},\hat{\rho}(t)\right] + \mathcal{D}(\hat{c})\hat{\rho}(t)\,, \tag{4.51}$$

where we used the superoperator

$$\mathcal{D}(\hat{c})\hat{\rho} = \hat{c}\,\hat{\rho}\,\hat{c}^\dagger - \frac{1}{2}\left(\hat{c}^\dagger\hat{c}\,\hat{\rho} + \hat{\rho}\,\hat{c}^\dagger\hat{c}\right)\,. \tag{4.52}$$

Note that by replacing $\hat{c}$ with $\sqrt{\gamma}\,\hat{a}$ in Equation (4.51) one recovers the damped-cavity master equation derived in Sec. 3.1.2 (Eq. (3.46)), reinforcing the idea that this minimal model is a good description of photodetection.

4.3.2 Photon counting: stochastic quantum jumps

Once that photon-counting monitoring is defined in the formalism of quantum measurement we are interested in studying the conditional evolution of the system, when it is submitted to this kind of monitoring. We will see that it is possible to describe this evolution through an "adapted" Schrödinger equation based on stochastic Poissonian increments.

Let us start by noting that the probability to obtain the result $r = 1$

$$p_1(t,\mathrm{d}t) = \mathrm{Tr}\Big\{\hat{M}_1(\mathrm{d}t)^\dagger\hat{M}_1(\mathrm{d}t)\hat{\rho}(t)\Big\} = \mathrm{d}t\,\mathrm{Tr}\big\{\hat{c}^\dagger\hat{c}\,\hat{\rho}(t)\big\} \tag{4.53}$$

is infinitesimal. This means that for almost all times the result of the continuous measurement will be $r = 0$, and that the system evolves according to $\hat{M}_0(\mathrm{d}t)$ in a continuous (but non-unitary) evolution. At random times, and precisely at the rate $p_1(t,\mathrm{d}t)/\mathrm{d}t$, a result $r = 1$ occurs. These relatively rare events are called *detections*, and they are accompanied by an abrupt discontinuous evolution, described by the measurement operator $\hat{M}_1(\mathrm{d}t)$, and that are called *quantum jumps*. This stochastic time evolution is illustrated in Fig. 4.1. It is important to have in mind the context in which we defined this stochastic behaviour. The detections are the result of a measurement, and quantum jumps are the conditional updates of the observer's knowledge of the system.

A convenient way to encode this kind of behaviour is through the so called *stochastic Schrödinger equation*. First of all, we need to introduce the discontinuous function $N(t)$ denoting the number of photodetections counted up to time t. This function allows to define the stochastic increment $\mathrm{d}N(t) = N(t+\mathrm{d}t) - N(t)$, that is equal 1

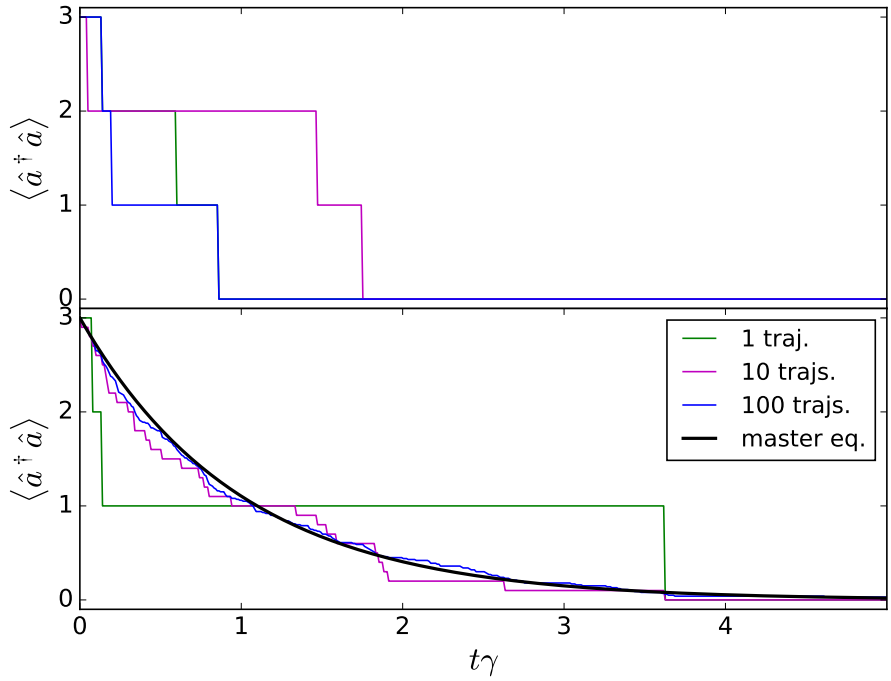

Figure 4.1 The quantum trajectories of a linear cavity relaxing from the three photon Fock state to the vacuum state, where γ quantifies the coupling to the environment. Top panel: three different realisations of quantum trajectories. The abrupt jumps correspond to the detection of photons. Bottom panel: the average of an increasing number of trajectories approaches the solution of the master equation.

when a photon is detected and 0 otherwise. From this definition it is straightforward to recognise the following properties of $\mathrm{d}N(t)$:

$$\mathrm{d}N(t)^2 = \mathrm{d}N(t)\,, \tag{4.54a}$$

$$\mathrm{E}[\mathrm{d}N(t)] = p_1(t,\mathrm{d}t) = \mathrm{d}t\,\langle\psi_c(t)|\hat{c}^\dagger\hat{c}|\psi_c(t)\rangle\ , \tag{4.54b}$$

where we are assuming that the system is in a maximal-knowledge pure state $|\psi_c(t)\rangle$ at time t, and where we introduced the ensemble expectation value $\mathrm{E}[\cdot]$. The subscript c in the state $|\psi_c(t)\rangle$, stands for conditional. From now on all the states considered are conditional on the result of the detection, and the brackets $\langle\,\cdot\,\rangle_c(t) = \langle\psi_c(t)|\cdot|\psi_c(t)\rangle$ denote the average on these states.

The conditional evolution defined by the measurement operators in Eqs. (4.49a)

and (4.49a) can alternatively be expressed as

$$\begin{aligned} \mathrm{d}\,|\psi_c(t)\rangle = \mathrm{d}N(t)\left(\frac{\hat{c}}{\sqrt{\langle\hat{c}^\dagger\hat{c}\rangle_c(t)}} - \hat{\mathbb{1}}_S\right)|\psi_c(t)\rangle \\ + [1-\mathrm{d}N(t)]\,\mathrm{d}t\left(\frac{\langle\hat{c}^\dagger\hat{c}\rangle_c(t)}{2} - \frac{\hat{c}^\dagger\hat{c}}{2} - i\hat{H}\right)|\psi_c(t)\rangle\,, \end{aligned} \tag{4.55}$$

where we used the expansion of the denominator in the state update associated to $\hat{M}_0$ to the first order in $\mathrm{d}t$:

$$|\psi_{c0}(t+\mathrm{d}t)\rangle = \frac{\hat{M}_0\,|\psi_c(t)\rangle}{\sqrt{\langle\hat{M}_0^\dagger\hat{M}_0\rangle_c}} = \left\{\hat{\mathbb{1}}_S - \mathrm{d}t\left[i\hat{H} + \frac{\hat{c}^\dagger\hat{c}}{2} - \frac{\langle\hat{c}^\dagger\hat{c}\rangle_c(t)}{2}\right]\right\}|\psi_c(t)\rangle\ . \tag{4.56}$$

The stochastic evolution in Equation (4.55) can be simplified further by considering that $\mathrm{d}N(t)\,\mathrm{d}t = o(\mathrm{d}t)$:

$$\mathrm{d}\,|\psi_c(t)\rangle = \left[\mathrm{d}N(t)\left(\frac{\hat{c}}{\sqrt{\langle\hat{c}^\dagger\hat{c}\rangle_c(t)}} - \hat{\mathbb{1}}_S\right) + \mathrm{d}t\left(\frac{\langle\hat{c}^\dagger\hat{c}\rangle_c(t)}{2} - \frac{\hat{c}^\dagger\hat{c}}{2} - i\hat{H}\right)\right]|\psi_c(t)\rangle\ . \tag{4.57}$$

This expression defines the stochastic Schrödinger equation for a photon-counting monitoring. Note that the equation is nonlinear in $|\psi_c(t)\rangle$ due to the presence of the averages $\langle\cdot\rangle_c$. The name of the equation comes from the fact that the equation acts on and is solved by pure states.

As we have seen in Equation (4.51) the unconditional state of the system evolves according to a Lindbladian master equation. In accordance with this, here we show that the ensemble average of $|\psi_c(t)\rangle$ evolves through the same master equation. Let us define the pure state density operator $\hat{\rho}_c(t) = |\psi_c(t)\rangle\langle\psi_c(t)|$. Its time evolution is given by (using the notation $|\mathrm{d}\psi_c(t)\rangle = \mathrm{d}\,|\psi_c(t)\rangle$)

$$\begin{aligned} \mathrm{d}\hat{\rho}_c(t) &= |\mathrm{d}\psi_c(t)\rangle\langle\psi_c(t)| + |\psi_c(t)\rangle\langle\mathrm{d}\psi_c(t)| + |\mathrm{d}\psi_c(t)\rangle\langle\mathrm{d}\psi_c(t)| \\ &= \Big\{\mathrm{d}N(t)\mathcal{G}(\hat{c}) - \mathrm{d}t\,\mathcal{H}(i\hat{H} + \hat{c}^\dagger\hat{c}/2)\Big\}\,\hat{\rho}_c(t) \end{aligned} \tag{4.58}$$

where we introduced the nonlinear superoperators

$$\mathcal{G}(\hat{r})\hat{\rho} = \frac{\hat{r}\hat{\rho}\hat{r}^\dagger}{\mathrm{Tr}\{\hat{r}^\dagger\hat{r}\hat{\rho}\}} - \hat{\rho}\,, \tag{4.59a}$$

$$\mathcal{H}(\hat{r})\hat{\rho} = \hat{r}\hat{\rho} + \hat{\rho}\hat{r} - \mathrm{Tr}\{\hat{r}\hat{\rho} + \hat{\rho}\hat{r}\}\,\hat{\rho}\,. \tag{4.59b}$$

The ensemble average state of the system is defined as

$$\hat{\rho}(t) = \mathrm{E}[\,\hat{\rho}_c(t)] = \sum_{\hat{\rho}_c}\hat{\rho}_c(t)p(\hat{\rho}_c, t)\,, \tag{4.60}$$

where the sum over all the possible $\hat{\rho}_c$ and $p(\hat{\rho}_c, t)$ is the probability to be in such $\hat{\rho}_c$ at time t. By using the relation

$$\mathrm{E}[\,\mathrm{d}N(t)\hat{\rho}_c(t)] = \sum_{\hat{\rho}_c} p_1(t,\mathrm{d}t)\, p(\hat{\rho}_c,t)\hat{\rho}_c(t) = \mathrm{d}t\,\mathrm{E}[\,\mathrm{Tr}\{\hat{c}^\dagger\hat{c}\,\hat{\rho}_c(t)\}\,\hat{\rho}_c(t)]\,, \tag{4.61}$$

one can easily retrieve the same Lindbladian master equation in Eq. (4.51)

$$\frac{\mathrm{d}\hat{\rho}(t)}{\mathrm{d}t} = -i\left[\hat{H},\hat{\rho}(t)\right] + \mathcal{D}(\hat{c})\hat{\rho}(t)\,. \tag{4.62}$$

This basically means that if we take an infinite number of solution to the stochastic Eq. (4.57), the average of them is a solution of the Lindbladian master equation, as illustrated in the bottom panel of Fig. 4.1. The Monte Carlo wave function (MCWF) method, one of the most used (numerical) method in the study of open quantum system is based on this idea [141–144]. The next section is devoted to introduce this method.

Furthermore, we would like to stress that this relation between quantum trajectories and Lindblad master equation clarifies the physical meaning of the latter. The Lindblad master equation describes the evolution of the density operator, representing our knowledge about the system, when we do not use any information about the environment. Information from photodetection measurement on the environment allows to infer a more precise estimation of the system state. In the ideal case in which all the photons escaping a cavity QED system are detected, our knowledge about the system can be described by a maximal-knowledge pure state at all times provided that the system was in a pure state at the initial time.

Monte Carlo wave function method

The existence of a mathematical map between the Lindblad master equation and stochastic state trajectories has been emphasised the first time in 1992 by Dalibard et al. [141]. This mathematical map has been later developed [142, 143], and extensively exploited for numerical approaches to open quantum system [144].

The idea is to approximate the solution of the Lindblad master equation by averaging a large number of quantum state trajectories. The numerical advantage behind the success of this method consists in the fact that, by simulating a stochastic Schrödinger equation, one only has to deal with a state of dimension d (the Hilbert space dimension), while working with density operator requires a space of order d^2. This means that this stochastic techniques, require less memory than a direct numerical integration, permitting to solve a master equation for larger values of d. In addition, the quantum trajectories can be sampled on different processors via parallel computing, that can considerably reduce the computing time of the method.

Let us consider the following general form for the Lindblad master equation

$$\frac{\mathrm{d}\hat{\rho}(t)}{\mathrm{d}t} = -i\left[\hat{H},\hat{\rho}(t)\right] + \sum_{\mu}\mathcal{D}(\hat{c}_\mu)\hat{\rho}(t)\,. \tag{4.63}$$

The stochastic Schrödinger equation whose average is equivalent to this master equation, is a generalised one in which the state of the system is conditional on different distinguishable type of detections labeled by μ:

$$\mathrm{d}\,|\psi_c(t)\rangle = \left[\mathrm{d}N_\mu(t)\left(\frac{\hat{c}_\mu}{\sqrt{\langle\hat{c}_\mu^\dagger\hat{c}_\mu\rangle_c(t)}} - \hat{\mathbb{1}}_S\right) + \mathrm{d}t\left(\frac{\langle\hat{c}_\mu^\dagger\hat{c}_\mu\rangle_c(t)}{2} - \frac{\hat{c}_\mu^\dagger\hat{c}_\mu}{2} - i\hat{H}\right)\right]|\psi_c(t)\rangle\ , \tag{4.64}$$

with

$$\mathrm{E}[\mathrm{d}N_\mu(t)] = p_\mu(t,\mathrm{d}t) = \mathrm{d}t\,\langle\hat{c}_\mu^\dagger\hat{c}_\mu\rangle_c(t)\,, \tag{4.65a}$$

$$\mathrm{d}N_\mu(t)\mathrm{d}N_\nu(t) = \mathrm{d}N_\mu(t)\delta_{\mu\nu}\,. \tag{4.65b}$$

The simplest method to solve this stochastic equation is to define a small time interval δt, and to compute the infinitesimal state evolution by random generation of the increments $\delta N_\mu(t) = 0, 1$.

However, since the increments $\delta N_\mu(t)$ are most of the time equal to zero, this is not the most efficient approach. A more efficient way to sample a quantum trajectory is through an iterative method, whose steps are listed above.

1. We choose the initial normalised state $|\psi_c(t_0)\rangle$ at times t_0.

2. A real number $r \in [0,1]$ is randomly generated.

3. Given the unnormalised state $|\widetilde{\psi}_c(t)\rangle$, whose evolution

$$\frac{\mathrm{d}\,|\widetilde{\psi}_c(t)\rangle}{\mathrm{d}t} = -\left(\sum_\mu \frac{\hat{c}_\mu^\dagger\hat{c}_\mu}{2} + i\hat{H}\right)|\widetilde{\psi}_c(t)\rangle\ , \tag{4.66}$$

   is not unitary, we let evolve this state from $|\widetilde{\psi}_c(t_0)\rangle = |\psi_c(t_0)\rangle$ up to the time t_1 in which the norm $\langle\widetilde{\psi}_c(t_1)|\widetilde{\psi}_c(t_1)\rangle = r$. The time t_1 is the time in which the next detection occurs.

4. For the detection at time t_1 we randomly generate its type μ_1, according to the following probabilities that are conditional on the detection occurrence:

$$\bar{p}_\mu(t_1) = \frac{p_\mu(t_1,\mathrm{d}t)}{\sum_\mu p_\mu(t_1,\mathrm{d}t)} = \frac{\langle\hat{c}_\mu^\dagger\hat{c}_\mu\rangle_c(t_1)}{\sum_\mu\langle\hat{c}_\mu^\dagger\hat{c}_\mu\rangle_c(t_1)}\,. \tag{4.67}$$

   Note that computing the averages $\langle\,\cdot\,\rangle_c$ on the unnormalised state $|\widetilde{\psi}_c(t_1)\rangle$ provides the good values for $\bar{p}_\mu(t_1)$.

5. The normalised state of the system at time t_1 is updated according to the occurred type of detection:

$$|\psi_c(t_1)\rangle = \frac{\hat{M}_{\mu_1}\,|\widetilde{\psi}_c(t_1)\rangle}{\sqrt{\langle\widetilde{\psi}_c(t)|\,\hat{M}_{\mu_1}^\dagger\hat{M}_{\mu_1}\,|\widetilde{\psi}_c(t_1)\rangle}} = \frac{\hat{c}_{\mu_1}\,|\widetilde{\psi}_c(t_1)\rangle}{\sqrt{\langle\widetilde{\psi}_c(t)|\,\hat{c}_{\mu_1}^\dagger\hat{c}_{\mu_1}\,|\widetilde{\psi}_c(t_1)\rangle}} \tag{4.68}$$

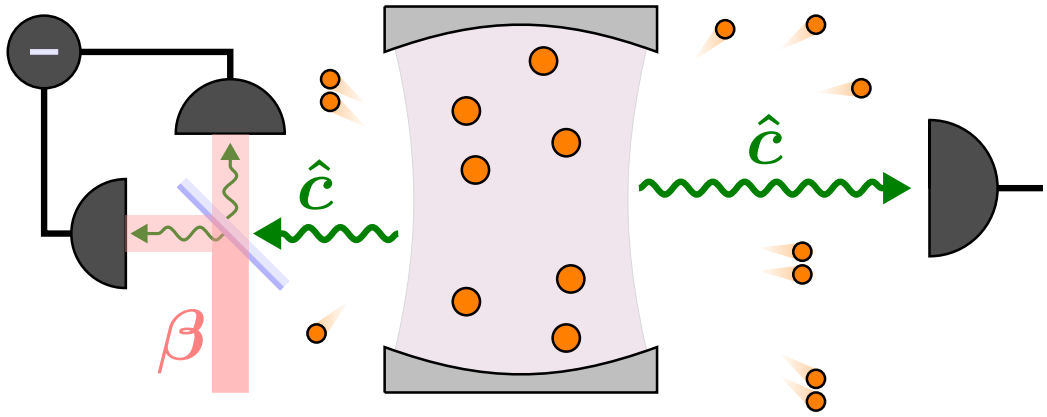

Figure 4.2 The two schemes of detection. Photon counting on the right side and homodyne detection on the left.

6. The method is iterated using $|\psi_c(t_1)\rangle$ as the initial state.

At the end of this procedure, we finish with a set of couples $\{(\mu_1, t_1); (\mu_2, t_2); \ldots; (\mu_n, t_n)\}$ (with $t_1 < t_2 < \ldots < t_n$), reporting the times and the types of registered detections, and that univocally defines a quantum trajectory.

The advantage of this method stays in the fact that since the detection are rare events it is convenient to generate the time of the next detection rather then generating the increments $\delta N_\mu(t)$ at each interval of time δt. The main numerical weight is represented by the integration in the step 3. However Eq. (4.66) is an ordinary linear differential equation that is efficiently solved by standard numerical techniques, such as Runge-Kutta integration.

Let us better clarify the meaning of step 3. The non-unitary evolution in Equation (4.66) is equivalently described by the (unnormalised) action of the non-detection measurement operator $\hat{M}_0(\mathrm{d}t) = \hat{\mathbb{1}}_S - \mathrm{d}t(\sum_\mu \hat{c}_\mu^\dagger \hat{c}_\mu/2 + i\hat{H})$. The norm of $|\widetilde{\psi}_c(t)\rangle$ is then equivalent to the probability of having no-detection up to time t. Thus it represents the right probability distribution to use in generating the random time of the next detection.

4.3.3 Homodyne detection: stochastic diffusive evolution

Beyond photon counting, another possible way to continuously monitor a quantum-optical system is through homodyne detection. It consists in a widely-used experimental technique which allows to access the cavity field quadratures [89, 138, 139].

The implementation of this kind of measurement is illustrated in Fig. 4.2. The cavity output field is mixed to a coherent field of a reference laser through a beam splitter. The mixed fields are then probed via (perfect) photodetectors. Assuming the beam splitter to be of perfect transmittance and the coherent field to have a large

amplitude, one can show that the measurement operator for the detection of this field is

$$\hat{M}_1(\mathrm{d}t) = \sqrt{\mathrm{d}t}\,(\hat{c} + \beta) \tag{4.69}$$

where β is the coherent field amplitude [126, 135] . In order to fulfill the completeness relation, the measurement operator for no-detection is required to be

$$\hat{M}_0(\mathrm{d}t) = -\mathrm{d}t\left[i\hat{H} + \frac{1}{2}\left(\beta^*\hat{c} - \beta\hat{c}^\dagger\right) + \frac{1}{2}\left(\hat{c}^\dagger + \beta^*\right)(\hat{c} + \beta)\right] \tag{4.70}$$

Note that these measurement operators can alternatively be obtained from the operators in Eqs. (4.49) through the transformation:

$$\hat{c} \to \hat{c} + \beta\,, \quad \hat{H} \to \hat{H} - i\frac{1}{2}(\beta^*\hat{c} - \beta\hat{c}^\dagger)\,. \tag{4.71}$$

Furthermore, the Lindblad master Equation (4.51) is invariant under this transformation. This means that the homodyne quantum trajectories generated by the measurement operators in Eqs. (4.69) and (4.70) are an alternative unraveling of the same master equation that describes the unconditional evolution of the system in the case of photon counting, Eq. (4.51).

The ideal limit of homodyne detection is when the coherent field amplitude β goes to infinity. In this case the number of detections per time unit is very large, and a stochastic Schrödinger equation based on point process increments $\mathrm{d}N(t)$ (see Eq. (4.57)), would not be the most convenient representation anymore. Indeed, a numerical implementation in these terms would require a too small time interval δt in order to ensure a negligible probability of multiple counting. The probability of a detection is indeed very large, and equal to

$$p_1(t, \mathrm{d}t) = \langle(\hat{c} + \beta)^\dagger(\hat{c} + \beta)\rangle_c(t)\,\mathrm{d}t \simeq \left[\beta^2 + \beta\langle\hat{c} + \hat{c}^\dagger\rangle_c(t)\right]\mathrm{d}t\,, \tag{4.72}$$

where the approximation is valid in the limit of $\beta \to \infty$. Note that here, and in the following, the amplitude β is for simplicity chosen to be real.

Even if detections are very frequent, the detected field is almost entirely due to the coherent field, associated to the operators β. This means that a single detection contains very little information about the system, and that the total jump operators $\hat{c} + \beta$ have a very small effect on its state. Indeed the action of the single detection measurement operator $\hat{M}_1$

$$\frac{\hat{M}_1\,|\psi_c(t)\rangle}{\sqrt{\langle\hat{M}_1^\dagger\hat{M}_1\rangle_c}} \simeq \frac{(\hat{c} + \beta)\,|\psi_c(t)\rangle}{\sqrt{\langle(\hat{c} + \beta)^\dagger(\hat{c} + \beta)\rangle_c(t)}} \tag{4.73}$$

approaches the identity in the limit of $\beta \to \infty$. In this limit, the occurrence of an infinite number of jumps is counterbalanced by their infinitesimally small effect on the

system. Indeed, it has been shown that the resulting effective dynamics is a stochastic diffusive evolution of the system state [142, 145]. Without entering the details of the calculations here we present the main concepts of this derivation.

Let us assume a small time interval δt with the precise scaling $\delta t = O(\beta^{-3/2})$. From Eq. (4.72), the number of detections within this time interval $\delta N = O(\beta^2 \delta t) = O(\beta^{1/2})$ is large, and the average change of the system, of $O(\delta t) = O(\beta^{-3/2})$ is small. Under this assumption, the average number of detections in the time interval δt reads

$$\mathrm{E}[\,\delta N(t)\,] \simeq p_1(t,\delta t) \simeq \left[\beta^2 + \beta \langle \hat{x} \rangle_c(t)\right] \delta t\,. \tag{4.74}$$

This is dominated by the contribution from the coherent field, and it is linear with the average field quadrature $\langle \hat{x} \rangle_c = \langle \hat{c} + \hat{c}^\dagger \rangle_c$. Since the system evolution during the time δt is small, the probability of a single detection per unit of time is constant. This implies that the statistics of $\delta N(t)$ is mostly Poissonian, thus we can conclude that its variance is

$$\mathrm{Var}[\,\delta N(t)\,] \simeq \beta^2 \delta t\,. \tag{4.75}$$

Furthermore, since the average is very large we can consistently attribute to $\delta N(t)$ a Gaussian statistics, and write

$$\delta N(t) = \beta^2 \delta t + \beta\, \langle \hat{x} \rangle_c(t)\, \delta t + \beta\, \delta W(t)\,, \tag{4.76}$$

where $\delta W(t)$ are a Wiener increments with a Gaussian statistics characterised by

$$\mathrm{E}[\,\delta W(t)\,] = 0 \quad \text{and} \quad \mathrm{E}[\,\delta W^2(t)\,] = \delta t\,. \tag{4.77}$$

These Wiener increments describe the fluctuation around the average value of the homodyne photocurrent.

At this stage we can write the unnormalised evolution of the conditional state of the system over the time interval δt as

$$|\widetilde{\psi}_c(t+\delta t)\rangle = \hat{N}(t+\delta t - t_m)(\hat{c}+\beta)\hat{N}(t_m - t_{m-1}) \cdots (\hat{c}+\beta)\hat{N}(t_1 - t)\,|\psi_c(t)\rangle\ , \tag{4.78}$$

where $t_1, t_2, \ldots, t_m$ are the times of the m detections recorded in the time δt, and where the time evolution between two detections is described by the operator

$$\hat{N}(t_1 - t) = \exp\left\{ -\left[i\hat{H} + \frac{1}{2}\left(2\beta\hat{c} + \hat{c}^\dagger \hat{c} + \beta^2\right)\right](t_1 - t)\right\}\,. \tag{4.79}$$

Note that this operator is obtained from the repeated action of the no-detection measurement operator $\hat{M}_0(\mathrm{d}t)$ in Eq. (4.70). Since the time interval δt is small, the system change over this time is typically small as well. This implies that the conditional state in Eq. (4.78) is approximatively independent on the detection times $t_1, t_2, \ldots, t_m$ [145]. This allows to move all the collapse operator at the beginning of the evolution and to rewrite the unnormalised conditional state as

$$|\widetilde{\psi}_c(t+\delta t)\rangle = \hat{N}(\delta t)\,(\hat{c}+\beta)^m\,|\psi_c(t)\rangle\ , \tag{4.80}$$

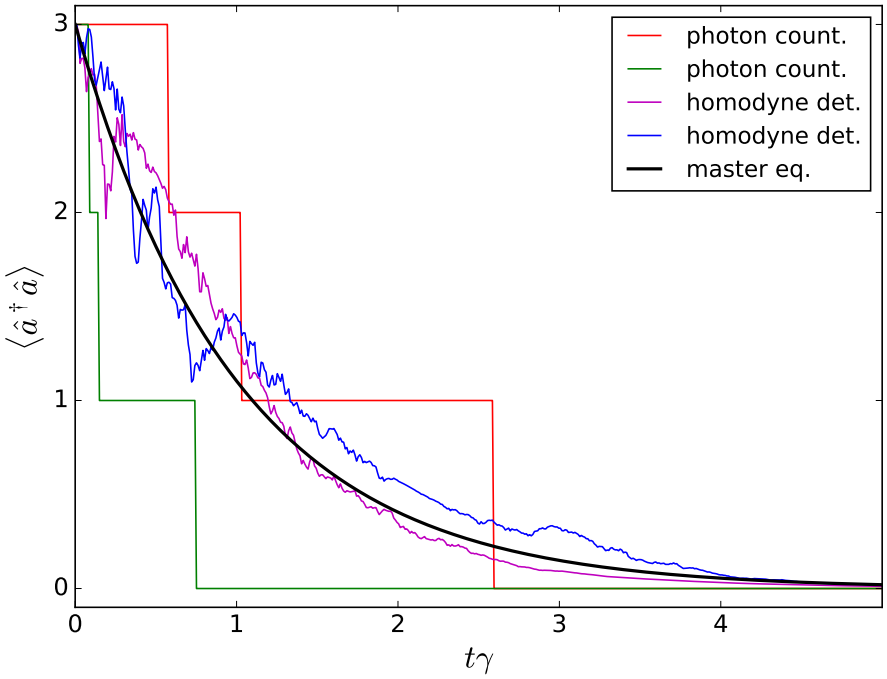

Figure 4.3 Comparison between the photon-counting and homodyne-detection quantum trajectories for a linear cavity relaxing from the three photon Fock state to the vacuum state (γ quantifies the coupling to the environment). The homodyne trajectories follow a diffusive evolution.

Since we are only considering the evolution of the unnormalised state we can drop the factor $\exp(\delta t\, \beta^2/2)\, \beta^m$ and write

$$|\widetilde{\psi}_c(t+\delta t)\rangle = \exp\left[-i\hat{H}\delta t - \frac{1}{2}\left(2\beta\hat{c} + \hat{c}^\dagger\hat{c}\right)\delta t\right]\left(\hat{\mathbb{1}}_S + \frac{\hat{c}}{\beta}\right)^m |\psi_c(t)\rangle \ . \tag{4.81}$$

Expanding this expression and substituting m with the expression of δN in Eq. (4.76), one obtains an approximated formulation for the conditional state that becomes exact in the limit of $\beta \to \infty$. In this continuous limit $\delta t \to \mathrm{d}t$, $\delta W(t) \to \mathrm{d}W(t)$ and, after renormalisation of the conditional state, it can be shown that the conditional time evolution under homodyne monitoring is

$$\begin{aligned} \mathrm{d}\,|\psi_c(t)\rangle = \Big\{ &-i\hat{H}\,\mathrm{d}t \ - \frac{1}{2}\left[\,\hat{c}^\dagger\hat{c} + 2\langle\hat{x}/2\rangle_c(t)\,\hat{c} + \langle\hat{x}/2\rangle_c^2(t)\,\right]\mathrm{d}t \\ &+ \left[\,\hat{c} - \langle\hat{x}/2\rangle_c(t)\,\right]\mathrm{d}W(t)\Big\}\,|\psi_c(t)\rangle \ . \end{aligned} \tag{4.82}$$

This equation defines the stochastic Schrödinger equation of homodyne detection. By this equation one can simulate the conditional quantum trajectory, taking a reasonably

small $\mathrm{d}t$ and generating stochastic Wiener increments at each time step. The initial state combined with the history of the occurred $\mathrm{d}W(t)$ completely define a singular homodyne conditional state trajectory. Note in Eq. (4.82) that, by performing the limit, we lost the dependence on the values of β. Even if the underlying measurement is detection, the quantum jumps of photon counting have been reduced to a continuous diffusive evolution, as illustrated in Fig. 4.3.

In a very similar way to what we did in Sec. (4.3.2) we can determine the stochastic evolution of the conditional density matrix $\hat{\rho}_c(t) = |\psi_c(t)\rangle\langle\psi_c(t)|$. Having in mind that $\mathrm{d}W^2(t) = \mathrm{d}t$, it is easy to prove that

$$\begin{aligned} \mathrm{d}\hat{\rho}_c(t) &= |\mathrm{d}\psi_c(t)\rangle\langle\psi_c(t)| + |\psi_c(t)\rangle\langle\mathrm{d}\psi_c(t)| + |\mathrm{d}\psi_c(t)\rangle\langle\mathrm{d}\psi_c(t)| \\ &= -i\left[\hat{H}, \hat{\rho}_c(t)\right]\mathrm{d}t + \mathcal{D}(\hat{c})\hat{\rho}_c(t)\,\mathrm{d}t + \mathcal{H}(\hat{c})\hat{\rho}_c(t)\,\mathrm{d}W(t), \end{aligned} \tag{4.83}$$

where the superoperator $\mathcal{H}$ has been defined in Eq. (4.59b) and $\mathcal{D}$ is the usual dissipation term of Lindblad master equation defined in Eq. (4.52).

As we mentioned at the beginning of the section, the unconditional evolution under homodyne monitoring is the same as in photon counting, i.e. the master Equation (4.51). Indeed the Wiener increments $\mathrm{d}W(t)$ are uncorrelated to the state of the system $\hat{\rho}_c(t)$, then we have

$$\mathrm{E}[\,\mathcal{H}(\hat{c})\hat{\rho}_c(t)\mathrm{d}W(t)] = \mathrm{E}[\,\mathcal{H}(\hat{c})\hat{\rho}_c(t)]\,\mathrm{E}[\,\mathrm{d}W(t)] = 0\,. \tag{4.84}$$

This implies that the average state of the system $\hat{\rho}(t) = \mathrm{E}[\,\hat{\rho}_c(t)]$ is a solution of the Lindblad master Equation (4.51)

$$\frac{\mathrm{d}\hat{\rho}(t)}{\mathrm{d}t} = -\,i\left[\hat{H}, \hat{\rho}(t)\right] + \mathcal{D}(\hat{c})\hat{\rho}(t)\,, \tag{4.85}$$

Once again we have seen that the Lindblad master equation describes the evolution of our knowledge about the system, when the information is lost in an unmonitored environment. Homodyne detection allows to retrieve this information and to describe the system in a state of maximal knowledge, a pure state. Note that the photon-counting and the homodyne detection trajectories are very different. One is characterised by quantum jumps, the other by a diffusive evolution, however both the evolution average to the same master equation. This means that the way in which we monitor the same environment, drastically condition the evolution of the system quantum state.

Chapter 5

Ancillary qubit spectroscopy of exotic vacua

In recent years, cavity quantum electrodynamics (QED) has thrived thanks to the possibility of controlling light-matter interaction at the quantum level, which is relevant for the study of fundamental quantum phenomena, the generation of artificial quantum systems, and quantum information applications [27]. The field has more recently blossomed in solid-state systems, particularly in superconducting circuit QED [41, 74] and semiconductor cavity QED [52].

In conventional cavity QED, photons are present only in the excited light-matter states of the system and can escape the cavity due to a finite transparency of the mirrors. The situation changes drastically in the so-called ultrastrong light-matter coupling regime[58, 61, 64–67], achieved when the light-matter interaction rate is comparable or larger than the photon frequency. Indeed, it can become energetically favorable to have photons in the ground state. However, such ground state photons are bound to the cavity and cannot escape, since that would violate energy conservation[146].

In the 'thermodynamic' limit where a large number N of two-level systems are (ultra)strongly coupled to a single bosonic mode, phase transitions can occur with non-trivial and degenerate vacua. The vacuum properties depend on the details of the light-matter coupling and on the Hamiltonian symmetries. These phase transitions are associated with symmetry breaking: it is a discrete $\mathbb{Z}_2$ symmetry for the phase transition [68–70, 73] in the Dicke model [28] where the non-rotating wave terms of light-matter interaction are considered; it is a continuous $U(1)$ symmetry in the case of the Tavis-Cummings model [30, 71] where non-rotating wave terms are absent. Such symmetries can be controlled in models where the two-level systems are coupled to both quadratures of the bosonic field [72]. On the other hand, in Hamiltonians containing a strong enough quadratic renormalisation of the cavity photon frequency (e.g., due to the squared electromagnetic vector potential term), the ground state is a two-mode squeezed vacuum, but no phase transition occurs [63]. This is the case for the Hopfield model [29], notably realised in semiconductor microcavities [64–67]. The fundamental meaning and validity of cavity and circuit QED quantization procedures is critically at play in the ultrastrong coupling regime, since different forms of Hamiltonians lead to extremely different physical phenomena [118–120]. Protocols to detect the properties of cavity vacua are therefore of strong significance, not only

for a study of intriguing ground states, but also as a sensitive test of fundamental microscopic theories.

In this context, a crucial question arises: how to detect ground state photon populations and correlations without destroying them? In principle bound photons in cavity (circuit) QED vacua can be released by a non-adiabatic, ultrafast modulation of the Hamiltonian parameters [64, 121–123, 147, 148], which can convert a ground state into an excited state. While non-adiabatic QED provides an interesting way of observing nonclassical quantum vacuum radiation, finding a non-invasive and sensitive probe of the ground state properties remains highly desirable. Some theoretical work [149, 150] in circuit QED has suggested to study the coupling between a Dicke system and an additional superconducting qubit, showing that Dicke criticality can be observed via current transport measurements. However, in Ref. [149] the considered effective dispersive interaction between the cavity system and the auxiliary qubit depends only on the cavity photon population, and not on the intracavity light-matter correlations; moreover the dissipation has not been treated with a master equation which is valid in the ultrastrong coupling regime [151], which is essential to avoid artifacts such as the instability of the ground state and the excitation of the system in the absence of driving [146, 151].

In this chapter, we show that the spectroscopy of an ancillary qubit, moderately coupled to a cavity QED system, depends sensitively on the type of vacuum. By driving this ancillary qubit and analyzing its frequency response, we show that it is possible to have distinct signatures of the ground state photon populations and correlations without destroying them. We explore this protocol by considering three different classes of systems described respectively by the Dicke, Tavis-Cummings and Hopfield models, whose Hamiltonian are introduced in Sec. 5.1. Each of these models has a ground state with different properties.

Sections 5.2 and 5.3 report our main results. We show numerically and analytically that the Lamb shift of the ancillary qubit transition is very sensitive both to the photon populations and correlations of exotic vacua. We explore the back-action of the ancillary qubit on the cavity ground state and determine the key physical quantities affecting the fidelity of the measurement, consistently including the dissipation effects in the ultrastrong coupling regime.

Finally in Sec. 5.4 we show how the finite temperature affects our measurement protocol and we provide a detailed derivation of effective Hamiltonians in the dispersive regime.

5.1 The model

As sketched in Fig. 5.1, we will consider an ancillary qubit M coupled to the bosonic mode of a cavity (circuit) QED system S. In particular, we will deal with the following

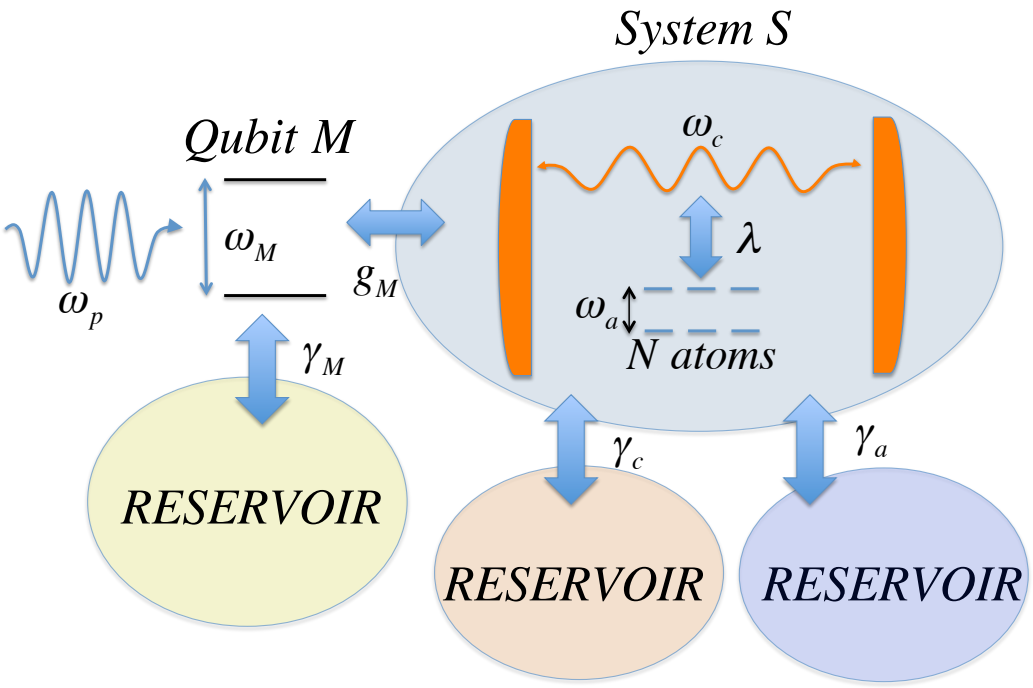

Figure 5.1 A sketch of a cavity (circuit) QED system S consisting of a single-mode resonator coupled to N two-level (artificial) atoms. An ancillary qubit M is also coupled to the resonator boson mode. The spectroscopy of the ancilla is used to probe quantum ground state properties of S. Note that in experimental realisations, also the ancillary qubit can be inserted inside the cavity.

time-dependent Hamiltonian ($\hbar = 1$),

$$\hat{H}(t) = \hat{H}_S + \frac{\omega_M}{2}\hat{\sigma}_z^{(M)} + g_M\left(\hat{a}^\dagger + \hat{a}\right)\hat{\sigma}_x^{(M)} + \Omega_p \cos(\omega_p t)\hat{\sigma}_x^{(M)}, \tag{5.1}$$

where $\hat{H}_S$ is the system Hamiltonian, g_M is the coupling between the measurement qubit and the boson field, whose boson annihilation operator is a. The $\hat{\sigma}_i^{(M)}$ Pauli operators act on the Hilbert space of the qubit M, whose transition frequency is ω_M, while Ω_p is the amplitude of the driving field (see Sec. 3.2) with frequency ω_p acting on M.

In the following, $\hat{H}_S$ will be one of the three Hamiltonians, describing respectively the Dicke, Tavis-Cummings and Hopfield-like models ($\hbar = 1$):

$$\hat{H}_{Dicke} = \omega_c \hat{a}^\dagger \hat{a} + \omega_a \hat{J}_z + \frac{\lambda}{\sqrt{N}}\left(\hat{a}^\dagger + \hat{a}\right)\left(\hat{J}_+ + \hat{J}_-\right), \tag{5.2a}$$

$$\hat{H}_{TC} = \omega_c \hat{a}^\dagger \hat{a} + \omega_a \hat{J}_z + \frac{\lambda}{\sqrt{N}}\left(\hat{a}^\dagger \hat{J}_- + \hat{a}\hat{J}_+\right), \tag{5.2b}$$

$$\hat{H}_{Hopfield} = \hat{H}_{Dicke} + D\left(\hat{a}^\dagger + \hat{a}\right)^2, \tag{5.2c}$$

where ω_c is the frequency of the bosonic mode, ω_a is the transition frequency of each of the N identical two-level atoms, λ is the collective coupling and $D = \lambda^2/\omega_a$ is the strength of the boson renormalisation term in the Hopfield model. The $\hat{J}_i$ are the angular momentum operators representing the collective pseudo-spin associated to the N two-level systems, namely

$$\hat{J}_z = \frac{1}{2}\sum_{i=1}^{N}\hat{\sigma}_z^{(i)}\,, \qquad \hat{J}_\pm = \sum_{i=1}^{N}\hat{\sigma}_\pm^{(i)}\,, \tag{5.3}$$

where the Pauli matrices here refer to each two-level system. Sec. 2.2.3 and Sec. 2.2.2 provide a more detailed description of these models.

5.2 Spectrum analysis and Lamb shift

We start by considering the energy levels of $\hat{H}_{S+M}$, describing the system S coupled to the measurement qubit M, namely:

$$\hat{H}_{S+M} = \hat{H}_S + \frac{\omega_M}{2}\hat{\sigma}_z^{(M)} + g_M\left(\hat{a}^\dagger + \hat{a}\right)\hat{\sigma}_x^{(M)}. \tag{5.4}$$

The eigenstates and their energies are defined by $\hat{H}_{S+M}|\epsilon\rangle = \epsilon|\epsilon\rangle$. System S will be of the Dicke, Tavis-Cummings or Hopfield type, as shown in Figs. 5.2 and 5.3. We consider a qubit transition frequency ω_M detuned with respect to the boson frequency $\omega_c = \omega_a$.

For $g_M = 0$, the driving field term, proportional to the operator $\hat{\sigma}_x^{(M)}$, induces a transition from the ground state $|G_S\rangle \otimes |g\rangle$ to the excited state $|G_S\rangle \otimes |e\rangle$, being $|G_S\rangle$ the ground state of S and $|g\rangle$ ($|e\rangle$) the ground (excited) state of the qubit M. For finite g_M, the coupling between S and M creates a mixing between states of the form $|\Psi_S\rangle \otimes |\psi_M\rangle$ and the driving induces a transition from the ground state $|G_{S+M}\rangle$ to excited states of $\hat{H}_{S+M}$. Therefore, in the spectroscopy the relevant excited states $|\epsilon\rangle$ are those having the largest values of $|\langle G_{S+M}|\hat{\sigma}_x^{(M)}|\epsilon\rangle|^2$. The colour scale of the levels in Figs. 5.2 and 5.3 is proportional to the value of such matrix elements.

The results show that, due to the off-resonant coupling, there is only one dominant spectroscopically-active level (black thick solid line), which originates from and has a strong overlap with the state $|G_S\rangle \otimes |e\rangle$. The right panels of Figs. 5.2 and 5.3, show the Lamb shift of the qubit transition frequency.

For $\lambda = 0$ the system S is like a bare cavity, so the spectral renormalisation is the standard Lamb shift [43] of the qubit due to the coupling to the normal vacuum in the cavity. By increasing λ the vacuum is modified and the Lamb-shift changes. It is apparent that the behaviour of the qubit shift is qualitatively different in the three cases. For the Dicke model (top panels of Fig. 5.2), the Lamb shift increases strongly with λ and becomes much bigger than in the case of the bare cavity ($\lambda = 0$).

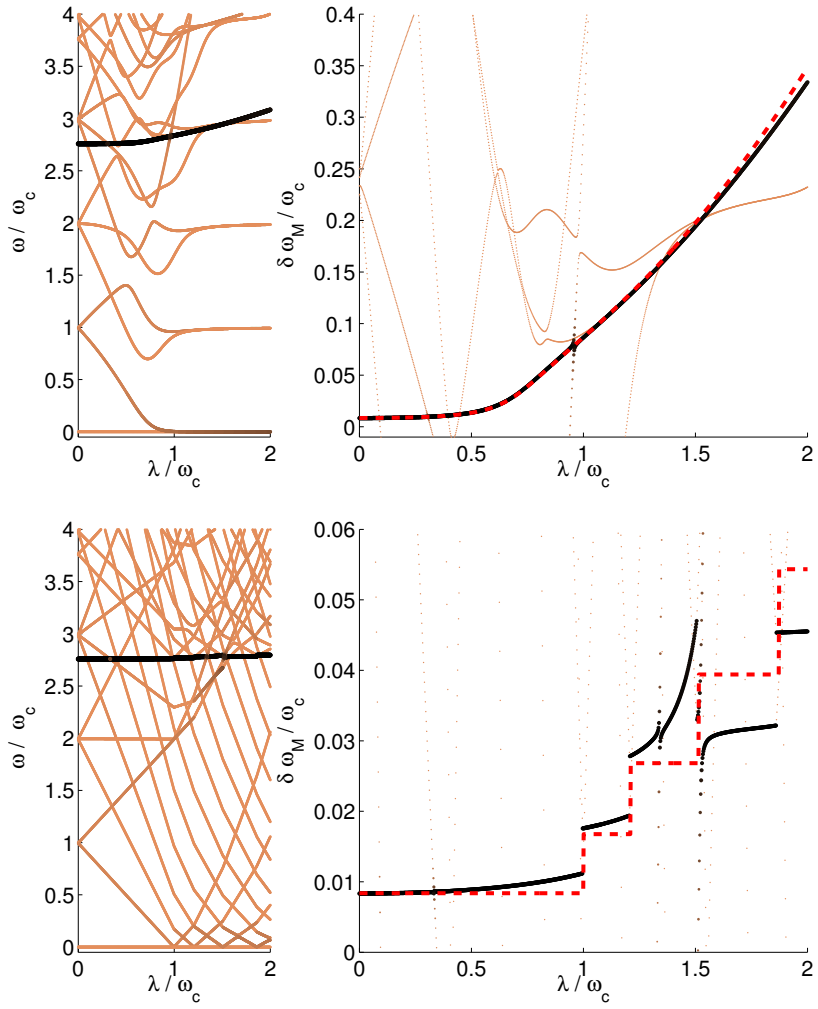

Figure 5.2 Left panels: excitation energies for the three considered systems S versus the coupling λ between the boson field and the N atoms. Right panels: the Lamb shift of the ancillary qubit transition. The red dashed lines are calculated via Eq. (5.5). Top panels: Dicke system. with $N = 3$, $\omega_c = \omega_a$, $\omega_M = 2.75\omega_c$, $g_M = 0.1\omega_c$. Bottom panels: Tavis-Cummings system with $N = 3$, $\omega_c = \omega_a$, $\omega_M = 2.75\omega_c$, $g_M = 0.1\omega_c$.

In the Tavis-Cummings case (bottom panels Fig. 5.2), the Lamb shift increases in a step-like way as a function of λ. In the Hopfield model (Fig. 5.3), instead the Lamb shift decreases with increasing value of λ.

As it will be detailed in Sec. 5.2.1, we have derived an analytical expression at the second order in g_M for the measurement qubit Lamb shift, namely

$$\delta\omega_M^{(S)} \simeq g_M^2\left(\frac{1}{\omega_M-\omega_c}+\frac{1}{\omega_M+\omega_c}\right)\langle(\hat{a}^\dagger+\hat{a})^2\rangle+g_M^2\left[\frac{1}{(\omega_M-\omega_c)^2}-\frac{1}{(\omega_M+\omega_c)^2}\right]\langle\hat{V}^{(S)}\rangle, \tag{5.5}$$

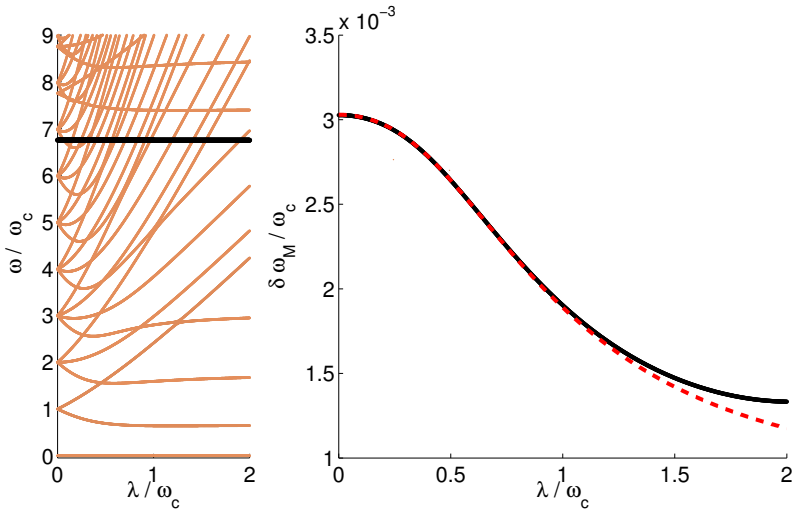

Figure 5.3 Left and right panels like in Fig. 5.2, but for the Hopfield system with $N = 3$, $\omega_c = \omega_a$, $\omega_M = 6.75\omega_c$ (chosen to avoid level crossing), $g_M = 0.1\omega_c$, $D = \lambda^2/\omega_a$.

where

$$\hat{V}^{(Dicke)} = \frac{\lambda}{\sqrt{N}}(\hat{a}^\dagger + \hat{a})\hat{J}_x\,, \tag{5.6a}$$

$$\hat{V}^{(TC)} = \frac{\lambda}{\sqrt{N}}(\hat{a}^\dagger \hat{J}_- + \hat{a}\hat{J}_+)\,, \tag{5.6b}$$

$$\hat{V}^{(Hopfield)} = \hat{V}^{(Dicke)} + 2\frac{\lambda^2}{\omega_a}(\hat{a}^\dagger + \hat{a})^2\,. \tag{5.6c}$$

Here the expectation values are calculated on the ground state $|G_S\rangle$ of the target system S. Importantly, the shift not only depends on the ground state photon population $\langle \hat{a}^\dagger \hat{a}\rangle$, but also on the anomalous expectation value $\langle \hat{a}^{\dagger 2} + \hat{a}^2\rangle$ and on the correlation between photon field and the N two-level systems. The red-dashed lines in the right panels of Figs. 5.2 and 5.3 depict the shift predicted by Eq. (5.5). The agreement between the numerical diagonalisation results and the analytical formula is excellent in the considered range of values for λ/ω_c, except for points where there are avoided crossings with other levels, as expected from the pertubative nature of our formula.

Criticality

In Fig. 5.4, we present the behaviour of the qubit spectral shift as a function of N. With increasing value of N, a critical point emerges for the Dicke Hamiltonian (left panels), but not for the Hopfield case (right panels). The behaviour of the qubit Lamb shift, already completely different for small values of N, becomes strikingly dissimilar. Already for $N = 30$, the shift has a considerable jump around the critical coupling.

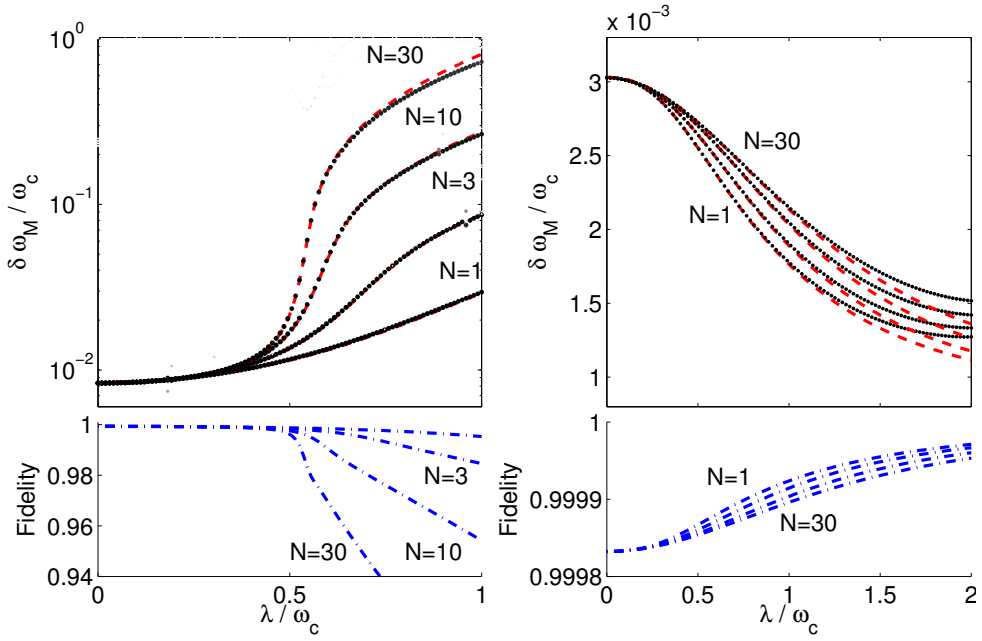

Figure 5.4 Top panels: Lamb shift of the ancillary qubit (black dots) versus λ for $N = 1, 3, 10$ and 30. Red-dashed lines are obtained via Eq. (5.5). Bottom panel: ground state fidelity $\mathcal{F}_G$. Left panels: Dicke model with $\omega_c = \omega_a$, $\omega_M = 2.75\omega_c$, $g_M = 0.1\omega_c$. Right panels: Hopfield model with $\omega_c = \omega_a$, $\omega_M = 6.75\omega_c$, $g_M = 0.1\omega_c$, $D = \lambda^2/\omega_a$.

The bottom panels shows the ground state fidelity

$$\mathcal{F}_G = Tr_{S,M}\left\{|G_{S+M}\rangle\langle G_{S+M}|(|G_S\rangle\langle G_S| \otimes \hat{1}^{(M)})\right\}, \tag{5.7}$$

quantifying the change of the cavity system ground state in presence of the ancilla qubit. In the considered conditions, $\mathcal{F}_G$ can be close to 1. However, for large values of λ/ω_c the fidelity strongly decreases in the Dicke case above the critical coupling, while it stays close to 1 for the Hopfield model. Since for $g_M \to 0$ the fidelity tends to 1 and the qubit shift is proportional to g_M^2, a trade-off between fidelity and size of the qubit shift can be found depending on the degree of level broadening, as it will be discussed later, when we will include the effect of dissipation.

5.2.1 Dispersive Hamiltonians and analytical derivation of vacuum-dependent Lamb shift

In Sec. 2.2.2 we introduced the dispersive regime and its effective Hamiltonian for atom-cavity interaction when the rotating wave approximation (RWA) is valid. Since the ancillary qubit and the cavity are strongly detuned compared to the interaction intensity g_M, the same approach can be used to simplify the complete Hamiltonians

$\hat{H}_{S+M}$. However, due to the presence of anti-resonant terms in the interaction between the ancillary qubit and the cavity, our approach must be adapted to be valid beyond the rotating wave approximation [115].

Let us start from the simple situation in which $\lambda = 0$. In this case our system reduces to only the boson mode and the coupled ancillary qubit. This is equivalent to the Rabi model whose Hamiltonian is:

$$\hat{H}_{C+M} = \omega_c \hat{a}^\dagger \hat{a} + \frac{\omega_M}{2}\hat{\sigma}_z^{(M)} + g_M \left(\hat{a}^\dagger + \hat{a}\right)\hat{\sigma}_x^{(M)}. \tag{5.8}$$

In the dispersive regime, i.e. $|\omega_M - \omega_c| \gg g_M$, it is possible to derive an effective Hamiltonian for this model. Let us define the operators $\hat{X}_\pm$ and $\hat{Y}_\pm$, exactly in the same way as in Ref. [115] (except for the sign of $\hat{Y}_-$):

$$\hat{X}_\pm = \hat{a}^\dagger \hat{\sigma}_-^{(M)} \pm \hat{a}\,\hat{\sigma}_+^{(M)}, \qquad \hat{Y}_\pm = \hat{a}\,\hat{\sigma}_-^{(M)} \pm \hat{a}^\dagger \hat{\sigma}_+^{(M)}. \tag{5.9}$$

Applying to $\hat{H}_{C+M}$ the unitary transformation

$$\hat{U}(\xi, \tilde{\xi}) = e^{\xi \hat{X}_- + \tilde{\xi}\hat{Y}_-}, \quad \text{where} \quad \xi = \frac{g_M}{\omega_M - \omega_c} \quad \text{and} \quad \tilde{\xi} = \frac{g_M}{\omega_M + \omega_c},$$

and keeping only the terms up to the second order in the small parameters ξ and $\tilde{\xi}$, the transformed Hamiltonian can be approximated as

$$\begin{aligned}\hat{H}_{C+M}^{(disp)} \simeq& \hat{U}^\dagger(\xi,\tilde{\xi})\hat{H}_{C+M}\hat{U}(\xi,\tilde{\xi}) \\ \simeq& \hat{H}_{C+M} + \left[\hat{H}_{C+M}, \xi\hat{X}_- + \tilde{\xi}\hat{Y}_-\right] + \left[\left[\hat{H}_{C+M}, \xi\hat{X}_- + \tilde{\xi}\hat{Y}_-\right], \xi\hat{X}_- + \tilde{\xi}\hat{Y}_-\right].\end{aligned} \tag{5.10}$$

The unitary transformation $\hat{U}^\dagger(\xi, \tilde{\xi})$ is a Schrieffer-Wolff transformation [113], and this is explicitly chosen to eliminate the interaction term to first order in g_M. As we have mentioned in Sec. 2.2.2, the approach is based on the idea that a unitary transformation leaves the spectrum of the Hamiltonian unchanged, thus $\hat{H}_{C+M}$ and its transformed $\hat{U}^\dagger(\xi,\tilde{\xi})\hat{H}_{C+M}\hat{U}(\xi,\tilde{\xi})$, have the same spectrum. By expanding $\hat{U}^\dagger(\xi,\tilde{\xi})\hat{H}_{C+M}\hat{U}(\xi,\tilde{\xi})$ to the second order in ξ and $\tilde{\xi}$, we obtain an effective Hamiltonian that has approximatively the same spectrum of $\hat{H}_{C+M}$.

Indeed, using the following commutation relations,

$$\begin{aligned}&\left[\omega_c\hat{a}^\dagger\hat{a} + \frac{\omega_M}{2}\hat{\sigma}_z^{(M)}, \xi\hat{X}_- + \tilde{\xi}\hat{Y}_-\right] = -(\omega_M - \omega_c)\hat{X}_+ - (\omega_M + \omega_c)\hat{Y}_+, \\ &\left[\hat{X}_+, \hat{X}_-\right] = (2\hat{a}^\dagger\hat{a} + 1)\hat{\sigma}_z^{(M)} + 1, \qquad \left[\hat{Y}_+, \hat{Y}_-\right] = (2\hat{a}^\dagger\hat{a} + 1)\hat{\sigma}_z^{(M)} - 1, \\ &\left[\hat{Y}_\pm, \hat{X}_\mp\right] = \pm(\hat{a}^{\dagger 2} + \hat{a}^2)\hat{\sigma}_z^{(M)}, \qquad \left[\hat{Y}_\pm, \hat{X}_\pm\right] = \pm(\hat{a}^{\dagger 2} - \hat{a}^2)\hat{\sigma}_z^{(M)},\end{aligned} \tag{5.11}$$

it is possible to obtain the effective dispersive Hamiltonian to the second order in ξ and $\tilde{\xi}$:

$$\hat{H}_{C+M}^{(disp)} \simeq \omega_c\hat{a}^\dagger\hat{a} + \frac{\omega_M}{2}\hat{\sigma}_z^{(M)} + \frac{g_M^2}{2}\left(\frac{1}{\omega_M - \omega_c} + \frac{1}{\omega_M + \omega_c}\right)(\hat{a} + \hat{a}^\dagger)^2\hat{\sigma}_z^{(M)}. \tag{5.12}$$

The resulting effective shift for the transition frequency of the qubit due to the coupling to the cavity ground state reads:

$$\delta_{\omega_M}^{(cav)} \simeq g_M^2 \left(\frac{1}{\omega_M - \omega_c} + \frac{1}{\omega_M + \omega_c} \right) \langle (\hat{a} + \hat{a}^\dagger)^2 \rangle. \tag{5.13}$$

Here and in the following, the expectation values are calculated on the ground state $|G_S\rangle$ of the target system S. In this case the system is the bare cavity, $|G_S\rangle$ is the standard vacuum and the last equation gives the standard Lamb shift.

Lamb shift for an exotic vacuum

On the other hand, when $\lambda \neq 0$ the vacuum is changed and correspondingly also the Lamb shift changes. We start by considering the Dicke model, its complete Hamiltonian when it is coupled to the measurement ancilla qubit reads:

$$\hat{H}_{Dicke+M} = \hat{H}_{C+M} + \omega_a \hat{J}_z + \frac{\lambda}{\sqrt{N}} \left(\hat{a}^\dagger + \hat{a} \right) \hat{J}_x \,. \tag{5.14}$$

We apply to this Hamiltonian the transformation $\hat{U}(\xi, \tilde{\xi})$ defined above. The $\hat{J}_i$ operators commute with $\hat{U}(\xi, \tilde{\xi})$ (i.e. $\hat{U}^\dagger(\xi, \tilde{\xi}) \hat{J}_i \hat{U}(\xi, \tilde{\xi}) = \hat{J}_i$), and, at second order in ξ and $\tilde{\xi}$, the cavity quadrature $(\hat{a} + \hat{a}^\dagger)$ transforms as

$$\hat{U}^\dagger(\xi, \tilde{\xi})(\hat{a} + \hat{a}^\dagger)\hat{U}(\xi, \tilde{\xi}) \simeq (\hat{a} + \hat{a}^\dagger) + (\xi - \tilde{\xi})\hat{\sigma}_x^{(M)} + \frac{1}{2}(\xi^2 - \tilde{\xi}^2)(\hat{a} + \hat{a}^\dagger)\hat{\sigma}_z^{(M)}. \tag{5.15}$$

The shift of the qubit M transition frequency due to coupling to the Dicke system, to the second order in ξ and $\tilde{\xi}$ reduces to:

$$\delta\omega_M^{(Dicke)} \simeq \delta_{\omega_M}^{(cav)} + g_M^2 \frac{\lambda}{\sqrt{N}} \left(\frac{1}{(\omega_M - \omega_c)^2} - \frac{1}{(\omega_M + \omega_c)^2} \right) \langle (\hat{a} + \hat{a}^\dagger) J_x \rangle \,. \tag{5.16}$$

where we used the fact that $\langle \hat{J}_x \rangle = 0$. It can be proved by considering that $\hat{H}_{Dicke}$ commutes with the parity operator $\hat{P} = \exp[i\pi(\hat{a}^\dagger \hat{a} + \hat{J}_z + N/2)]$. Indeed, since $[\hat{H}_{Dicke}, \hat{P}] = 0$, the eigenstates of $\hat{H}_{Dicke}$ are also eigenstates of $\hat{P}$, this means that

$$\langle G_S | \hat{J}_\pm | G_S \rangle = \langle G_S | \hat{P}^\dagger \hat{J}_\pm \hat{P} | G_S \rangle = -\langle G_S | \hat{J}_\pm | G_S \rangle \Rightarrow \langle G_S | \hat{J}_\pm | G_S \rangle = 0 \,, \tag{5.17}$$

where we have used the fact that $\hat{P}^\dagger \hat{J}_\pm \hat{P} = -\hat{J}_\pm$. The same reasoning leads to prove that $\langle \hat{a} \rangle = \langle \hat{a}^\dagger \rangle = 0$.

Let us consider now the Hopfield model, characterised by the quadratic renormalisation of the cavity photon frequency. The total Hamiltonian reads

$$\hat{H}_{Hopfield+M} = \hat{H}_{Dicke+M} + \omega_a \hat{J}_z + \frac{\lambda^2}{\omega_a} \left(\hat{a} + \hat{a}^\dagger \right)^2 . \tag{5.18}$$

Using the fact that $\hat{U}^\dagger(\xi,\tilde{\xi})(\hat{a}+\hat{a}^\dagger)^2\hat{U}(\xi,\tilde{\xi}) = (\hat{U}^\dagger(\xi,\tilde{\xi})(\hat{a}+\hat{a}^\dagger)\hat{U}(\xi,\tilde{\xi}))^2$, we obtain:

$$\hat{U}^\dagger(\xi,\tilde{\xi})(\hat{a}+\hat{a}^\dagger)^2\hat{U}(\xi,\tilde{\xi}) \simeq \left[(\hat{a}+\hat{a}^\dagger) + (\xi-\tilde{\xi})\hat{\sigma}_x^{(M)} + \frac{1}{2}(\xi^2-\tilde{\xi}^2)(\hat{a}+\hat{a}^\dagger)\hat{\sigma}_z^{(M)}\right]^2 . \tag{5.19}$$

Developing the square up to the second order in ξ and $\tilde{\xi}$, we get

$$\hat{U}^\dagger(\xi,\tilde{\xi})(a+a^\dagger)^2\hat{U}(\xi,\tilde{\xi}) \simeq (a+a^\dagger)^2+2(\xi-\tilde{\xi})(a+a^\dagger)\sigma_x^{(M)}+(\xi^2-\tilde{\xi}^2)(a+a^\dagger)^2\sigma_z^{(M)}+(\xi-\tilde{\xi})\hat{1}\,. \tag{5.20}$$

Since $\langle\hat{a}+\hat{a}^\dagger\rangle = 0$, the shift of the ancilla transition due to coupling to the Hopfield system, to the second order in ξ and $\tilde{\xi}$, is:

$$\delta\omega_M^{(Hop)} \simeq \delta_{\omega_M}^{(Dicke)} + 2g_M^2\frac{\lambda^2}{\omega_a}\left(\frac{1}{(\omega_M-\omega_c)^2}-\frac{1}{(\omega_M+\omega_c)^2}\right)\langle(\hat{a}+\hat{a}^\dagger)^2\rangle\,. \tag{5.21}$$

Finally we consider the case of the Tavis-Cummings model, in this case the complete Hamiltonian of the ancilla qubit plus the cavity system reads:

$$\hat{H}_{TC+M} = \hat{H}_{C+M} + \omega_a J_z + \frac{\lambda}{\sqrt{N}}\left(\hat{a}\hat{J}_+ + \hat{a}^\dagger\hat{J}_-\right). \tag{5.22}$$

Considering that

$$\hat{U}^\dagger(\xi,\tilde{\xi})\hat{a}\hat{U}(\xi,\tilde{\xi}) = \hat{a} + (\xi\hat{\sigma}_-^{(M)} - \tilde{\xi}\hat{\sigma}_+^{(M)}) + \frac{1}{2}(\xi^2-\tilde{\xi}^2)\hat{a}\hat{\sigma}_z^{(M)} + o(\xi^2,\tilde{\xi}^2,\xi\tilde{\xi}), \tag{5.23}$$

the action of the unitary transformation on the interaction term of Tavis-Cummings model to the second order in ξ and $\tilde{\xi}$, is:

$$\begin{aligned}\hat{U}^\dagger(\xi,\tilde{\xi})\left(\hat{a}\hat{J}_+ + \hat{a}^\dagger\hat{J}_-\right)\hat{U}(\xi,\tilde{\xi}) \simeq{}& \hat{a}\,\hat{J}_+ + \hat{a}\,\hat{J}_- + (\xi-\tilde{\xi})\left(\hat{\sigma}_-^{(M)}\hat{J}_+ + \hat{\sigma}_+^{(M)}\hat{J}_-\right)\\ &+ \frac{1}{2}(\xi^2-\tilde{\xi}^2)\left(\hat{a}\hat{J}_+ + \hat{a}^\dagger\hat{J}_-\right)\hat{\sigma}_z^{(M)}.\end{aligned} \tag{5.24}$$

Since $\langle\hat{J}_-\rangle = \langle\hat{J}_+\rangle = 0$, the second-order shift of the ancillary qubit transition due to the coupling to the Tavis-Cummings system is:

$$\delta\omega_M^{(TC)} \simeq \delta_{\omega_M}^{(cav)} + g_M^2\frac{\lambda}{\sqrt{N}}\left(\frac{1}{(\omega_M-\omega_c)^2}-\frac{1}{(\omega_M+\omega_c)^2}\right)\langle(\hat{a}\hat{J}_+ + \hat{a}^\dagger\hat{J}_-)\rangle.$$

The three expressions obtained for the shift of the qubit M transition can finally be condensed in the compact expression in Eq. (5.5).

5.3 Spectroscopy of the ancillary qubit: consistent master equation

Taking into account drive and dissipation, here we show how the spectroscopy of the ancilla qubit will allow us to measure the Lamb shift. In order to include dissipation consistently with the ultrastrong coupling regime, we need to consider a master

equation for the density matrix where the quantum jumps occur between the actual eigenstates of the Hamiltonian $\hat{H}_{S+M}$ [151, 152]. We consider three decay channels, associated to the bosonic mode, the N two-level systems and the measurement qubit, with dissipation rates γ_c, γ_a and γ_M respectively (see Fig. 5.1). Namely:

$$\partial_t\hat{\rho} = -i[\hat{H}(t),\hat{\rho}] + \frac{\gamma_c}{2}\mathcal{D}_-(\hat{a}^\dagger + \hat{a})\hat{\rho} + \frac{\gamma_a}{2}\mathcal{D}_-(\hat{J}_x)\hat{\rho} + \frac{\gamma_M}{2}\mathcal{D}_-(\hat{\sigma}_x^{(M)})\hat{\rho}\,. \tag{5.25}$$

Here $\mathcal{D}_-(\hat{S})\hat{\rho} = \left(2\hat{S}_-\hat{\rho}\hat{S}_-^\dagger - \hat{\rho}\hat{S}_-^\dagger\hat{S}_- - \hat{S}_-^\dagger\hat{S}_-\hat{\rho}\right)$ and $\hat{S}_- = \sum_{\epsilon'>\epsilon}\langle\epsilon|\hat{S}|\epsilon'\rangle|\epsilon\rangle\langle\epsilon'|$, define respectively the dissipation term and the jump operators. Here we are considering reservoirs at zero temperature (they can only absorb energy from the system $S+M$). This Lindblad master equation corresponds to the one in Eq. (3.41), that has been microscopically derived in Sec. 3.1 for a generic system and a single dissipative coupling. Note that Eq. (5.25) allows to solve the pathological behaviour of the standard Lindblad equation with bare excitation operators as in Ref. [149], in which the ground state of the whole system $\hat{H}_{S+M}$ is unstable and the reservoir excites the system even at zero temperature.

For cavity QED systems with infrared transitions at cryogenic temperatures, it is experimentally feasible to have $k_BT \ll \hbar\omega_C$, which is equivalent to the zero-temperature limit. For circuit QED systems based on superconductors [153] with microwave resonators and dilution fridge cryogenic conditions, the thermal energy can be a fraction of the photon energy: to give an example, a temperature of 50 mK and a resonator transition frequency $\omega_c/(2\pi) = 5$ GHz corresponds to $k_BT/(\hbar\omega_c) \simeq 0.21$. In this range of temperatures the main effect is a moderate thermal broadening of the ancilla qubit transition resonance (see section 5.4 for more details).

We can now apply the master equation in Eq. (5.25) to describe the spectroscopy when the qubit M is driven as described by Eq. (5.1). We have determined the steady-state density matrix $\hat{\rho}_{S+M}$ and consequently the reduced density matrix of the qubit M and system S , namely

$$\hat{\rho}_M = Tr_S\left\{\hat{\rho}_{S+M}\right\} \quad \text{and} \quad \hat{\rho}_S = Tr_M\left\{\hat{\rho}_{S+M}\right\}\,. \tag{5.26}$$

In Fig. 5.5, we show results for the qubit excited state population

$$n_e^{(M)} = Tr_{S,M}\left\{\hat{\rho}_{S+M}(1+\hat{\sigma}_z^{(M)})/2\right\} \tag{5.27}$$

versus the driving frequency ω_p and the collective atom-photon coupling λ. The ancilla excited state population spectrum shows a resonant peak that provides direct access to the vacuum-dependent qubit Lamb shift discussed so far and well described by the formula in Eq. (5.5).

Measurement back action

Within our framework, we can evaluate the degree of back-action on the system S. In particular we can calculate the measurement fidelity

$$\mathcal{F} = Tr_S\left\{\hat{\rho}_S|G_S\rangle\langle G_S|\right\}\,, \tag{5.28}$$

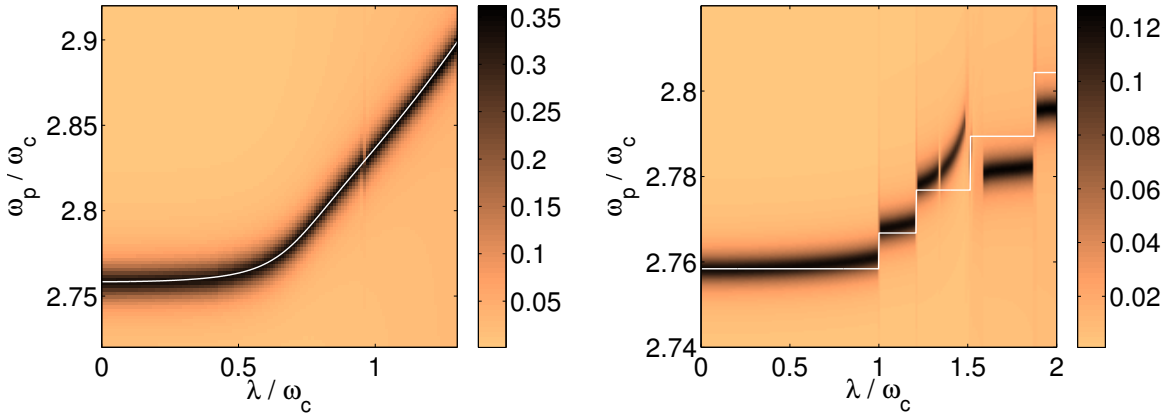

Figure 5.5 Excited state population of the ancilla qubit M versus the coherent drive frequency ω_p for different values of collective coupling λ, that controls the cavity vacuum. Left panel: Dicke model with $\Omega_p = 0.5\gamma_M$. Right panel: Tavis-Cummings model with $\Omega_p = 0.2\gamma_M$. Dissipation parameters: $\gamma_M = \gamma_c = \gamma_a = 0.01\omega_c$ for the left panel and $0.005\omega_c$ for the right panel. The other parameters are as in Fig. 5.2. The white line corresponds to the analytical curve in Eq. (5.5).

depending on the coupling between S and M, the driving of the qubit and the dissipation rates. $\mathcal{F} = 1$ means that the system stays in its ground state $|G_S\rangle$ during the measurement process. In Fig. 5.6, we show $\mathcal{F}$ versus ω_p for different values of λ and of the dissipation rates. The moderate dip at the resonance frequency is due to creation of real excitations in the system S via the driving of the qubit M. When the driving amplitude $\Omega_p \to 0$, the dip disappears (not shown). Out of resonance, $\mathcal{F} \to \mathcal{F}_G$, the fidelity depending only on the level mixing between qubit M and system S (see Fig. 5.4), quantified by the ground state fidelity $\mathcal{F}_G$. Concerning the dissipation, our results show that when the cavity system S dissipation rates γ_c, γ_a are much smaller than the ancilla qubit dissipation rate γ_M, then the most pronounced fidelity dip is obtained (black solid-lines in Fig. 5.6 are for vanishing dissipation in the system S). Indeed, in such conditions a significant steady-state population of excited states can be created in S due to the low dissipation rates, implying that the ancilla qubit cannot 'read' faithfully the ground state of the system. Instead in the opposite limit, the fidelity dip disappears ($\mathcal{F}(\omega_{dip}) \to \mathcal{F}_G$) as the excited state populations in S can be dissipated efficiently.

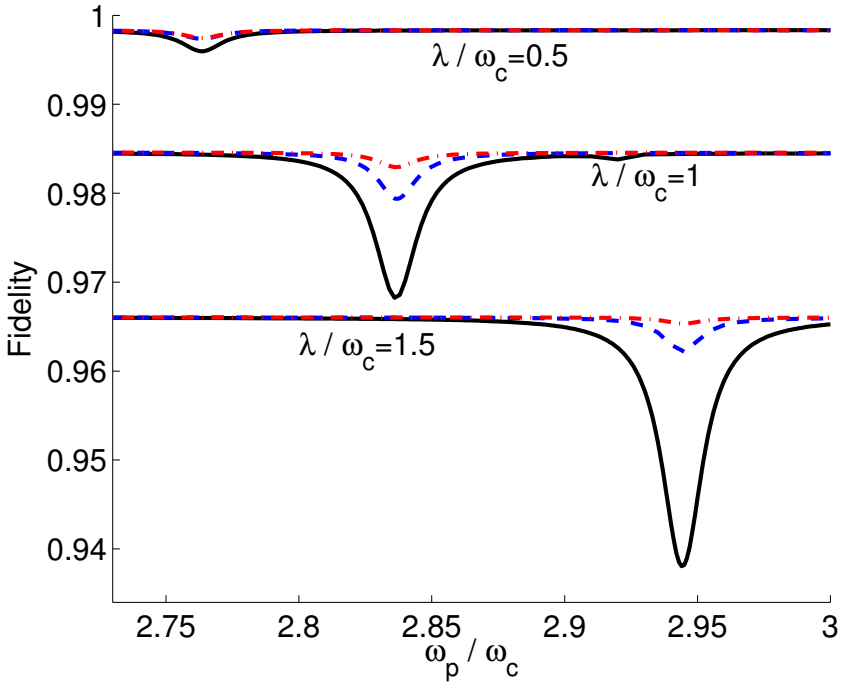

Figure 5.6 Measurement fidelity $\mathcal{F}$ (see definition in the text) for different values of λ for the Dicke model and for different dissipation rates $\gamma_c = \gamma_a = \eta\gamma_M$ and $\gamma_M = 0.01\omega_c$. Solid line: $\eta = 0$. Dashed line: $\eta = 1$. Dot-dashed line: $\eta = 10$. Other parameters as in Fig. 5.5.

5.4 Finite temperature and dephasing

All the results shown up to now have been obtained considering reservoirs at zero temperature, because the focus is the physics of the ground state. In this section, we consider the effect of a finite temperature bath and of dephasing on the ancillary qubit spectroscopy.

In order to include the effect of temperature, we need to consider the following master equation, that is derived in detail in Section 3.1:

$$\partial_t\hat{\rho} = -i[\hat{H}(t),\rho] + \frac{\gamma_c}{2}\mathcal{D}_T(\hat{S}_c)\hat{\rho} + \frac{\gamma_a}{2}\mathcal{D}_T(\hat{S}_a)\hat{\rho} + \frac{\gamma_M}{2}\mathcal{D}_T(\hat{S}_M)\hat{\rho} \tag{5.29}$$

where the dissipative term $\mathcal{D}_T$ are defined in the following energy conserving form

$$\begin{aligned}\mathcal{D}_T(\hat{S}_i)\hat{\rho} = &\sum_{\omega>0}\widetilde{G}(\omega)(1+N(\omega))\left\{2\hat{S}_i(\omega)\rho\hat{S}_i^\dagger(\omega) - \rho\hat{S}_i^\dagger(\omega)\hat{S}_i(\omega) - \hat{S}_i^\dagger(\omega)\hat{S}_i(\omega)\rho\right\}\\ &+\sum_{\omega>0}\widetilde{G}(\omega)\,N(\omega)\left\{2\hat{S}_i^\dagger(\omega)\rho\hat{S}_i(\omega) - \rho\hat{S}_i(\omega)\hat{S}_i^\dagger(\omega) - \hat{S}_i(\omega)\hat{S}_i^\dagger(\omega)\rho\right\}.\end{aligned} \tag{5.30}$$

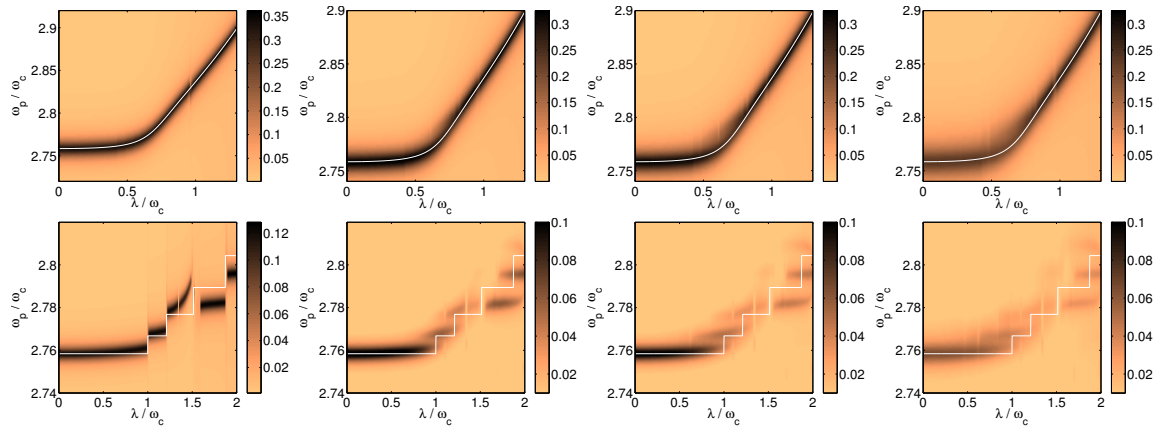

Figure 5.7 Excited state population of the ancilla M versus the coherent drive frequency ω_p for different values of collective coupling λ at finite temperature. In the four columns from left to right, the value of the temperature is respectively $k_BT/(\hbar\omega_c) = 0$, 0.105, 0.21 and 0.42. Top panels are for the Dicke model with $\Omega_p = 0.5\gamma_M$ and dissipation parameters $\gamma_M = \gamma_c = \gamma_a = 0.01\omega_c$. Bottom panels are for the Tavis-Cummings model with $\Omega_p = 0.2\gamma_M$ and dissipation parameters $\gamma_M = \gamma_c = \gamma_a = 0.005\omega_c$ (note that in some areas of the figures the colour scale is saturated in order to improve the contrast). Other parameters: $N = 3$, $\omega_c = \omega_a$, $\omega_M = 2.75\omega_c$, $g_M = 0.1\omega_c$.

where $N(\omega)$ is the bosonic thermal distribution and the jumps operator $\hat{S}_i(\omega)$ are defined as

$$\hat{S}_i(\omega) \stackrel{\text{def}}{=} \sum_{\epsilon'-\epsilon=\omega} \langle l|\hat{S}_i|l'\rangle |l\rangle\langle l'|.$$

The operators $\hat{S}_i$ are those involved in the coupling to the reservoir, namely $\hat{S}_c = \hat{a}^\dagger + \hat{a}$ for the bosonic mode, $\hat{S}_0 = \hat{J}_x$ for the two-level systems and $\hat{S}_M = \hat{\sigma}_x^{(M)}$ for the ancilla. The spectral function $\widetilde{G}(\omega)$ depends on the density-of-states of the reservoir excitations. When the bath is a 3D electromagnetic field, we have $\widetilde{G}(\omega) \propto \omega^3$, hence it vanishes while $\omega \to 0$ [125, 126]. An ohmic reservoir scales instead as $\widetilde{G}(\omega) \propto \omega$.

In Fig. 5.7 , we show the ancillary transition spectrum as a function of the coupling λ for different values of temperature, namely $k_BT/\hbar\omega_c = 0$, 0.105, 0.21 and 0.42 (from bottom to top) for the Dicke (left panels) and Tavis-Cummings model (right panel). As we mentioned in Sec. 5.3, these values for $k_BT/\hbar\omega_c$ are realistic values in circuit QED realisation. We conclude that the Lamb shifts are still well measurable and that the main effects is a moderate broadening of the Lamb-shifted ancillary qubit resonances.

We have also checked that the behaviour at low frequency does not affect the results in a significant way. In Fig. 5.8, we show a typical ancilla spectrum with three different reservoirs with $\widetilde{G}(\omega) \propto \omega^\alpha$ and $\alpha = 1$ (ohmic), $\alpha = 2$ and $\alpha = 3$. It is apparent that the differences are negligible, indeed the broadening is dominated by

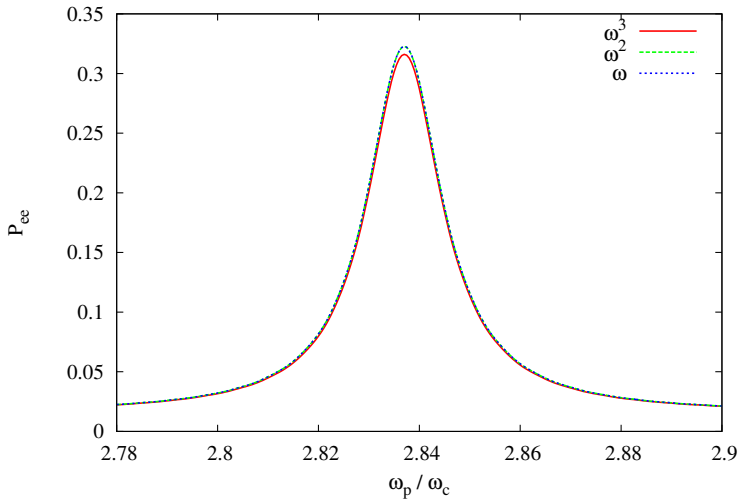

Figure 5.8 Example of ancilla spectrum dependence on reservoir density of states ($J(\omega) \propto \omega^{\alpha}$ with $\alpha = 1, 2, 3$) for a finite temperature ($k_B T/(\hbar\omega_c) = 0.21$). Dicke model, parameters: $\lambda/\omega_c = 1$, $\gamma_c = \gamma_M = \gamma_a = 0.01\omega_C$. Other parameters: $N = 3$, $\omega_c = \omega_a$, $\omega_M = 2.75\omega_c$, $g_M = 0.1\omega_c$.

the spectra dependence around the ancilla qubit transition.

Dephasing noise

We have also tested the robustness of the ancillary spectroscopy under the effect of noise mechanisms different from flip errors. More precisely we considered the effect produced by jump operator $\hat{\sigma}_z^{(M)}$ and $\hat{J}_z$, which correspond to pure dephasing respectively on the ancilla and on the intra-cavity two-level systems. At zero temperature, we account for this kind of noise by adding to the master equation in Eq. (5.29) the term $\frac{\gamma_d}{2}\mathcal{D}_0(\hat{S}_d)\hat{\rho}$, which is defined as

$$\mathcal{D}_0(\hat{S}_d)\hat{\rho} = \sum_{\omega>0} \left\{ 2\hat{S}_d(\omega)\hat{\rho}\hat{S}_d^{\dagger}(\omega) - \hat{\rho}\hat{S}_d^{\dagger}(\omega)\hat{S}_d(\omega) - \hat{S}_d^{\dagger}(\omega)\hat{S}_d(\omega)\hat{\rho} \right\} , \tag{5.31}$$

where we assumed a constant spectral function $\widetilde{G}(\omega) = 1$ and where the operator $\hat{S}_d(\omega)$ is defined as above, using the jump operators $\hat{S}_d = \hat{\sigma}_z^{(M)}$ or $\hat{J}_z$. We have checked that the ancillary qubit spectroscopy is robust with respect to pure dephasing, which gives a similar effect to what produced by dissipation (population finite lifetime). In Fig. 5.9 we show different spectra by varying the ratio between dissipation and pure dephasing produced by the jump operator $\hat{J}_z$. The broadening effect due to pure dephasing is suppressed for larger values of coupling λ between the cavity and the two-level systems. This kind of suppression is due to collective symmetry and is consistent with results obtained in other works on ultrastrongly coupled systems

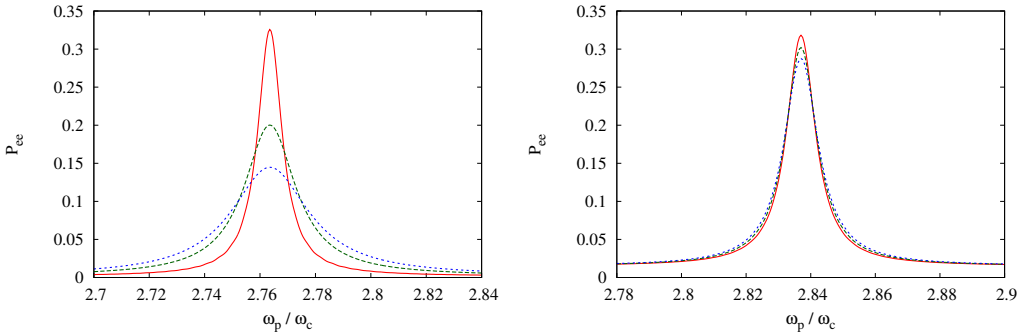

Figure 5.9 Ancilla spectrum of the Dicke model at zero temperature when the pure dephasing rate is tuned from $\gamma_d = 0$ (solid red), 0.5 (dashed green) to $1\,\gamma_c$ (dotted blue). Left panel: $\lambda = 0.5\,\omega_C$. Right panel: $\lambda = 1\,\omega_C$. Other parameters: $\gamma_c = \gamma_M = \gamma_a = 0.006\omega_C$, $N = 3$, $\omega_c = \omega_a$, $\omega_M = 2.75\omega_c$, $g_M = 0.1\omega_c$.

[76, 152]. We do not show the well known results about the effect of pure dephasing produced by the jump operator $\hat{\sigma}_z^{(M)}$, which only causes an additional broadening of the ancilla transition. What is mainly relevant in the ancilla spectroscopy is the total broadening affecting the spectral linewidth more than the specific nature of its origin. We emphasise that in our work, we have conservatively considered spectral linewidths, which are considerably larger than what achievable in state-of-the-art circuit QED systems [152, 154].

5.5 Conclusion and perspectives on the ancillary qubit spectroscopy

In conclusion, we have shown theoretically that the spectroscopy of an ancillary qubit coupled to a cavity (circuit) QED system is a very sensitive probe of its ground state properties. The spectral Lamb shift of the ancillary qubit transition is vacuum-dependent, namely it depends on the ground state populations and correlations. The Lamb shift behaves qualitatively in a different way for systems described by the Dicke, Tavis-Cummings and Hopfield models, whose exotic vacua are qualitatively different. By a consistent solution of the master equation to include dissipation in the ultrastrong coupling regime, we have studied the measurement fidelity by accounting for level-mixing between system and measurement qubit, driving and dissipation. The present work demonstrates that ancillary qubit spectroscopy of cavity QED systems is a promising tool to study non-destructively the rich physics of QED vacua in the ultrastrong light-matter coupling regime.

Chapter 6

Photonic Schrödinger cat and their feedback control

Even if the quantization of light was at the heart of the development of quantum mechanics, for a very long time it was impossible to exploit photons to investigate quantum many-body physics. It was only recently that this idea became reality. In particular, the development of new experimental platforms, such as semiconductor cavities[37, 38, 51] and superconducting circuits [44, 47], made possible to create effective photon-photon interactions via the meditation of the electronic degrees of freedom of the materials. Thanks to these developments, it was possible to study many-body quantum physics with light [155]. Because of its out-of-equilibrium nature, this physics profoundly differs from its atomic counterpart. The continuous leak of photons from a resonator can not be neglected, and therefore photons must be continuously pumped into the system. The competition between drive, dissipation, and interactions in such kind of out-of-equilibrium quantum systems enriches even more the physical scenario. Indeed, this non-equilibrium regime has been at the centre of a vast theoretical and experimental exploration: from quantum fluids of light (e.g. [55] and references therein), to dissipative phase transition (both in spin systems [156, 157] and in softcore bosons [158]) the interest in the subject has been considerable.

At the same time, the new field of reservoir engineering achieved extraordinary results. The objective is to shape the photon exchanges between a resonator and the environment, so to realise non-trivial drive and dissipation [78–85]. In this direction moved the idea of quantum computation with light. If one can exploit the environment so to force the system into a nonclassical superposition of orthogonal states, those can be used as the logic basis of computation. The advantage in this procedure is that those states will be, for their own construction, impervious to decoherence. In particular, it has been proven that Schrödinger cats (and coherent states) can be used as (quasi-)orthogonal states in quantum computation [75, 77, 159, 160]. Those states are defined as the superposition of two coherent states and have the form:

$$|\mathcal{C}_\alpha^\pm\rangle = \frac{|\alpha\rangle \pm |-\alpha\rangle}{\sqrt{1 \pm e^{-2|\alpha|^2}}}. \tag{6.1}$$

We recall that the coherent state $|\alpha\rangle = e^{-|\alpha|^2/2} \sum_n (n!)^{-1/2} \alpha^n |n\rangle$ is the eigenstate of the destruction operator: $\hat{a}|\alpha\rangle = \alpha|\alpha\rangle$. Coherent states are the states of the

electromagnetic field that are the closest to the classical ones, since they have a well defined mean amplitude $|\alpha|$ and phase (being $|n\rangle$ the n-photon Fock state). Cat states become particularly interesting in the limit $\langle\hat{n}\rangle = |\alpha|^2 \gg 1$. In this limit of high number of photons, in fact, $\langle\alpha| - \alpha\rangle \simeq 0$ and therefore the Schrödinger cat is a superposition of two (almost) orthogonal (semi) classical states. The state $|\mathcal{C}_\alpha^+\rangle$ is called the even cat, since it can be written as a superposition of solely even Fock states, while $|\mathcal{C}_\alpha^-\rangle$ is the odd cat.

In this chapter we report our work on a class of two-photon driven-dissipative resonators that is particularly promising for the realisation of these interesting states. We start by showing in Sec. 6.1, that the steady state of this kind of systems could be very well approximated by a statistical mixture of two photonic Schrödinger cats [96]. Even if in the transient dynamics of the cavity it is still possible to detect some quantumness [85], the steady state was mathematically proven to be fully classical (i.e. with a totally positive Wigner function). By studying the quantum trajectories of the system we realised that this loss of quantumness is mainly due to one-photon dissipation and that under photon-counting monitoring the state of the system is always quantum. This quantum trajectory analysis, that is largely discussed in Section 6.2, leads to envisioning a feedback mechanism that exploits the action of one-photon dissipation to effectively protect a chosen cat state. In Sec. 6.3 we analyse in more detail this feedback protocol, by discussing its effect on the system, providing both an analytical and a numerical description.

6.1 The model: two-photon driven-dissipative resonators

The system under consideration is a single nonlinear Kerr resonator (see Sec. 2.2.1) subject to a parametric two-photon driving and to one- and two-photon dissipation processes, see Fig. 6.1. This class of exotic resonators have been realised experimentally, and interestingly it was shown in Ref. [85] that in the transient dynamics toward the steady state some features of photonic Schrödinger cats were still present. In the absence of pumping our Hamiltonian reads ($\hbar = 1$)

$$\hat{H}_0 = \omega_c\, \hat{a}^\dagger \hat{a} + \frac{U}{2} \hat{a}^\dagger \hat{a}^\dagger \hat{a} \hat{a}, \tag{6.2}$$

where ω_c is the cavity mode frequency, U is the strength of photon-photon interaction (see Sec. 2.2.1), $\hat{a}$ and $\hat{a}^\dagger$ are, respectively, the annihilation and creation operator for photons inside the resonator. As shown in Ref.[85], a two-photon coherent drive with amplitude G and frequency $2\omega_p$ can be realised through a parametric processes. It allows to coherently inject pairs of photons in the system and it can be described by

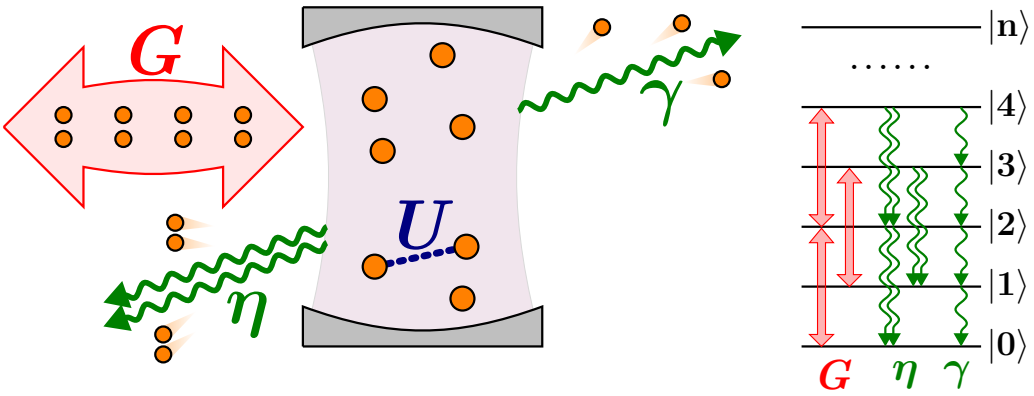

Figure 6.1 A sketch of the considered class of systems. The photon-photon interaction of a Kerr nonlinear resonator is quantified by U. The resonator is also subject to a coherent two-photon driving of amplitude G, one- and two-photon losses with rates γ and η. On the right, we sketch the effects of these physical processes on the Fock (number) states $|n\rangle$.

the following time-dependent Hamiltonian term :

$$\hat{H}_{\text{2ph}} = \frac{G}{2} e^{-i2\omega_p t} \hat{a}^\dagger \hat{a}^\dagger + \frac{G^*}{2} e^{i2\omega_p t} \hat{a}\hat{a}, \tag{6.3}$$

where G is the pump amplitude and ω_2 its frequency (see Sec. 3.2 for a microscopical derivation of a driving Hamiltonian). In order to remove the time-dependence from the Hamiltonian we consider the unitary transformation $\hat{U}(t) = e^{i\omega_p \hat{a}^\dagger \hat{a} t}$. This transformation allows us to describe the system in the reference in a frame rotating at the coherent pump frequency ω_p. In this rotating frame the Hamiltonian is time-independent and it reads:

$$\hat{H} = -\Delta \hat{a}^\dagger \hat{a} + \frac{U}{2} \hat{a}^\dagger \hat{a}^\dagger \hat{a}\hat{a} + \frac{G}{2} \hat{a}^\dagger \hat{a}^\dagger + \frac{G^*}{2} \hat{a}\hat{a}, \tag{6.4}$$

where $\Delta = \omega_p - \omega_c$ is the pump-cavity detuning (more detail on the derivation of the rotating frame Hamiltonian are provided at the end of Sec. 3.2). Here and in the rest of the manuscript we will consider the case of resonant pumping, i.e $\omega_p = \omega_c$ and $\Delta = 0$. With any loss of generality we can arbitrarly choose the two-photon pumping phase in such a way to have a real amplitude G. Under this two assumptions the Hamiltonian reducesf to a very simplified form:

$$\hat{H} = \frac{U}{2} \hat{a}^\dagger \hat{a}^\dagger \hat{a}\hat{a} + \frac{G}{2} \left(\hat{a}^\dagger \hat{a}^\dagger + \hat{a}\hat{a} \right), \tag{6.5}$$

Despite the high quality factor of state-of-the-art cavities, a confined photon has always a finite lifetime due to the coupling to the environment. The environment is in general a system with a huge number of degrees of freedom in which the system

dissipates photons. As detailed in Sec. 3.1, an excellent description of the coupling to the environment is provided by a Lindblad dissipation super-operator $\mathcal{D}(\hat{A})$ of the form

$$\mathcal{D}(\hat{A})\,\hat{\rho} = 2\,\hat{A}\,\hat{\rho}\,\hat{A}^\dagger - \hat{A}^\dagger\hat{A}\,\hat{\rho} - \hat{\rho}\,\hat{A}^\dagger\hat{A}, \tag{6.6}$$

where $\hat{A}$ is the quantum jump operator corresponding to the specific dissipation process. To include the interaction with the environment, it is usually enough to consider one-photon losses, whose jump operator is given by the annihilation operator (see Sec. 3.1.2). In addition, we also consider two-photon losses, which naturally emerge together with the engineered two-photon pumping [85]. These losses are included through the jump operator $\hat{a}^2$. The resulting Lindblad master equation describing the evolution of the the system density matrix $\hat{\rho}$ is

$$\frac{\partial\hat{\rho}}{\partial t} = i\left[\hat{\rho}, \hat{H}\right] + \frac{\gamma}{2}\,\mathcal{D}(\hat{a})\,\hat{\rho} + \frac{\eta}{2}\,\mathcal{D}(\hat{a}^2)\,\hat{\rho} = \mathcal{L}\hat{\rho}, \tag{6.7}$$

where γ and η are, respectively, the one- and two-photon dissipation rates and $\hat{H}$ is the one given in Eq. (6.5). We recall that together with the initial condition, the time evolution of $\hat{\rho}$ is completely defined by the Lindbladian superoperator $\mathcal{L}$. Note that we are assuming the environment to be at zero temperature. Indeed according to the two dissipators in Eq. (6.7) the photons are only going from the system to the environment. On the other hand these losses are balanced by the two-photon pump that keep the population of the cavity finite. We emphasise that only the one-photon dissipation term in the Lindblad master equation (6.7) is not preserving the parity of the cavity field $\hat{P} = \exp(i\pi\hat{a}^\dagger\hat{a}) = \exp(i\pi\hat{N})$.

6.1.1 Exact solution for the steady state

Despite the many different contributing terms, this master equation has an exact analytic solution for the steady density matrix [161]. The solution has been recently found following a technique first introduced in Ref. [162] via the so-called P-representation of the density matrix. In this representation the Lindblad master Equation (6.7) maps into a Fokker-Planck equation whose stationary solution is known. Remarkably, this solution can be integrated, providing the analytic expression of the stationary density matrix in the Fock basis of number states:

$$\langle n|\,\hat{\rho}_{\rm ss}\,|m\rangle = \frac{1}{\mathcal{N}}\sum_{\ell=0}^{\infty}\frac{1}{\ell!\sqrt{n!\,m!}}\,\mathcal{F}(g,c,\ell+n)\,\mathcal{F}^*(g,c,\ell+m), \tag{6.8}$$

where $\mathcal{N}$ is the normalisation factor, chosen such that $\mathrm{Tr}\{\hat{\rho}_{\rm ss}\} = 1$. $\mathcal{F}(g,c,\ell) = (i\sqrt{g})^\ell\ {}_2F_1(-\ell,-c;-2c;2)$, ${}_2F_1$ being the Gaussian hypergeometric function [163]. In spite of the several parameters in the model, the solution depends only on two dimensionless quantities, namely

$$\begin{aligned} c &= (\Delta + i\,\gamma/2)/(U - i\,\eta)\,, \\ g &= G/(U - i\ \eta)\,. \end{aligned} \tag{6.9}$$

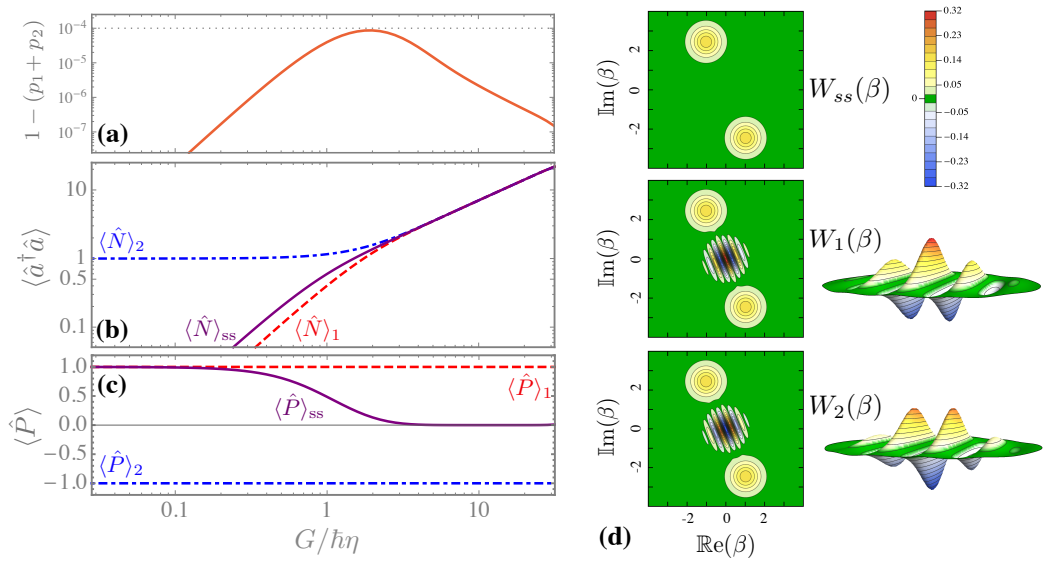

Figure 6.2 Exact results for the steady-state. The corresponding density matrix can be expressed as $\hat{\rho}_{\rm ss} = \sum_\kappa p_\kappa |\Psi_\kappa\rangle\langle\Psi_\kappa|$, where p_1 and p_2 are the probabilities of the two most probable eigenstates. The parameters are set to: $\Delta = 0$, $U = 1\eta$, $\gamma = 0.1\,\eta$. Panel (a): residual probability $1 - p_1 - p_2$ versus the two-photon drive amplitude G normalised to the two-photon loss rate η, showing that the density matrix is dominated by the first two eigenstates. Panel (b): as a function of G/η, mean number of photons $\langle \hat{N} \rangle_{\rm ss}$ and its contributions $\langle \hat{N} \rangle_1$ and $\langle \hat{N} \rangle_2$. Panel (c): as a function of G/η, the mean parity $\langle \hat{P} \rangle_{\rm ss}$ and its contributions $\langle \hat{P} \rangle_1$ and $\langle \hat{P} \rangle_2$. Panel (d): for $G = 10\eta$, contour plots of the Wigner function $W_{\rm ss}(\beta)$ for the density matrix $\hat{\rho}_{\rm ss}$, together with the Wigner functions $W_1(\beta)$ and $W_2(\beta)$ associated to the two most probable eigenstates. For the latter, we also show a 3D zoom of the central region $|\beta| \leq 1.6$.

The former can be seen as a complex single-particle detuning $\Delta + i\,\gamma/2$ divided by a complex interaction energy $U - i\,\eta$; g is instead the two-photon pump intensity normalised by the same quantity. We recall that we will only consider here the resonant pump case $\Delta = 0$, thus the dimensionless quantity c reduces to $c = i\,\gamma/2(U - i\,\eta)$. Notably, $\mathcal{F}(g, c, \ell) = 0$ for ℓ odd, meaning that, for any finite value of the system parameters, there will be no even-odd coherences in the steady state. More detail on this analytic solution of the stationary density matrix is provided in Ref. [161].

To further characterise the steady state, we consider its spectral decomposition

$$\hat{\rho}_{\rm ss} = \sum_\kappa p_\kappa |\Psi_\kappa\rangle\langle\Psi_\kappa| \,, \tag{6.10}$$

with $|\Psi_\kappa\rangle$ the $\kappa^{\rm th}$ eigenstate of $\hat{\rho}_{\rm ss}$ with eigenvalue p_κ. The latter corresponds to the probability of finding the system in $|\Psi_\kappa\rangle$. The eigenstates are sorted in such a way that $p_\kappa \geq p_{\kappa+1}$. For a pure state, $p_1 = 1$ and all the other probabilities p_κ are zero. For the steady state in Eq. (6.8) only two eigenstates dominate the density matrix.

As shown in Fig. 6.2(a), typically

$$p_1 + p_2 \simeq 1\,, \quad \text{and} \quad \hat{\rho}_{\rm ss} \simeq p_1\,|\Psi_1\rangle\,\langle\Psi_1| + p_2\,|\Psi_2\rangle\,\langle\Psi_2|\,. \tag{6.11}$$

The aforementioned absence of even-odd coherences implies that $|\Psi_{1(2)}\rangle$ is composed of only even (odd) Fock states. Furthermore, we find that $|\Psi_{1,2}\rangle$ are nearly equal to the photonic Schrödinger Cat states $|\mathcal{C}_\alpha^{\pm}\rangle$ where the coherence α depends on physical parameters of the system:

$$\alpha = \sqrt{\frac{-G}{U - i\eta}}\,, \tag{6.12}$$

where an explanation for this formula is given in Section 6.1.2. In order to give an idea of how close $|\Psi_{1,2}\rangle$ are to the cat states $|\mathcal{C}_\alpha^{\pm}\rangle$ we compute the inner product between these state for the parameters of Fig. 6.2(d). The value we obtain is very close to one: $\langle\Psi_{1,2}|\mathcal{C}_\alpha^{+(-)}\rangle \simeq (1 - 8\times10^{-6})$ for $\alpha \approx 2.7\,e^{2.0\,i}$. Hence the steady-state density matrix $\hat{\rho}_{\rm ss}$ is well approximated by the statistical mixture of two orthogonal cat states:

$$\hat{\rho}_{\rm ss} \simeq p_1\ |\mathcal{C}_\alpha^{+}\rangle\langle\mathcal{C}_\alpha^{+}| + p_2\ |\mathcal{C}_\alpha^{-}\rangle\langle\mathcal{C}_\alpha^{-}|\,, \tag{6.13}$$

The coefficients $p_{1,2}$ can be interpreted as the probabilities of the system of being found in the corresponding cat state. Using the linearity of the trace, for any operator $\hat{O}$ one can write

$$O_{\rm ss} = {\rm Tr}\Big\{\hat{\rho}_{\rm ss}\,\hat{O}\Big\} \simeq p_1 O_1 + p_2 O_2, \quad \text{where} \quad O_\kappa = \langle\Psi_\kappa|\hat{O}|\Psi_\kappa\rangle\,. \tag{6.14}$$

In Fig. 6.2(b) we plot, as a function of the pump amplitude G, the steady-state mean density $\langle\hat{N}\rangle_{\rm ss}$, together with the mean density $\langle\hat{N}\rangle_{1,2}$ of the two contributing cat-like states $|\Psi_{1,2}\rangle$. The mean number of photons of these two states become large and equal in the limit of a very intense pumping. As a confirmation that $|\Psi_{1,2}\rangle \simeq |\mathcal{C}_\alpha^{\pm}\rangle$, in Fig. 6.2(c), we have that the $\langle\hat{P}\rangle_{1,2}$ are always close to ±1, that are the eigenvalues of $\hat{P}$. A valuable tool to visualise the non-classicality of a state is the Wigner function defined as:

$$W(\beta) = \frac{2}{\pi}{\rm Tr}\Big\{\hat{\rho}\,\hat{D}_\mu\hat{P}\hat{D}_\mu^\dagger\Big\}\,, \quad \text{where} \quad \hat{D}_\mu = e^{\beta\hat{a}^\dagger - \beta^*\hat{a}} \tag{6.15}$$

is the displacement operator [164]. Indeed, negative values of $W(\beta)$ indicate that we are in presence of non-classicality [27, 165]. More concretely, in the context of quantum computation, negative valued Wigner representation are considered a necessary resource for computational speed-up [166, 167].

The Wigner function corresponding to the stationary density matrix in Eq. (6.8) is always positive, while the separate contributions $W_1(\beta)$ and $W_2(\beta)$ exhibit an interference pattern with negative regions, typical of cat states [cf. Fig. 6.2(d)].

From Fig. 6.2(b,c) it is clear that in the regime of intense pumping ($G \gg U, \gamma, \eta$), one has $|\alpha| \gg 1$ and $p_1 \simeq p_2 \simeq 1/2$. Under these conditions Eq. (6.13) can be recast as:

$$\hat{\rho}_{\rm ss} \simeq \frac{1}{2}\,|\alpha\rangle\langle\alpha| + \frac{1}{2}\,|-\alpha\rangle\langle-\alpha|\,. \tag{6.16}$$

Hence, the steady state can be seen as well as a statistical mixture of two coherent states of opposite phase. Since $\hat{\rho}_{\rm ss}$ is anyhow a mixture of two (quasi-)orthogonal states, the steady state is bimodal. Such a bimodality can be visualised, for instance, through the Wigner function Fig. 6.2(d) [96, 161]. Now, the pivotal question is: if one monitors the evolution of the system, in which states will it be? The orthogonal cat states in Eq. (6.13), the two coherent states with opposite phases in Eq. (6.16), or none of them in particular? As we will show in Section 6.2, the answer dramatically depends on the type of measurement scheme employed to monitor the trajectory of the system.

6.1.2 Evolution in the cat subspace

To obtain a useful insight on the property of this system, let us consider a different approach to the solution of Eq. (6.7). Let us divide the Liouvillian into a two-photon part and a one photon one, i.e. $\mathcal{L} = \mathcal{L}_2 + \mathcal{D}_1$, where $\mathcal{L}_2\hat{\rho} = i\left[\hat{\rho}, \hat{H}\right] + \frac{\eta}{2}\mathcal{D}(\hat{a}^2)\,\hat{\rho}$ and $\mathcal{D}_1\hat{\rho} = \frac{\gamma}{2}\mathcal{D}(\hat{a})\hat{\rho}$. In the most simple case, there exists a class of steady state density matrices $\hat{\rho}$ which separately are zero under the action of $\mathcal{L}_2$ and $\mathcal{D}_1$. In this spirit, one may try to simplify the description of the system time evolution. First, one identifies a set of density matrices $\hat{\rho}_i$ for which $\mathcal{L}_2\hat{\rho}_i = 0$. If $\mathcal{D}_1$ simply couples the $\hat{\rho}_i$ between them, then the evolution of a system on this reduced subspace greatly simplifies.

The Schrödinger cats states $|\mathcal{C}_\alpha^\pm\rangle\langle\mathcal{C}_\alpha^\pm|$, defined in Eq. (6.1), are steady state of $\mathcal{L}_2$, indeed

$$\begin{aligned}\mathcal{L}_2\,|\mathcal{C}_\alpha^\pm\rangle\langle\mathcal{C}_\alpha^\pm| = &\left(-i\frac{U}{2}\alpha^2 - i\frac{G}{2} - \frac{\eta}{2}\alpha^2\right)\hat{a}^\dagger\hat{a}^\dagger\,|\mathcal{C}_\alpha^\pm\rangle\langle\mathcal{C}_\alpha^\pm| \\ &+\left(-i\frac{U}{2}\alpha^2 - i\frac{G}{2} - \frac{\eta}{2}\alpha^2\right)|\mathcal{C}_\alpha^\pm\rangle\langle\mathcal{C}_\alpha^\pm|\,\hat{a}\,\hat{a} \\ &+\left(-i\frac{G}{2}\alpha^2 + i\frac{G}{2}\alpha^{*\,2} + \eta|\alpha|^4\right)|\mathcal{C}_\alpha^\pm\rangle\langle\mathcal{C}_\alpha^\pm|\ ,\end{aligned} \tag{6.17}$$

and it is straightforward to check that the brackets cancel for $\alpha = \sqrt{-G/(U-i\eta)}$. Any statistical mixture of the Schrödinger cat states $\hat{\rho} = p^+\,|\mathcal{C}_\alpha^+\rangle\langle\mathcal{C}_\alpha^+| + p^-\,|\mathcal{C}_\alpha^-\rangle\langle\mathcal{C}_\alpha^-|$ is also a steady state of $\mathcal{L}_2$, i.e. $\mathcal{L}_2\hat{\rho} = 0$.

Let us now consider the effect of $\mathcal{D}_1$ on this mixed state:

$$\begin{aligned}\mathcal{D}_1\hat{\rho} = &\,\gamma\left[|\alpha|^2 p^-\,|\mathcal{C}_\alpha^+\rangle\langle\mathcal{C}_\alpha^+| + |\alpha|^2 p^+\,|\mathcal{C}_\alpha^-\rangle\langle\mathcal{C}_\alpha^-|\right] \\ &-\frac{\gamma}{2}\left[\alpha\,p^+\hat{a}^\dagger\,|\mathcal{C}_\alpha^-\rangle\langle\mathcal{C}_\alpha^+| + \alpha\,p^-\hat{a}^\dagger\,|\mathcal{C}_\alpha^+\rangle\langle\mathcal{C}_\alpha^-|\right] \\ &-\frac{\gamma}{2}\left[\alpha^* p^+\,|\mathcal{C}_\alpha^+\rangle\langle\mathcal{C}_\alpha^-|\,\hat{a} + \alpha^* p^-\,|\mathcal{C}_\alpha^-\rangle\langle\mathcal{C}_\alpha^+|\,\hat{a}\right]\ .\end{aligned} \tag{6.18}$$

This equation is not zero except for $\gamma = 0$. However it interestingly approaches a very simplified expression in the regime of intense pumping, in which $|\alpha| \gg 1$. Let us

express all the terms of the form $\hat{a}^\dagger |\mathcal{C}_\alpha^\pm\rangle$ in Eq. (6.18) as $\hat{a}^\dagger |\mathcal{C}_\alpha^\pm\rangle - \alpha^* |\mathcal{C}_\alpha^\mp\rangle + \alpha^* |\mathcal{C}_\alpha^\mp\rangle$:

$$\begin{aligned}\mathcal{D}_1\hat{\rho} =& \gamma \left[|\alpha|^2(p^- - p^+) |\mathcal{C}_\alpha^+\rangle\langle\mathcal{C}_\alpha^+| + |\alpha|^2(p^+ - p^-) |\mathcal{C}_\alpha^-\rangle\langle\mathcal{C}_\alpha^-|\right] \\ &- \frac{\gamma}{2}\left[\alpha p^+ \left(\hat{a}^\dagger |\mathcal{C}_\alpha^-\rangle - \alpha^* |\mathcal{C}_\alpha^+\rangle\right)\langle\mathcal{C}_\alpha^+| + \alpha p^- \left(\hat{a}^\dagger |\mathcal{C}_\alpha^+\rangle - \alpha^* |\mathcal{C}_\alpha^-\rangle\right)\langle\mathcal{C}_\alpha^-|\right] \\ &- \frac{\gamma}{2}\left[\alpha^* p^+ |\mathcal{C}_\alpha^+\rangle\left(\langle\mathcal{C}_\alpha^-| \hat{a} - \alpha \langle\mathcal{C}_\alpha^+|\right) + \alpha^* p^- |\mathcal{C}_\alpha^-\rangle\left(\langle\mathcal{C}_\alpha^+| \hat{a} - \alpha \langle\mathcal{C}_\alpha^-|\right)\right] .\end{aligned} \tag{6.19}$$

For $|\alpha| \gg 1$, the last two terms are negligible with respect to the first one. Indeed, the norm of the states $\left(\hat{a}^\dagger |\mathcal{C}_\alpha^\pm\rangle - \alpha^* |\mathcal{C}_\alpha^\mp\rangle\right)$ is equal to 1 for any value of α, so the last two terms in Eq. (6.19) are of order $O(|\alpha|)$, while the first two terms are of order $O(|\alpha|^2)$. Thus, we have proved that the overall effect of $\mathcal{D}_1$ is simply to evolve the populations of the even ad odd cats:

$$\mathcal{D}_1\hat{\rho} \simeq \gamma \left[|\alpha|^2(p^- - p^+) |\mathcal{C}_\alpha^+\rangle\langle\mathcal{C}_\alpha^+| + |\alpha|^2(p^+ - p^-) |\mathcal{C}_\alpha^-\rangle\langle\mathcal{C}_\alpha^-|\right] . \tag{6.20}$$

Note that this equation reduces to zero for $p^+ = p^- = 1/2$ and that the projection on cat subspace is valid and stable as soon as γ is small compared to the other parameters G, U and η, that are the parameters of $\mathcal{L}_2$ whose action is to stabilise the cat states.

Summarising, in the regime of strong pumping and weak one-photon dissipation $G \gg U, \eta \gg \gamma$, the behaviour and the properties of the system can be faithfully described by considering the subspace spanned by the two cat states $|\mathcal{C}_\alpha^\pm\rangle$. The effect of $\mathcal{D}_1$ will be to evolve the system towards an equal mixture of odd and even cats. We have therefore developed a tool which allows to study both the steady state and the evolution of the density matrix passing from an infinite dimensional space to one of dimension two. We will also see how this tool can be used to analyse the action of a feedback control, as detailed in Sec. 6.3.

6.2 Quantum trajectories approach to bimodality

From a theoretical point of view, a Lindblad master equation describes the out-of-equilibrium dynamics of a system coupled to a Markovian (i.e., memoryless) environment. As we have seen in Chapter 4, the density matrix $\hat{\rho}(t)$ solving Eq. (6.7) also encodes the average evolution of the system when no information is collected about the environment state. On the other hand, one can imagine to keep track of the system state by continuously probing the environment. Doing so, the time evolution of the system would change at each realisation, as expected from the intrinsic randomness of quantum measurement. However, $\hat{\rho}(t)$ can be retrieved by averaging over an infinite number of such "monitored" realisations.

The Montecarlo wavefunction method [144, 168, 169] has been developed relying exactly on this idea. It is based on the stochastic simulation of the system evolution when one continuously gathers information from the environment. Each simulation of the stochastic evolution of the system gives a single quantum trajectory. The results

obtained by solving the master Equation (6.7) are recovered by averaging over many trajectories. In order to simulate the quantum trajectories, it is necessary to explicitly model how an observer measures the environment, thus affecting the system evolution itself (a detailed discussion on this subject is given in Ref. [27]). Interestingly, several different measures can be associated with the same master equation. Depending on the chosen measurement, contrasting results and interpretations can emerge. Those incompatibilities are, however, harmonised once the mean value over many trajectories is taken.

As it stems from Eqs. (6.13) and (6.16), the steady-state density matrix of the system can be cast as the statistical mixture of only two pure states. This bimodality is an intrinsic propriety of the Lindblad master Equation (6.7) and, being an average propriety of the system, it should somehow appear also on a single experimental realisation. In other words, the quantum trajectory approach should show a bimodal behaviour. However, the states between which the system switches, as well as the characteristic time scales, can not be inferred from the form of $\hat{\rho}_{\rm ss}$, and are not manifest in the Lindblad master equation, but depend on the measurement process. After a brief reminder of the basic definitions, we present the quantum trajectory behaviour under two different measurement protocols that both average to the same master Equation (6.7): photon counting and homodyne detection.

6.2.1 Photon counting and jumping Schrödinger cats

The most natural way to observe the exchanges between the Kerr resonator and the environment is to just detect every leaked photon (both individually and in couples). At every detection of leaked photons the knowledge of the system is updated via the action of the one-photon jump operator $\hat{J}_1 = \sqrt{\gamma}\,\hat{a}$ and the two-photon one $\hat{J}_2 = \sqrt{\eta}\,\hat{a}^2$ (see Sec. 4.3 for more details). Indeed, in typical realisations (e.g. in Ref. [85]) the one- and two-photon dissipation channels are discernible. Hence, we can assume that the photodetector is capable of distinguishing between one- and two-photon losses. The photon-counting trajectory is then simulated by discretising the system time evolution. At each time step, one stochastically determines if a single photon or a couple of them has been detected. To do so, one considers that the probability of a one- and two-photon detection in a time step dt are, respectively,

$$p_1(t,\mathrm{d}t) = \langle \hat{J}_1^\dagger \hat{J}_1\rangle(t)\mathrm{d}t = \gamma\langle \hat{a}^\dagger\hat{a}\rangle(t)\mathrm{d}t, \qquad p_2(t,\mathrm{d}t) = \langle \hat{J}_2^\dagger \hat{J}_2\rangle(t)\mathrm{d}t = \eta\langle \hat{a}^{\dagger\,2}\hat{a}^2\rangle(t)\mathrm{d}t\,. \tag{6.21}$$

If a jump occurs, the system state abruptly changes under the action of the corresponding jump operator according to

$$|\Psi(t+\mathrm{d}t)\rangle = \frac{\hat{J}_\nu\,|\Psi(t)\rangle}{\sqrt{\langle\Psi(t)|\hat{J}_\nu^\dagger\hat{J}_\nu|\Psi(t)\rangle}}, \qquad \nu = 1,2\,. \tag{6.22}$$

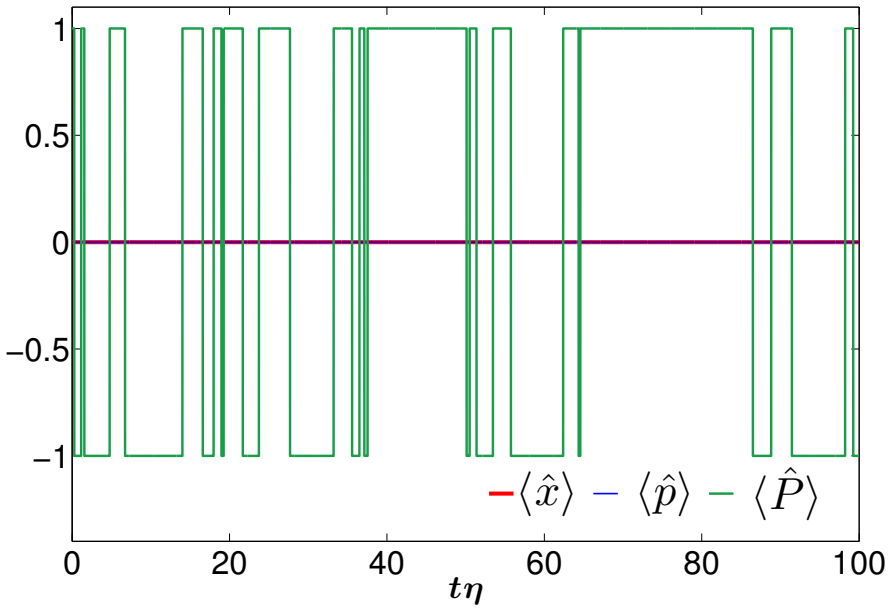

Figure 6.3 Time evolution of $\langle\hat{x}\rangle$, $\langle\hat{p}\rangle$, and $\langle\hat{P}\rangle$ along single photon-counting quantum trajectories for the master Equation (6.7).The system parameters are set to $U = 1\eta$, $G = 5\eta$, and $\gamma = 0.1\eta$. Simulations were performed on a truncated Fock basis with $n_{\max} = 15$, ensuring convergence.

If no jump occurs, the unnormalised state $|\widetilde{\Psi}(t)\rangle$ evolves under the action of an effective non-hermitian Hamiltonian operator:

$$\frac{\mathrm{d}\,|\widetilde{\Psi}(t)\rangle}{\mathrm{d}t} = -i\left(\hat{H} - \frac{i}{2}\sum_{\nu=1,2}\hat{J}_\nu^\dagger\hat{J}_\nu\right)|\widetilde{\Psi}(t)\rangle\,, \tag{6.23}$$

where here and below, the averages are computed on the conditional state of the system $|\Psi(t)\rangle$ at time t (note that respect to Sec. 4.3, we have let drop the subscript c standing for "conditional"). We stress that dt must be sufficiently small to ensure $p_{1,2}(t, \mathrm{d}t) \ll 1$, such to avoid multiple jumps in the same time step. A photon-counting trajectory is then characterised by a smooth evolution given by an effective non-hermitian Hamiltonian and by abrupt jumps corresponding to the projective measure associated to the detection of one or two photons.

As shown in Section 6.1, the Hamiltonian (6.5) and the two-photon dissipation preserve the parity of the cavity and tend to stabilise photonic cat states. On the other hand the single-photons annihilation does not preserve the parity and its action on the even cat state is to switch it into the odd one and *vice versa*: $\hat{a}\,|\mathcal{C}_\alpha^\pm\rangle \propto \alpha\,|\mathcal{C}_\alpha^\mp\rangle$. Thus one-photon dissipation, described by the jump operator $\hat{J}_1 = \sqrt{\gamma}\,\hat{a}$, induces random jumps between the two cat states at a rate proportional to $\gamma\,\langle\hat{a}^\dagger\hat{a}\rangle$. This picture is confirmed by the simulations of photon-counting trajectories, an example

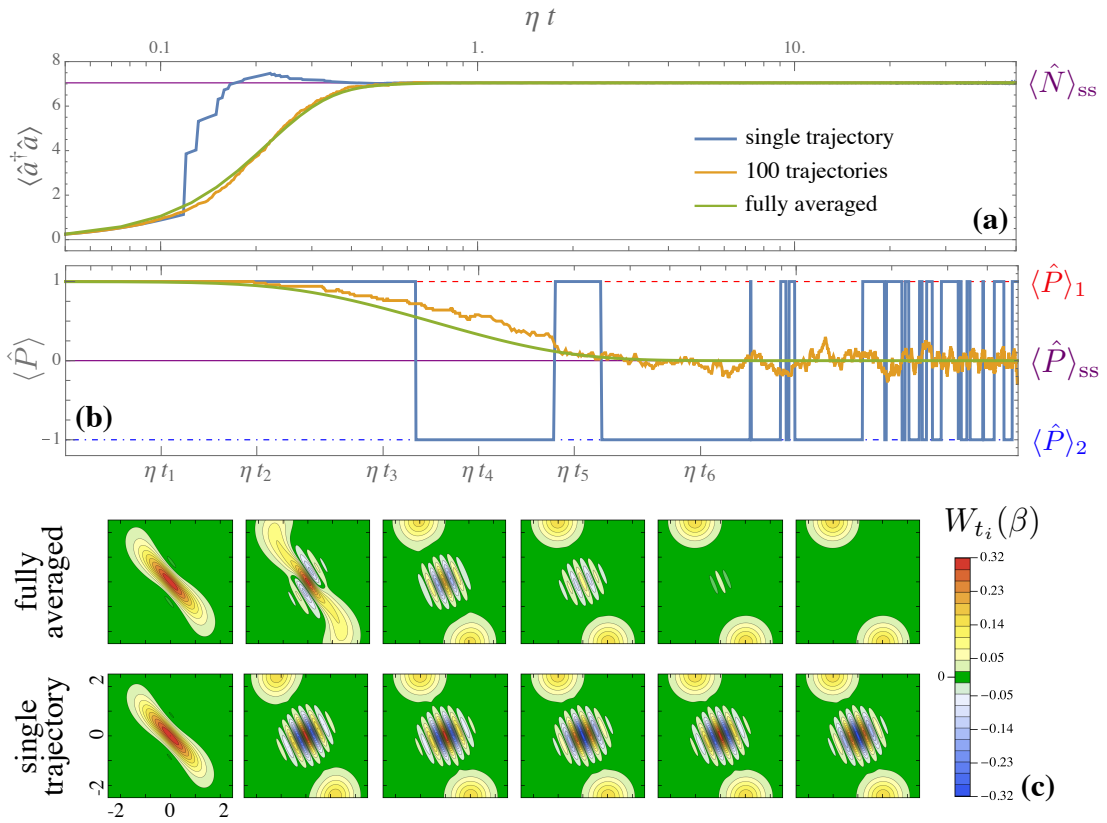

Figure 6.4 Dynamics of averaged quantities versus single quantum trajectories. Panel (a): dynamics (time is in logarithmic scale) of the photon population for a single quantum trajectory (blue line), an average of 100 trajectories (orange line) and the fully averaged (green line) density-matrix. Panel (b): same as (a) but for the expectation value of the photon parity operator. Panel (c): snapshots of the Wigner functions at times $t_1, t_2, \ldots, t_6$ indicated in panel (b). The system parameters are $\Delta = 0$, $U = 1\eta$, $G = 10\eta$, and $\gamma = 0.1\eta$.

of which is given in Fig. 6.3. The expectation value of the parity operator $\hat{P} = e^{i\pi\hat{a}^\dagger\hat{a}}$ jumps between its eigenvalues ± 1. We recall that cat states are orthogonal eigenstates of the parity operator $\hat{P}$, this suggests that along a single trajectory the system intermittently and randomly switches between the two cat states. As a confirmation of this picture, the mean values of the field quadratures $\hat{x} = \left(\hat{a}^\dagger + \hat{a}\right)/2$ and $\hat{p} = i\left(\hat{a}^\dagger - \hat{a}\right)/2$ are practically zero along the trajectory, as expected for any cat state.

In order to have a definitive confirmation of how the trajectories behave we consider the evolution of the system Wigner function. The fully-averaged and single-trajectory evolutions of the Wigner function are shown in panel (c) of Fig. 6.4 . Starting from the vacuum state as initial condition, an even-cat transient appears in the average behaviour, but negativities are eventually washed out for $\eta t, \gamma t \gg 1$ [85, 170, 171]. On

a single trajectory, two-photon processes initially dominate, driving $W(\beta, t)$ towards the Wigner function of $|\mathcal{C}_\alpha^+\rangle$. Even if many two-photon losses are detected, they do not affect the state parity, indeed $\hat{J}_2 \, |\mathcal{C}_\alpha^\pm\rangle \propto \hat{a}^2 \, |\mathcal{C}_\alpha^\pm\rangle = \alpha^2 \, |\mathcal{C}_\alpha^\pm\rangle$. This is why the system remains close to the even cat state until a one-photon loss occurs. At this point, since $\hat{J}_1 \, |\mathcal{C}_\alpha^\pm\rangle \propto \hat{a} \, |\mathcal{C}_\alpha^\pm\rangle \propto |\mathcal{C}_\alpha^\mp\rangle$, the Wigner function of the system abruptly switches to that of $|\mathcal{C}_\alpha^-\rangle$ [171], then back at each one-photon jump.

Hence, if the quantum trajectory is monitored via photon counting [126], the system can only be found nearby $|\mathcal{C}_\alpha^+\rangle$ or $|\mathcal{C}_\alpha^-\rangle$. Furthermore, we may interpret $p_{\rm ss}^\pm$ in Eq. (6.13) as the asymptotic probabilities to find the system in one of the two cat states. In the panels (a) and (b) of Fig. 6.4, we compare the evolution of the Wigner function evolution with the evolution of the average photon number $\langle \hat{N} \rangle$ and parity $\langle \hat{P} \rangle$. Since $\langle \hat{N} \rangle_{1,2} \approx \langle \hat{N} \rangle_{\rm ss}$, it is impossible to discern the cats' jumps by tracking the photon density. It is in particular impossible to determine in which cat state the system is by measuring the photon loss intensity. A parity measurement, contrarily, would be suitable [88] to unravel the bimodal behaviour of the system when is monitored by photon-counting detection. In Fig. 6.4(a) and (b) we also show the average over 100 trajectories, which, as expected, converges to the master equation solution. The latter corresponds to the full average over an infinite number of realisations.

6.2.2 Homodyne detection and switching coherent states

Another possible way to monitor a quantum-optical system is through homodyne detection, a widely-used experimental technique which allows to access the field quadratures [89, 138, 139]. To implement this kind of measurement, the cavity output field is mixed to the coherent field of a reference laser through a beam splitter (here assumed of perfect transmittance). Then, the mixed fields are probed via (perfect) photodetectors, whose measures are described by new jump operators. We stress that both the coherent and the cavity fields are measured simultaneously.

In our case, we want to probe independently the two dissipation channels. To distinguish between one- and two-photon losses, one can exploit a nonlinear element acting on the cavity output field. Indeed, in experimental realisations such as in Ref. [85], a nonlinear element is already part of the system and is the key ingredient to realise two-photon processes. More specifically, one-photon losses are due to the finite quality factor of the resonator. They can be probed by directly mixing the output field of the cavity with a coherent beam of amplitude β_1 acting as local oscillator. Therefore, the homodyne jump operator for one-photon losses can be cast as $\hat{K}_1 = \hat{J}_1 + \beta_1 \hat{\mathbb{1}}$. Two-photon losses are, instead, mediated by a nonlinear element (a Josephson junction in Ref. [85]), which converts two cavity photons of frequency ω_c into one photon of frequency ω_{nl}. Hence, the field coming out of the nonlinear element can be mixed to a second independent oscillator. This whole process can be seen as the action

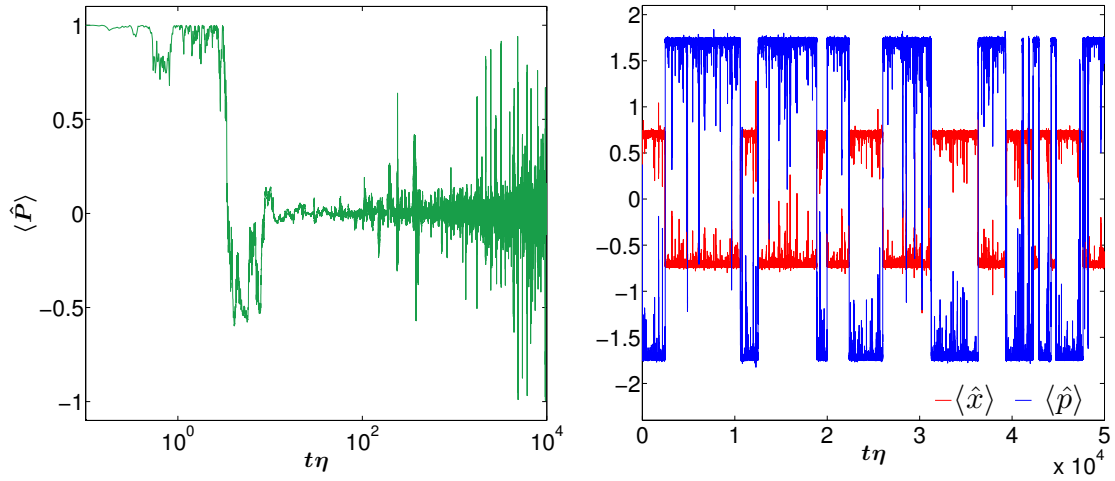

Figure 6.5 Time evolution of $\langle \hat{x} \rangle$, $\langle \hat{p} \rangle$ (right panel), and $\langle \hat{P} \rangle$ (left panel) along single homodyne quantum trajectories for the master Equation (6.7). The system parameters are set to $U = 1\eta$, $G = 5\eta$, and $\gamma = 0.1\eta$. Simulations were performed on a truncated Fock basis with $n_{\max} = 15$, ensuring convergence.

of a nonlinear beam splitter which mixes pairs of dissipated photons with a reference oscillator of amplitude β_2. Therefore, the homodyne two-photon jump operator takes the form $\hat{K}_2 = \hat{J}_2 + \beta_2 \hat{\mathbb{1}}$. Without loss of generality, in the following, we assume the amplitudes $\beta_{1,2}$ to be real [135].

From the definitions of the jump operators, one extracts the jump probabilities

$$\begin{aligned} p_1(t, \mathrm{d}t) &= \langle \hat{K}_1^\dagger \hat{K}_1 \rangle(t)\mathrm{d}t = \langle (\sqrt{\gamma}\hat{a} + \beta_1 \hat{\mathbb{1}})^\dagger (\sqrt{\gamma}\hat{a} + \beta_1 \hat{\mathbb{1}}) \rangle(t)\mathrm{d}t \\ &\simeq [\beta_1^2 \hat{\mathbb{1}} + \beta_1 \sqrt{\gamma} \langle \hat{a} + \hat{a}^\dagger \rangle(t)]\mathrm{d}t, \\ p_2(t, \mathrm{d}t) &= \langle \hat{K}_2^\dagger \hat{K}_2 \rangle(t)\mathrm{d}t = \langle (\sqrt{\eta}\hat{a}^2 + \beta_2 \hat{\mathbb{1}})^\dagger (\sqrt{\eta}\hat{a}^2 + \beta_2 \hat{\mathbb{1}}) \rangle(t)\mathrm{d}t \\ &\simeq \left[\beta_2^2 \hat{\mathbb{1}} + \beta_2 \sqrt{\eta} \langle \hat{a}^2 + \hat{a}^{\dagger\,2} \rangle(t)\right] \mathrm{d}t, \end{aligned} \tag{6.24}$$

where the approximations are valid in the ideal limit $\beta_{1,2} \gg 1$. In this regime, for any time interval, there would be a huge number of total field detections. This would make computationally very demanding to follow the same procedure as in Sec. 6.2.1, since one should take an extremely small time step. However, the detected field is almost entirely due to the reference lasers, associated to the operators $\beta_{1,2}\hat{\mathbb{1}}$. This means that a single detection contains very few information on the resonator field, and that the total jump operators $\hat{K}_{1,2}$ have a very small effect on its state. In the ideal limit $\beta_{1,2} \to \infty$, the occurrence of an infinite number of jumps is counterbalanced by their infinitesimal effect on the resonator, resulting in an effective diffusive evolution of the cavity state. The latter, indeed, is found to obey to a stochastic Schrödinger equation

of the form

$$\begin{aligned} \mathrm{d}|\psi(t)\rangle = &-i\,\mathrm{d}t\,\hat{H}\;|\psi(t)\rangle + \sum_{\nu=1,2}\left\{\left[\hat{J}_\nu - \frac{\langle \hat{J}_\nu + \hat{J}_\nu^\dagger\rangle(t)}{2}\hat{\mathbb{1}}\right]\mathrm{d}W_\nu(t)\right. \\ &\left.-\frac{1}{2}\left[\hat{J}_\nu^\dagger\hat{J}_\nu - \langle \hat{J}_\nu + \hat{J}_\nu^\dagger\rangle(t)\hat{J}_\nu + \frac{\langle \hat{J}_\nu + \hat{J}_\nu^\dagger\rangle^2(t)}{4}\hat{\mathbb{1}}\right]\mathrm{d}t\right\}|\psi(t)\rangle\,, \end{aligned} \tag{6.25}$$

where $\hat{J}_{1,2}$ are the resonator jump operators and $\mathrm{d}W_{1,2}$ are stochastic Wiener increments of zero expectation value satisfying $\mathrm{d}W_\nu(t)\mathrm{d}W_\mu(t) = \delta_{\nu\mu}\,\mathrm{d}t$ (a more detailed description of the main formal steps to derive this equation is given in Sec. 4.3.3).

Those Wiener processes describe the fluctuation of the homodyne signal. Using the stochastic Schrödinger Equation (6.25), one can simulate the trajectory by taking a reasonably small dt and generating stochastic Wiener increments at each time step. Note that Eq. (6.25) does not depend on the values of $\beta_{1,2}$, which are both infinitely large. In conclusion, the homodyne detection reduces to a continuous diffusive evolution of the wave function.

As shown in Sec. 6.2.1, quantum trajectory analysis based on photon counting seems to privilege a mixture of cat states (Eq. (6.13)) over the mixture of coherent states (Eq. (6.16)) as the more truthful picture of the steady state. This is no more the case if we consider homodyne quantum trajectories. In Fig. 6.5(b), we present (in a log-linear scale) the mean parity $\langle\hat{P}\rangle$ along a single homodyne trajectory, taking the vacuum as initial state. In spite of the "switching cat" picture, the parity rapidly approaches zero, and than just fluctuates around this value. These fluctuations are due to the diffusive nature of Eq. (6.25), which rules the stochastic time evolution of the system wave function under homodyne detection. The bimodal behaviour, instead, is clear in the time evolution of $\langle\hat{x}\rangle$ and $\langle\hat{p}\rangle$, shown in Fig. 6.5(c). This appears compatible with the picture given by Eq. (6.16): at the steady state the system switches between the coherent states $|\pm\alpha\rangle$. We point out that the phase switches observed for homodyne trajectories have a much smaller rate than parity switches in photon-counting trajectories. This is a consequence of the metastable nature of the coherent states $|\pm\alpha\rangle$ [85, 96].

For finite γ the considered system has always a unique steady-state. However, the temporal relaxation towards the steady-state dramatically depends on the initial state. This is revealed by the time-dependent fidelity with respect to the steady-state

$$f[\hat{\rho}_{\mathrm{ss}};\hat{\rho}(t)] = \mathrm{Tr}\left\{\sqrt{\sqrt{\hat{\rho}_{\mathrm{ss}}}\,\hat{\rho}(t)\,\sqrt{\hat{\rho}_{\mathrm{ss}}}}\right\}, \tag{6.26}$$

that in Fig. 6.6 has been obtained by numerical integration of the master equation. In particular, initialising the system in one of the coherent states $|\pm\alpha\rangle$ composing the steady-state cats, it remains nearby for a time several orders of magnitude longer than $1/\gamma$ and $1/\eta$. More precisely, this is the same time (of the order of $10^4/\eta$) that

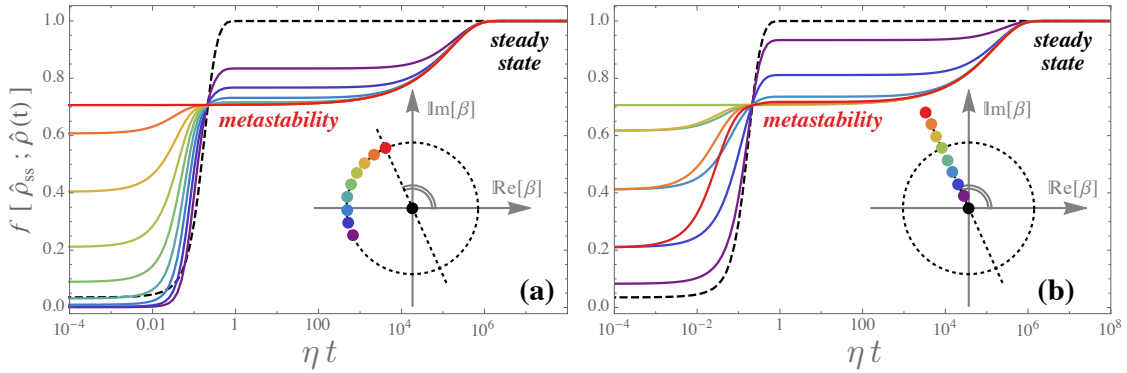

Figure 6.6 Metastable versus steady-state regime. The curves depict the time-dependent fidelity of the density matrix $\hat{\rho}(t)$ with respect to the unique steady-state density matrix $\hat{\rho}_{\rm ss}$ by taking as initial condition a pure coherent state, i.e., $\hat{\rho}(t = 0) = |\beta\rangle\langle\beta|$. The fidelity $f[\hat{\rho}_{\rm ss}; \hat{\rho}(t)]$ is defined in Eq. (6.26). The values of β and the corresponding colours are indicated in the inset. In the top panel, the phase of the initial coherent state is varied, while in the bottom panel the amplitude is changed. The dashed line corresponds to the vacuum as initial state. Parameters: $\Delta = 0$, $U = 1\eta$, $G = 10\eta$, $\gamma = 0.1\eta$.

one has to wait in average to have a switch in the homodyne trajectory (Fig. 6.5(c)). Hence, we proved that $|\pm\alpha\rangle$ are metastable states of the systems, improving the previous dominant interpretation that was considering them as multiple stable steady states [85].

6.2.3 One-photon driven resonators

It is legitimate to question if the abrupt switches observed in the quantum trajectories presented in Fig. 6.5 are an intrinsic property of the system or is just an effect of the measurement protocol. To dispel all doubts, we calculated single photon-counting and homodyne trajectories for a resonator subject to a resonant one-photon driving of frequency ω_c. In the frame rotating at ω_c, the corresponding Hamiltonian reads

$$\hat{H} = \frac{U}{2}\,\hat{a}^\dagger\hat{a}^\dagger\hat{a}\hat{a} + F\left(\hat{a}^\dagger + \hat{a}\right). \tag{6.27}$$

We stress that, differently from the case discussed above, the steady state of this system is not an equiprobable statistical mixture of two states [140, 162]. A photon-counting trajectory for $\langle\hat{P}\rangle$ and homodyne trajectories for $\langle\hat{x}\rangle$ and $\langle\hat{p}\rangle$ are shown, respectively, in Fig. 6.7(a) and (b). Clearly, the trajectory does not show the same kind of abrupt switches observed in Fig. 6.5. This proves that the behaviour discussed in Sec. 6.2.1 and Sec. 6.2.2 is not caused solely by the measurement protocol, but is indeed linked to the bimodal character of the steady state.

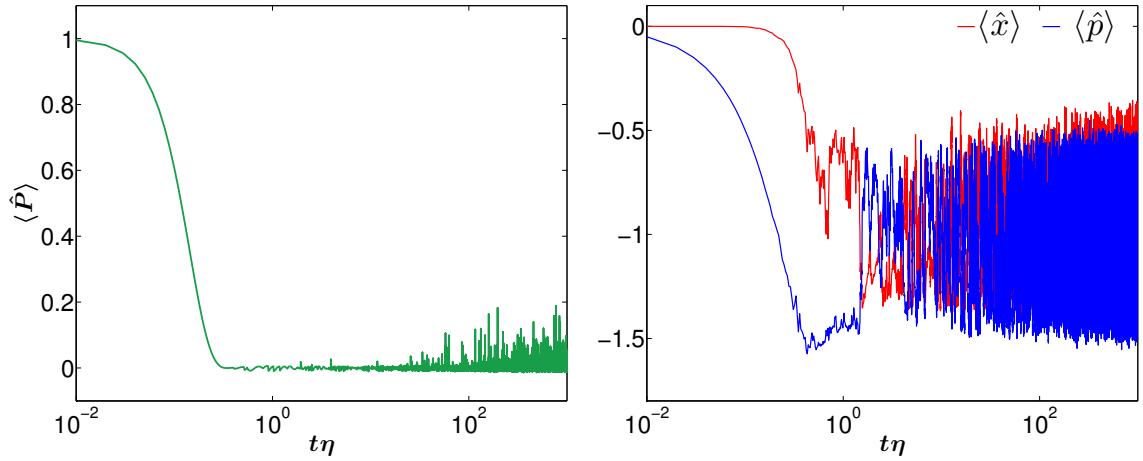

Figure 6.7 Left Panel: Time evolution of $\langle \hat{P} \rangle$ along a single photon-counting trajectory. Righ Panel: Time evolution of $\langle \hat{x} \rangle$ and $\langle \hat{p} \rangle$ along a single homodyne trajectory. Both plots refers to the Lindblad Equation (6.7) for the one-photon-driving Hamiltonian (6.27). We set the system parameters to $U = 1\eta$, $F = 5\eta$, and $\gamma = 0.1\eta$ (we stress that here $G = 0$). Simulations were performed on a truncated Fock basis with $n_{\max} = 15$, ensuring convergence.

6.2.4 Conclusion on trajectory analysis

In this section we have studied the behaviour of interacting photons in a nonlinear resonator subject to engineered two-photon processes. The objective has been to point out and characterise the bimodal nature of the system steady state, which can be seen, equivalently, as the statistical mixture of photonic Schrödinger cat states (Eq. (6.13)) or of coherent states with same amplitude and opposite phases (Eq. (6.16)). The behaviour of the system along a single quantum trajectory dramatically depends on the measurement protocol adopted. For photon-counting measurements on the environment, the system switches between the parity-defined cat states appearing in Eq. (6.13). Under homodyne detection, the states explored along a single quantum trajectory are the coherent ones in Eq. (6.16). In other words, one may assign a physical meaning to the probabilities appearing in the mixed-state representation of $\hat{\rho}_{\rm ss}$ only upon specification of the single-trajectory protocol.

However, the average behaviour is exactly the same for the two detection protocols, which are described by the same Lindblad master Equation (6.7). Finally, we have also studied the quantum trajectories for a one-photon-driven resonator in a regime where its steady state is not bimodal. The absence of abrupt switches in parity or quadratures proves that the ones observed in Fig. 6.5 are not artefacts of the quantum trajectory approach, but a feature linked to the steady-state bimodality.

6.3 Feedback control on cat states

In the previous sections we saw that the class of systems described by the Lindblad master equation (6.7) is very promising for the realisation of Schrödinger cat states. Cat states have been observed in the transient dynamics of this kind of systems [85]. These states are highly nonclassical and very promising for computation applications [75, 77, 159, 160]. On the other hand they are fragile to one-photon decoherence and their lifetime is very short.

The question is: how can we protect photonic Schrödinger cats from one-photon decoherence? As we showed, when considering photon-counting quantum trajectories, the system intermittently jumps between an even and an odd cat states. We recall that quantum trajectories can be thought as the description of an actual experiment in which a continuous measurement is performed on the environment [126, 135, 144]. Photon counting is, in this regard, the most natural way to monitor the system: each time a photon escapes the cavity it is measured by a photon counter. In particular, if it was possible to collect all the leaked photons, one would be able to reconstruct the state of the cavity. In this regard, i.e. under perfect photon counting, the system would be anyhow in one of the two cats, and one would know in which one. Now, what can we say about the cavity if we consider non-perfect photodetection? As discussed in Ref. [27] for a closely related example, one would progressively lose its knowledge about the system. As the time passes and the number of missed photon increases, there will be an equal probability to be in the even or in the odd cat: hence one retrieve the statistical mixture in Eq. (6.13).

We stress that, even if both $|\mathcal{C}_\alpha^{\pm}\rangle$ in Eq. (6.13) are highly nonclassical states, it was proved in Ref. [96, 161] that the steady state of Eq. (6.13) has lost all the quantumness, i.e. there are no negativities in the Wigner function (cf. Fig 6.2). Thus, in order to retrieve some of the quantum features of the Schrödinger cats, it is necessary to contrast the one-photon dissipation. A possible way could be to actively control the system through a feedback protocols. This is the topic of the following sections.

6.3.1 Feedback by conditioning of one-photon dissipation

In Sec. 6.2.1 we saw that the main effect of one-photon dissipation is to induce abrupt and totally random jumps from one cat state to the other with opposite parity. This process drive the system toward a mixed state with equal probability 1/2 for the two cat states. In this stationary state the coherence between $|\alpha\rangle$ and $|-\alpha\rangle$ is completely lost and system is in a classical state.

Thus one-photon dissipation is the main obstacle toward the stabilisation of one of the two cat states. On the other hand, because of its central role, one could imagine to control the system state by controlling the intensity of one-photon dissipation. In

particular one could try to recover a cat-like steady state by unbalancing the even and odd contribution to $\hat{\rho}_{\rm ss}$ (Eq. (6.13)). In a quantum trajectory picture, if the jump rate from the even to the odd cat state is, for instance, smaller than the jump rate from the odd to the even cat state then the latter will be dominant. The resulting stationary state will be a cat-like state and the coherence between $|\alpha\rangle$ and $|-\alpha\rangle$ is recovered. In one of our works [96], we proposed the realisation of this idea through a parity-triggered feedback mechanism [172–175]. The idea is to repeatedly perform a non-destructive parity measurements at times t_i and to open an addition one-photon loss channel when the undesired value is measured. We point out that a similar measure has already been realised in the context of superconducting circuits [86, 88].

Let us describe a general evolution of the system under repeated measurement and a Liouvillian that depends on the result of the measure. As detailed in Sec. 4.2.1, any observable $\hat{M}$ can be written in terms of its eigenspace projectors $\hat{\Pi}_\mu$ and the associated eigenvalues μ: $\hat{M} = \sum_\mu \mu\, \hat{\Pi}_\mu$. The probability of obtaining the result μ, upon measure of $\hat{M}$, is therefore $p_\mu = \mathrm{Tr}\left\{\hat{\rho}\hat{\Pi}_\mu\right\}$. After obtaining the outcome μ from the measurement of $\hat{M}$, the density matrix become

$$\hat{\rho}_\mu = \frac{\hat{\Pi}_\mu \hat{\rho} \hat{\Pi}_\mu}{\mathrm{Tr}\left\{\hat{\Pi}_\mu \hat{\rho}\right\}} = \frac{\mathcal{M}_\mu\, \hat{\rho}}{p_\mu}, \tag{6.28}$$

where we have introduced the measurement superoperator of the form $\mathcal{M}_\mu \hat{\rho} = \hat{\Pi}_\mu \hat{\rho} \hat{\Pi}_\mu$. Now, we are interested in the description of the mean effect of the measure on the master equation, i.e. what are the quantities which can be retrieved from performing several times the same experiment . Thus, if we call $\hat{\rho}$ the density matrix describing the system just before the measure, the effect of $\mathcal{M}$ is

$$\mathcal{M}\hat{\rho} = \sum_\mu p_\mu\, \hat{\rho}_\mu = \sum_\mu \mathcal{M}_\mu\, \hat{\rho}\,. \tag{6.29}$$

We suppose to perform a measure on the system at every time t_i, while the system evolves under the action of the Liouvillian for $\Delta t = t_{i+1} - t_i$. Let us define the conditional Liouvillian $\mathcal{L}_\mu$, that is chosen according to the result of the measurement. The mean evolution of the system in between two measures is:

$$\hat{\rho}(t) = \sum_\mu e^{\mathcal{L}_\mu (t-t_i)} \mathcal{M}_\mu\, \hat{\rho}(t_i) \;= \sum_\mu e^{\mathcal{L}_\mu (t-t_i)} \hat{\Pi}_\mu \hat{\rho}(t_i) \hat{\Pi}_\mu\;, \tag{6.30}$$

where $\hat{\rho}(t_i)$ is the system state at the moment of the last measurement. So the average action on the density matrix of one feedback cycle (measurement followed by control) is given by:

$$\hat{\rho}(t_{i+1}) = \sum_\mu e^{\mathcal{L}_\mu \Delta t} \mathcal{M}_\mu \hat{\rho}(t_i)\,. \tag{6.31}$$

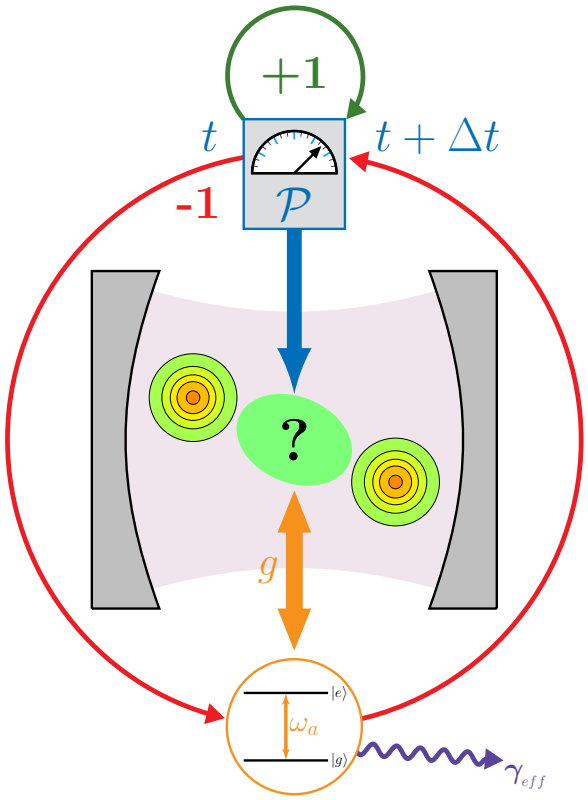

Figure 6.8 A schematic representation of the proposed feedback protocol. The system is probed by a parity measurement $\mathcal{P}$ at time t. If the result is $+1$ we go directly to the next measurement at time $t + \Delta t$. Otherwise, if the result is -1 a strongly dissipating two-level system is tuned in resonance with the cavity and we come back to measure. This enhances the one-photon dissipation bringing the system toward the target even state.

A possible way to distinguish between cat states is a parity measure. In fact, the even and odd cats are compound only by even or odd states, respectively, and thus are eigenstate with eigenvalue ± 1 of the parity operator $\hat{P} = e^{i\pi \hat{a}^\dagger \hat{a}}$. Thus, in the description our protocol to obtain cat-like states we can exploit parity measurement superoperators $\mathcal{P}_\pm \hat{\rho} = \hat{\Pi}_\pm \hat{\rho}\, \hat{\Pi}_\pm$, where parity projectors have the form

$$\hat{\Pi}_\pm = \frac{1}{2}\left[\hat{\mathbb{1}} \pm e^{i\pi \hat{a}^\dagger \hat{a}}\right] . \tag{6.32}$$

Note that, correctly, $\hat{\Pi}_-^\dagger \hat{\Pi}_- + \hat{\Pi}_+^\dagger \hat{\Pi}_+ = \hat{\mathbb{1}}$ and that measurement superoperators $\mathcal{P}_\pm$ project the density matrix on the even-odd manifold.

Following the proposal in Ref. [96], we condition the value of γ on the result of parity measurement. A proposal to realise the conditional dissipation is to increase it by tuning in resonance with the cavity a strongly dissipating two-level system (as detailed in the appendix. A). Figure 6.8 provides schematic representation of the

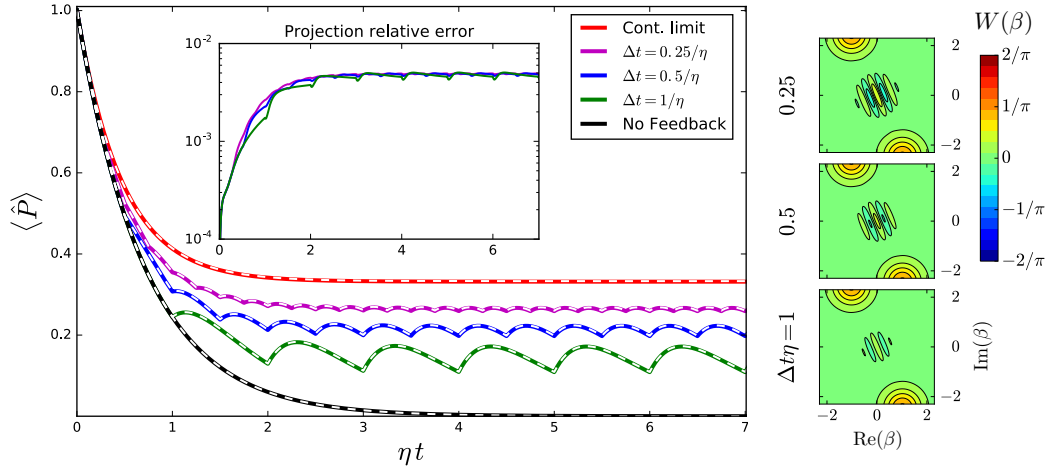

Figure 6.9 Left panel: evolution of the expectation value of the parity $\hat{P}$ for different durations Δt of the feedback cycle. Parameters are $G = 10\eta$, $U = 1\eta$, $\gamma_+ = 0.1\eta$ and $\gamma_- = 2\gamma_+$; the initial state is the even cat state $|\mathcal{C}_\alpha^+\rangle$. The solid lines represent the mean on the full density matrix, while the white dashes are obtained using the populations $p^\pm$ of the reduced space. Inset left panel: relative error in determining the parity using the projection procedure. Right panel: the Wigner function of the system density operator at time $\eta\, t = 7$.

feedback protocol.

The conditional Lindbladian superoperators act as $\mathcal{L}_\pm \hat{\rho} = i\,[\hat{\rho}, \hat{H}] + \mathcal{D}_2 \hat{\rho} + \mathcal{D}_1^\pm \hat{\rho} = (\mathcal{L}_2 + \mathcal{D}_1^\pm)\hat{\rho}$, where we have introduced the parity-dependent one-photon dissipation:

$$\mathcal{D}_1^\pm\, \hat{\rho} = \frac{\gamma_\pm}{2} \left(2\hat{a}\hat{\rho}\hat{a}^\dagger - \hat{a}^\dagger\hat{a}\hat{\rho} - \hat{\rho}\hat{a}^\dagger\hat{a}\right) . \tag{6.33}$$

The evolution of the system in Eq. (6.30) now reads:

$$\hat{\rho}(t) = \sum_{\mu=\pm} e^{\mathcal{L}_\mu (t-t_i)} \mathcal{P}_\mu \hat{\rho}(t_i) = \left[e^{(\mathcal{L}_2 + \mathcal{D}_1^+)(t-t_i)} \mathcal{P}_+ + e^{(\mathcal{L}_2 + \mathcal{D}_1^-)(t-t_i)} \mathcal{P}_- \right] \hat{\rho}(t_i) . \tag{6.34}$$

In Fig. 6.9 we plot the evolution of the parity according to Eq. (6.34) for different values of Δt. The initial pure even cat state quickly decay toward a zero-parity state, until the effect of the measurement-feedback procedure intervene. At every measurement we have a discontinuity in the first derivative of system time evolution. Between the two subsequent measurements the parity evolution is continuous and after few feedback cycles it stabilises on a precise repeated behaviour.

In Fig. 6.9 we choose to plot the average parity of the system because it is a good indicator of how close we are to realise a cat state, that is the target of our feedback protocol. In absence of feedback the two cats become equally probable, and the Wigner function of the steady state has no negativity (see Fig. 6.2). Introducing a feedback with $\gamma_- = 2\gamma_+$, the odd cat state is more fragile then the even one and some

quantum features will emerge (see the Wigner functions in Fig. 6.9). The resulting system state is closer to the even cat state as Δt decreases. Indeed in the Wigner functions showed in Fig. 6.9 we see that the smaller is Δt the more the fringes are marked. In order to explain that effect one has to consider that, after every measurement, the one-photon dissipation deteriorate the acquired information. For more frequent measurement the degrading effect of one-photon dissipation is smaller and the feedback is more efficient.

Finally, let us consider the continuous limit, i.e. $\Delta t \ll \gamma_-$, the feedback protocol is maximally efficient in this limit (see Fig. 6.9). As we will prove at the end of Sec. 6.3.5, this continuous limit is effectively described by an additional parity-dependent dissipation channel to the bare master equation in Eq. (6.7). More precisely this additional dissipation is described by the jump operator $\hat{a}_f = \hat{a}\,\frac{1}{2}(\hat{\mathbb{1}} - \hat{P}) = \hat{a}\,\hat{\Pi}_-$ and the corresponding dissipator

$$\mathcal{D}_f\hat{\rho} = \frac{\gamma_f}{2}\left(2\hat{a}_f\hat{\rho}\hat{a}_f^\dagger - \hat{a}_f^\dagger\hat{a}_f\hat{\rho} - \hat{\rho}\hat{a}_f^\dagger\hat{a}_f\right). \tag{6.35}$$

Qualitatively, $\mathcal{D}_f$ leaves the even cat undisturbed, while it enhances the dissipation for the odd one. Making the link to the parameters of our feedback protocol $\gamma_f = \gamma_- - \gamma_+$ and $\gamma = \gamma_+$.

In Fig. 6.10(a) we show the time evolution of $\langle\hat{P}\rangle$ for three different values of γ_f. At the steady state, $\langle\hat{P}\rangle$ increases with increasingly γ_f, indicating that the positive cat has a larger weight in $\hat{\rho}_{\rm ss}$. In Fig. 6.10(b) we show the corresponding steady-state Wigner functions $W(\beta)$. For finite γ_f, negative fringes appear in the Wigner function. They are more pronounced as γ_f is increased, revealing a highly nonclassical state. In the limit $\gamma_f \gg \gamma$, $\hat{\rho}_{\rm ss} \simeq |\mathcal{C}_\alpha^+\rangle\langle\mathcal{C}_\alpha^+|$. Note that, by using instead the jump operator $\hat{a}_f = \hat{a}\,\frac{1}{2}(\hat{\mathbb{1}} + \hat{P})$, one can similarly stabilise the odd cat state.

6.3.2 Projection on cat states

In Section 6.1.2, we saw that in the strong pumping and weak one-photon dissipation regime, the description of the system can be restricted to the subspace spanned by the cat states and that only the cat populations really matter (and not their coherences).

Let us use the same idea to project Eq. (6.34) on the subspace of the cat states. If at time t_i the system is in a statistical mixture of the two cats of the form $\hat{\rho}(t_i) = p^+(t_i)\,|\mathcal{C}_\alpha^+\rangle\langle\mathcal{C}_\alpha^+| + p^-(t_i)\,|\mathcal{C}_\alpha^-\rangle\langle\mathcal{C}_\alpha^-|$, the density matrix at time $t \in (t_i, t_{i+1})$ between the two measurements is given by

$$\begin{aligned}\hat{\rho}(t) &= \sum_\mu e^{\mathcal{L}_\mu(t-t_i)}\mathcal{P}_\mu\hat{\rho}(t_i) = e^{\mathcal{L}_+(t-t_i)}\,p^+(t_i)\,|\mathcal{C}_\alpha^+\rangle\langle\mathcal{C}_\alpha^+| + e^{\mathcal{L}_-(t-t_i)}\,p^-(t_i)\,|\mathcal{C}_\alpha^-\rangle\langle\mathcal{C}_\alpha^-| \\ &= p^+(t_i)\,e^{(\mathcal{L}_2+\mathcal{D}_1^+)(t-t_i)}\,|\mathcal{C}_\alpha^+\rangle\langle\mathcal{C}_\alpha^+| + p^-(t_i)\,e^{(\mathcal{L}_2+\mathcal{D}_1^-)(t-t_i)}\,|\mathcal{C}_\alpha^-\rangle\langle\mathcal{C}_\alpha^-|\ .\end{aligned} \tag{6.36}$$

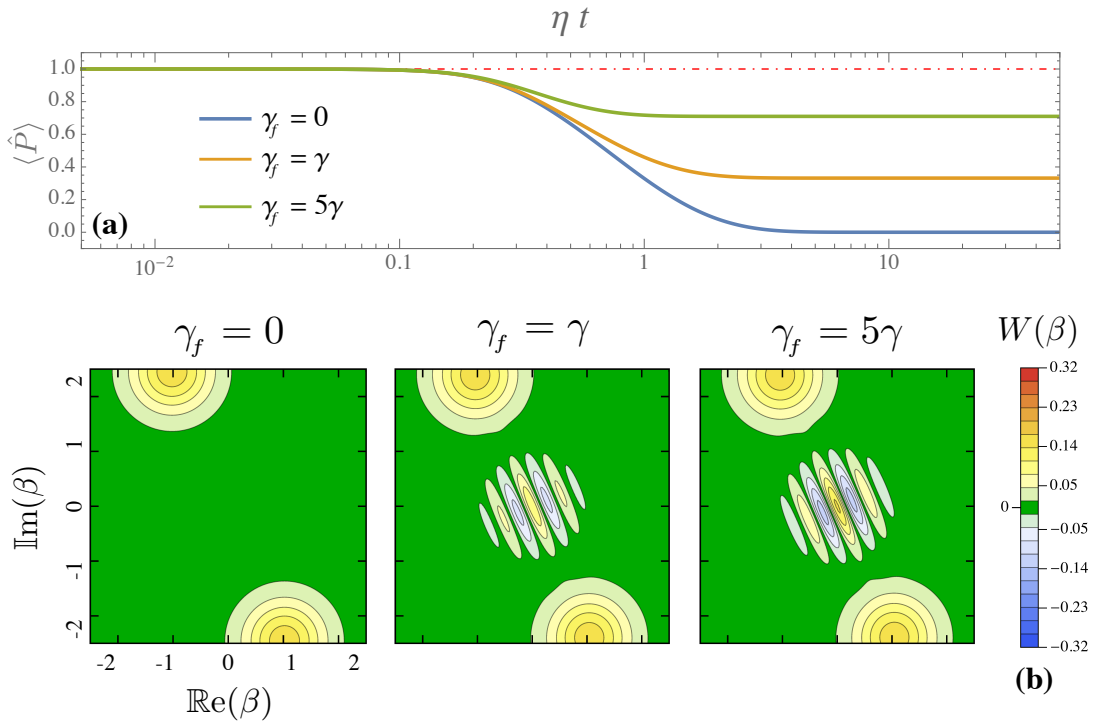

Figure 6.10 Effects of the considered feedback. These results are obtained by taking the vacuum as initial condition and for same system parameters as in Fig. 6.4. Panel (a): time evolution of the steady-state parity mean-value in presence of the feedback described by Eq. (6.35) for different values of γ_f (cf. legend). Panel (b): steady-state Wigner function ($t \to +\infty$) exhibiting negativities for $\gamma_f > 0$.

As we have seen in Sec. 6.1.2, for $\alpha = \sqrt{-G/(U - i\eta)}$ we have $\mathcal{L}_2 |\mathcal{C}_\alpha^\pm\rangle\langle\mathcal{C}_\alpha^\pm| = 0$, and then the Eq. (6.36) become:

$$\hat{\rho}(t) = p^+(t_i)\, e^{\mathcal{D}_1^+(t-t_i)}\, |\mathcal{C}_\alpha^+\rangle\langle\mathcal{C}_\alpha^+| + p^-(t_i)\, e^{\mathcal{D}_1^-(t-t_i)}\, |\mathcal{C}_\alpha^-\rangle\langle\mathcal{C}_\alpha^-| \,. \tag{6.37}$$

The action of the propagators $e^{\mathcal{D}_1^\pm(t-t_i)}$ on a generic mixture of the cat states is equivalent to the time evolution given by the following differential equation:

$$\frac{\partial}{\partial t}\left[p^+(t)\, |\mathcal{C}_\alpha^+\rangle\langle\mathcal{C}_\alpha^+| + p^-(t)\, |\mathcal{C}_\alpha^-\rangle\langle\mathcal{C}_\alpha^-|\right] = \mathcal{D}_1^\pm\left[p^+(t)\, |\mathcal{C}_\alpha^+\rangle\langle\mathcal{C}_\alpha^+| + p^-(t)\, |\mathcal{C}_\alpha^-\rangle\langle\mathcal{C}_\alpha^-|\right] \tag{6.38}$$

As we saw in Section 6.1.2, for $G \gg U, \eta \gg \gamma$ (i.e. $|\alpha| \gg 1$), the effect of superoperators $\mathcal{D}_1^\pm$ is to evolve the cat populations. Let us define the subspace of cat state population, in which we define the following representation of an arbitrary mixture of cat states:

$$a\, |\mathcal{C}_\alpha^+\rangle\langle\mathcal{C}_\alpha^+| + b\, |\mathcal{C}_\alpha^-\rangle\langle\mathcal{C}_\alpha^-| \stackrel{\text{def}}{=} \begin{pmatrix} a \\ b \end{pmatrix} \tag{6.39}$$

The action of $\mathcal{D}_1^\pm$, that we have determined in Eq. (6.20), can be expressed in the

basis of cat states populations:

$$\mathcal{D}_1^{\pm}\left[p^+(t)\,|\mathcal{C}_\alpha^+\rangle\langle\mathcal{C}_\alpha^+| + p^-(t)\,|\mathcal{C}_\alpha^-\rangle\langle\mathcal{C}_\alpha^-|\right] \stackrel{\text{def}}{=} \mathcal{D}_1^{\pm}\begin{pmatrix}p^+(t)\\p^-(t)\end{pmatrix} \simeq \begin{bmatrix}-\gamma_\pm|\alpha|^2 & +\gamma_\pm|\alpha|^2\\ +\gamma_\pm|\alpha|^2 & -\gamma_\pm|\alpha|^2\end{bmatrix}\begin{pmatrix}p^+(t)\\p^-(t)\end{pmatrix}. \tag{6.40}$$

Using the same representation we can now recast the Eq. (6.38) in the following rate equations:

$$\frac{\partial}{\partial t}\begin{pmatrix}p^+(t)\\p^-(t)\end{pmatrix} \simeq \gamma_\pm\bar{N}\begin{bmatrix}-1 & +1\\ +1 & -1\end{bmatrix}\begin{pmatrix}p^+(t)\\p^-(t)\end{pmatrix}, \tag{6.41}$$

in which we introduce the average number of photons $\bar{N} \simeq |\alpha|^2$. In the regime we are considering, the time evolution given by these rate equations is approximately equivalent to those produced by the propagators $e^{\mathcal{D}_1^{\pm}(t-t_i)}$. One can solve the rate equations by diagonalizing it and then determine the action of the propagators:

$$e^{\mathcal{D}_1^{+}(t-t_i)}\,|\mathcal{C}_\alpha^+\rangle\langle\mathcal{C}_\alpha^+| = \frac{1+e^{-2\bar{N}\gamma_+(t-t_i)}}{2}\,|\mathcal{C}_\alpha^+\rangle\langle\mathcal{C}_\alpha^+| + \frac{1-e^{-2\bar{N}\gamma_+(t-t_i)}}{2}\,|\mathcal{C}_\alpha^-\rangle\langle\mathcal{C}_\alpha^-|\,, \tag{6.42a}$$

$$e^{\mathcal{D}_1^{-}(t-t_i)}\,|\mathcal{C}_\alpha^-\rangle\langle\mathcal{C}_\alpha^-| = \frac{1-e^{-2\bar{N}\gamma_-(t-t_i)}}{2}\,|\mathcal{C}_\alpha^+\rangle\langle\mathcal{C}_\alpha^+| + \frac{1+e^{-2\bar{N}\gamma_-(t-t_i)}}{2}\,|\mathcal{C}_\alpha^-\rangle\langle\mathcal{C}_\alpha^-|\,. \tag{6.42b}$$

Using these expressions for the propagators, the Equation (6.37) reads:

$$\begin{aligned}\hat{\rho}(t) =& p^+(t)\,|\mathcal{C}_\alpha^+\rangle\langle\mathcal{C}_\alpha^+| + p^-(t)\,|\mathcal{C}_\alpha^-\rangle\langle\mathcal{C}_\alpha^-|\\ =& \frac{1}{2}\left[1 + p^+(t_i)\,e^{-2\bar{N}\gamma_+(t-t_i)} - p^-(t_i)\,e^{-2\bar{N}\gamma_-(t-t_i)}\right]|\mathcal{C}_\alpha^+\rangle\langle\mathcal{C}_\alpha^+| +\\ & \frac{1}{2}\left[1 + p^-(t_i)\,e^{-2\bar{N}\gamma_-(t-t_i)} - p^+(t_i)\,e^{-2\bar{N}\gamma_+(t-t_i)}\right]|\mathcal{C}_\alpha^-\rangle\langle\mathcal{C}_\alpha^-|\,.\end{aligned} \tag{6.43}$$

In Fig. 6.9 we plot the evolution of $\langle\hat{P}\rangle$ under the parity dependent feedback both for the full solution and for the projection on the cat states. The density operator, initialised in the even cat state, rapidly loses its quantum features if no feedback is applied, and the reduced basis perfectly captures this feature. The projection method produces very reliable quantitative results with respect to the full simulation also in presence of the parity dependent feedback. In the inset of Fig. 6.9 is also plotted the relative error between the projected evolution of Eq. (6.37) and the full simulation. We stress that the error is never bigger than 1%, confirming the validity of the approach.

As one may notice from Fig. 6.9, after a sufficiently long time the system stabilises on a repeated evolution of period $\Delta t = t_{i+1} - t_i$, the delay between two subsequent parity measurements. In other words, after a certain time $\hat{\rho}(t_{i+1}) = \hat{\rho}(t_i)$ and the state of the system only depend on the time τ passed between two subsequent measurements, precisely $\tau = t - t_i$ and $\tau \in [0, \Delta t]$.

In this regard it is possible to define the stroboscopic stationary state $\hat{\sigma}(\tau)$ and its the stroboscopic stationary populations $s^+(\tau)$ and $s^-(\tau)$, in analogy with Eq. (6.43):

$$\begin{aligned}\hat{\sigma}(\tau) =& s^+(\tau)\ |\mathcal{C}_\alpha^+\rangle\langle\mathcal{C}_\alpha^+| + s^-(\tau)\ |\mathcal{C}_\alpha^-\rangle\langle\mathcal{C}_\alpha^-| \\ =& \frac{1}{2}\left[1 + s^+(0)\, e^{-2\bar{N}\gamma_+\tau} - s^-(0)\, e^{-2\bar{N}\gamma_-\tau}\right] |\mathcal{C}_\alpha^+\rangle\langle\mathcal{C}_\alpha^+| + \\ & \frac{1}{2}\left[1 + s^-(0)\, e^{-2\bar{N}\gamma_-\tau} - s^+(0)\, e^{-2\bar{N}\gamma_+\tau}\right] |\mathcal{C}_\alpha^-\rangle\langle\mathcal{C}_\alpha^-|\,.\end{aligned} \tag{6.44}$$

With this definitions the the fact that $\hat{\rho}(t_{i+1}) = \hat{\rho}(t_i)$ implies that $\sigma(\Delta t) = \sigma(0)$ and that

$$\begin{aligned}s^+(\Delta t) &= \frac{1}{2}\left[1 + s^+(0)\, e^{-2\bar{N}\gamma_+\Delta t} - s^-(0)\, e^{-2\bar{N}\gamma_-\Delta t}\right] = s^+(0)\,, \\ s^-(\Delta t) &= \frac{1}{2}\left[1 + s^-(0)\, e^{-2\bar{N}\gamma_-\Delta t} - s^+(0)\, e^{-2\bar{N}\gamma_+\Delta t}\right] = s^-(0)\,.\end{aligned} \tag{6.45}$$

Solving these equations for $s^\pm(0)$ we obtain

$$s^\pm(0) = \frac{1 - e^{-2\bar{N}\gamma_\mp\Delta t}}{2 - e^{-2\bar{N}\gamma_+\Delta t} - e^{-2\bar{N}\gamma_-\Delta t}}\,. \tag{6.46}$$

It follows that the stroboscopic stationary density matrix is

$$\begin{aligned}\hat{\sigma}(\tau) =& \frac{1}{2}\left[1 + \frac{e^{-2\bar{N}\gamma_+\tau}\left(1 - e^{-2\bar{N}\gamma_-\Delta t}\right) - e^{-2\bar{N}\gamma_-\tau}\left(1 - e^{-2\bar{N}\gamma_+\Delta t}\right)}{2 - e^{-2\bar{N}\gamma_+\Delta t} - e^{-2\bar{N}\gamma_-\Delta t}}\right] |\mathcal{C}_\alpha^+\rangle\langle\mathcal{C}_\alpha^+| + \\ & \frac{1}{2}\left[1 + \frac{e^{-2\bar{N}\gamma_-\tau}\left(1 - e^{-2\bar{N}\gamma_+\Delta t}\right) - e^{-2\bar{N}\gamma_+\tau}\left(1 - e^{-2\bar{N}\gamma_-\Delta t}\right)}{2 - e^{-2\bar{N}\gamma_+\Delta t} - e^{-2\bar{N}\gamma_-\Delta t}}\right] |\mathcal{C}_\alpha^-\rangle\langle\mathcal{C}_\alpha^-|\,.\end{aligned} \tag{6.47}$$

and the average value of parity for this stroboscopic steady state is

$$\langle\hat{P}\rangle_\sigma(\tau) = \frac{e^{-2\bar{N}\gamma_+\tau}\left(1 - e^{-2\bar{N}\gamma_-\Delta t}\right) - e^{-2\bar{N}\gamma_-\tau}\left(1 - e^{-2\bar{N}\gamma_+\Delta t}\right)}{2 - e^{-2\bar{N}\gamma_+\Delta t} - e^{-2\bar{N}\gamma_-\Delta t}}\,. \tag{6.48}$$

Notice that, in accordance to Fig. 6.9, all these expressions depend on Δt. Moreover, for $\Delta t \to \infty$ one correctly retrieves the no feedback solution $s^+ = s^- = 1/2$, while for $\Delta t \to 0$ the ratio between the population is of the form $s^+/s^- = \gamma_+/\gamma_-$. For the chosen parameters ($\gamma_- = 2\gamma_+$) this would lead to an average parity of $\langle\hat{P}\rangle = (\gamma_- - \gamma_+)/(\gamma_- + \gamma_+) = 1/3$, that is in very good agreement with the numerical simulation of the continuous limit (see Fig. 6.9).

It is interesting, at this point, to explore the feedback efficiency by studying how close the stroboscopic steady state is to the even cat state. In order to further characterise the effectiveness of this feedback, in Fig. 6.11 we plot, for different values of Δt, the fidelity of the stroboscopic stationary density matrix $\hat{\rho}(\tau = 0)$ (full simulation) with respect to $\hat{\rho}^+ = |\mathcal{C}_\alpha^+\rangle\langle\mathcal{C}_\alpha^+|$ as a function of γ_-/γ_+. We recall that the fidelity between two density matrices $\hat{\rho}$ and σ is defined as $f(\hat{\rho}, \hat{\sigma}) = \mathrm{Tr}\{\sqrt{\sqrt{\hat{\rho}}\hat{\sigma}\sqrt{\hat{\rho}}}\}$. Clearly, an

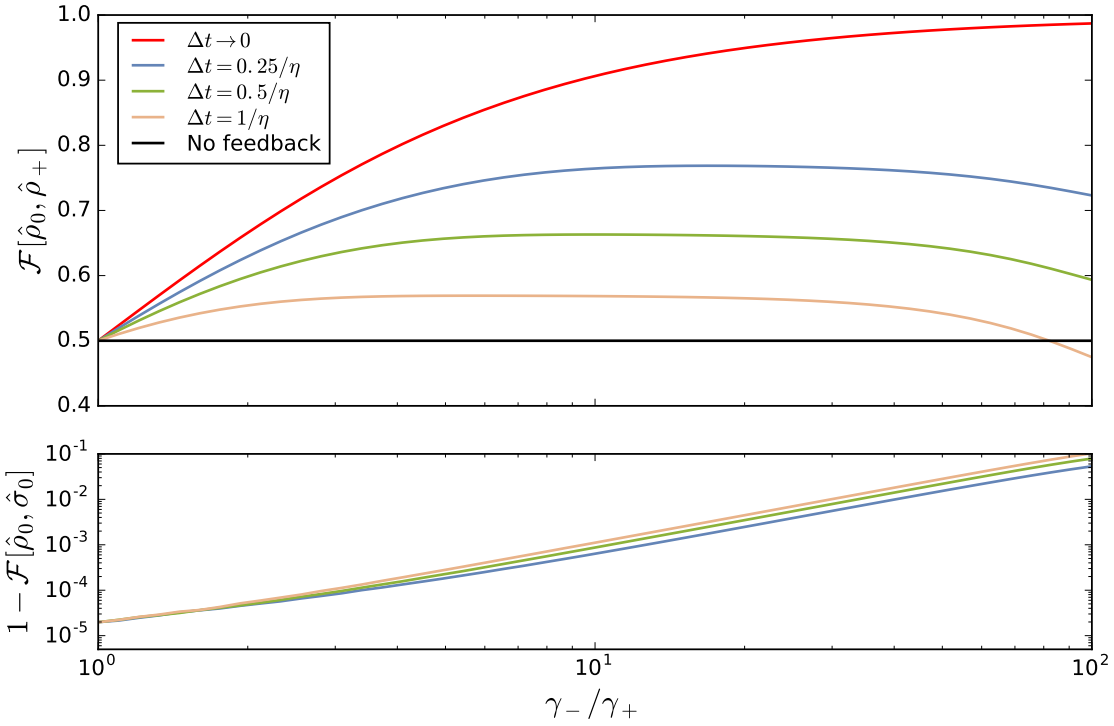

Figure 6.11 Fidelity as a function of the strength of the parity-selective dissipation for different values of the feedback characteristic time Δt. The parameters are $G = 10\eta$, $U = 1\eta$, $\gamma_+ = 0.1\eta$ and $\gamma_- = 2\gamma_+$. Top panel: fidelity between the even cat $\hat{\rho}^+ = |\mathcal{C}_\alpha^+\rangle\langle\mathcal{C}_\alpha^+|$ and the density matrix of the full simulation $\hat{\rho}_0 \stackrel{\text{def}}{=} \hat{\rho}(\tau = 0)$ at the stroboscopic steady state. Bottom panel: fidelity between the projected stroboscopic density matrix $\hat{\sigma}_0 \stackrel{\text{def}}{=} \hat{\sigma}(\tau = 0)$ and the density matrix of the full simulation $\hat{\rho}_0 \stackrel{\text{def}}{=} \hat{\rho}(\tau = 0)$.

interesting interplay between γ_-/γ_+ and Δt takes place. In the continuous limit the parity is continuously measured and an increasing value of γ_-/γ_+ will always increase the probability of being in the even cat. More interesting are the intermediate regimes. In fact, for a certain value γ_-/γ_+ the purity of the system starts to decrease. This poses a theoretical limit to the purification toward a even cat state which depends on the repetition rate of the parity measure. A qualitative explanation is the following. As γ_- increases, the system spends less and less time in the odd cat. This time is proportional to $1/\gamma_-$, when it is too small compared to Δt the measurements are not frequent enough to have an updated knowledge of the system and the feedback is not efficient anymore.

Moreover, for further increasing γ_- the approximations done in Sec. 6.1.2 are no more valid. In particular, for strong γ_-, the dissipator $\mathcal{D}_1^-$ is leading the system out of a statistical mixture of cat states with amplitude $\alpha = \sqrt{-G/(U - i\eta)}$. The

bottom panel of Fig. 6.11 show the limits of our approximation beyond which the description in terms of the two cat states breaks. To quantify the error committed by the cat state projection approach, the dashed line represent the fidelity between the approximated stroboscopic steady state and the full simulation one. Clearly, for $\gamma_- \gg 1/\Delta t$ the approximation is optimal, and one has a fidelity close to one, while for big γ_- the system cannot be described in the subspace spanned by the two considered cats. This also explain the further decrease of the stroboscopic stationary density matrix $\hat{\rho}(\tau = 0)$ and the even cat $\hat{\rho}^+ = |\mathcal{C}_\alpha^+\rangle\langle\mathcal{C}_\alpha^+|$.

6.3.3 Imperfect parity measurement

Let us study now the more realistic case in which the parity measurement is not perfect. In this case a certain outcome of the parity measurement does not allow to project the system state on the associated projector uniquely. More concretely, in the framework defined by Eq. (6.31), we will use the measurement superoperators $\mathcal{M}_\mu \overset{\text{def}}{=} (1-p_e)\,\mathcal{P}_\pm + p_e\,\mathcal{P}_\mp$, where p_e is the error probability allowing to take into account the imperfection of the parity measurement (also introduced in Sec. 4.2.2).

This measurement superoperators lead to the following expression for system evolution:

$$\begin{aligned}\hat{\rho}(t) &= \sum_{\beta=\pm} e^{\mathcal{L}_\mu(t-t_i)}\left[(1-p_e)\,\mathcal{P}_\mu + p_e\,\mathcal{P}_{-\beta}\right]\hat{\rho}(t_i) \\ &= \left\{e^{(\mathcal{L}_2+\mathcal{D}_1^+)(t-t_i)}\left[(1-p_e)\,\mathcal{P}_+ + p_e\,\mathcal{P}_-\right] + e^{(\mathcal{L}_2+\mathcal{D}_1^-)(t-t_i)}\left[(1-p_e)\,\mathcal{P}_- + p_e\,\mathcal{P}_+\right]\right\}\hat{\rho}(t_i),\end{aligned} \tag{6.49}$$

where we use the same definitions as in Eq. (6.34). In the same regime of the previous section, and following the same steps, this equation can be recast in the two-dimensional subspace of cat state populations:

$$\begin{aligned}\hat{\rho}(t) = p^+(t_i)\,&\left[(1-p_e)\,e^{\mathcal{D}_1^+(t-t_i)} + p_e\,e^{\mathcal{D}_1^-(t-t_i)}\right]|\mathcal{C}_\alpha^+\rangle\langle\mathcal{C}_\alpha^+| + \\ &p^-(t_i)\,\left[(1-p_e)\,e^{\mathcal{D}_1^-(t-t_i)} + p_e\,e^{\mathcal{D}_1^+(t-t_i)}\right]|\mathcal{C}_\alpha^-\rangle\langle\mathcal{C}_\alpha^-|\,.\end{aligned} \tag{6.50}$$

By properly inserting the action of $e^{\mathcal{D}_1^\pm(t-t_i)}$ given in Eq. (6.42), one gets:

$$\begin{aligned}\hat{\rho}(t) = \frac{1}{2}\Big[&1 + p^+(t_i)\,e^{-2\bar{N}\gamma_+(t-t_i)} - p^-(t_i)\,e^{-2\bar{N}\gamma_-(t-t_i)} \\ &+p_e\left(e^{-2\bar{N}\gamma_-(t-t_i)} - e^{-2\bar{N}\gamma_+(t-t_i)}\right)\Big]|\mathcal{C}_\alpha^+\rangle\langle\mathcal{C}_\alpha^+| \\ +\frac{1}{2}\Big[&1 + p^-(t_i)\,e^{-2\bar{N}\gamma_-(t-t_i)} - p^+(t_i)\,e^{-2\bar{N}\gamma_+(t-t_i)} \\ &+p_e\left(e^{-2\bar{N}\gamma_-(t-t_i)} - e^{-2\bar{N}\gamma_+(t-t_i)}\right)\Big]|\mathcal{C}_\alpha^-\rangle\langle\mathcal{C}_\alpha^-|\,.\end{aligned} \tag{6.51}$$

As in the case of perfect measurement, after few feedback cycles the system stabilises in a repeated evolution of period Δt. It is then possible to define the stroboscopic stationary density matrix $\sigma(\tau)$ and the populations $s^{\pm}(\tau)$ (see Eq. (6.44)), explicitly including the effect of errors in the parity measurement. In particular, the stroboscopic populations and the average parity at time $\tau = 0$ (equivalent to $\tau = \Delta t$) are given by:

$$s^{\pm}(\tau = 0) = \frac{1 - e^{-2\bar{N}\gamma_{\mp}\Delta t} \pm p_e \left(e^{-2\bar{N}\gamma_{-}\Delta t} - e^{-2\bar{N}\gamma_{+}\Delta t}\right)}{2 - e^{-2\bar{N}\gamma_{+}\Delta t} - e^{-2\bar{N}\gamma_{-}\Delta t}}\,, \tag{6.52a}$$

$$\langle \hat{P} \rangle_{\sigma}(\tau = 0) = \frac{(1 - 2p_e)\left(e^{-2\bar{N}\gamma_{+}\Delta t} - e^{-2\bar{N}\gamma_{-}\Delta t}\right)}{2 - e^{-2\bar{N}\gamma_{+}\Delta t} - e^{-2\bar{N}\gamma_{-}\Delta t}}\,. \tag{6.52b}$$

We recall that the parity is a good indicator of how close the system is to a cat state. For parity close to 1 (-1) the system is roughly in a even (odd) cat state, while for vanishing parity the two cat states are equally mixed, resulting in strictly positive Wigner functions. In equation (6.52b) the effect of imperfections in the parity measurement are explicit. For maximally imperfect measurement, i.e. $p_e = 0.5$, the average parity is zero, the system is in a equally weighted mixture of the two cat states and the Wigner function is positive.

6.3.4 Feedback by conditional pumping

While Section 6.3.1 reported our results on a feedback protocol based in conditioning the one-photon dissipation channel, in this section we show how a conditional change of pumping parameters can affect the steady state of the system. More precisely, we will show that it is possible to yield a negative valued Wigner function in the steady state by switching the phase or the intensity of the pumping.

Conditional pumping intensity

Let us repeatedly perform a projective parity measurement and conditionally tune the pumping intensity, depending on the measurement outcome. In Fig. 6.12 we show the steady state for continuous measurement limit $\hat{\rho}_{\rm ss}$ when $G_+/G_- = 5/12$ (at this ratio the effects of the feedback protocol are particularly apparent) and all the other parameters are independent of the measurement result, i.e. $U_+ = U_-$, $\gamma_+ = \gamma_-$ and $\eta_+ = \eta_-$. As the even sector is less pumped than the odd one, one would expect to see the odd sector more populated then the even one, but it is not the case. Indeed the system stabilises to a state that is closer to the even cat state, recovering the characteristic negative fringes in the Wigner function. This is explained as follows. The two sectors are approaching independently two cat states with two different values of α corresponding to the two different pumping intensities, in accordance with the formula $\alpha = \sqrt{-G/(U - i\eta)}$. Because of this, the two cat states have two different number of photons and, as the one-photon dissipation is

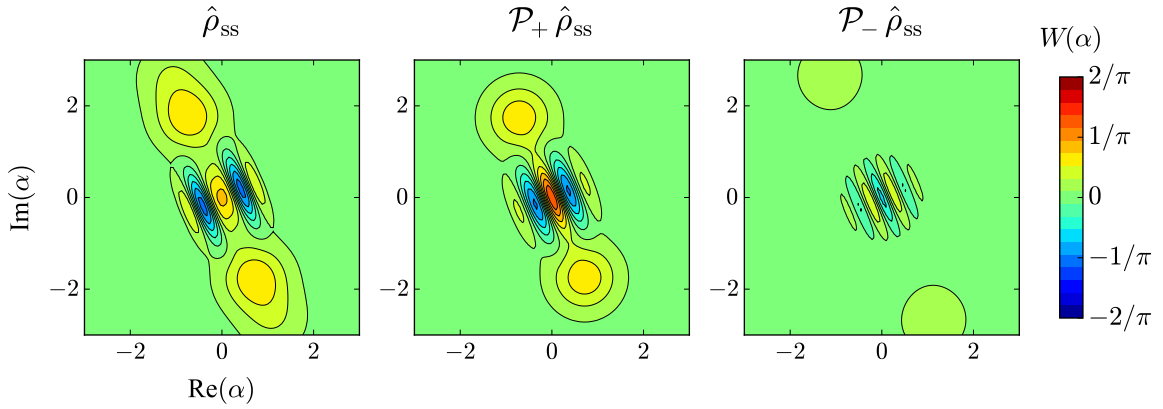

Figure 6.12 Continuous limit stationary state for conditional intensity of the pumping. Wigner function of the stationary state $\hat{\rho}_{\rm ss}$ (left panel), and of its even (middle panel) and odd (right panel) contributions. The parameter are $U = 1\eta$, $\gamma = 0.1\eta$, $G_+ = 5\eta$ and $G_- = 12\eta$.

proportional to the number of photons, it results in a stronger dissipation for the odd cat state that is then less populated. The state represented in Fig. 6.12 has an average parity of around $\langle \hat{P} \rangle \simeq 0.4$, it is dominated by even cat states, nevertheless we can still see the reminiscence of the of the odd cat state in the deformation of the positive lobes of the Wigner function. The coherent states composing the odd cat state have a larger amplitude α than the ones in the even cat state, and they appear at the extrema of the even cat state lobes.

Conditional pumping phase

Let us now consider the the case in which we conditionally pump the cavity with two opposite phases. The action of this feedback protocol for finite Δt is described again by Eq. (6.31) in which $G_+ = -G_-$ and all the other parameters are independent of the measurement result, i.e. $U_+ = U_-$, $\gamma_+ = \gamma_-$ and $\eta_+ = \eta_-$. In Fig. 6.13 we plot the Wigner function of the stationary and stroboscopic stationary state (see Sec. 6.3.2 for its definition), respectively for the continuous measurement limit and for finite Δt.

As mentioned in Sec. (6.1), without feedback our system evolve into a statistical mixture of $|\mathcal{C}_\alpha^+\rangle$ and $|\mathcal{C}_\alpha^-\rangle$. The value of α is determined by the system parameters, in particular if $G \to -G$ then $\alpha \to i\alpha$. In the feedback protocol considered here we pump the two parity sector with opposite phase ($G_+ = -G_-$), thus the even sector will tend to the state $|\mathcal{C}_\alpha^+\rangle$ while the odd sector will tend to $|\mathcal{C}_{i\alpha}^-\rangle$. In the continuous limit of this feedback protocol the steady state, showed in Figure (6.13, left), is given by:

$$\hat{\rho}_{\rm ss} \simeq p_{\rm ss}^+ \, |\mathcal{C}_\alpha^+\rangle\langle\mathcal{C}_\alpha^+| + p_{\rm ss}^- \, |\mathcal{C}_{i\alpha}^-\rangle\langle\mathcal{C}_{i\alpha}^-| \, , \tag{6.53}$$

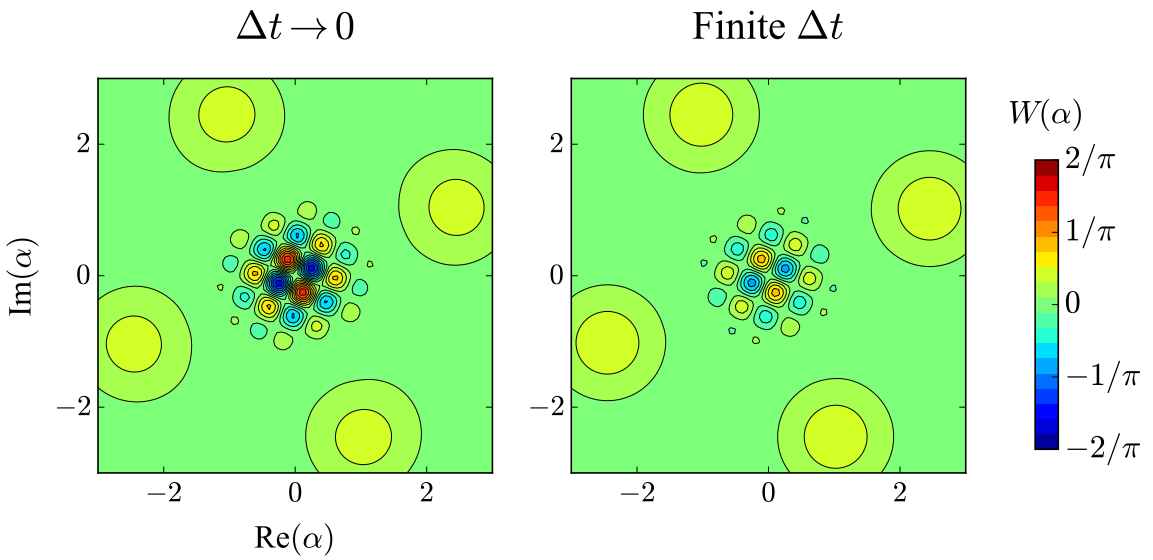

Figure 6.13 Feedback by conditional pumping phase. Wigner function of the stationary and the stroboscopic stationary state (see Sec. 6.3.2 for its definition), respectively for the continuous limit (left panel) and for $\Delta t = 0.5/\eta$ (right panel). The parameter are $U = 1\eta$, $\gamma = 0.1\eta$, $G_+ = 10\eta$ and $G_- = -G_+$

where in the intense pumping regime $p^+_{\rm ss} \simeq p^-_{\rm ss} \simeq 1/2$. If Δt is finite on the other hand, the one-photon dissipation has the time to introduce an error that modifies the stationary state of the feedback. In this case the pseudo stationary state has the form:

$$\hat{\rho}_{\rm ss} \simeq p^+_\alpha \ |\mathcal{C}^+_\alpha\rangle\langle\mathcal{C}^+_\alpha| + p^-_{i\alpha} \ |\mathcal{C}^-_{i\alpha}\rangle\langle\mathcal{C}^-_{i\alpha}| + p^-_\alpha \ |\mathcal{C}^-_\alpha\rangle\langle\mathcal{C}^-_\alpha| + p^+_{i\alpha} \ |\mathcal{C}^+_{i\alpha}\rangle\langle\mathcal{C}^+_{i\alpha}| \ , \tag{6.54}$$

where the last two terms are due to the error introduced by the one photon dissipation.

6.3.5 Projection of the feedback evolution on the parity subspaces

Let us consider the action of a feedback cycle, given by Eq. (6.31), in the more general case in which any parameter of the system can be controlled. It is not possible in general to do the same we did in the Section 6.3.2, and reduce the problem to the basis of the cat state populations. In this section we show that in the continuous measurement limit it is possible to neglect the odd-even photon number coherences and to reduce the problem to the parity defined subspaces.

In order to yield the continuous measurement limit of the general feedback proto-

col, let us expand for small Δt the conditional propagator in Eq. (6.31):

$$\begin{aligned}\hat{\rho}(t_{i+1}) &= \sum_{\mu} e^{\mathcal{L}_\mu \Delta t}\mathcal{P}_\mu\hat{\rho}(t_i) \simeq \sum_{\mu}(1+\mathcal{L}_\mu\Delta t)\,\mathcal{P}_\mu\hat{\rho}(t_i) = \sum_{\mu}\mathcal{P}_\mu\hat{\rho}(t_i) + \Delta t\sum_{\mu}\mathcal{L}_\mu\mathcal{P}_\mu\hat{\rho}(t_i)\\ &= \hat{\rho}(t_{i+1}) = (\mathcal{P}_- + \mathcal{P}_+)\,\hat{\rho}(t_i) + \Delta t\,(\mathcal{L}_-\mathcal{P}_- + \mathcal{L}_+\mathcal{P}_+)\,\hat{\rho}(t_i)\,.\end{aligned} \tag{6.55}$$

In the perspective of the continuous limit ($\Delta t \to \mathrm{d}t$ and $t_{i+1} \simeq t_i \to t$) we can express this equation as

$$\hat{\rho}(t+\mathrm{d}t) = (\mathcal{P}_- + \mathcal{P}_+)\,\hat{\rho}(t) + \mathrm{d}t\,(\mathcal{L}_-\mathcal{P}_- + \mathcal{L}_+\mathcal{P}_+)\,\hat{\rho}(t)\,. \tag{6.56}$$

It is not possible in general to obtain a differential equation from this expression, but this becomes possible when we consider its projection on the parity defined subspaces. Let us study, for example, the projection on the even space by applying the superoperator $\mathcal{P}_+[\cdot] = \hat{\Pi}_+[\cdot]\hat{\Pi}_+^\dagger$ to Eq. (6.56):

$$\mathcal{P}_+\hat{\rho}(t+\mathrm{d}t) = \mathcal{P}_+\,(\mathcal{P}_- + \mathcal{P}_+)\,\hat{\rho}(t) + \mathrm{d}t\,\mathcal{P}_+\,(\mathcal{L}_-\mathcal{P}_- + \mathcal{L}_+\mathcal{P}_+)\,\hat{\rho}(t)\,. \tag{6.57}$$

Note that $\hat{\Pi}_+\hat{\Pi}_- = 0$ and that $\hat{\Pi}_\pm^2 = \hat{\Pi}_\pm$, this implies that $\mathcal{P}_+\mathcal{P}_- = 0$ and that $\mathcal{P}_\pm^2 = \mathcal{P}_\pm$. Using these properties of the projectors, the expression (6.57) can be simplified to:

$$\mathcal{P}_+\hat{\rho}(t+\mathrm{d}t) = \mathcal{P}_+\,\hat{\rho}(t) + \mathrm{d}t\,\mathcal{P}_+\,(\mathcal{L}_-\mathcal{P}_- + \mathcal{L}_+\mathcal{P}_+)\,\hat{\rho}(t)\,. \tag{6.58}$$

From Equations (6.7) and (6.6) one can see that, a part for the first term of the one-photon dissipator, every term of the time evolution defined by the Lindbladian superoperators $\mathcal{L}_\pm$ preserves the parity. Taking into account this property and defining $\hat{\rho}_\pm \overset{\text{def}}{=} \mathcal{P}_\pm\hat{\rho}$, we obtain:

$$\frac{\hat{\rho}_+(t+dt) - \hat{\rho}_+(t)}{\mathrm{d}t} \equiv \partial_t\hat{\rho}_+ = i\,[\hat{\rho}_+, \hat{H}_+] + \mathcal{D}_2^+\hat{\rho}_+ + \mathcal{P}_+\mathcal{D}_1^-\hat{\rho}_- + \mathcal{P}_+\mathcal{D}_1^+\hat{\rho}_+\,, \tag{6.59}$$

where we switched Eq. (6.58) into a differential equation and we omitted for simplicity the explicit time dependence. The same procedure can be performed for the projection on the odd subspace. We finally obtain two coupled master equation for the parity projected density matrix $\hat{\rho}_+$ and $\hat{\rho}_-$:

$$\begin{aligned}\partial_t\hat{\rho}_+ &= i\,[\hat{\rho}_+, \hat{H}_+] + \eta_+\left[\hat{a}\hat{a}\hat{\rho}_+\hat{a}^\dagger\hat{a}^\dagger - \frac{1}{2}\left\{\hat{a}^\dagger\hat{a}^\dagger\hat{a}\hat{a}, \hat{\rho}_+\right\}\right] - \frac{\gamma_+}{2}\left\{\hat{a}^\dagger\hat{a}, \hat{\rho}_+\right\} + \gamma_-\,\hat{a}\hat{\rho}_-\hat{a}^\dagger\,,\\ \partial_t\hat{\rho}_- &= i\,[\hat{\rho}_-, \hat{H}_-] + \eta_-\left[\hat{a}\hat{a}\hat{\rho}_-\hat{a}^\dagger\hat{a}^\dagger - \frac{1}{2}\left\{\hat{a}^\dagger\hat{a}^\dagger\hat{a}\hat{a}, \hat{\rho}_-\right\}\right] - \frac{\gamma_-}{2}\left\{\hat{a}^\dagger\hat{a}, \hat{\rho}_-\right\} + \gamma_+\,\hat{a}\hat{\rho}_+\hat{a}^\dagger\,,\end{aligned} \tag{6.60}$$

where the subscripts denote the dependence of the piecewise-constant parameters on the measurement outcome.

We stress that these coupled equations do not represent a master equation in the full space as $\mathcal{P}_+ + \mathcal{P}_- \neq \mathbb{1}$. These equations disregard the coherences between even and odd sectors, that is valid for our problem in which these coherences are cancelled by the continuous parity measurement and in which any term of the dynamic couples the to parity defined sectors in a coherent manner. As a sanity check we can see that $\mathrm{Tr}\{\partial_t\hat{\rho}_+ + \partial_t\hat{\rho}_-\} = 0$, whereas the traces are not individually conserved $\mathrm{Tr}\{\partial_t\hat{\rho}_\pm\} \neq 0$. The expression obtained for the density matrix evolution under the effect of the feedback in Eq. (6.60), allows to study the system in large range of situation and in a more simplified representation.

Imperfect parity measurement

As we did in Section 6.3.3 we could be interested in the effect of the measurement error on these two coupled master equations. We use the same measurement superoperator $\mathcal{M}_\mu \overset{\text{def}}{=} (1-p_e)\,\mathcal{P}_\pm + p_e\,\mathcal{P}_\mp$ and we follow the same procedure as in Section 6.3.3. One can show that the same coupled master equations hold in this case, with the only effect of modifying their parameters:

$$\hat{H}'_\pm = (1-p_e)\,\hat{H}_\pm + p_e\,\hat{H}_\mp\,, \tag{6.61a}$$
$$\eta'_\pm = (1-p_e)\,\eta_\pm + p_e\,\eta_\mp\,, \tag{6.61b}$$
$$\gamma'_\pm = (1-p_e)\,\gamma_\pm + p_e\,\gamma_\mp\,. \tag{6.61c}$$

The case of maximally imperfect measurement, i.e. $p_e = 1/2$, is perfectly equivalent to the absence of feedback control: $\hat{H}'_+ = \hat{H}'_-$, $\eta'_+ = \eta'_-$ and $\gamma'_+ = \gamma'_-$. Remarkably for this kind of feedback the presence of a measurement error is equivalent to a reduced pumping amplitude. Considering that $G_+ = -G_-$, Eq. (6.61a) implies that $G'_\pm = (1-2p_e)G_\pm$ that is by definition smaller than $G_\pm$.

Equivalence with the effective parity-dependent dissipation

At the end of Sec. 6.3.1 we have described the continuous limit of our feedback protocol through the effective parity-dependent dissipation in Eq. (6.35). By projecting on the parity subspaces we can prove the equivalence between the continuous limit of our parity triggered feedback protocol and this effective dissipation. From Eq. (6.35), we recall his expression:

$$\mathcal{D}_f\hat{\rho} = \frac{\gamma_f}{2}\left(2\hat{a}_f\hat{\rho}\hat{a}_f^\dagger - \hat{a}_f^\dagger\hat{a}_f\hat{\rho} - \hat{\rho}\hat{a}_f^\dagger\hat{a}_f\right). \tag{6.62}$$

where $\hat{a}_f = \hat{a}\,\frac{1}{2}(\hat{\mathbb{1}} - \hat{P}) = \hat{a}\,\hat{\Pi}_-$ is a parity selective jump operator. By projecting the dissipator $\mathcal{D}_f$ on the parity defined subspaces we obtain:

$$\begin{aligned}\mathcal{P}_+\mathcal{D}_f\hat{\rho} &= \gamma_f\,\hat{a}\hat{\rho}_-\hat{a}^\dagger\,;\\ \mathcal{P}_-\mathcal{D}_f\hat{\rho} &= \frac{\gamma_f}{2}\,\left\{\hat{a}^\dagger\hat{a},\hat{\rho}_-\right\}\,.\end{aligned} \tag{6.63}$$

Imagine that we are not applying any feedback, it means that all the parameters are independent on the parity, i.e. $\hat{H}_+ = \hat{H}_- = \hat{H}$, $\eta_+ = \eta_- = \eta$ and $\gamma_+ = \gamma_- = \gamma$. By comparing Eqs. (6.63) and Eqs. (6.60), it is clear that by adding the dissipator $\mathcal{D}_{\gamma_f}$ one is effectively increasing by γ_f the value of γ_-, i.e. $\gamma_+ \equiv \gamma$ and $\gamma_- \equiv \gamma + \gamma_f$. Note that the equivalence is only true in the parity defined subspaces.

6.4 Conclusions and perspectives on photonic Schrödinger cat state generation

In this chapter we presented our results on the study of quantum trajectories and feedback control of two-photons driven-dissipative resonators. Studying quantum trajectories turned out to be very convenient in interpreting the characteristic bimodality of this kind of systems. Investigating the onset of bimodality in driven-dissipative resonators is particularly interesting since the components of the resulting mixed steady state,

$$\hat{\rho}_{\rm ss} \simeq p_1 \, |\mathcal{C}_\alpha^+\rangle\langle\mathcal{C}_\alpha^+| + p_2 \, |\mathcal{C}_\alpha^-\rangle\langle\mathcal{C}_\alpha^-| \quad \text{or} \quad \hat{\rho}_{\rm ss} \simeq \frac{1}{2}\,|\alpha\rangle\langle\alpha| + \frac{1}{2}\,|-\alpha\rangle\langle-\alpha|\,,$$

can be used as (quasi-)orthogonal states in quantum computation [75, 77, 159, 160]. To exploit the two-photon driven resonator in this context, one can envision a feedback mechanism which unbalances the steady-state mixture in favour of one of the two components [96]. Based on this idea we explored the properties and possibilities of a parity measurement triggered feedback. We considered some simplified approaches to the problem, that proved to be very efficient and accurate and we studied the effect of the several sources of error entering the feedback protocol.

From a perspective point of view, it would be interesting to define a precise realistic protocol to exctract information about the parity in this kind of two-photons driven-dissipative resonators. In Ref. [88], Sun et al. have been able to track photon jumps by repeated measurements of parity. However, in this experiment they measured the parity of a free linear cavity, while our system is driven and nonlinear. Some preliminary analysis, that we did not present in this thesis, have proved that it is indeed possible to extract partial information on the parity of our two-photons driven-dissipative resonators, by coupling and measuring an ancillary qubit. This partial information can be used to protect the quantum properties of optical Schrödinger cat states through a feedback protocols of the kind that we presented in this chapter.

Chapter 7

Conclusion and perspectives

In this thesis we have explored theoretically the measurement and the control of highly nonclassical states of quantum optical systems. After an introduction of some paradigmatic models of quantum optics in Chapter 2, and a presentation of the theoretical framework in Chapters 3 and 4, we have detailed the original results of this thesis in Chapters 5 and 6.

In Chapter 5 we have presented our proposal for a non-destructive measurement of populations and correlations of exotic ground states in the ultrastrong coupling regime [94]. Cavity (circuit) QED systems in the ultrastrong coupling regime are characterised by exotic vacua that contain photons. The precise nature of these vacua is directly related to the fundamental symmetries of the considered cavity (circuit) QED systems. In the case of the Dicke model for example, the ground state is a light-matter Schrödinger cat state. Due to energy conservation, the photons contained in these exotic ground states are bound to the cavity, and cannot be emitted into the environment. This means that we can not explore and control them by simple photodetection. With our work we have proven that the Lamb shift of an ancillary two-level atom (qubit) coupled to a cavity (circuit) QED system in the ultrastrong coupling regime contains direct information on the populations and the coherences of the system ground state.

Another important part of our work has been focused on the realisation of photonic Schrödinger cat states in two-photon driven-dissipative resonators [96]. The results of this work have been reported in Chapter 6. Through reservoir engineering, it is possible to shape an out-of equilibrium system, in which, except for the presence of one-photon dissipation, the parity of the system is conserved [160]. It has been proved, that this symmetry allows to observe photonic Schrödinger cats in the transient dynamics of the system [85]. However, due to the unavoidable one-photon dissipation, the stationary state of the system is a classical state, and more precisely it is a statistical mixture of the two photonic Schrödinger cat states with opposite parity. The big challenge here is to protect one of the two cat state against one-photon dissipation, and to recover the distinctive quantum features of these states. Based on a detailed analysis of the system quantum state trajectories [95], we have proposed and explored the different regimes of a parity-triggered feedback control that is intended to recover the quantum features of photonic Schrödinger cat states.

It is worth spending a few words on the analogies and the differences between the two types of systems considered in this thesis. First of all, we note that in both

systems the generation of highly nonclassical states of light and matter is associated to the underlying symmetry of the system. Both the ground state of a (Dicke) system in the ultrastrong coupling regime, and the out-of-equilibrium stationary state of two-photon driven-dissipative resonators, are both in the form of Schrödinger cat states. These kind of states are very interesting because they are a coherent superposition of macroscopically different states. However, the access to the quantum correlations of these systems is non-trivial: our work in this thesis has been to address this problem.

Furthermore, we find important to discuss the relation of this research with the problem of quantum-to-classical boundaries. In order to have a macroscopic state, we need the Schrödinger cat state to have a large number of photons. However, it is precisely in that condition that the effect of decoherence is stronger. Indeed, for a large number of photons, the ground state and the first excited state in the ultrastrong coupling regime are quasi-degenerate. This makes these system more vulnerable to the effect of thermal equilibrium, that for a large enough temperature of the bath, leads the system to a classical mixture of ground and first exited state. In an analogous way, since one-photon dissipation is proportional to the number of photons, the lifetime of photonic Schrödinger cats in two-photon driven-dissipative resonators is inversely proportional to number of photons. In a few words, these superposition of macroscopic states are more fragile as their size increases.

Along this thesis, we have insisted on the crucial role of information in quantum physics. Another field in which this concept haa a very central role is the thermodynamics. Indeed, Jaynes reinterpretation of thermodynamics principles in terms of Shannon's theory of information [13, 14], cast a new light on the field [15, 16]. According to this view, observer knowledge and information are the central concepts, on which modern thermodynamics is built [176].

In this regard, a very promising field to develop the role of information in physics, is represented by quantum thermodynamics [177, 178]. Furthermore, the enormous experimental advances in tracking the quantum state trajectories [86–89], represent a concrete resource to explore the thermodynamics of quantum systems [90–93, 179, 180]. Being among the main processes of information managing, quantum measurement and feedback control might play a very central role in this research.

Appendix A

A realistic model of an artificial dissipation

As a possible model for the parity-selective dissipation, let us consider to conditionally couple the cavity to a two-level system. For sake of simplicity, let us suppose that we want to stabilise the even cat, and let us consider the following feedback. At time $t = 0$, we perform the parity measure: if the right parity is measured, we keep the two-level system decoupled, i.e. the spin stays in its ground state $|0\rangle\langle 0|$ and the cat state evolves according to $e^{\mathcal{L}t}$. Instead, if the wrong one is measured, we activate a qubit which enters in resonance with the cavity, and whose interaction is given by:

$$\hat{H}_g = g\left(\hat{a}^\dagger\hat{\sigma}^- + \hat{a}\hat{\sigma}^+\right), \tag{A.1}$$

where $\hat{\sigma}^\pm$ are the spin creation/annihilation operators. Now, we measure the qubit with a frequency $\Delta\tau$. We suppose that, initially, the qubit is in its ground state, and therefore the evolution of the system for $t \in [0, \Delta\tau]$ is given by:

$$\begin{aligned}
\hat{\rho}(t) = e^{(\mathcal{L}+\mathcal{L}_g)t}\hat{\rho}(0) &\simeq \left(\mathbb{1} + (\mathcal{L}+\mathcal{L}_g)t + \frac{(\mathcal{L}+\mathcal{L}_g)^2t^2}{2}\right)|\mathcal{C}_\alpha^-\rangle\langle\mathcal{C}_\alpha^-| \otimes |0\rangle\langle 0| \\
&= \left(\mathbb{1} + \mathcal{L}t + \frac{\mathcal{L}^2t^2}{2} + \mathcal{L}_g t + \frac{\mathcal{L}_g^2t^2}{2} + (\mathcal{L}\mathcal{L}_g + \mathcal{L}_g\mathcal{L})\frac{t^2}{2}\right)|\mathcal{C}_\alpha^-\rangle\langle\mathcal{C}_\alpha^-| \otimes |0\rangle\langle 0| \\
&\simeq \left(e^{\mathcal{L}t} + \mathcal{L}_g t + \frac{\mathcal{L}_g^2t^2}{2} + (\mathcal{L}\mathcal{L}_g + \mathcal{L}_g\mathcal{L})\frac{t^2}{2}\right)|\mathcal{C}_\alpha^-\rangle\langle\mathcal{C}_\alpha^-| \otimes |0\rangle\langle 0|\,.
\end{aligned} \tag{A.2}$$

At time $t = \Delta\tau$ we perform the measure on the system. Therefore, coherences will disappear after the measure. This translates into the fact that the only relevant terms to determine the outcome of the measure are those quadratic in $\mathcal{L}_g$. Therefore one has

$$\hat{\rho}(t) \simeq \left(e^{\mathcal{L}t} + \frac{\mathcal{L}_g^2t^2}{2}\right)|\mathcal{C}_\alpha^-\rangle\langle\mathcal{C}_\alpha^-| \otimes |0\rangle\langle 0|\,. \tag{A.3}$$

The evolution of the first term is given by Eq. (6.42). For the second term, we have that

$$\begin{aligned}
\frac{\mathcal{L}_g^2 t^2}{2}\hat{\rho}(0) &= -\frac{t^2}{2}\left[\hat{H}_g, \left[\hat{H}_g, |\mathcal{C}_\alpha^-\rangle\langle\mathcal{C}_\alpha^-| \otimes |0\rangle\langle 0|\right]\right] \\
&= -\frac{gt^2}{2}\left[\hat{H}_g, \left[\hat{a}^\dagger\hat{\sigma}^- + \hat{a}\hat{\sigma}^+, |\mathcal{C}_\alpha^-\rangle\langle\mathcal{C}_\alpha^-| \otimes |0\rangle\langle 0|\right]\right] \\
&= -\frac{gt^2}{2}\left[\hat{H}_g, \alpha\,|\mathcal{C}_\alpha^+\rangle\langle\mathcal{C}_\alpha^-| \otimes |1\rangle\langle 0| - \alpha^*\,|\mathcal{C}_\alpha^-\rangle\langle\mathcal{C}_\alpha^+| \otimes |0\rangle\langle 1|\right] \\
&= -\frac{g^2t^2}{2}\left(\alpha\hat{a}^\dagger\,|\mathcal{C}_\alpha^+\rangle\langle\mathcal{C}_\alpha^-| + |\alpha|^2\,|\mathcal{C}_\alpha^-\rangle\langle\mathcal{C}_\alpha^-|\right) \otimes |0\rangle\langle 0| \\
&\qquad\qquad -\frac{g^2t^2}{2}\left(|\alpha|^2\,|\mathcal{C}_\alpha^+\rangle\langle\mathcal{C}_\alpha^+| + \alpha^*\,|\mathcal{C}_\alpha^+\rangle\langle\mathcal{C}_\alpha^-|\,\hat{a}\right) \otimes |1\rangle\langle 1| \\
&\simeq -g^2t^2\bar{N}\left(|\mathcal{C}_\alpha^-\rangle\langle\mathcal{C}_\alpha^-| \otimes |0\rangle\langle 0| - |\mathcal{C}_\alpha^+\rangle\langle\mathcal{C}_\alpha^+| \otimes |1\rangle\langle 1|\right),
\end{aligned} \tag{A.4}$$

where we recall that $\bar{N} = |\alpha|^2$.

Combining in Eq. (A.3) the results from Eqs. (6.42) and (A.4), and tracing out the two-level system degrees of freedom we eventually obtain

$$\begin{aligned}
\hat{\rho}(t) &\simeq \frac{1 - e^{-2\bar{N}\gamma t} + 2g^2t^2\bar{N}}{2}\,|\mathcal{C}_\alpha^+\rangle\langle\mathcal{C}_\alpha^+| + \frac{1 + e^{-2\bar{N}\gamma t} - 2g^2t^2\bar{N}}{2}\,|\mathcal{C}_\alpha^-\rangle\langle\mathcal{C}_\alpha^-| \\
&\simeq \frac{1 - e^{-2\bar{N}\gamma_{\text{eff}} t}}{2}\,|\mathcal{C}_\alpha^+\rangle\langle\mathcal{C}_\alpha^+| + \frac{1 + e^{-2\bar{N}\gamma_{\text{eff}} t}}{2}\,|\mathcal{C}_\alpha^-\rangle\langle\mathcal{C}_\alpha^-|
\end{aligned} \tag{A.5}$$

where we have introduced $\gamma_{\text{eff}} = \gamma + g^2 t$. In other words, we have proved that the Hamiltonian coupling to a two-level system and a measurement on it can effectively result in an additional one-photon dissipation for the cavity.

Bibliography

[1] E. Schrödinger. *"Nature and the Greeks" and "Science and Humanism"*. Reissue. Canto Classics. Cambridge University Press, 2014.

[2] W. Heisenberg. *Physics and Philosophy: The Revolution In Modern Science*. World Perspectives Vol. Nineteen. Harper Perennial Modern Classics, 2007.

[3] M. Schlosshauer, J. Kofler, and A. Zeilinger. *A snapshot of foundational attitudes toward quantum mechanics*. Studies in History and Philosophy of Science Part B: Studies in History and Philosophy of Modern Physics **44** (2013), pp. 222–230.

[4] M. F. Pusey, J. Barrett, and T. Rudolph. *On the reality of the quantum state*. Nature Physics **8** (2012), pp. 475–478.

[5] N. D. Mermin. *Physics: QBism puts the scientist back into science*. Nature **507** (2014), pp. 421–423.

[6] C. A. Fuchs and R. Schack. *Quantum-Bayesian coherence*. Reviews of Modern Physics **85** (2013), pp. 1693–1715.

[7] A. Cabello, S. Severini, and A. Winter. *Graph-Theoretic Approach to Quantum Correlations*. Physical Review Letters **112** (2014), p. 040401.

[8] *Interpretations of quantum mechanics*. *Wikipedia*. Page Version ID: 794489025.

[9] A. Cabello. *Interpretations of quantum theory: A map of madness*. arXiv:1509.04711 [quant-ph] (2015).

[10] R. Feynman, R. B. Leighton, and M. Sands. *Lectures on physics*. Vol. Volume 3. AW, 1964.

[11] W. Heisenberg. *Über den anschaulichen Inhalt der quantentheoretischen Kinematik und Mechanik*. Zeitschrift für Physik **43** (1927), pp. 172–198.

[12] E. Dolnick. *The Clockwork Universe: Isaac Newton, the Royal Society, and the Birth of the Modern World*. 1St Edition. Harper, 2011.

[13] C. E. Shannon. *A mathematical theory of communication*. The Bell System Technical Journal **27** (1948), pp. 379–423.

[14] C. E. Shannon. *A mathematical theory of communication*. The Bell System Technical Journal **27** (1948), pp. 623–656.

[15] E. T. Jaynes. *Information Theory and Statistical Mechanics*. Physical Review **106** (1957), pp. 620–630.

[16] E. T. Jaynes. *Information Theory and Statistical Mechanics. II*. Physical Review **108** (1957), pp. 171–190.

[17] P. Goyal. *Information Physics—Towards a New Conception of Physical Reality*. Information **3** (2012), pp. 567–594.

[18] K. Friston. *The free-energy principle: a unified brain theory?* Nature Reviews Neuroscience **11** (2010), pp. 127–138.

[19] A. G. Dimitrov, A. A. Lazar, and J. D. Victor. *Information theory in neuroscience*. Journal of computational neuroscience **30** (2011), pp. 1–5.

[20] W. Hermanns and A. Einstein. *Einstein and the Poet: In Search of the Cosmic Man*. en. Branden Press, 1983.

[21] A. Einstein, B. Podolsky, and N. Rosen. *Can Quantum-Mechanical Description of Physical Reality Be Considered Complete?* Physical Review **47** (1935), pp. 777–780.

[22] J. S. Bell. *On the Einstein–Podolsy–Rosen paradox*. Phisics **1** (1964), pp. 195–200.

[23] N. Bohr. *Can Quantum-Mechanical Description of Physical Reality be Considered Complete?* Physical Review **48** (1935), pp. 696–702.

[24] M. Planck. *Über das Gesetz der Energieverteilung im Normalspektrum*. SpringerLink (1901), pp. 178–191.

[25] A. Einstein. *Über einen die Erzeugung und Verwandlung des Lichtes betreffenden heuristischen Gesichtspunkt*. Annalen der Physik **322** (1905), pp. 132–148.

[26] B. Niels. *I. On the constitution of atoms and molecules*. Philosophical Magazine **26** (1913), pp. 1–25.

[27] S. Haroche and J.-M. Raimond. *Exploring the quantum: atoms, cavities, and photons*. 1st ed. Oxford Graduate Texts. Oxford University Press, USA, 2006.

[28] R. H. Dicke. *Coherence in Spontaneous Radiation Processes*. Physical Review **93** (1954), pp. 99–110.

[29] J. J. Hopfield. *Theory of the Contribution of Excitons to the Complex Dielectric Constant of Crystals*. Physical Review **112** (1958), pp. 1555–1567.

[30] M. Tavis and F. W. Cummings. *Exact Solution for an N-Molecule—Radiation-Field Hamiltonian*. Physical Review **170** (1968), pp. 379–384.

[31] E. T. Jaynes and F. W. Cummings. *Comparison of quantum and semiclassical radiation theories with application to the beam maser*. Proceedings of the IEEE **51** (1963), pp. 89–109.

[32] A. D. Greentree, J. Koch, and J. Larson. *Fifty years of Jaynes– Cummings physics*. Journal of Physics B: Atomic, Molecular and Optical Physics **46** (2013), p. 220201.

[33] J. M. Raimond, M. Brune, and S. Haroche. *Manipulating quantum entanglement with atoms and photons in a cavity*. Reviews of Modern Physics **73** (2001), pp. 565–582.

[34] R. Miller, T. E. Northup, K. M. Birnbaum, A. Boca, A. D. Boozer, and H. J. Kimble. *Trapped atoms in cavity QED: coupling quantized light and matter*. Journal of Physics B: Atomic, Molecular and Optical Physics **38** (2005), S551.

[35] C. J. Hood, M. S. Chapman, T. W. Lynn, and H. J. Kimble. *Real-Time Cavity QED with Single Atoms*. Physical Review Letters **80** (1998), pp. 4157–4160.

[36] M. Brune, F. Schmidt-Kaler, A. Maali, J. Dreyer, E. Hagley, J. M. Raimond, and S. Haroche. *Quantum Rabi Oscillation: A Direct Test of Field Quantization in a Cavity*. Physical Review Letters **76** (1996), pp. 1800–1803.

[37] C. Weisbuch, M. Nishioka, A. Ishikawa, and Y. Arakawa. *Observation of the coupled exciton-photon mode splitting in a semiconductor quantum microcavity*. Physical Review Letters **69** (1992), pp. 3314–3317.

[38] B. Deveaud. *The physics of semiconductor microcavities: from fundamentals to nanoscale devices*. Wiley-VCH, 2007.

[39] M. H. Devoret, J. M. Martinis, and J. Clarke. *Measurements of Macroscopic Quantum Tunneling out of the Zero-Voltage State of a Current-Biased Josephson Junction*. Physical Review Letters **55** (1985), pp. 1908–1911.

[40] J. M. Martinis, M. H. Devoret, and J. Clarke. *Energy-Level Quantization in the Zero-Voltage State of a Current-Biased Josephson Junction*. Physical Review Letters **55** (1985), pp. 1543–1546.

[41] A. Wallraff, D. I. Schuster, A. Blais, L. Frunzio, R.-S. Huang, J. Majer, S. Kumar, S. M. Girvin, and R. J. Schoelkopf. *Strong coupling of a single photon to a superconducting qubit using circuit quantum electrodynamics*. Nature **431** (2004), pp. 162–167.

[42] D. I. Schuster, A. A. Houck, J. A. Schreier, A. Wallraff, J. M. Gambetta, A. Blais, L. Frunzio, J. Majer, B. Johnson, M. H. Devoret, S. M. Girvin, and R. J. Schoelkopf. *Resolving photon number states in a superconducting circuit*. Nature **445** (2007), pp. 515–518.

[43] A. Fragner, M. Göppl, J. M. Fink, M. Baur, R. Bianchetti, P. J. Leek, A. Blais, and A. Wallraff. *Resolving Vacuum Fluctuations in an Electrical Circuit by Measuring the Lamb Shift*. Science **322** (2008), pp. 1357–1360.

[44] R. J. Schoelkopf and S. M. Girvin. *Wiring up quantum systems*. Nature **451** (2008), pp. 664–669.

[45] J. M. Fink, M. Göppl, M. Baur, R. Bianchetti, P. J. Leek, A. Blais, and A. Wallraff. *Climbing the Jaynes–Cummings ladder and observing its nonlinearity in a cavity QED system*. Nature **454** (2008), pp. 315–318.

[46] J. M. Fink. *Dressed Collective Qubit States and the Tavis-Cummings Model in Circuit QED*. Physical Review Letters **103** (2009).

[47] J. Q. You and F. Nori. *Atomic physics and quantum optics using superconducting circuits*. Nature **474** (2011), pp. 589–597.

[48] V. E. Manucharyan, A. Baksic, and C. Ciuti. *Resilience of the quantum Rabi model in circuit QED*. Journal of Physics A: Mathematical and Theoretical **50** (2017), p. 294001.

[49] B. D. Josephson. *Possible new effects in superconductive tunnelling*. Physics Letters **1** (1962), pp. 251–253.

[50] P. W. Anderson and J. M. Rowell. *Probable Observation of the Josephson Superconducting Tunneling Effect*. Physical Review Letters **10** (1963), pp. 230–232.

[51] M. Saba, C. Ciuti, J. Bloch, V. Thierry-Mieg, R. André, L. S. Dang, S. Kundermann, A. Mura, G. Bongiovanni, J. L. Staehli, and B. Deveaud. *High-temperature ultrafast polariton parametric amplification in semiconductor microcavities*. Nature **414** (2001), pp. 731–735.

[52] K. Hennessy, A. Badolato, M. Winger, D. Gerace, M. Atatüre, S. Gulde, S. Fält, E. L. Hu, and A. Imamoğlu. *Quantum nature of a strongly coupled single quantum dot–cavity system*. Nature **445** (2007), pp. 896–899.

[53] G. Bastard. *Wave mechanics applied to semiconductor heterostructures*. Monographies de physique. EDP Science, 1992.

[54] B. Deveaud and International School of Physics Enrico Fermi, eds. *Electron and photon confinement in semiconductor nanostructures: proceedings of the International School of Physics "Enrico Fermi", Course CL, Varenna on Lake Como, Villa Monastero, 25 June - 5 July 2002*. OCLC: 249530376. Amsterdam: IOS Press [u.a.], 2003. 421 pp. ISBN: 978-1-58603-352-1 978-4-274-90597-1.

[55] I. Carusotto and C. Ciuti. *Quantum fluids of light*. Rev. Mod. Phys. **85** (2013), pp. 299–366.

[56] J. Kasprzak, M. Richard, S. Kundermann, A. Baas, P. Jeambrun, J. M. J. Keeling, F. M. Marchetti, M. H. Szymańska, R. André, J. L. Staehli, V. Savona, P. B. Littlewood, B. Deveaud, and L. S. Dang. *Bose–Einstein condensation of exciton polaritons*. Nature **443** (2006), pp. 409–414.

[57] A. Amo, J. Lefrère, S. Pigeon, C. Adrados, C. Ciuti, I. Carusotto, R. Houdré, E. Giacobino, and A. Bramati. *Superfluidity of polaritons in semiconductor microcavities*. Nature Physics **5** (2009), pp. 805–810.

[58] M. Devoret, S. Girvin, and R. Schoelkopf. *Circuit-QED: How strong can the coupling between a Josephson junction atom and a transmission line resonator be?* Annalen der Physik **16** (2007), pp. 767–779.

[59] J. Bourassa, J. M. Gambetta, A. A. Abdumalikov, O. Astafiev, Y. Nakamura, and A. Blais. *Ultrastrong coupling regime of cavity QED with phase-biased flux qubits*. Physical Review A **80** (2009), p. 032109.

[60] B. Peropadre, P. Forn-Díaz, E. Solano, and J. J. García-Ripoll. *Switchable Ultrastrong Coupling in Circuit QED*. Physical Review Letters **105** (2010), p. 023601.

[61] T. Niemczyk, F. Deppe, H. Huebl, E. P. Menzel, F. Hocke, M. J. Schwarz, J. J. Garcia-Ripoll, D. Zueco, T. Hümmer, E. Solano, A. Marx, and R. Gross. *Circuit quantum electrodynamics in the ultrastrong-coupling regime*. Nature Physics **6** (2010), pp. 772–776.

[62] P. Nataf and C. Ciuti. *Vacuum Degeneracy of a Circuit QED System in the Ultrastrong Coupling Regime*. Phys. Rev. Lett. **104** (2010), p. 023601.

[63] P. Nataf and C. Ciuti. *No-go theorem for superradiant quantum phase transitions in cavity QED and counter-example in circuit QED*. Nature Communications **1** (2010), p. 72.

[64] C. Ciuti, G. Bastard, and I. Carusotto. *Quantum vacuum properties of the intersubband cavity polariton field*. Physical Review B **72** (2005), p. 115303.

[65] A. A. Anappara, S. De Liberato, A. Tredicucci, C. Ciuti, G. Biasiol, L. Sorba, and F. Beltram. *Signatures of the ultrastrong light-matter coupling regime*. Physical Review B **79** (2009), p. 201303.

[66] Y. Todorov, A. M. Andrews, R. Colombelli, S. De Liberato, C. Ciuti, P. Klang, G. Strasser, and C. Sirtori. *Ultrastrong Light-Matter Coupling Regime with Polariton Dots*. Physical Review Letters **105** (2010), p. 196402.

[67] G. Scalari, C. Maissen, D. Turčinková, D. Hagenmüller, S. D. Liberato, C. Ciuti, C. Reichl, D. Schuh, W. Wegscheider, M. Beck, and J. Faist. *Ultrastrong Coupling of the Cyclotron Transition of a 2D Electron Gas to a THz Metamaterial*. Science **335** (2012), pp. 1323–1326.

[68] H. J. Carmichael, C. W. Gardiner, and D. F. Walls. *Higher order corrections to the Dicke superradiant phase transition*. Physics Letters A **46** (1973), pp. 47–48.

[69] F. Dimer, B. Estienne, A. S. Parkins, and H. J. Carmichael. *Proposed realization of the Dicke-model quantum phase transition in an optical cavity QED system*. Physical Review A **75** (2007), p. 013804.

[70] K. Baumann, C. Guerlin, F. Brennecke, and T. Esslinger. *Dicke quantum phase transition with a superfluid gas in an optical cavity*. Nature **464** (2010), pp. 1301–1306.

[71] K. Hepp and E. H. Lieb. *On the superradiant phase transition for molecules in a quantized radiation field: the dicke maser model*. Annals of Physics **76** (1973), pp. 360–404.

[72] A. Baksic and C. Ciuti. *Controlling Discrete and Continuous Symmetries in "Superradiant" Phase Transitions with Circuit QED Systems*. Physical Review Letters **112** (2014), p. 173601.

[73] C. Emary and T. Brandes. *Chaos and the quantum phase transition in the Dicke model*. Physical Review E **67** (2003), p. 066203.

[74] A. Blais, R.-S. Huang, A. Wallraff, S. M. Girvin, and R. J. Schoelkopf. *Cavity quantum electrodynamics for superconducting electrical circuits: An architecture for quantum computation*. Physical Review A **69** (2004), p. 062320.

[75] A. Gilchrist, K. Nemoto, W. J. Munro, T. C. Ralph, S. Glancy, S. L. Braunstein, and G. J. Milburn. *Schrödinger cats and their power for quantum information processing*. Journal of Optics B: Quantum and Semiclassical Optics **6** (2004), S828.

[76] P. Nataf and C. Ciuti. *Protected Quantum Computation with Multiple Resonators in Ultrastrong Coupling Circuit QED*. Phys. Rev. Lett. **107** (2011), p. 190402.

[77] M. Mirrahimi, Z. Leghtas, V. V. Albert, S. Touzard, R. J. Schoelkopf, L. Jiang, and M. H. Devoret. *Dynamically protected cat-qubits: a new paradigm for universal quantum computation*. New Journal of Physics **16** (2014), p. 045014.

[78] J. F. Poyatos, J. I. Cirac, and P. Zoller. *Quantum Reservoir Engineering with Laser Cooled Trapped Ions*. Physical Review Letters **77** (1996), pp. 4728–4731.

[79] F. Verstraete, M. M. Wolf, and J. Ignacio Cirac. *Quantum computation and quantum-state engineering driven by dissipation*. Nature Physics **5** (2009), pp. 633–636.

[80] H. Tan, G. Li, and P. Meystre. *Dissipation-driven two-mode mechanical squeezed states in optomechanical systems*. Physical Review A **87** (2013), p. 033829.

[81] Y. Lin, J. P. Gaebler, F. Reiter, T. R. Tan, R. Bowler, A. S. Sørensen, D. Leibfried, and D. J. Wineland. *Dissipative production of a maximally entangled steady state of two quantum bits*. Nature **504** (2013), pp. 415–418.

[82] C. Arenz, C. Cormick, D. Vitali, and G. Morigi. *Generation of two-mode entangled states by quantum reservoir engineering*. Journal of Physics B: Atomic, Molecular and Optical Physics **46** (2013), p. 224001.

[83] M. Asjad and D. Vitali. *Reservoir engineering of a mechanical resonator: generating a macroscopic superposition state and monitoring its decoherence*. Journal of Physics B: Atomic, Molecular and Optical Physics **47** (2014), p. 045502.

[84] A. Roy, Z. Leghtas, A. D. Stone, M. Devoret, and M. Mirrahimi. *Continuous generation and stabilization of mesoscopic field superposition states in a quantum circuit*. Physical Review A **91** (2015), p. 013810.

[85] Z. Leghtas, S. Touzard, I. M. Pop, A. Kou, B. Vlastakis, A. Petrenko, K. M. Sliwa, A. Narla, S. Shankar, M. J. Hatridge, M. Reagor, L. Frunzio, R. J. Schoelkopf, M. Mirrahimi, and M. H. Devoret. *Confining the state of light to a quantum manifold by engineered two-photon loss*. Science **347** (2015), pp. 853–857.

[86] P. Campagne-Ibarcq, E. Flurin, N. Roch, D. Darson, P. Morfin, M. Mirrahimi, M. H. Devoret, F. Mallet, and B. Huard. *Persistent Control of a Superconducting Qubit by Stroboscopic Measurement Feedback*. Phys. Rev. X **3** (2013), p. 021008.

[87] M. E. Roch N.and Schwartz, F. Motzoi, C. Macklin, A. W. Vijay R. and Eddins, A. N. Korotkov, K. B. Whaley, M. Sarovar, and I. Siddiqi. *Observation of Measurement-Induced Entanglement and Quantum Trajectories of Remote Superconducting Qubits*. Physical Review Letters **112** (2014), p. 170501.

[88] L. Sun, A. Petrenko, Z. Leghtas, B. Vlastakis, G. Kirchmair, K. M. Sliwa, A. Narla, M. Hatridge, S. Shankar, J. Blumoff, L. Frunzio, M. Mirrahimi, M. H. Devoret, and R. J. Schoelkopf. *Tracking photon jumps with repeated quantum non-demolition parity measurements*. Nature **511** (2014), pp. 444–448.

[89] P. Campagne-Ibarcq, P. Six, L. Bretheau, A. Sarlette, M. Mirrahimi, P. Rouchon, and B. Huard. *Observing Quantum State Diffusion by Heterodyne Detection of Fluorescence*. Physical Review X **6** (2016), p. 011002.

[90] S. Pigeon, L. Fusco, A. Xuereb, G. De Chiara, and M. Paternostro. *Thermodynamics of trajectories of a quantum harmonic oscillator coupled to N baths*. Physical Review A **92** (2015), p. 013844.

[91] S. Pigeon, L. Fusco, A. Xuereb, G. D. Chiara, and M. Paternostro. *Thermodynamics of trajectories and local fluctuation theorems for harmonic quantum networks*. New Journal of Physics **18** (2016), p. 013009.

[92] P. Strasberg, G. Schaller, T. Brandes, and M. Esposito. *Thermodynamics of quantum-jump-conditioned feedback control*. Physical Review E **88** (2013), p. 062107.

[93] M. Esposito, U. Harbola, and S. Mukamel. *Nonequilibrium fluctuations, fluctuation theorems, and counting statistics in quantum systems*. Reviews of Modern Physics **81** (2009), pp. 1665–1702.

[94] J. Lolli, A. Baksic, D. Nagy, V. E. Manucharyan, and C. Ciuti. *Ancillary Qubit Spectroscopy of Vacua in Cavity and Circuit Quantum Electrodynamics*. Physical Review Letters **114** (2015), p. 183601.

[95] N. Bartolo, F. Minganti, J. Lolli, and C. Ciuti. *Homodyne versus photon-counting quantum trajectories for dissipative Kerr resonators with two-photon driving*. The European Physical Journal Special Topics **226** (2017), pp. 2705–2713.

[96] F. Minganti, N. Bartolo, J. Lolli, W. Casteels, and C. Ciuti. *Exact results for Schrödinger cats in driven-dissipative systems and their feedback control*. Scientific Reports **6** (2016), p. 26987.

[97] W. Greiner, J. Reinhardt, and D. A. Bromley. *Field Quantization*. 1st ed. Springer, 1996.

[98] P. A. M. Dirac. *The Principles of Quantum Mechanics (Fourth Edition, Revised)*. International Series of Monographs on Physics 27. Oxford University Press, 1967.

[99] C. Cohen-Tannoudji, J. Dupont-Roc, and G. Grynberg. *Photons and atoms: Introduction to quantum electrodynamics*. Wiley Professional. Wiley-VCH, 1997.

[100] J.-M. Raimond. *Lecture notes: Atoms and Photons*.

[101] C. Fabre. *Lecture notes: Atomes et lumière. Interaction matière rayonement*. fr. Nov. 2011.

[102] E. H. Kennard. *Zur Quantenmechanik einfacher Bewegungstypen*. Zeitschrift für Physik **44** (1927), pp. 326–352.

[103] H. P. Robertson. *The Uncertainty Principle*. Physical Review **34** (1929), pp. 163–164.

[104] P. J. Coles, M. Berta, M. Tomamichel, and S. Wehner. *Entropic uncertainty relations and their applications*. Reviews of Modern Physics **89** (2017), p. 015002.

[105] M. Born and P. Jordan. *Zur Quantenmechanik*. Zeitschrift für Physik **34** (1925), pp. 858–888.

[106] P. A. M. Dirac. *Lectures on quantum mechanics*. Dover Publications, 2001.

[107] P. A. M. Dirac. *Generalized Hamiltonian dynamics*. Canadian Journal of Mathematics **2** (1950), pp. 129–148.

[108] W. Heisenberg and H. Euler. *Folgerungen aus der Diracschen Theorie des Positrons*. Zeitschrift für Physik **98** (1936), pp. 714–732.

[109] M. Hillery and L. D. Mlodinow. *Quantization of electrodynamics in nonlinear dielectric media*. Physical Review A **30** (1984), pp. 1860–1865.

[110] M. O. Scully and M. S. Zubairy. *Quantum optics*. 1st ed. Cambridge University Press, 1997.

[111] G. Grynberg, A. Aspect, and C. Fabre. *Introduction to Quantum Optics: From the Semi-classical Approach to Quantized Light*. Cambridge University Press, 2010.

[112] M. Maggiore. *A modern introduction to quantum field theory*. Oxford master series in physics 12. Oxford University Press, 2005.

[113] J. R. Schrieffer and P. A. Wolff. *Relation between the Anderson and Kondo Hamiltonians*. Physical Review **149** (1966), pp. 491–492.

[114] V. Denner and M. Wagner. *Diagonalization of the Rabi Hamiltonian by means of a unitary transformation*. Zeitschrift für Physik B Condensed Matter **58** (1985), pp. 255–258.

[115] D. Zueco, G. M. Reuther, S. Kohler, and P. Hänggi. *Qubit-oscillator dynamics in the dispersive regime: Analytical theory beyond the rotating-wave approximation*. Physical Review A **80** (2009), p. 033846.

[116] W. E. Lamb and R. C. Retherford. *Fine Structure of the Hydrogen Atom by a Microwave Method*. Physical Review **72** (1947), pp. 241–243.

[117] H. A. Bethe. *The Electromagnetic Shift of Energy Levels*. Physical Review **72** (1947), pp. 339–341.

[118] O. Viehmann, J. von Delft, and F. Marquardt. *Superradiant Phase Transitions and the Standard Description of Circuit QED*. Physical Review Letters **107** (2011), p. 113602.

[119] C. Ciuti and P. Nataf. *Comment on "Superradiant Phase Transitions and the Standard Description of Circuit QED"*. Physical Review Letters **109** (2012), p. 179301.

[120] D. Nagy, G. Kónya, G. Szirmai, and P. Domokos. *Dicke-Model Phase Transition in the Quantum Motion of a Bose-Einstein Condensate in an Optical Cavity*. Phys. Rev. Lett. **104** (2010), p. 130401.

[121] S. D. Liberato, C. Ciuti, and I. Carusotto. *Quantum Vacuum Radiation Spectra from a Semiconductor Microcavity with a Time-Modulated Vacuum Rabi Frequency*. Physical Review Letters **98** (2007), p. 103602.

[122] J. R. Johansson, G. Johansson, C. M. Wilson, and F. Nori. *Dynamical Casimir Effect in a Superconducting Coplanar Waveguide*. Physical Review Letters **103** (2009), p. 147003.

[123] S. De Liberato, D. Gerace, I. Carusotto, and C. Ciuti. *Extracavity quantum vacuum radiation from a single qubit*. Physical Review A **80** (2009), p. 053810.

[124] A. Klein and E. R. Marshalek. *Boson realizations of Lie algebras with applications to nuclear physics*. Reviews of Modern Physics **63** (1991), pp. 375–558.

[125] H.-P. Breuer and F. Petruccione. *The Theory of Open Quantum Systems*. Oxford University Press, 2002. 648 pp.

[126] C. Gardiner and P. Zoller. *Quantum noise: A Handbook of Markovian and Non-Markovian Quantum Stochastic Methods with Applications to Quantum Optics*. 2nd enlarged ed. Springer series in synergetics. Springer, 2004.

[127] J. Dalibard. *Lecture notes: Cohérence quantique et dissipation*. 2006.

[128] I. Dotsenko, M. Mirrahimi, M. Brune, S. Haroche, J.-M. Raimond, and P. Rouchon. *Quantum feedback by discrete quantum nondemolition measurements: Towards on-demand generation of photon-number states*. Phys. Rev. A **80** (2009), p. 013805.

[129] E. Schrödinger. *Die gegenwärtige Situation in der Quantenmechanik*. Naturwissenschaften **23** (1935), pp. 807–812.

[130] D. Bohm. *A Suggested Interpretation of the Quantum Theory in Terms of "Hidden" Variables. I*. Physical Review **85** (1952), pp. 166–179.

[131] D. Bohm and B. J. Hiley. *The undivided universe: an ontological interpretation of quantum theory*. First. Routledge, 1993.

[132] *Bulletin of the Atomic Scientists*. en. Educational Foundation for Nuclear Science, Inc., 1963.

[133] B. D. Finetti, A. Machi, and A. Smith. *Theory of Probability: A Critical Introductory Treatment*. Wiley Series in Probability & Mathematical Statistics v. 1 & 2. John Wiley & Sons, 1992.

[134] C. M. Caves, C. A. Fuchs, and R. Schack. *Unknown quantum states: The quantum de Finetti representation*. Journal of Mathematical Physics **43** (2002), pp. 4537–4559.

[135] H. M. Wiseman and G. J. Milburn. *Quantum Measurement and Control*. Cambridge University Press, 2009.

[136] M. Born. *Zur Quantenmechanik der Stoßvorgänge*. Zeitschrift für Physik **37** (1926), pp. 863–867.

[137] M. A. Nielsen and I. L. Chuang. *Quantum computation and quantum information*. 1st ed. Cambridge Series on Information and the Natural Sciences. Cambridge University Press, 2004.

[138] D. T. Smithey, M. Beck, M. G. Raymer, and A. Faridani. *Measurement of the Wigner distribution and the density matrix of a light mode using optical homodyne tomography: Application to squeezed states and the vacuum*. Physical Review Letters **70** (1993), pp. 1244–1247.

[139] A. Zavatta, S. Viciani, and M. Bellini. *Tomographic reconstruction of the single-photon Fock state by high-frequency homodyne detection*. Physical Review A **70** (2004), p. 053821.

[140] D. F. Walls and G. J. Milburn. *Quantum Optics*. 2nd ed. Springer, 2008.

[141] J. Dalibard, Y. Castin, and K. Mølmer. *Wave-function approach to dissipative processes in quantum optics*. Physical Review Letters **68** (1992), pp. 580–583.

[142] H. Carmichael. *An Open Systems Approach to Quantum Optics: Lectures Presented at the Université Libre de Bruxelles, October 28 to November 4, 1991*. Springer Science & Business Media, 1993. 192 pp.

[143] R. Dum, A. S. Parkins, P. Zoller, and C. W. Gardiner. *Monte Carlo simulation of master equations in quantum optics for vacuum, thermal, and squeezed reservoirs*. Physical Review A **46** (1992), pp. 4382–4396.

[144] M. B. Plenio and P. L. Knight. *The quantum-jump approach to dissipative dynamics in quantum optics*. Reviews of Modern Physics **70** (1998), pp. 101–144.

[145] H. M. Wiseman and G. J. Milburn. *Quantum theory of field-quadrature measurements*. Physical Review A **47** (1993), pp. 642–662.

[146] C. Ciuti and I. Carusotto. *Input-output theory of cavities in the ultrastrong coupling regime: The case of time-independent cavity parameters*. Phys. Rev. A **74** (2006), p. 033811.

[147] C. M. Wilson, G. Johansson, A. Pourkabirian, M. Simoen, J. R. Johansson, T. Duty, F. Nori, and P. Delsing. *Observation of the dynamical Casimir effect in a superconducting circuit*. Nature **479** (2011), pp. 376–379.

[148] S. Fedortchenko, S. Huppert, A. Vasanelli, Y. Todorov, C. Sirtori, C. Ciuti, A. Keller, T. Coudreau, and P. Milman. *Output squeezed radiation from dispersive ultrastrong light-matter coupling*. Physical Review A **94** (2016), p. 013821.

[149] N. Lambert, Y.-n. Chen, R. Johansson, and F. Nori. *Quantum chaos and critical behavior on a chip*. Physical Review B **80** (2009), p. 165308.

[150] S. Felicetti, T. Douce, G. Romero, P. Milman, and E. Solano. *Parity-dependent State Engineering and Tomography in the ultrastrong coupling regime*. Scientific Reports **5** (2015).

[151] F. Beaudoin, J. M. Gambetta, and A. Blais. *Dissipation and ultrastrong coupling in circuit QED*. Physical Review A **84** (2011), p. 043832.

[152] F. Nissen, J. M. Fink, J. A. Mlynek, A. Wallraff, and J. Keeling. *Collective Suppression of Linewidths in Circuit QED*. Physical Review Letters **110** (2013), p. 203602.

[153] Y. Makhlin, G. Schön, and A. Shnirman. *Quantum-state engineering with Josephson-junction devices*. Reviews of Modern Physics **73** (2001), pp. 357–400.

[154] V. E. Manucharyan, J. Koch, L. I. Glazman, and M. H. Devoret. *Fluxonium: Single Cooper-Pair Circuit Free of Charge Offsets*. Science **326** (2009), pp. 113–116.

[155] K. Le Hur, L. Henriet, A. Petrescu, K. Plekhanov, G. Roux, and M. Schiró. *Many-body quantum electrodynamics networks: Non-equilibrium condensed matter physics with light*. Comptes Rendus Physique. Polariton physics / Physique des polaritons **17** (2016), pp. 808–835.

[156] J. Jin, A. Biella, O. Viyuela, L. Mazza, J. Keeling, R. Fazio, and D. Rossini. *Cluster Mean-Field Approach to the Steady-State Phase Diagram of Dissipative Spin Systems*. Physical Review X **6** (2016), p. 031011.

[157] R. M. Wilson, K. W. Mahmud, A. Hu, A. V. Gorshkov, M. Hafezi, and M. Foss-Feig. *Collective phases of strongly interacting cavity photons*. Physical Review A **94** (2016), p. 033801.

[158] M. Foss-Feig, P. Niroula, J. T. Young, M. Hafezi, A. V. Gorshkov, R. M. Wilson, and M. F. Maghrebi. *Emergent equilibrium in many-body optical bistability*. Physical Review A **95** (2017), p. 043826.

[159] T. C. Ralph, A. Gilchrist, G. J. Milburn, W. J. Munro, and S. Glancy. *Quantum computation with optical coherent states*. Physical Review A **68** (2003), p. 042319.

[160] S. Puri, S. Boutin, and A. Blais. *Engineering the quantum states of light in a Kerr-nonlinear resonator by two-photon driving*. npj Quantum Information **3** (2017), p. 18.

[161] N. Bartolo, F. Minganti, W. Casteels, and C. Ciuti. *Exact steady state of a Kerr resonator with one- and two-photon driving and dissipation: Controllable Wigner-function multimodality and dissipative phase transitions*. Physical Review A **94** (2016).

[162] P. D. Drummond and D. F. Walls. *Quantum theory of optical bistability. I. Nonlinear polarisability model*. Journal of Physics A: Mathematical and General **13** (1980), p. 725.

[163] W. N. Bailey. *Generalized hypergeometric series*. New edition. Cambridge Tracts in Mathematics. Hafner Publishing Co Ltd, 1973.

[164] E. Wigner. *On the Quantum Correction For Thermodynamic Equilibrium*. Physical Review **40** (1932), pp. 749–759.

[165] H. Carmichael. *Statistical Methods in Quantum Optics 1: Master Equations and Fokker-Planck Equations*. Springer Science & Business Media, 1998. 400 pp.

[166] V. Veitch, C. Ferrie, D. Gross, and J. Emerson. *Negative quasi-probability as a resource for quantum computation*. New Journal of Physics **14** (2012), p. 113011.

[167] N. Delfosse, P. Allard Guerin, J. Bian, and R. Raussendorf. *Wigner Function Negativity and Contextuality in Quantum Computation on Rebits*. Physical Review X **5** (2015), p. 021003.

[168] K. Mølmer, Y. Castin, and J. Dalibard. *Monte Carlo wave-function method in quantum optics*. Journal of the Optical Society of America B **10** (1993), p. 524.

[169] H. J. Carmichael. *Quantum trajectory theory for cascaded open systems*. Physical Review Letters **70** (1993), pp. 2273–2276.

[170] L. Gilles, B. M. Garraway, and P. L. Knight. *Generation of nonclassical light by dissipative two-photon processes*. Physical Review A **49** (1994), pp. 2785–2799.

[171] L. Krippner, W. J. Munro, and M. D. Reid. *Transient macroscopic quantum superposition states in degenerate parametric oscillation: Calculations in the large-quantum-noise limit using the positive P representation*. Physical Review A **50** (1994), pp. 4330–4338.

[172] D. Vitali, S. Zippilli, P. Tombesi, and J.-M. Raimond. *Decoherence control with fully quantum feedback schemes*. Journal of Modern Optics **51** (2004), pp. 799–809.

[173] S. Zippilli, D. Vitali, P. Tombesi, and J.-M. Raimond. *Scheme for decoherence control in microwave cavities*. Physical Review A **67** (2003), p. 052101.

[174] C. Sayrin, I. Dotsenko, X. Zhou, B. Peaudecerf, T. Rybarczyk, S. Gleyzes, P. Rouchon, M. Mirrahimi, H. Amini, M. Brune, J.-M. Raimond, and S. Haroche. *Real-time quantum feedback prepares and stabilizes photon number states*. Nature **477** (2011), pp. 73–77.

[175] X. Zhou, I. Dotsenko, B. Peaudecerf, T. Rybarczyk, C. Sayrin, S. Gleyzes, J. M. Raimond, M. Brune, and S. Haroche. *Field Locked to a Fock State by Quantum Feedback with Single Photon Corrections*. Physical Review Letters **108** (2012), p. 243602.

[176] J. M. R. Parrondo, J. M. Horowitz, and T. Sagawa. *Thermodynamics of information*. Nature Physics **11** (2015), pp. 131–139.

[177] J. Millen and A. Xuereb. *Perspective on quantum thermodynamics*. New Journal of Physics **18** (2016), p. 011002.

[178] J. Goold, M. Huber, A. Riera, L. d. Rio, and P. Skrzypczyk. *The role of quantum information in thermodynamics—a topical review*. Journal of Physics A: Mathematical and Theoretical **49** (2016), p. 143001.

[179] N. Cottet, S. Jezouin, L. Bretheau, P. Campagne-Ibarcq, Q. Ficheux, J. Anders, A. Auffèves, R. Azouit, P. Rouchon, and B. Huard. *Observing a quantum Maxwell demon at work*. Proceedings of the National Academy of Sciences **114** (2017), pp. 7561–7564.

[180] C. Elouard, D. A. Herrera-Martí, M. Clusel, and A. Auffèves. *The role of quantum measurement in stochastic thermodynamics*. npj Quantum Information **3** (2017), p. 9.